

Synthesis of Novel Tetrahydroisoquinoline-related Estrogen Receptor Modulators

by

Tanya Mabank

*Dissertation presented in fulfilment of the requirements for the
degree of Doctor of Philosophy*



**at
Stellenbosch University**

Supervisor: Prof. W. A. L. van Otterlo

Co-supervisor: Dr. S. C. Pelly

Department of Chemistry and Polymer Science

Faculty of Science

April 2019

Declaration

By submitting this dissertation electronically, I declare that the entirety of the work contained therein is my own original work, that I am the authorship owner thereof (unless to the extent explicitly otherwise stated) and that I have not previously in its entirety or in part submitted it for obtaining any qualification.

Signature:

Date:

Acknowledgements

I would like to thank Professor Ivan Green for the guidance once my MSc project was complete. My sincerest gratitude to Professor Willem van Otterlo for providing me with the opportunity gain an immense amount of knowledge relating to synthetic chemistry, development of laboratory skills, life skills and the patience to tolerate mistakes which accompany learning valuable lessons learned. Once accepted for the project, I can only thank God almighty for the perseverance, patience, also a major thanks to the extremely helpful and welcoming personalities of so many lab members who passed through labs 2007, 2008, 2020 and 2021 whom I have met and worked with over the years who were patiently willing to help when required.

None of this would have possible without Stellenbosch University (for the opportunity to study here), NRF (for funding) and CAF facilities (for the hands-on experience gained and analysis of laboratory results). Not to be forgotten, the people who rarely get considered and value taken for granted, the CAF analytical and technical staff, without these people the smooth functioning, acquiring of chemicals, acquiring of results and assistance with their interpretation. No words or gifts could ever encapsulate the gratitude I have or would like to transfer to these people.

Abstract

The tetrahydroisoquinoline (THIQ) core has displayed a rich history as a biologically active natural product and is an interesting scaffold to use in drug discovery. Its structural skeleton is present in a number of structurally diverse natural products exhibiting a wide range of biological, pharmaceutical and estrogen receptor (ER) activities.¹⁻⁵ Estrogen is a steroid hormone which influences the functioning of many target tissues. However, the normal existence of estradiol in women affected with breast cancer may worsen the infection; and a deficiency may increase the risk of various hormone related diseases. Estradiol is the natural ligand responsible for modulating the expression and/or repression of specific estrogen gene transcriptions.^{6,7} In this project, we therefore considered the synthesis of four small sets of THIQ-based compounds with the potential ability to bind the ER with affinities competing with that of estradiol. The THIQ compounds generated included structures with or without linker groups, and a lactam core without a linker group.

The compounds were structurally designed by making use of Schrodinger and Accelrys Discovery Studio software, to accommodate the receptors binding pocket and improve the potency and selectivity toward the ER β . With the successful synthesis of the THIQ compounds generated, which included structures with or without linker groups, and a lactam core without a linker group, further biochemical studies were explored. During the synthesis of these final compounds, it was found that once demethylated, the final compounds showed some degree of decomposition and sedimentation upon preparation for bioevaluations. Whole cell testing however, only revealed that only one compound showed potential activity, with the rest showing quite poor activity. In terms of the cell proliferation, this compound (65%) compared well to the medicinal agent, Fulvestrant, which slowed growth to 63.5%.

Uitreksel

Die tetrahydroisokinolien (THIQ) kern het 'n ryk geskiedenis as dit kom by natuurlike aktiewe tetrahydroisokinoliene en is 'n struktuur wat dikwels gebruik word gedurende die ontdekking van nuwe medisinale middels. Die struktuur kom in baie verskillende natuurlike produkte voor en het biologiese, farmaseutiese en estrogeen reseptor (ER) aktieweiteite.¹⁻⁵ Baie organe word beïnvloed deur die funksionering van die steroïde hormoon estrogeen. In vrouens wat aan borskanker ly kan estrogeen 'n nadelige uitwerking hê, hoewel te min estrogeen tot ander hormoonverwante siektes kan ly. Estradiol is die natuurlike bindingsmiddel wat verantwoordelik is vir die modulering van en/of die onderdrukking van spesifieke estrogeen gene transkripsies.^{6,7} In hierdie projek stel ons die sintese van vier stelsels voor wat die THIQ kern bevat. Die molekules het die potensiaal om in die binding met die ER, met estradiol te kompeteer. Die molekules wat gesinteseer is, het die volgende algemene strukture wat op trifluorometielsulfoniel THIQ – gebaseerd is: THIQ met bindings groepe, geen bindings groep en die laktam kern sonder die bindings groep.

Die molekules was ontwerp deur gebruik te maak van die Schrodinger en Acclerys Discovery Studio sagteware, om sodoende interaksies met die ER β , en dus selektiwiteit, te verbeter. Met die suksesvolle sintese van die molekules, dws trifluorometielsulfoniel THIQ – gebaseerd, met bindings groepe, geen bindings groep en die laktam kern sonder die bindings groep, is verder biochemiese toetse gedoen. Gedurende die sintese van hierdie finale molekules is dit bevind dat die demetieleerde weergawes degradasie en sedimentasie ondergaan gedurende voorbereiding vir bio-evaluasie. Biochemiese en heel sel toetse het gewys dat van die molekules potensieel aktief is, terwyl die meeste minder aktief was. Een van die molekules het 'n sel groei persentasie waarde van 65.0% getoon, teenoor die wel bekende Fulvestrant wat die groei tot 63.5% vertraag het.

List of Abbreviations

AF	Activation function	MS	Mass spectroscopy
AIB	Amplified in breast cancer	NCoA	Nuclear receptor coactivator
ATP	Adenosine triphosphate	NCoR	Nuclear receptor corepressor
CARM	Coactivator associated arginine methyl transferase	NMR	Nuclear magnetic resonance
CBP	CREB binding protein	p/CAF	p300/CBP associated factor
CC	Column chromatography	p300	E1A binding protein
CDI	1,1-Carbonyldiimidazole	RIP	Receptor interacting protein
D	Doublet	S	Singlet
DBD	DNA binding domain	SERM	Selective estrogen receptor modulator
DCM	Dichloromethane	SMRT	Silencing mediator of retinoid and thyroid
DNA	Deoxyribonucleic acid	SRA	Steroid receptor RNA activator
E2	Estradiol	SRC	Steroid receptor coactivator
equiv.	Equivalent	T	Triplet
ER	Estrogen receptor	TCDI	1,1-Thiocarbonyldiimidazole
ERE	Estrogen response elements	THF	Tetrahydrofuran
FC	Flash chromatography	THIQ	Tetrahydroisoquinoline
HAT	Histone acetyl transferase	TIF	Transcriptional intermediary factor
IR	Infrared spectroscopy	TLC	Thin layer chromatography
LBD	Ligand binding domain	TRIM	Tripartite motif containing
M	Multiplet		

Table of Contents

Declaration	1
Acknowledgements.....	2
Abstract.....	3
Uitreksel.....	4
List of Abbreviations.....	5
Chapter 1	1
General Introduction	1
1.1 The significant and multifaceted role of hormones	1
1.2 Established link between hormones and the development of carcinomas	4
1.3 Estrogen’s distinct contribution toward breast carcinoma development.....	4
1.3.1 Estradiol metabolism pathways and the unfavourable resulting DNA adducts	5
1.4 The diverse source and characteristics of mammary gland carcinomas	7
1.5 The evolutionary development in therapeutic strategies toward alleviating carcinomas	9
1.5.1 Surgical techniques used for the removal of carcinomas.....	9
1.5.2 Eradication of carcinomas with radiation	10
1.5.3 A chemical approach toward treating carcinomas	10
1.5.4 The manipulation of hormones for promoting cellular health	12
1.5.5 Immunotherapy treatment targeting gene specific tumors.....	12
1.6 Carcinomas: An overall understanding, therapeutic challenges and the way forward.....	13
1.7 Feasibility for this research study	13
Chapter 2.....	16
Literature review	16
Part 1: Estrogen modulation	16
2.1 The distribution and physiological importance presented by the ER isoforms... 16	16

2.2 The structural architecture of estradiol and its binding sites	18
2.3 The ERs and their associated binding domains	21
2.3.1 The amino terminal domain.....	21
2.3.2 The DNA binding domain	22
2.3.3 The D- and E/F-domain.....	23
2.4 Estradiol instrumentation and its mechanism of action	25
2.4.1 Effector machinery responsible for the orchestration of ER modulation.....	26
2.4.2 All pathways lead to gene transcription	28
Literature review	32
Part 2: Evaluation of past and present SERMs	32
2.5 Synthetic ligands and selectively mediating estrogenic gene transcription	32
2.6 The general SERM binding interaction mechanism	33
2.7 The gradual development of the SERM generations	34
2.8 First generation SERMs: Triphenylethylene analogues	34
2.8.1 Victories and challenges associated with tamoxifen	35
2.8.2 The structural modification of tamoxifen to toremifene	36
2.8.3 The triphenylethylene analogue: Droloxifene	37
2.8.4 The triphenylethylene analogue: Idoxifene.....	37
2.9 Second generation SERMs: Benzothiophene analogues	38
2.10 Third generation SERMs	40
2.10.1 Redemption of the benzothiophene scaffold with the development of arzoxifene	40
2.10.2 Redemption of the triphenylethylene analogue with the development of ospemifene ..	41
2.10.3 The naphthalene analogue: Lasofoxifene.....	42
2.10.4 The indole analogue: Bazedoxifene	43
2.11 Fourth generation SERMs: Benzopyrans	43
2.12 The metabolic pathways undergone by SERMs	44
2.12.1 Metabolic pathways followed by the triphenylethylene analogues	44
2.12.2 Metabolic pathways followed by the benzothiophene analogues.....	46

2.12.3 Metabolic pathway followed by benzopyran analogues	49
2.13 Drug discovery and its development rooted from natural products	50
2.14 The tetrahydroisoquinoline alkaloids: Natural and synthetic substrates	50
2.15 Major research objectives of this project	54
Chapter 3.....	59
Synthesis of THIQ analogues.....	59
3.1 Introduction.....	59
3.2 Background chemistry on tetrahydroisoquinoline syntheses.....	62
3.3 Synthesis of the	
2-[(trifluoromethyl)sulfonyl]-1,2,3,4-tetrahydroisoquinolin-6-ol	65
3.3.1 Synthesis of the 6-methoxy-1,2,3,4-tetrahydroisoquinoline hydrochloride salt	66
3.3.2 Synthesis of the trifluoromethyl sulfonamide 3.34	67
3.3.4 Demethylation of the aryl methyl ether	68
3.4 The synthesis of the C4 analogues 3.49	70
3.4.1 Synthetic protocol for alkylation of 2-(3-methoxyphenyl)acetonitrile	72
3.4.2 Reduction of nitriles 3.46a – d to amines 3.47a – d	74
3.4.3 Synthesis of the THIQ salts 3.52a – d	74
3.4.4 Synthesis of the trifluoromethyl sulfonamide analogues.....	75
3.4.5 Demethylation of aryl methyl ethers 3.53a – d	77
3.5 Summary and concluding remarks	78
Chapter 4.....	79
Investigation of linker group effects on the THIQ analogues.....	79
4.1 Initial motivation for the design of the second library	79
4.2 The synthesis of 1,2,3,4-tetrahydroisoquinolin-6-ol peptidyl-linked analogues.....	83
4.3 The synthesis of 1,2,3,4-tetrahydroisoquinolin-6-ol urea-linked analogues	88
4.3.1 Coupling agents used for the synthesis of urea bonds.....	90
4.3.2 Isocyanates as an intermediate towards the urea moiety	91

4.3.3 Carbamoyl transfer agents for the synthesis of THIQ–urea analogues	93
4.4 The synthesis of 1,2,3,4–tetrahydroisoquinolin–6–ol thiourea–linked analogues.....	99
4.4.1 Synthesis of THIQ–thiocarbamoyl imidazolium iodide salt	100
4.4.2 Coupling of THIQ–thiocarbamoyl imidazolium iodide salt with amines.....	101
4.4.3 Isothiocyanate to the rescue: Generating thiocarbamoyl analogues.....	103
4.5 The synthesis of 1,2,3,4–tetrahydroisoquinolin–6–ol sulfonylurea–linked analogues.....	109
4.5.1 Evaluation of protocols developed for the synthesis of the sulfonyl amide moiety	109
4.5.2 Synthesis of 1,1'–sulfonylbis(1 <i>H</i> –imidazolium) triflate salt.....	110
4.5.3 Synthesis of 1–{[6–methoxy–3,4–dihydroisoquinolin–2(1 <i>H</i>)–yl]sulfonyl}–3–methyl–1 <i>H</i> –imidazol–3–ium triflate salt.....	112
4.5.4 Coupling of the THIQ–sulfonyl imidazolium triflate salt 4.76 with amines	113
4.6 Deprotection of aryl methyl ethers	115
4.7 Summary and concluding remarks	119
Chapter 5.....	121
Isochromanones: surprisingly valuable intermediates.....	121
5.1 Introduction.....	121
5.2 Retrosynthetic analysis 1: Metal–mediated coupling protocol for synthesizing THIQ analogues	122
5.2.1 Investigation toward the feasibility of Ullmann condensation for synthesizing <i>N</i> –aromatic THIQ analogues	128
5.3 Retrosynthetic analysis 2: Intramolecular cyclization as an approach to synthesizing THIQ analogues.....	130
5.3.1 Reductive amination reactions	131
5.3.2 Nucleophilic substitution reactions	133
5.3.3 Acylation of secondary amines	134
5.3.4 Intramolecular Friedel–Crafts cyclization reactions	135
5.4 Isochroman: A valuable intermediate for the synthesis of THIQ analogues.....	139

5.4.1 Synthesis of THIQ analogues from an isochroman	139
5.4.2 Synthesis of an isochroman analogue from 3-methoxyphenyl acetic acid.....	141
5.4.3 Ring-opening and halogenation of the 6-methoxyisochroman	145
5.5 Isochromanone as an intermediate toward the synthesis of THIQ analogues ...	148
5.5.1 Synthesis of THIQ analogues promoted through coupling reactions	151
5.6 Demethylating routes toward obtaining 5.1 and 5.56 THIQ analogues.....	154
5.7 Summary and concluding remarks	156
Chapter 6.....	158
Computational and Biological evaluation of the THIQ analogues	158
6.1 Computational evaluation of the synthesized compounds	158
6.1.1 Ligand-ER efficiency docking results	159
6.1.1.1 Computational results obtained for set 1 compounds	160
6.1.1.2 Computational results obtained for set 2 compounds	161
6.1.1.3 Computational results obtained for set 3 compounds	162
6.1.1.4 Computational results obtained for set 4 compounds	163
6.1.1.5 Computational results obtained for set 5 compounds	164
6.1.1.6 Computational results obtained for set 6 compounds	165
6.1.1.7 Overall results obtained for Table 6.1 to 6.6	166
6.2 EC₅₀ results obtained for set 1 compounds	166
6.3 Methodology used in screening of sets 2 – 6 against MCF7	169
6.3.1 MCF7 cellular anti-proliferation results and discussion	170
6.4 Summary and concluding remarks	171
Chapter 7.....	172
Future work	172
7.1 Addressing solubility problems	173
7.2 Maintaining solubility while retaining the phenoxy functional group – a possible pro-drug strategy	173

7.3 Modification to the synthesis of the thiourea linked compounds 4.66	174
7.4 Boron-containing phenol-fused heterocycles to potentially mimic the tetrahydroisoquinoline scaffold	175
7.5 Concluding remarks	176
Chapter 8.....	178
Experimental and Analytical results	178
8.1 Glassware preparation	178
8.2 Reagent preparation	178
8.3 Temperature control	178
8.4 Chromatography	178
8.5 Characterization	179
General experimental methods.....	180
8.6 Synthesis of 2-[(trifluoromethyl)sulfonyl]-1,2,3,4-tetrahydroisoquinolin-6-ol 3.34	180
8.6.1 General procedure for the synthesis of bis[6-methoxy-3,4-dihydroisoquinolin-2(1 <i>H</i>)-yl]methane 3.36	180
8.6.2 General procedure for the synthesis of 6-methoxy-1,2,3,4-tetrahydroisoquinoline hydrochloride 3.37	180
8.6.3 General procedure for the preparation of 6-methoxy-2-[(trifluoromethyl)sulfonyl]-1,2,3,4-tetrahydroisoquinoline 3.38	181
8.6.4 General procedure for the synthesis of 2-[(trifluoromethyl)sulfonyl]-1,2,3,4-tetrahydroisoquinolin-6-ol 3.34	182
8.7 Synthesis of the C4 analogues of 2-[(trifluoromethyl)sulfonyl]-1,2,3,4-tetrahydroisoquinolin-6-ol analogues 3.49	182
8.7.1 General alkylation procedure for 2-(3-methoxyphenyl)acetonitrile 3.47a – d	182
8.7.2 General procedure for the reduction of nitriles 3.47a – d	184
8.7.3 General procedure for the synthesis of 3.51a – d	185
8.7.4 General procedure for the synthesis of THIQ hydrochloride salts 3.52a – d	186
8.7.5 General procedure for the synthesis of trifluorosulfonamides 3.53a – d	187

8.7.6 General procedure for the demethylation of aryl ethers 3.53a – d	189
8.8 Synthesis of urea analogues	190
8.8.1 General procedure for the synthesis of THIQ–carbamoyl imidazoles	190
8.8.2 General procedure for the synthesis of THIQ–carbamoyl imidazolium salts	191
8.8.3 Coupling of THIQ – carbamoyl imidazolium salts with heteroaryls amines	192
8.8.3.1 General procedure for the synthesis of compound 4.54	195
8.8.3.2 General procedure for the synthesis of compounds 4.54	195
8.8.3.3 General procedure for the synthesis of compounds 4.54c – g	196
8.9 Synthesis of thiourea analogues	197
8.9.1 General procedure for the synthesis of [3,4-dihydroisoquinolin-2(1 <i>H</i>)-yl] (1 <i>H</i> -imidazol-1-yl)methanethione	197
8.9.2 General procedure for the synthesis of 1-[3,4 dihydroisoquinolin-2(1 <i>H</i>)-yl]- 3'- methyl-1 <i>H</i> -imidazole-3-ium iodide	198
8.9.3 General procedure for the coupling of THIQ thiocarbamoyl imidazolium salts with heteroaryl amines	199
8.9.4 Method A: General procedure for the synthesis of isothiocyanates 4.64 from hydroxy anilines	201
8.9.5 Method B: General procedure for the synthesis of isothiocyanates 4.64 from haloanilines	201
8.9.6 General procedure for the coupling of isothiocyanates 4.64 with 4.65	202
8.10 Synthesis of sulfonyl urea analogues	205
8.10.1 General procedure for the synthesis of 1,1 – sulfonyl bisimidazole 4.72	205
8.10.2 General procedure for the preparation of sulfamoyl imidazolium salts 4.73	205
8.10.3 General procedure for the synthesis of 2-[(1 <i>H</i> -Imidazol-1-yl)sulfonyl]-1,2,3,4- tetrahydroisoquinolines 4.64 and 4.75	206
8.10.4 General procedure for the coupling of 4.76 with heteroaryl amines.....	207
8.11 Deprotection of aryl methyl ethers	210
8.11.1 General procedure for the demethylation using BBr ₃	210
8.11.2 General procedure for the synthesis of demethylation using AlI ₃	212

8.11.3 Debenzylation of 6-[Benzyloxy-3,4-dihydroisoquinolin-2(1 <i>H</i>)-yl](morpholino) methanone.....	216
8.12 Coupling protocols for the synthesis of THIQ analogues.....	217
8.12.1 2'-[3,4-Dihydroisoquinolin-2(1 <i>H</i>)-yl]thiazole 5.5a	217
8.12.2 4'-[3,4-Dihydroisoquinolin-2(1 <i>H</i>)-yl]thiazole 5.5b	218
8.12.3 2-Phenyl-1,2,3,4-tetrahydroisoquinoline 5.5c	218
8.13 Intramolecular Friedel-Crafts cyclization protocol toward synthesis of THIQ analogues.....	219
8.13.1 Procedure for the synthesis of <i>N</i> -benzylaniline 5.16	219
8.13.2 S _N 2 substitution protocol for the synthesis of THIQ analogues.....	219
8.13.2.1 Method A: General procedure for of <i>N</i> -benzyl-5-methylthiazol-2-amine 5.1	221
8.13.2.2 Method B: General procedure for 5.19 using the Ullmann conditions	221
8.13.3 General procedure for acylation of amines	220
8.13.3.1 Chloroacetylation of amines (a and b)	221
8.13.3.2 2-[Benzyl(phenyl)amino]-2-oxoacetyl chloride 5.33	222
8.13.4 <i>N</i> -Benzyl- <i>N</i> -(2-chloroethyl)aniline 5.22	221
8.14 Synthesis of isochromanone as a route to THIQ analogues.....	222
8.14.1 Reduction of phenyl acetic acid to 2-phenylethanol 5.35	222
8.14.2 Isochroman 5.36	223
8.14.3 1-(2-Iodoethyl)-2-(iodomethyl)benzene 5.37	223
8.14.4 General procedure for the THIQ formation from 5.37	223
8.14.5 6-Methoxyisochroman 5.44	224
8.14.6 2-[2-(Hydroxymethyl)-5-methoxyphenyl]ethanol 5.48	225
8.14.7 General procedure for the halogenation of diol 5.48	226
8.14.7.1 2-(2-Bromoethyl)-1-(bromomethyl)-4-methoxybenzene 5.49	227
8.14.7.2 2-(2-Chloroethyl)-1-(chloromethyl)-4-methoxybenzene 5.49	227
8.15 Synthesis of isochromanone as a route to THIQ analogues.....	226

8.15.1 General procedure for the synthesis of 6-methoxyisochroman-3-one 5.47	226
8.15.2 General procedure for the lactamisation 5.47	227
8.15.3 Synthesis of THIQ analogues <i>via.</i> , amide formation	229
8.15.3.1 Coupling of amines with carboxylic acid 5.45	231
8.15.3.2 General procedure for the reduction of the carbonyl function.....	233
8.15.3.3 General procedure for the Pictet–Spengler cyclization of amines 5.54	234
8.15.4 General procedure for the reduction of Isochromanones 5.43	234
8.16 Demethylation protocols for 6-hydroxy THIQ analogues	235
8.16.1 Method A: Using BBr ₃	235
8.16.2 Method B: Using AlI ₃	237
References	240

Chapter 1

General Introduction

This Chapter, briefly introduces a few important concepts, aimed toward generating a link between our dependence on hormones, their function and the modes of action they assume when transmitting valuable genetic information throughout the body. These concepts provide an understanding to the varied complexities associated with hormones, which allow them to function optimally, as well as effects caused when the malfunctioning of one system occurs. The focus then converges towards the estrogen hormone, fostering the general understanding of its versatility and association to the development of breast cancer (further elaborated in Chapter 2). In this chapter, further discussions on the introduction of cancer, the evolutionary development of cancer therapeutics and the current need for further development, especially in third world countries, will briefly be discussed.

1.1 The significant and multifaceted role of hormones

Hormones are critical biological messengers which function at a cellular level conveying specific chemical information, thereby controlling vital processes in the body such as metabolic homeostasis, growth, development and reproduction, which are listed in Table 1.1.⁸

Table 1.1. Transcriptional activity mediated by major glands within the endocrine system.⁸

Gland	Hormone	Physiological effects
Pituitary	Antidiuretic hormone	Regulates the retention of water in kidneys and blood pressure
	Corticotropin (ACTH)	Regulates the production and secretion of hormones from the adrenal glands
	Growth hormone (GH)	Regulates growth and development, as well as promotes protein production

	Luteinizing hormone (LH)	Regulates the physiological function of the reproductive gland in males and females
	Oxytocin	Aids in childbirth and lactation processes
	Prolactin	Facilitates the production of milk in mammary glands
	Thyroid stimulating hormone (TSH)	Regulates the production and secretion of hormones from the thyroid glands
Parathyroid	Parathyroid hormone	Regulates the functioning and excretion of calcium and phosphorous ions
Thyroid	Thyroid hormone	Regulates metabolic processes
		Regulates the salt and water content of the kidneys
Adrenal	Aldosterone	Maintains the blood sugar level, blood pressure and muscle strength
	Cortisol	Induces anti-inflammatory functions
		Regulates salt and water content
	Dehydroepiandrosterone (DHEA)	Influences skeletal health, mood and immune system
	Epinephrine and Norepinephrine	Stimulates the functioning of blood vessels, heart, lungs and nervous system
Pancreas	Glucagon	Increases blood-sugar level
		Decreases blood-sugar level
	Insulin	Regulates the metabolism of sugar, proteins and lipids
Gonads	Ovaries: Estrogen	Regulates the development of female sex characteristics and the reproductive system
	Progesterone	Prepares the body for impregnation

Testes: Testosterone	Regulates the development of male sex characteristics and the reproductive system
----------------------	-----------------------------------------------------------------------------------

In mammals, these hormones are secreted by the endocrine system, which is composed of the pineal, pituitary, parathyroid (thymus), thyroid, adrenal, pancreas and the gonads (ovaries in females and testes in males), to mention a few of the major glands responsible for the secretion of hormones. Hormones can be classified into three major categories *viz.*, steroid hormones (composed of the adrenal cortical and sex hormones), peptide hormones (which include insulin and glucagon) and amino acid derivatives (such as thyroidal hormones).^{7,8} The hormones secreted by these glands are directly translocated into the blood stream, where the hormone receptor is responsible to either express or repress the modulation of particular physiological effect. Hormone receptors are classed into two groups, described as steroidal and nuclear receptors, which are designated by their agonistic and/or antagonistic mediation of gene expression. Steroid receptors regulate gene transcription with the aid of a binding site (agonistically) for a specific steroid hormone, whereas nuclear receptors are ligand activated (antagonistically) when expressing their gene transcriptions.

The importance of these hormones is reflected by their synergistic and independent ability to effect important physiological functions within the body, shown in Table 1.1. It can thus be expected, that a cascade of adverse physiological events would occur if one system (gland) malfunctions. However, it is important to note, that the optimal functioning of hormones is not only dependent on the endocrine system, but can significantly be influenced by lifestyle decisions.^{9,10} The exponential growth in the world's population has generated the need for food to be grown at faster rates, resulting in the incorporation of synthetic chemicals such as hormones in milk, antibiotics in meat and pesticides in agricultural produce.¹¹ Research contributions by Key *et al.*,¹² suggests that exposure to high concentrations, as well as long term exposure to low concentrations, of these synthetic chemicals may result in a number of adverse physiological side effects within the body.¹² In addition to chemical stimuli, the evolution of technology, coupled with busier lifestyles and the exposure to numerous radiation sources, has further influenced healthy living (which include exercise and enough rest), usually required to assist in the regeneration of new or damaged cells.¹⁰ Regular exercise is essential not only for maintaining a healthy body, but also for reducing the production of cholesterol. Interestingly, estrogen is a side product generated from

processes, in which cholesterol is produced. Work reported by Tsuchiya and co-workers, have suggested that estrogen concentrations were found to be lower in women that exercise.¹³

1.2 Established link between hormones and the development of carcinomas

The development of carcinoma cells can be attributed to a number of diverse and complex processes within the body, with the major argument being related to the unregulated cell growth that occurs at an alarming rate (normally controlled by certain members of the endocrine system). Since certain hormones are responsible for the regulation of growth and cell differentiation (described in Table 1.1), a link has been confirmed between hormones and the development of certain cancers.¹⁴ The term tumour (associated with carcinomas), often refers to growths caused by cancerous cells. However, not all tumours are necessarily malignant since numerous benign tumours are known to exist. It should be noted that unlike malignant tumours, the latter do not invade the surrounding cellular environments.

1.3 Estrogen's distinct contribution toward breast carcinoma development

For the purpose of this dissertation, the main focus is on the hormone estrogen and its receptors, and their implication in the development of certain breast cancers experienced in women.

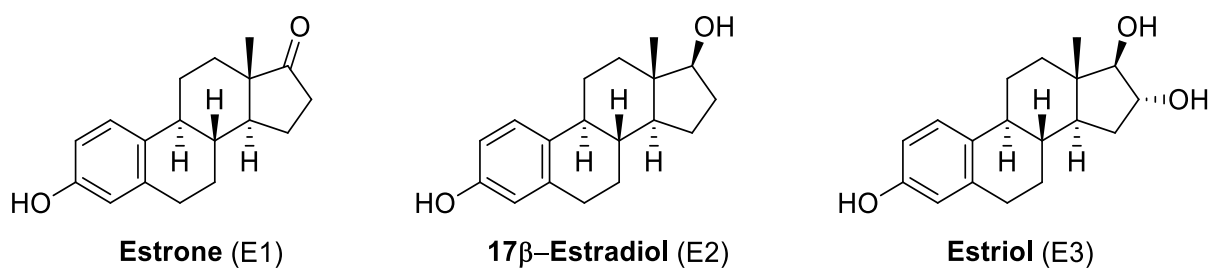


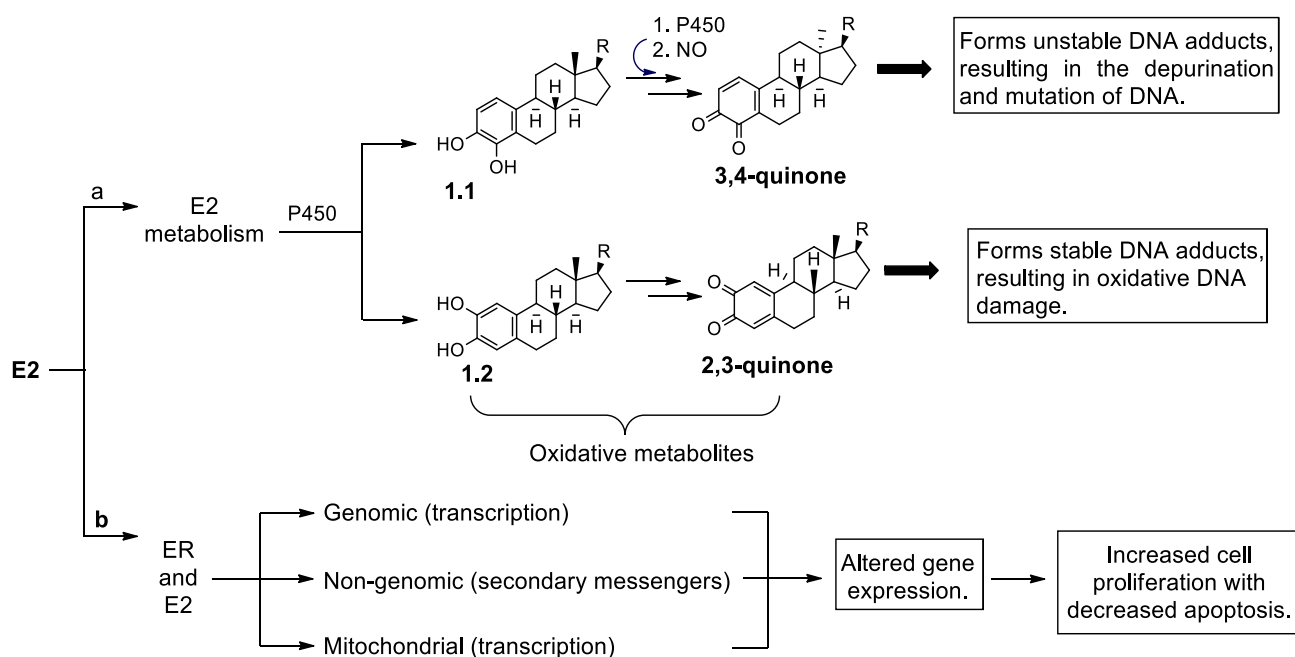
Figure 1.1. Three essential estrogenic hormones secreted by the female body.

The estrogens (Figure 1.1), namely estrone (E1), 17β-estradiol (E2) and estriol (E3) are the natural (or endogenous) ligands for the estrogen receptor subtypes (ERα and ERβ).¹⁵ E2 is the most important estrogen, which is responsible for modulating the expression and/or repression of specific gene transcriptions.^{6,7} An insightful review by Gustafsson and co-workers,¹⁶ has revealed the intricate distribution and functioning of both ERα and ERβ subtypes within the body. Both ER-subtypes contain overlapping distributions, with ERα being responsible for reproductive functions and is dominantly expressed in the uterus and

mammary glands. ER β on the other hand, is more generally expressed within skeletal tissue, the central nervous and cardiovascular system, as well as the uterus and liver.^{6,7} Both ER-subtypes display similar binding affinities toward the hormone E2 (for which further elaboration will be reported in Chapter 2), which can be explained by the modes of binding adopted by estrogen and its receptors. Unlike other hormones, reports by Gustafsson,¹⁶ Korach¹⁷ and co-workers suggest that estrogens do not follow the classical protein-protein binding mode, when mediating their transcriptional effects. This feature confirms that the ER's mechanisms, which influence gene transcriptions, are more complex than initially thought. Since E2 and its receptors are important mediators involved in the proliferation and differentiation within reproductive tissues, it appears to hold one of the keys in understanding the development of breast cancer.^{14,18-20}

1.3.1 Estradiol metabolism pathways and the unfavourable resulting DNA adducts

It has been postulated that a number of mechanistic routes are responsible for the development of carcinogenesis in breast tissue. A number of reports indicated that the ER α was associated with playing a key role in the development and progression of breast cancer.^{11,14} It is considered that the complex hormonal binding mode mechanisms are responsible for the development of this malignancy.²¹ Due to key contributions by the E2 ligand in modulating ER-subtypes to exert specific transcriptional effects in multiple tissues, it can be postulated that this ligand may stimulate desirable effects in some tissues and undesirable effects in others. It is important to note that E2 and ER do not function independently but involve many cellular processes which could have a domino effect. If one receptor is repressed or expressed more dominantly than the other, adverse effects might well be expected. Scheme 1.1 is an illustration of the two pathways, in which the metabolism of E2 can initiate the development and progression of estrogen positive breast cancer.¹⁸ The metabolism of estrogen, results in the formation of genotoxic mutagenic metabolites *via.*, the protein cytochrome P450 (in Scheme 1.1).^{13,19} The second receptor ER β , has likewise been detected in breast cancers, which may additionally contribute to hormonal sensitivity and resistance experienced by many patients undergoing hormonal therapeutic treatment.²²



Glucuronidation *viz.*, UDP-glucuronosyltransferase
 Sulfation *viz.*, sulfotransferase
 O-Methylation *viz.*, catechol O-methyltransferase (COMT)

Scheme 1.1. Two pathways in which estrogen could initiate carcinogenesis. **a)** Metabolism: 16- α -hydroxyestrone **1.1** and 2-hydroxyestrone, 2-hydroxyestradiol, 4-hydroxyestrone, 4-hydroxyestradiol **1.2**. **b)** Altered gene expression.¹⁸ (Source: Modified from Yagar, J. D.; Davidson, N. E. *N. Engl. J. Med.* **2006**, 354, 270)

Unlike other hormones (in Table 1.1), the ERs are able to mediate gene transcription in the absence of their natural ligand (E2), leading to an important question as to whether it could be considered as a versatile mechanism for gene transcription.^{6,7} This dynamic feature has allowed scientists to take advantage of this unique property to further develop synthetic ligands with improved and selective estrogenic activity. Both ER-subtypes differ on the basis of their gene transcription responses due to their agonistic and antagonistic binding, which can be explained by the inherent differences presented on the binding domains of the individual receptor.²³⁻²⁵

The metabolism of E2 includes its oxidation by the cytochrome (CYP) P450 protein, which is a heme-containing superfamily of monooxygenases, and is responsible for the oxidative metabolism of many biological agents.^{13,18} It is composed of three families namely CYP1, CYP2 and CYP3, which catalyse the oxidative metabolism of both exo- and endogenous ligands of ER.¹³ The enzymes CYP1A1, CYP1A2 and CYP3A4 modulate catalytic activity toward generating the 2-hydroxylation species, rather than the 4-hydroxylation species of E2. In contrast, the CYP1B1 and CYP3A5 enzymes, exhibited specific catalytic activity

toward generating the 4-hydroxylation of the estrogen metabolite.¹³ CYP1A1 is not expressed in the liver, therefore the 2-hydroxylation metabolite in the liver is mainly catalyzed by the enzymes CYP1A2 and CYP3A,¹³ which are usually associated breast, uterine, placenta, brain and pituitary tissues.¹³

The E2 metabolites, contribute to the initiation of carcinogenesis by the resulting harmful adducts (**1.1** and **1.2**) formed during metabolism, as illustrated in Scheme 1.1. Additional metabolic reactions generate radicals from the oxidized estradiol and estrone metabolites, which are both catalyzed by the P450 enzyme. These radicals and their unique corresponding quinones (for example the 3,4-quinones) can form unstable adducts with the adenine and guanine residues within the DNA sequence, thus mutating and depurating the nucleic base and thereby damaging the DNA sequence. The presence of these unstable adducts and damaged DNA sequences in human breast cancer tissue, further support the claim that estrogen metabolites are essential in understanding the development of breast cancer.^{13,18,19}

1.4 The diverse source and characteristics of mammary gland carcinomas

Breast cancer is a term broadly used for the description of a number of mammary gland tumours. The most common breast cancer originates from cells that line the ducts and lobules in mammary glands, while others originate within other tissues and metastasize. Despite this, benign breast tumours do exist and are known as fibro adenomas. Unlike many other malignancies, breast cancers are developed sporadically but can also be inherited from shared familial genetic traits.²⁶

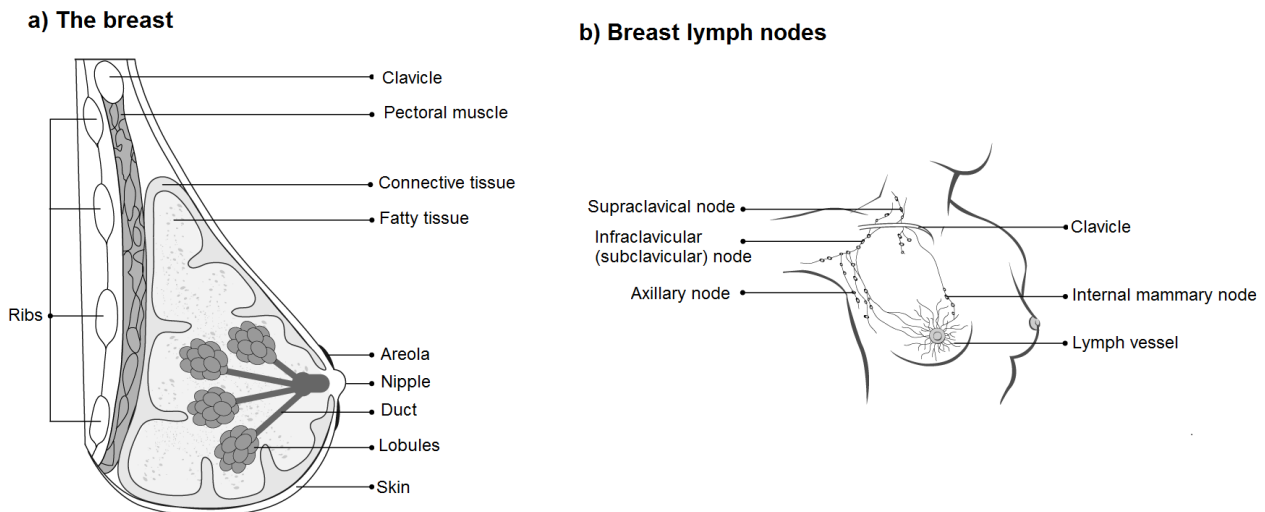


Figure 1.2. Anatomical description of mammary glands and their associated lymph nodes.²⁶
(Source: www.cancer.ca/en/cancer-information/cancer-type/breast/breast-cancer/the-breast/?region=on)

The lymphatic system is of paramount importance, as it is involved with the immune responses within the body. The lymphatic system is composed of lymph nodes (a collection of immune system cells), which are connected to lymphatic vessels that further consist of small veins responsible for carrying lymph fluid away from the breast (as shown in Figure 1.2). Lymph fluid is a composition of waste products and immune system cells. Unfortunately, breast cancer cells can enter lymphatic vessels and grow within these lymph nodes. As illustrated in Figure 1.2, lymph nodes within the breast are connected to axillary nodes (found under the arm), internal mammary nodes (found in the chest), *supra-* and *infra-*clavicular nodes (found above and below the clavicle). Once cancer cells metastasize to lymph nodes, it can further permeate other cells and tissues within the body. The most common breast cancers are developed in epithelial cells (cells lining organs and tissues) and are known as adenocarcinomas. Cancers which develop within the cells of muscles, lipids or connective tissues are known as sarcomas.

Ductal carcinoma *in situ* (DCIS), also known as intra ductal carcinoma, is considered to be a non-invasive or pre-invasive breast cancer. Non-invasive cancers are not able to metastasize but do contain the ability to become invasive (hence its pre-invasive breast cancer category). Invasive ductal carcinoma (IDC) originates within the milk ducts, which easily move through the cell wall and grows into the adipose tissue of the breast. Once the growth is present within the adipose tissue, it is able to metastasize, thereby infiltrating other tissues and organs.²⁷ Like IDC, invasive lobular carcinoma (ILC) develops within the lobules and has the ability to metastasize infecting healthy tissues and organs.²⁸ More rare forms of

breast cancer include the inflammatory breast cancer (IBC), which affects 1 – 3% of women, where lymph vessels blocked by cancerous cells result in swelling of the affected breast. The growth initiated within the ducts, is spread outward to the areola, with mastectomy often employed as a treatment. Phyllode tumors are rare and benign, and even more rarely have the ability to become malignant. This type of tumor often develops within the stroma caused by complications experienced during radiation therapy, which leads to the development of cancer within the cells that line blood vessels and/or lymph vessels, and is known as angiosarcoma.²⁶

1.5 The evolutionary development in therapeutic strategies toward alleviating carcinomas

It has been reported by Sudhakar and co-workers, that this ancient and non-communicable disease (cancer) has been recorded throughout time, with the first symptoms of this dreaded disease being reported by the Egyptians in 3000 B.C.²⁹ The first diagnosis was recorded in the 1700s, with chimney sweepers being the unfortunate victims during this time.²⁹ With the passing of time, the collective research by many scientists, with the development of technology, has clarified the understanding of this disease.²⁹ In earlier days, the lack of proper instrumentation and knowledge prevented any comprehensive study of the disease. This resulted in many theories being established, primarily believing that cancer resulted from an imbalance of fluids in the body, which later gave rise to the humoral theory. A second theory included the belief that lymph nodes played a role in the development of cancer, thus a lymph theory arose. These theories later fell in abeyance with new ones taking their place *viz.*, blastema, chronic irritation, trauma and finally the parasite theory (where it was believed that cancer was contagious).²⁹ As time progressed, the evolution of scientific discoveries made the studying and treatment of cancer possible. Today science might not have all the answers, but the developed theories have been able to explain a good deal about cancer, as our current inputs will hopefully impact future decades.

1.5.1 Surgical techniques used for the removal of carcinomas

Since 50 A.D., the Greeks and Romans utilized cautery and surgical techniques for the elimination of small tumours. With the passing of time (after 1590 A.D.), autopsies presented scientists with the unique opportunity to further study and gain an improved understanding of internal tumours. Shortly thereafter, with the discovery of the microscope during 1600 A.D., scientists were afforded the opportunity to study cancer at the cellular level. The 1840

– 1900's era led to the discovery of anaesthesia, which granted surgeons novel therapeutic opportunities to surgically remove small tumours, as implemented by Bilroth, Handley and Halsted. With increased knowledge, it was later discovered that primary tumours had the ability to spread *via* the bloodstream, by a process now known as metastasis, originally identified by Paget.²⁹ This was key in understanding the limitations surgery offered as a treatment, but this area of medicine soon evolved with the use of more sophisticated applications for treating tumours.

1.5.2 Eradication of carcinomas with radiation

The late 1800's (1895) brought with it the discovery and development of x-rays, which played a vital role in the diagnosis and treatment of cancer, as founded by Roentgen.²⁹ However, it was later realized that this form of radiation not only alleviated cancer, but in certain instances it had also unfortunately promoted its growth. This was an important realization, which led to the understanding that only very specific forms of radiation can be implemented in such a treatment regime. Today, radiation therapy has progressed to the use of a conformal proton beam, where X-rays are exchanged for a beam of protons. The inclusion of stereotactic surgery includes the use of a gamma knife and is commonly utilized on brain tumours, with its outstanding merit being that no harm is caused to healthy cells. Lastly, intra-operative radiation therapy, which includes the surgical removal of tumours in conjunction with radiation to adjacent cells, has also been utilized.²⁹

1.5.3 A chemical approach toward treating carcinomas

Later, chemotherapy was identified as a therapeutic treatment in targeting a broad range of cancerous cell lines. However, the major problems associated with chemotherapeutic agents include the lack of selectivity, metastasis of the initial tumour, heterogeneity of the disease and multidrug resistance.³⁰ During the initial stages of chemotherapy, cytotoxic nitrogen mustard agents (see for example the structures of representative steroidal nitrogen mustard agents depicted in Figure 1.3) were developed to avoid these unfavourable effects.³⁰

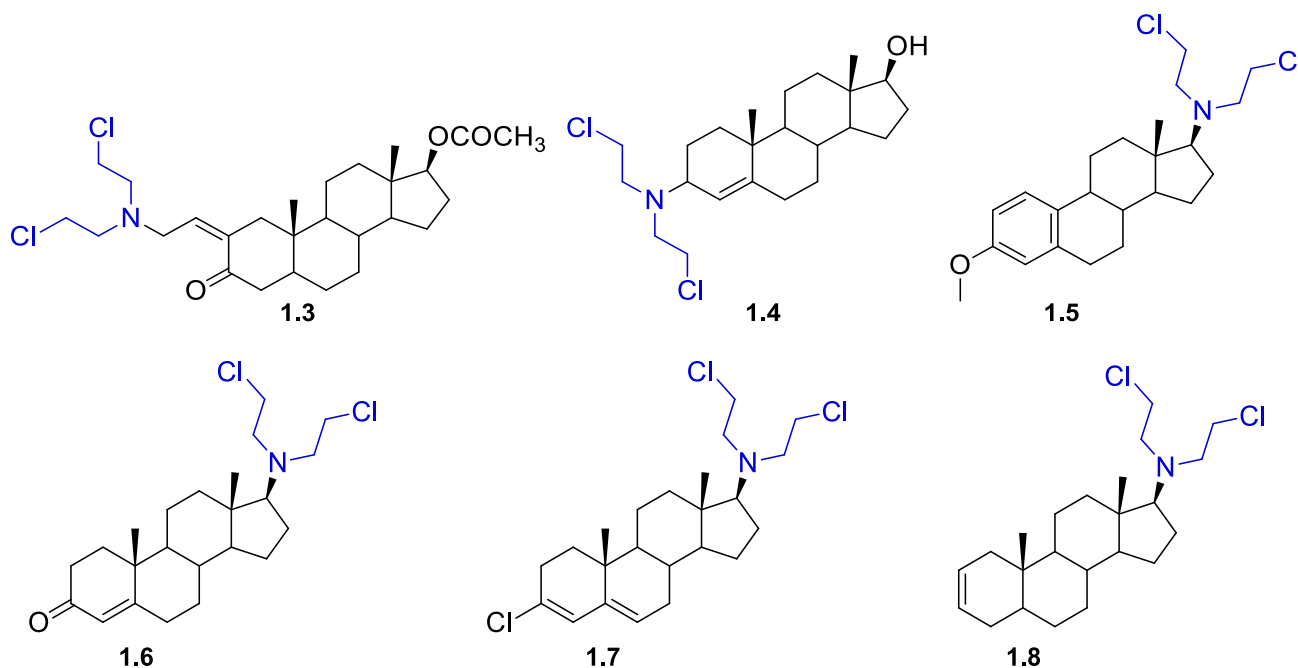
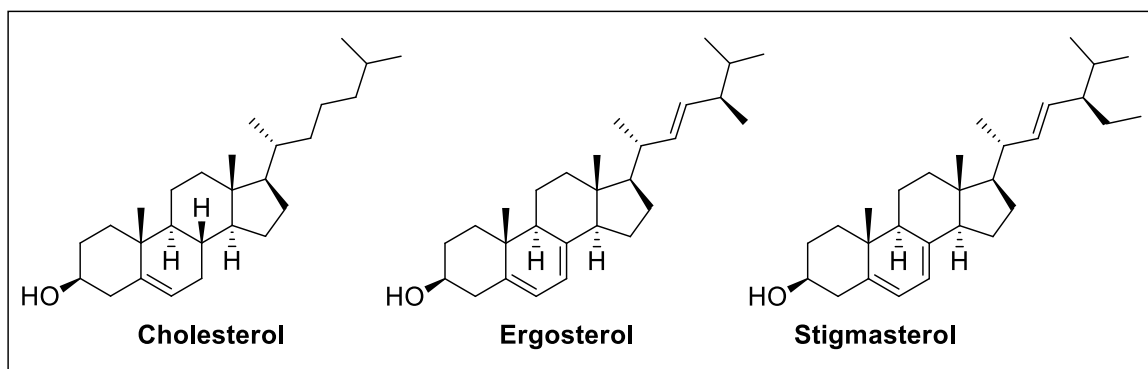


Figure 1.3. *N*-Substituted steroidal-based mustard agents tested. *N*-mustard agents refer to the *N*-haloalkyl substituents which have substituted the hydroxyl group at C17 (**1.5 – 1.8**) on various cholesterol-based compounds.³⁰ (Source: Reported in Bansal, R.; Acharya, P. C. *Chem. Rev.* **2014**, *114*, 6986)

The structural characteristics for these mustard agents (**1.3 – 1.8**) were adopted from the structural skeleton of molecules such as cholesterol, ergosterol and stigmasterol in Figure 1.3. These compounds generated by Bansal and co-workers were extensively utilized as chemotherapeutics, based on animal studies.³⁰ The steroidal-type moiety was included for the enhancement of binding with the DNA adducts within the tumour's tissue. Thus, leading to DNA damaging effects with reduced toxicity. These compounds showed a delay in cell division and the induction of apoptosis suggesting that the mustard agents (**1.5 – 1.8**) presented a certain binding mode. Upon testing, compound **1.3** showed less toxicity upon comparison to compounds **1.4 – 1.8** but the antitumor activity was found to be reduced.³⁰ Compounds **1.4** and **1.5** showed a 100% increase in the lifespan of mice with Gardner ascites tumours.³⁰ An interesting report by Jones *et al.*, in the review by Bansal and

co-workers, showed that the treatment of 7,12-dimethylbenz[a]anthracene (DMBA)-induced mammary gland tumours when treated with compounds **1.6** and **1.7** proved ineffective toward proliferation, with compound **1.8** showing a moderate regression.³⁰ This was later replaced by the use of a combination of drugs and therapeutics, monoclonal antibody therapy, hematopoietic stem cell transplantation and with agents to overcome multidrug resistance, and adjuvant therapy (co-administration of chemotherapy implemented after surgical treatment).^{29,30}

1.5.4 The manipulation of hormones for promoting cellular health

The late 1800s (1878) brought forth new knowledge about a ground-breaking link between the ovaries (where certain hormones are produced) and mammary glands, was established by Thomas Beatson.²⁹ This concept proved to be validated later when hormones were connected to the growth of cancer cells.^{11,21} Since then, hormone replacement therapy (HRT) has proven to be effective in the treatment of breast cancer, but like alternate cancer treatments, it is not without risk. HRT was primarily employed for the enhancement of hormone levels in women (especially undergoing menopause), by treatment with estrogen on its own or co-administered with progesterone. The use of estrogen improved skeletal and cardiovascular related ailments, but it was soon realized that its implementation was responsible for an increased incidence of both breast and uterine cancers.¹ The adverse effects associated with HRT, resulted in the use of estrogen receptors being targeted for pharmacological interest. Since the connection between breast cancer and estrogen has emerged, attempts have been made to antagonize estrogen's biological effects as a therapeutic strategy for women with breast cancer. This led to a more modern approach, where synthetic estrogenic ligands have been developed to behave agonistically in some tissues and antagonistically in others. These compounds are known as selective estrogen receptor modulators (SERMs) and display tissue selective behaviour by mimicking estrogen quite effectively.^{31,32} The development of these compounds were aimed toward reducing adverse effects (such as the increased incidence of certain cancers), associated with HRT.¹ Further elaboration on SERMs will be reported in Chapter 2.

1.5.5 Immunotherapy treatment targeting gene specific tumours

Immunotherapy treatment includes the use of biological agents (for example antibodies), intended to mimic signals within the body for controlling tumour growth. In the 1900s scientists developed two therapeutic monoclonal antibodies *viz.*, rituximab and trastuzumab, targeting specific cancer cell lines.²⁹ Rituximab was approved by the Food and Drug

Administration (FDA) in 1998 in the treatment of lymphoma and in 1999 trastuzumab was soon approved for the treatment of breast cancer cell lines.³³ Rituximab is an antibody responsible for targeting the CD20-cells present in healthy B lymphocytes, as well as induce apoptosis directly. Whereas the antibody trastuzumab's action is mediated by binding to the human epidermal growth factor receptor (HER2) by blocking the transduction signal.³⁴ Apart from this, reports by Dillman revealed a large number of side effects associated with these agents due to antigen-antibody interactions within certain cells.³³ These effects included ailments such as, nausea, fever and abdominal pain, which are but a few associated with both rituximab and trastuzumab.³³ The application of these agents as therapeutics for malignant cancers were soon abandoned and the search for improved therapeutic agents continued.

1.6 Carcinomas: An overall understanding, therapeutic challenges and the way forward

With the enhancements in therapeutic strategies over time and gained understanding it has been noticed, that the normal existence of estrogen within women who have breast cancer and are undergoing hormonal therapy, can cause them to experience a number of adverse hormonal side effects such as osteoporosis, cardiovascular disease and obesity, as well as problems associated with the central nervous and immune system.¹⁵ As described by Marino and co-workers these adverse effects, associated with current hormonal treatment and antiestrogenic drugs, have had a diminished efficiency and thus as a consequence, the search for novel drugs, which can selectively bind to a specific ER continues.¹⁵ Despite the excellent progress made by science in this area, there are still quite a number of drawbacks which include; the lack of selectivity, metastatic spreading and the heterogeneity of the disease as well as resistance.³⁰ In spite of this, a number of preventative measures have been put in place, where treatment such as surgical applications, radiation, chemotherapy and HRT (used singularly or in combination with additional forms of treatment), have increased the life span of sufferers, with the inclusion of a better quality of life.³⁵ However, despite the valuable information provided, the development of cancers are still not completely understood.

1.7 Feasibility for this research study

Research efforts and evidence reported by Jemal and co-workers, do indicate that cancer is not just a global health epidemic, but increasing in Africa with 715 000 new cancer cases

and 542 000 cancer deaths recorded during 2008, which is further expected to double within the following 20 years.^{10,36}

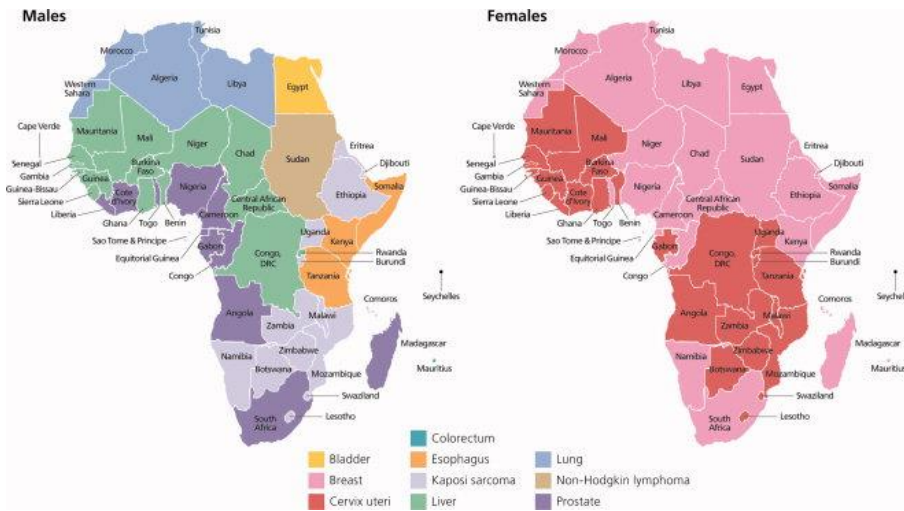


Figure 1.4. A demonstration of the gender related cancers prevalent during 2008.¹⁰ (Source: Figure taken from Jemal, A. *et al.*, *Cancer* **2012**, 118, 4372)

The cancers frequented by women in Africa are generally associated with reproductive organs demonstrated in Figure 1.4 and by the statistics reported in the graph Figure 1.5. The graph in Figure 1.5, provides the cancer statistics associated with 2008. However, the predicted increase of these values for 2028 presents an irksome view and future challenges posed to the scientific community. Despite many newly reported cases and the predicted increase, as a preventative measure early detection has been put in place.

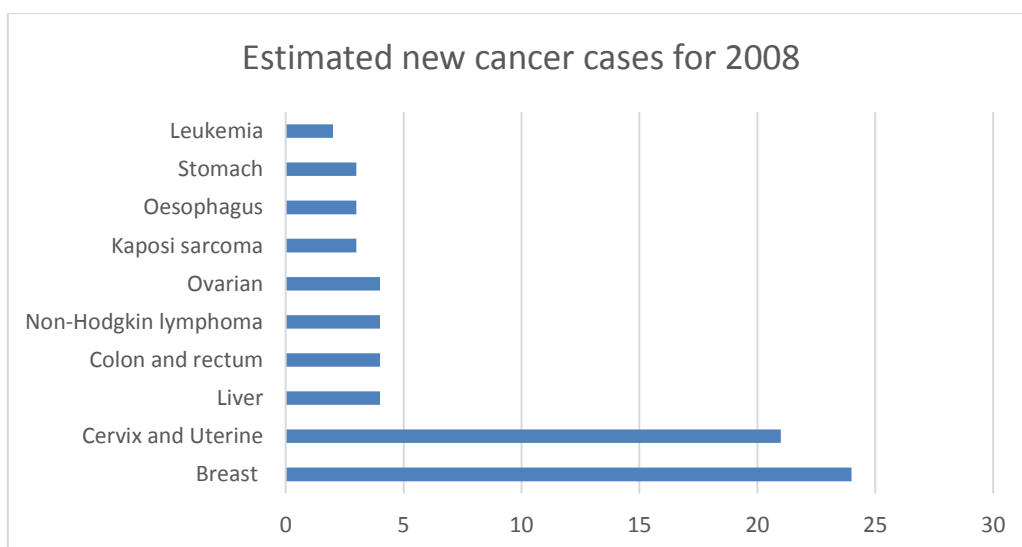


Figure 1.5. Common cancers experienced by African women.¹⁰ (Source: Taken from Jemal, A. *et al.*, *Cancer* **2012**, 118, 4372)

Apart from what is reported in the graph, reports by Jemal and co-workers imply that breast cancer is the most prevalent cancer experienced by women in Southern Africa.¹⁰ The advancements in technology and therapeutic strategies have led to a better quality of life, as well as a prolonged lifespan for women burdened with breast cancer. There is thus an urgent need to focus on some economically effective treatments, as well as screening techniques to improve on current preventative strategies for breast cancer in Africa. These findings highlight the importance of further exploration into this research topic.^{11,37}

Chapter 2

Literature review

Part 1: Estrogen modulation

In part one of this chapter, a detailed focus will address both estrogen receptors, their distribution and overlapping functions of the receptors in the body. Furthermore, the individual characteristics of both ERs will be explored. These characteristics would provide some understanding toward their binding domains by providing an explanation for the affinity at which endo- and exogenous ligands bind with ER. Lastly, and most importantly, the transcriptase machinery and the varied modes of binding, will be discussed to provide some explanation for the complexities associated with ERs including its ability to effectively express gene transcription, even in the absence of its endogenous ligand.

2.1 The distribution and physiological importance presented by the ER isoforms

E2 is the principle ligand responsible for the elucidation of a number of physiological responses in tissues and biological systems of the body *viz.*, the ERs.^{38,39} These ERs exist as two main subtypes, namely the alpha and beta (ER α and ER β) species, and are from the class of biochemical entities known as nuclear receptors.⁴⁰

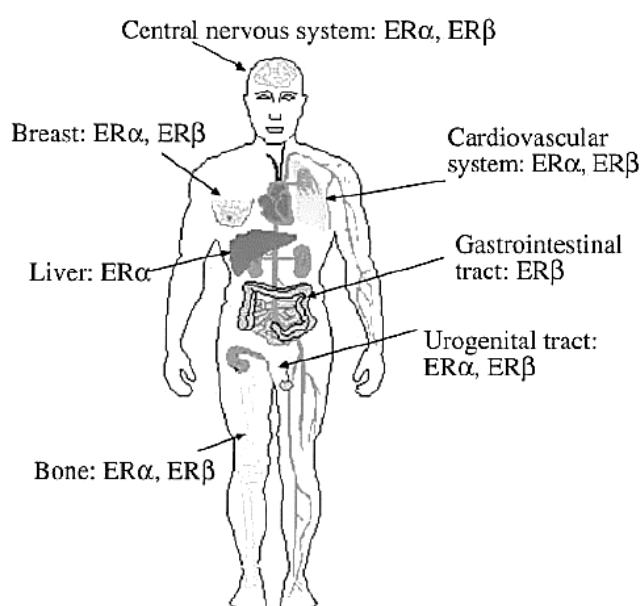


Figure 2.1. The ER α and ER β distribution within target tissues.¹⁶ (Source: Figure taken from Gustafsson, J. Å. *J. Endocrinol.* **1999**, 163, 379)

These two ER-subtypes are expressed throughout the body, with ER α being more dominantly expressed than ER β , and for which E2 is the endogenous ligand.³⁹ Both ER-subtypes possess overlapping distributions as illustrated in Figure 2.1, but instigate distinct functions within their designated tissues.¹⁶ Apart from the diverse expression of these receptors, reports by Ascenzi¹⁵ and Gustafsson^{16,41-44} and co-authors, have further substantiated the importance of their role in maintaining the healthy functioning of the body. As previously mentioned, ER α is mainly implicated in reproductive processes and is thus generally expressed in mammary glands and the uterus.¹⁵ The more generally distributed ER β , is expressed within the central nervous system (CNS), skeletal tissues, the cardiovascular system, the gastrointestinal tract, liver and the urogenital tract, in Figure 2.1.⁴⁵ The necessary requirement of E2 within these tissues was realised after a comprehensive screening process, in which the treatment of a number of breast cancer patients with antiestrogens interestingly, revealed many patients experiencing many adverse effects.⁴⁶ Reports by Howell,³² Rahman,⁴⁷ Martinkovich⁴⁸ and co-workers, suggest that the alleviation of these effects could be improved by compounds, which would include both an agonistic, as well as an antagonistic, mode of binding for modulating gene transcription. These many observations thus leading up to the development of SERMs, to further improve on therapeutic agents with limited side effects.³²

In the CNS, the hypothalamus is responsible for regulating target functions of the endocrinal system. Here, E2 contributes to the maintenance of mental health by regulating hormones such as serotonin and dopamine (usually associated with alleviating stress and depression), as well as choline (involved in memory and delaying the development of Alzheimer's), aiding in the healthy functioning of the CNS.^{15,42} The optimal functioning of the cardiovascular system can also be attributed to contributions from the E2 ligand, where regulating low density lipoprotein (LDL) and high density lipoprotein (HDL), as well as reduce the development of venous thrombosis, which could eventually lead to additional secondary ailments for example, a stroke and coronary heart disease. However, more commonly associated with the reproductive tissue, E2 has also proved essential in facilitating the proliferation and differentiation in premalignant cells (during adolescence), as well as malignant breast epithelial cells.^{16,42,49,50}

In addition, the metabolism and homeostasis of skeletal tissue also relies on both ER-subtypes.⁴³ E2 is but one of the molecules responsible for the development and growth

of bone during early developmental stages and adolescence. In addition to regulation of bone mass density in pre- and postmenopausal women, E2 is also a key element hindering the progression of ailments such as osteoporosis and osteopenia.^{15,43} Apart from regulating bone mass density, a number of essential metabolic processes in the liver, where enzymes in addition to ERs are responsible for regulatory functions, which include processes such as aiding in blood clotting and the removal of damaged blood cells by preventing their circulation through the body.^{16,42,49,50} Despite E2's physiological importance, the over- or under-expression of E2 may result in a cascade of adverse events *viz.*, mental illness and venous thrombosis (already mentioned), which are often experienced by women affected with breast cancer and are undergoing a combination of treatments with hormone therapy being one of the components.¹⁶ The normal existence of E2 can worsen the associated symptoms, but a deficiency would further increase the risk of hormone-related ailments in breast cancer patients.⁵¹

2.2 The structural architecture of estradiol and its binding sites

The active site in which the E2 ligand binds, consists of two hydrophobic pockets reported by Anstead,⁵² Marino¹⁵ and co-workers and Maalouf *et al.*²³ This entails the A- and D-rings of the E2 molecule, which interact with a water molecule and/or amino acid residues respectively, within the binding site. In addition to this, the E2 ligand consists of a phenolic ring, ring-A, two six membered aliphatic fused ring systems referred to as the B- and C-rings, and a D-ring comprised of a five membered aliphatic ring containing a hydroxyl functional group.^{24,52} Contributions by Anstead and co-workers, have reported that the A-ring of E2 is non-polar and not very tolerant of polar substituents.⁵² However, despite its hydrophobic nature, it can interact with water molecules *via* hydrogen bonding with the hydroxyl groups present on both the A- and D-rings of E2. These hydroxyl functional groups provide the primary hydrogen donor sources, required for anchoring the ligand to residues as illustrated in Figure 2.2 (amino acid residues are listed in Figure 2.3). Once the ligand is anchored to the glutamic acid residue (Glu353/305), it is able to undergo conformational changes within the binding site and further undergo proton bond donor/acceptor interactions with other key residues within the proximity, for example the arginine (Arg394/346) and histidine (His524/475) in Figure 2.2.^{24,53}

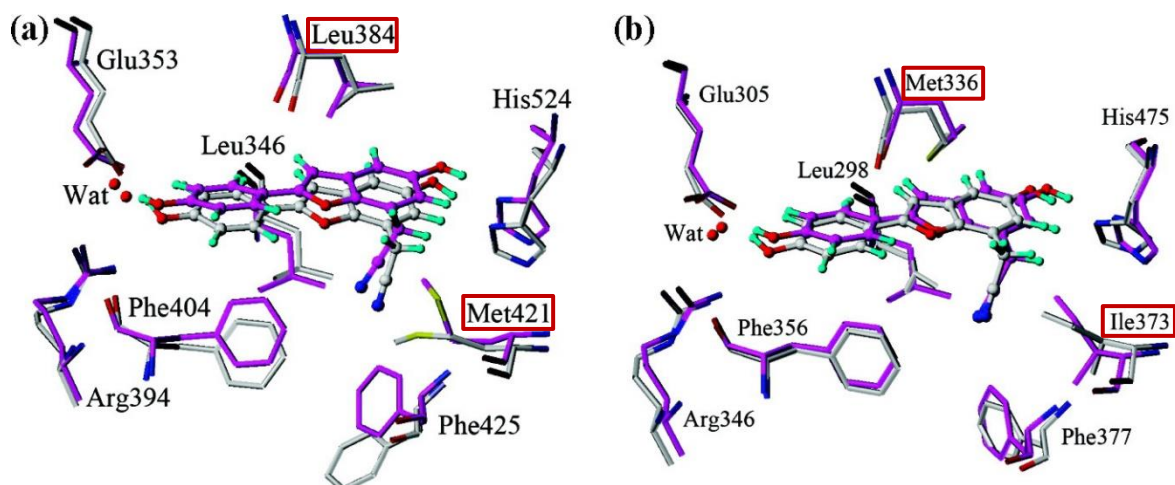


Figure 2.2. Binding mode of **a)** ER α and **b)** ER β in the ligand binding domain.⁵⁴ (Source: Figures taken from Zeng, J. Li, W.; Zhao, Y.; Liu, G.; Tang, Y.; Jiang, H. *J. Phys. Chem. B* **2008**, 112, 2719)

Regardless of the number of residues as illustrated in Figure 2.2, it is important to note that a significant number of residues are present within the receptor's active site. However, the aim of Figure 2.2 is to illustrate a few important target residues, which play a role in providing certain residue interactions. From Figure 2.2, one may appreciate that both ER-subtypes possess a certain degree of similarity within their binding site, with a variation of two important residues highlighted in Figure 2.2. The ER α (shown in frame a, of Figure 2.2) contains the residues Leu384/Met421, and ER β (shown in frame b, of Figure 2.2) contains the residues Met336/Ile373.⁵⁴ In Figure 2.3 below, a structural depiction of a few important residues within the ER active site are shown as they relate to Figure 2.2.

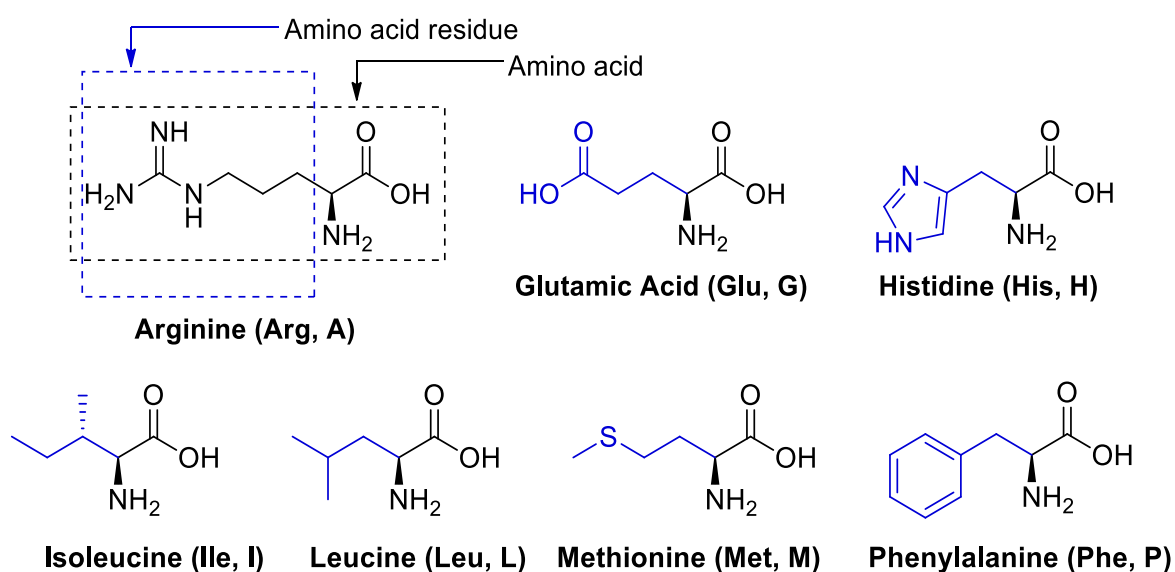
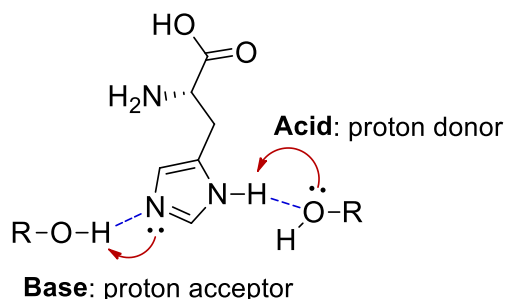


Figure 2.3. There are three and one letter codes used in the identification of amino acid residues, these describe the residues within the ER binding cavity.⁵⁵ (Source: Taken and edited from Patrick, G. L. *An introduction to medicinal chemistry*, 5th ed.; Oxford University Press, **2013**)

Apart from the A-ring, the E2 ligand contains two fused cyclohexyl B- and C-rings, which contribute a certain degree of conformational freedom to the molecule, thus allowing E2 to adopt a range of structural orientations enhancing complexation of the ligand with the ER. The limited conformational freedom within this region is essential for initiating binding with a specific ER subtype. The newly formed E2-ER bound complex is forced to undergo allosteric conformational changes dictating how the E2-ER complex fits into a particular binding cavity which affects the recruitment of transcriptional proteins (cofactors) by either enhancing or repressing a particular transcriptional effect.^{44,54}

The D-ring's terminal C17 hydroxyl motif serves as a proton donor/acceptor depending on the positioning of the ligand to His524/475 and is situated in the second hydrophobic binding cavity of the receptor, where its polar character undergoes hydrogen bonding interactions with the His residues (His524/475 as illustrated in Scheme 2.1). Additionally, the D-ring also contributes a certain degree of flexibility, further allowing for the accommodation of conformational changes to enhance the proton donor/acceptor required interactions, which are also dependent on the orientation of the His-residue within the cavity.^{24,52}



The mesoionic character, as well as the orientation of the imidazole residue of the amino acid within the binding cavity, enables either a proton donor or acceptor activity by the ligand.

Scheme 2.1. Proposed mode of proton bond interactions induced by the His-residue.

An interesting structural feature of the His-residue derived from its mesoionic ability, in which six π -electrons (four attributed to the two double bonds and two from the lone pair on the nitrogen of the diazine ring system), are involved. This affords it the ability to form both bond interactions, as well as partake in π -stacking interactions, and the side chain additionally allowing ligand coordination with metalloproteins and catalytic sites of varied enzymes. Depending on the orientation of the His-residue, it thus behaves either as a proton source (for enzymes of interest) or a proton acceptor as illustrated in Scheme 2.1. Understanding the structural architecture of the E2 ligand and the ER residues is vital in understanding its function, as well as assisting in the structural design for the development

of novel compounds with the potential of mimicking important biological processes by promoting specific target residue interactions.

2.3 The ERs and their associated binding domains

As with most nuclear receptors, both ER α and ER β contain six structurally conserved domains (A – F), which are distinct regions serving functions common to the physiology of most nuclear receptors.^{23,44} In Figure 2.4, the diagram illustrates the binding domains for both ER-subtypes.

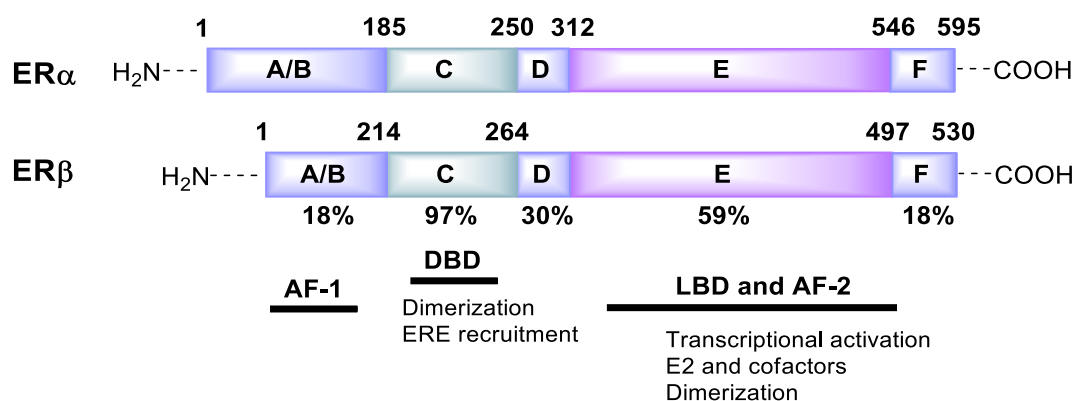


Figure 2.4. The six distinct binding domain regions which define nuclear receptors.^{16,53,56} (Source: Modified from Levin, E. R. *J. Appl. Physiol.* **2001**, *91*, 1860) A/B: Amino-terminal or transcriptional activation function (AF-1) responsible for the recruitment of coregulatory proteins. C: DNA binding domain where dimerization occurs. D: hinge region. E: Ligand binding domain, responsible for secondary dimerization and the recruitment of coregulatory proteins. F: Carboxyl-terminal or transcriptional function (AF-2).

The difference within these regions enable the binding of endo- or exogenous ligands and affect the affinity, to which specific ER subtype binding occurs. As illustrated in Figure 2.4, each ER is encoded on different chromosomes with ER α consisting of a 595 sequence of amino acid residues, while a significantly smaller number of residues (530) are observed for the ER β subtype.^{16,17,22} A certain degree of homology is displayed between these two receptors in the C-domain, which roughly shows a 97% similarity in Figure 2.4.²³ It is important to note that these similarities play a crucial role in the congruent binding affinities and efficacies displayed toward both ER α and ER β .¹⁶

2.3.1 The amino terminal domain

The A/B domain harbours the activation function (AF)-1. This region contributes to the transcriptional activity and is also known as the amino terminal. Reports by Heldring *et al.*,⁴² suggest that the amino/N-terminal domain is not conserved (as illustrated in Figure 2.4) and

is illustrated by the variation of residues within this domain and thus represents the most varied domain (18%).⁷ AF-1 is known to function by encoding ligand independent activation, achieved by the recruiting of protein-protein interactions with the transcriptional activation for targeted gene expression.^{15,43} The activation function of this domain can be attributed to the negative charges and hydrophobic residues provided within this region.¹⁵ Within the ER α , this domain binds antagonistically to E2 and is responsible for stimulating gene expression *viz.*, a variety of estrogen response elements (ERE), which vary depending on the cell line.^{7,15,43,57} However, the same conditions are inconsequential for the ER β subtype, which binds purely agonistically to E2 within this domain.⁴³

2.3.2 The DNA binding domain

The C-domain or DNA binding domain (DBD) contains approximately 70 residues, with 97% being almost identical for both receptor subtypes (in Figure 2.4).²³ The DBD is the most central and conserved binding domain, consisting of two zinc finger motifs, which are tetrahedrally coordinated, with two groups of the four sulfur atoms on the eight cysteine residues present (see Figure 2.5).^{15,44} Interestingly, the nucleophilic motif on the cysteine residue not only allows co-ordination of the zinc, but also enables its participation in a number of enzymatic and binding interactions.⁵⁸ Of importance is that in this domain, dimerization of the bound receptor and ligand does occur. Dimerization is essential as it is a prerequisite for the recruitment of specific ERE and is thus responsible for initiating the gene transcription processes (Figure 2.5). The DBD domain in both ER-subtypes are homologized, enhancing their ability to bind with similar affinities and specifications to various ERE.^{23,43}

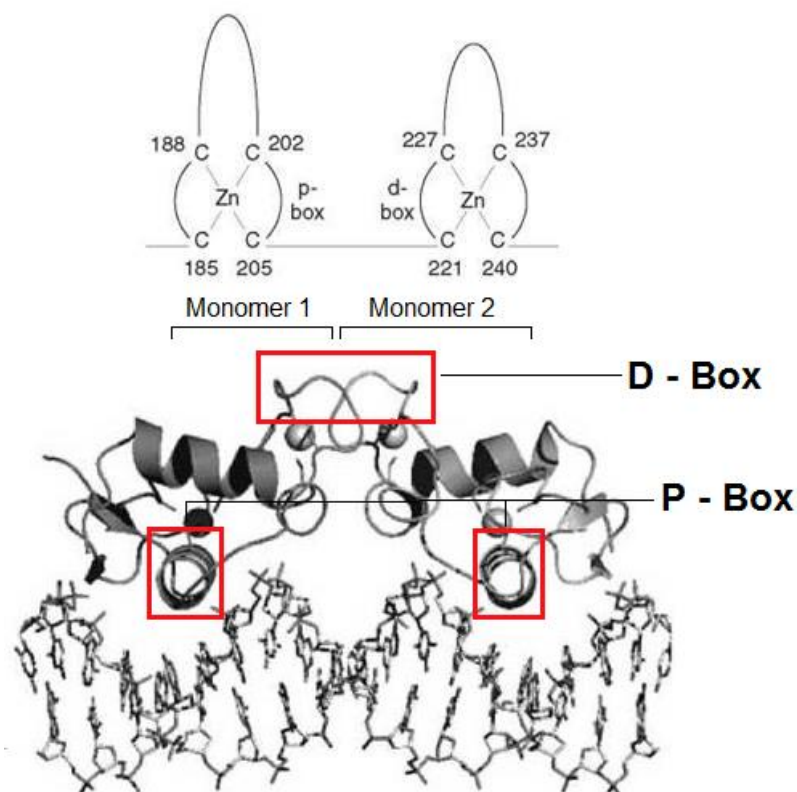


Figure 2.5. Demonstration of the DBD complexed with ERE.²⁵ (Source: The diagram was taken and modified from Ruff, M.; Gangloff, M.; Wurtz, J. M.; Moras, D. *Breast Cancer Res.* **2000**, 2, 353)

This domain can further be divided into two subdomains known as the proximal box (responsible for DNA recognition) and distal box (responsible for DNA dependent dimerization in the DBD), also known as the P-box and D-box respectively.^{15,44} The P-box for both ER-subtypes are identical, thus enabling both receptors to bind with similar affinities to EREs, where the role of the D-box provides the topography suited for accommodating the head to head dimerization undergone by the ligand and the ER bound complex.¹⁵

2.3.3 The D- and E/F-domain

The D-domain, also known as the hinge region, and is the most variable region within the receptor subtypes. The carboxyl/COOH-terminal is linked to the E/F-domain or ligand binding domain (LBD) by way of the hinge region.⁴⁴ The LBD is the second most conserved domain, which harbours an activation function (AF-2) governed by the E2-ER complex. This region mediates binding of the ligand, as well as the homo- and heterodimerization required for nuclear translocation processes and the transactivation of specified gene expression.⁴³ Regardless of the shared homology in the E/F-domain, with both ER-subtypes being able to bind with similar affinities during ERE activation.²³ However, variation of the two residues in Figure 2.6 enables both ER-subtypes to bind with different

affinities by recruiting EREs, providing selectivity and explaining the versatility associated with the ER-subtypes and their binding affinities. This domain is also involved with the recruitment of chaperone proteins that are responsible for the stabilization of folded proteins during protein-protein translocation. These chaperone proteins [also known as heat-shock proteins (Hsp)] are additionally responsible for the inhibition of the synthesis of ligands crucial for cell growth, thus enabling the ER-subtypes to modulate transcriptions in the absence of its endogenous ligand.¹⁵

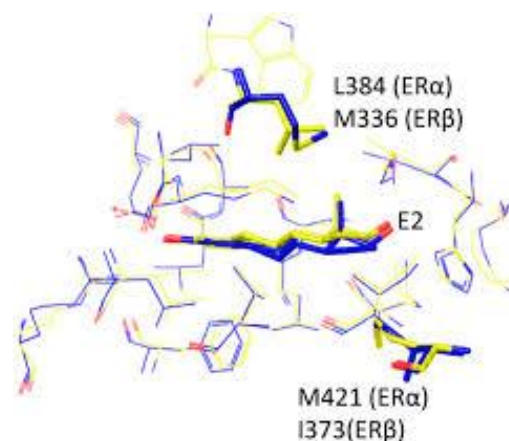


Figure 2.6. The two distinguishing residues within the ER binding cavity.⁶ M = Met, L = Leu and I = Ile are the different residues present within the ER α and ER β , which present the factor of selectivity within the LBD.⁶ (Source: Figure taken from Wen Ng, H.; Perkins, R.; Tong, W.; Hong, H. *Int. J. Environ. Res. Public Health* **2014**, *11*, 8709)

A key element to the AF-2 conformational orientation is the short helical region (helix 12) located at the carboxyl terminal of the LBD, shown in Figure 2.7.⁴² The helical elements consist of a three layered antiparallel α -helices which comprises the AF-2 region.¹⁵

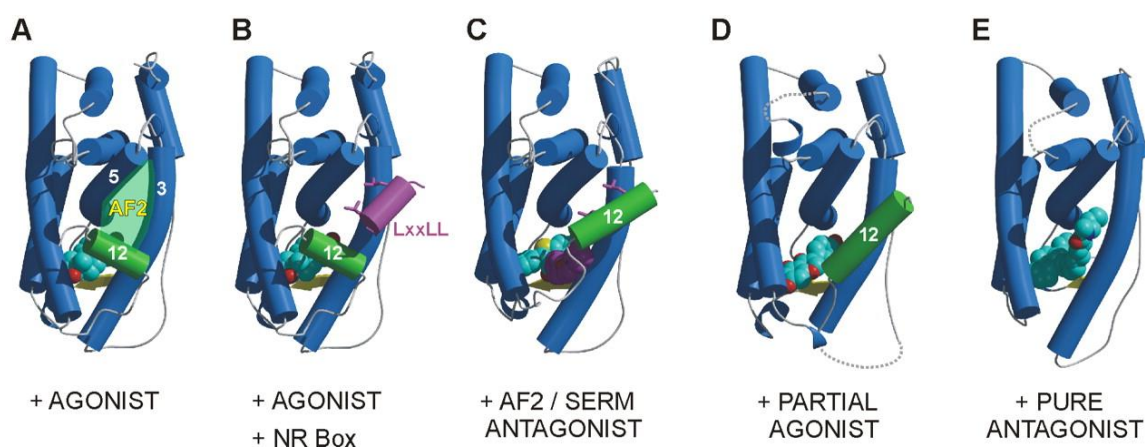
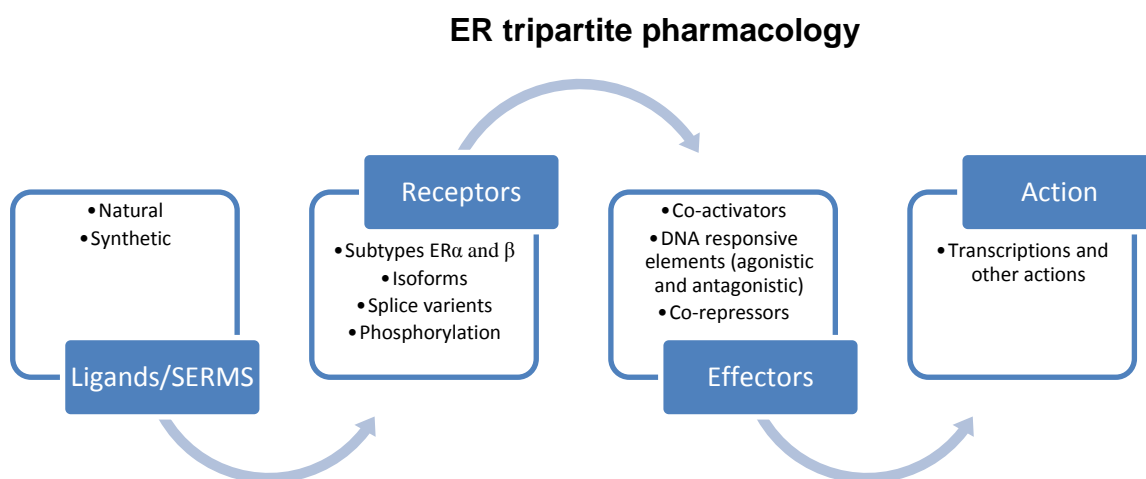


Figure 2.7. Illustration of the helix12's conformational orientations permitting different ER modes of binding.⁴² (Source: Figure taken from Heldring, N. *et al.*, *Physiol. Rev.* **2007**, *87*, 905)

The helices (helix 4 – helix 11) assemble to form a shallow hydrophobic binding cavity for leucine-rich motifs (LXXLL, where L refers to leucine and X, to the additional residues attached to the DNA sequence) of nuclear receptor coactivators.⁴⁴ As illustrated in Figure 2.7, in cases where helix 12 is not stabilized (the agonist conformation, frame A), the helix is re-orientated to bind along and occlude the AF-2 groove, thus blocking the recruitment site. In contrast, receptor antagonists interfere with the orientation of the helix 12, which results in an ER conformation unable to complete the recruitment of coactivators. The removal of the helix 12 greatly enhances the ER's ability to interact with traditional nuclear receptor corepressors (illustrated in frame E).⁴² Of importance is that the ligand binding site for both ER-subtypes is quite generous in size, further allowing a number of exogenous ligands to bind with the receptor.⁴²

2.4 Estradiol instrumentation and its mechanism of action

With the general understanding of the receptor's binding domains previously introduced, this section further elaborates on the overall biochemical machinery (EREs), which permit the gene transcription for ERs.^{43,59} Scheme 2.2 provides the general layout of the major instrumentation required for orchestrating the physiological transcriptions modulated by E2.



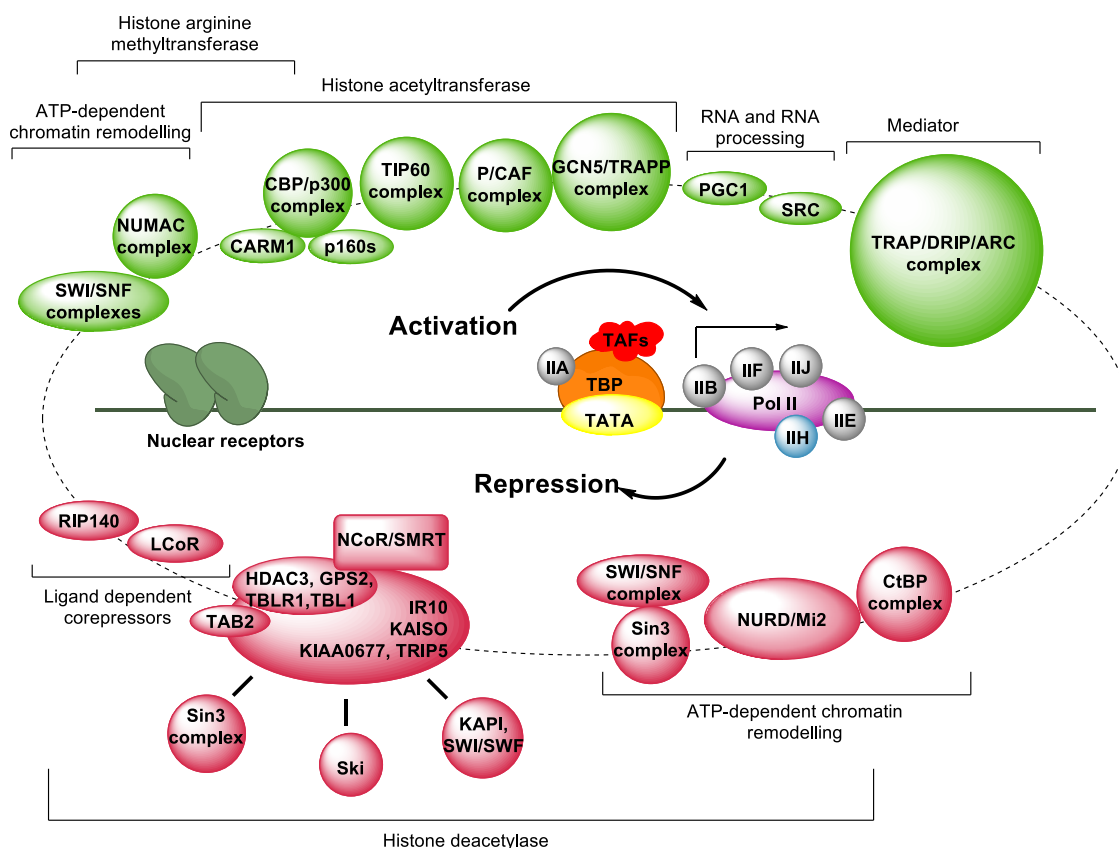
Scheme 2.2. The three components (ligands, receptors, and effectors), which together orchestrate transcriptional responses to the estrogens in target tissues.⁶⁰ (Source: Modified from Katzenellenbogen, B. S.; Katzenellenbogen, J. A. *Breast Cancer Res.* **2000**, *2*, 335)

The overall mechanistic process is initiated by the E2 (ligand), which binds to the ER α and/or ER β (receptors). The resultant E2-ER bound complex further undergoes dimerization, which is essential for phosphorylation of the receptor's protein chain, and gives rise to either the heterodimer (ER α /ER β) or the homodimer (ER α /ER α or ER β /ER β) complex, which

occurs within the DBD domain.⁷ Dimerization is vital, as it further allows the E2-ER dimerized complex to recruit specific DNA sequences known as ERE (or coregulatory proteins) to either express or repress transcriptional information.⁴⁶ The homo/heterodimer status is important and plays a distinct and sometimes opposite role in the regulation of gene transcription.⁵⁸ The recruitment of coregulatory proteins regulate gene transcription, which consists of coactivators that enhances estrogenic gene transcription, and corepressors responsible for repressing ER's gene transcription.⁴⁴ These coregulatory proteins enforce gene transcription by altering the chromatin structure with enzymatic processes implemented by the recruitment of DNA polymerase. This either masks or reveals active sites on the AF-2 domain, thus enhancing/reducing the structural topography required for the efficient binding of coregulatory proteins.⁴² These coregulatory proteins are further discussed in the section below and as illustrated in Scheme 2.3.

2.4.1 Effector machinery responsible for the orchestration of ER modulation

With previous attention focused on the E2 ligand and its receptors, attention is now shifted toward the effector machinery and their contribution to enhancing and repressing estrogenic transcription. The coregulatory proteins are the major transcriptional mediators, responsible for fostering cooperation between cofactors (coactivators and corepressors with a few illustrated in Scheme 2.3) mediated by specific DNA sequences (LXXLL), known as the nuclear receptor box (NR box), or LCD/LXD. The NR box is the primary docking site within the AF-2 domain.^{15,43,61} During which, coactivators serve as a bridge between the receptor and basal transcription machinery required for the enhancement of gene transcription.



Scheme 2.3. A summary of the major ER coregulators.⁶² (Source: Scheme taken from Perissi, V. and Rosenfeld, M. G. *Nat. Rev. Mol. Cell Biol.* **2005**, *6*, 542)

Scheme 2.3 presents a summarized description of the coregulatory components, with the green shaded components representing the coactivator family, while the red shaded component represents the corepressor family and lastly, the centre components are the basal transcription machinery. It is important to note that despite the opposing functions these coregulators offer, they can be found within similar protein complexes.⁴² The coactivator family consists of p160/steroid receptor coactivators (SRC), which can further be expanded into three subgroups.^{43,44} These subgroups include the SRC-1 and the nuclear receptor coactivator (NCoA-1). The SRC-2 coactivator includes the transcriptional intermediary factor-2 (TIF2), glutamate receptor interacting protein-1 (GRIP1), and NCoA-2. The third subgroup SRC-3, is composed of the co-integrator associated protein (p/CIP), the activator of thyroid and retinoic acid receptor (ACTR), amplified in breast cancer-1 (AIB1), receptor-associated coactivator-3 (RAC3), and TRAM1 summarized in Scheme 2.3.^{15,43,44}

The SRC coactivators contain two separate activation domains (AD)-1 and AD-2. AD-1 is responsible for the recruitment of the co-integrator CBP/p300, usually involved in multiple

signalling pathways, which include acetyl transferase, associated with the RNA polymerase II.⁴⁴ The AD-2 domain recruits secondary protein modifying enzymes, known as the coactivator associated arginine methyl transferase (CARM1) that incorporates the use of histone acetyl transferase (HAT) enzymes. These HAT enzymes further consist of the SRC, CBP/p300 and/or p/CAF/GCNS, which function by recruiting chromatin modifying enzymatic activities to the ligand activated nuclear receptor, regulating target gene transcription.^{43,63} The RNA processing unit, aided by PGC1 and SRA promotes the RNA transcription of coactivator complexes by acting as a protein binding scaffold.¹⁵ Mediators such as TRAP/SMCC/DRIP/ARC complexes, form a bridge directly linking the ER to the basal transcription machinery promoting gene transcription.⁴³

Recent work by Gustafsson and co-workers, suggest that both the agonist and antagonistically bound ERs are able to recruit a variety of corepressor proteins,⁴² which in turn decrease the rate of gene transcription by stimulating specific transcriptional effects.⁶⁰ Coactivators function by way of histone acetylation, thus altering the chromatin structure. Conversely, the corepressor functions by repressing gene transcription by blocking off the AF-2 domain, and inhibiting the recruitment of coactivators.⁶² Baniahmad and co-workers,⁶⁴ further support these findings, suggesting that the histone deacetylase offers a platform enhancing protein-protein interactions, by bridging the DNA bound transcriptional silencers with chromatin modifying enzymes (also known as silencing factors).⁶⁴ The transcriptional silencing factors are comprised of nuclear receptor corepressors (NCoR) and the silencing mediator of retinoid and thyroid (SMRT) that function by recruiting protein complex histone deacetylase (HDAC).⁶⁵ Work by Nilsson *et al.*⁴³ further reports that repressors function by antagonizing the AF-2 proteins of SRC-1 by the recruiting of ligand dependent corepressors such as RIP140 or ICoR, which block the recruitment of HAT enzymes.⁴³ The repression of gene transcription can also be obtained by employing ATP-dependent chromatin remodelling complexes (such as SWI/SNF, NURD/Mi2, Sin3 and CtBP complexes in Scheme 2.3), which compete for the AF-2 domain on the SRC-1 coactivator.^{15,43,62} Despite the use of coregulators in gene transcription, reports by Gustafsson has established that many more complex processes further contribute to the recognition of coregulators, critical for the functioning of estrogenic gene transcription.⁴²

2.4.2 All pathways lead to gene transcription

The multifaceted role exhibited by the E2 ligand and its receptors, can be associated with its ability to bind in both an agonistic and antagonistic binding mode. The agonistic mode of

binding adopted by the ER follows a direct binding path and is ligand dependent, whereas the antagonistic mode of binding follows a more indirect path, which is ligand independent. In the absence of its endogenous ligand, the receptor recruits cofactors able to enhance the transcription of gene expression.⁶⁶ Once the ligand and receptor binds, the bound complex (ligand-ER) undergoes a number of structural conformational changes, allowing for the recruitment of coregulatory proteins, modulating either the expression or repression of gene transcription *via* a number of secondary routes. The structural conformations adopted by the bound complex, suggests that the binding site is quite flexible and accommodating to these conformations.⁶ Apart from endogenous ligands such as E1, E2 and E3, the ER has proved its ability to bind with a diverse series of exogenous ligands (in Figure 2.8).

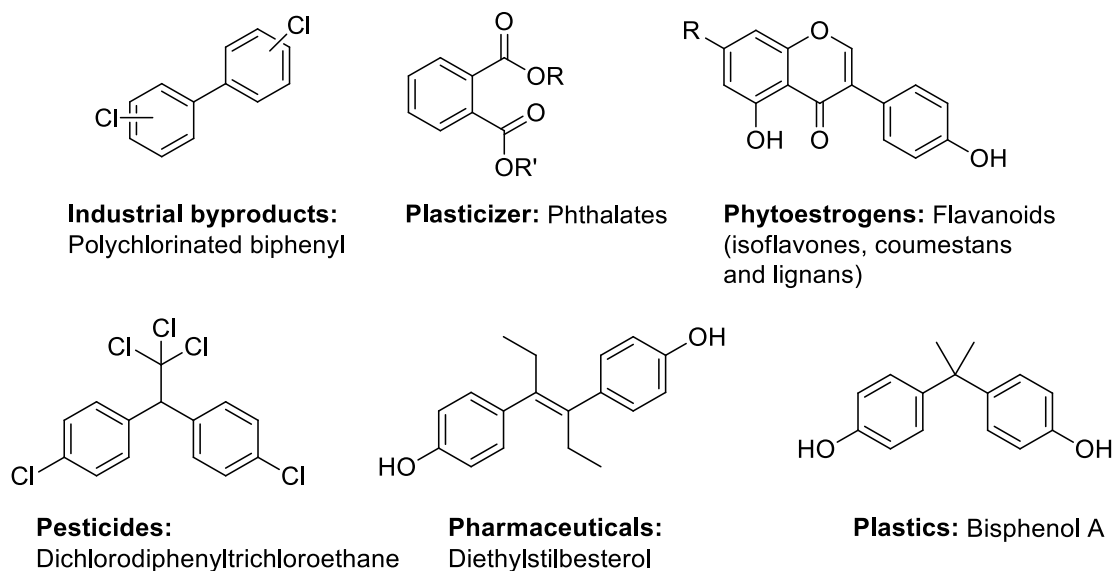
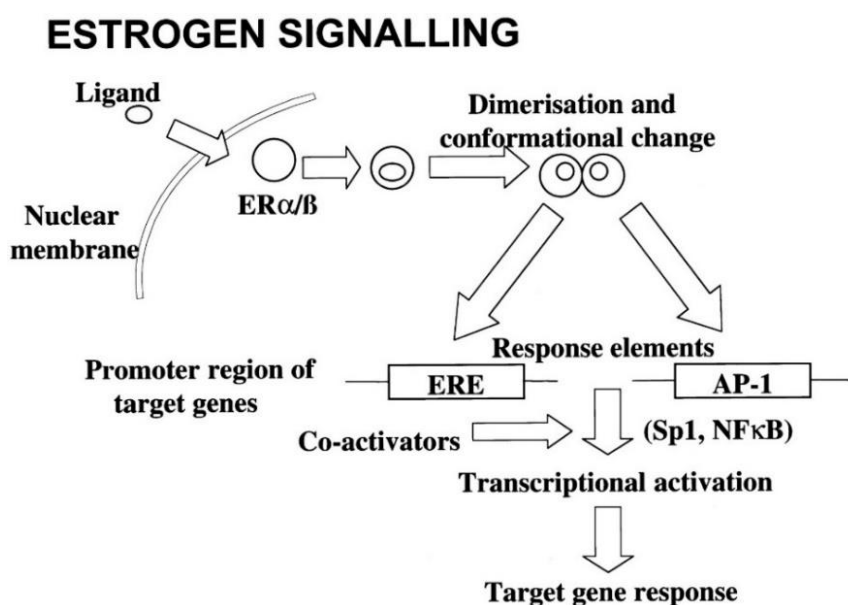


Figure 2.8. Xenoestrogens composed of synthetic and natural chemical compounds compatible with ER binding.⁶ (Source: Taken from the work reported by Wen Ng, *et al.*; *Int. J. Environ. Res. Public Health* **2014**, *11*, 8709)

These compounds range from industrial by-products, to plastics, phytoestrogens, pesticides and pharmaceuticals, further substantiating that the ER does not bind according to the conventional lock and key binding models hypothesized by Fischer.⁶ However, its mode of binding has been better supported by Koshlands theory, where the transcriptional processes are catalyzed by the receptor recruiting certain cofactors.^{6,55} The ability of ER to bind with numerous endo- and exogenous ligands accommodates its unconventional transcription methods. This can be attributed to a number of complex procedures briefly as illustrated by Scheme 2.4, which further illustrates the ligand dependent and independent binding modes.

2.4.2.1 ERs general binding modes

The ligand dependent ER mode of binding includes a process where the E2-ER bound complex undergoes dimerization. The activated homo/heterodimer undergoes translocation from the plasma membrane into the nucleus, where it directly binds with the response element machinery. This triggers transcription factors that recruit coregulators, further altering the chromatin structure and thus facilitating the recruitment of RNA polymerase II transcriptional machinery in Scheme 2.4 (in addition to Table 2.1), which either decreases or enhances gene transcription.^{17,46}



Scheme 2.4. General signalling transcriptional pathways followed by estrogen.^{7,67} (Source: Diagram taken from the Compston, J. E. *Physiol. Rev.* **2001**, *81*, 419)

Table 2.1. Summary of signaling pathways followed by ERs.

Ligand	Response elements	Transcription factors	Coregulators
Dependent	ERE	/	Coactivators and corepressors ^{42,43}
Dependent	AP1	Jun/Fos ^{7,17,43,68}	Coactivators: CBP and GRIP ⁶⁹
Dependent	SP1	GF, EGF and IGF-1 ^{42,68}	Coactivators

Independent	NFkB	Protein kinases (MAPK/ERK, P13K/AKT, cAMP, PKA) tyrosine kinase	Phosphorylation <i>viz.</i> , kinase cascades (MAPK and P13K–Akt) ¹⁸
-------------	------	--------------------------------------------------------------------------	---------------------------------------------------------------------------------------

CREB-binding protein: CBP; glucocorticoid receptor interacting protein: GRIP; growth factors: GF; epidermal growth factor: EGF; insulin-like growth factor-1: IGF-1; nuclear factor-kB: NFkB.

The multiple binding modes adopted by estrogen receptors create many challenges in the design and development of molecules required to selectively modulate their target transcriptions. Thus, a few antiestrogens have been developed as an initial strategy to block the estrogen receptor's transcription. However, a number of hormonal related ailments were soon realized and antiestrogens were soon replaced by SERMs with the aim of selectively allowing gene transcription in certain tissues by the design of molecules, which could behave agonistically and/or antagonistically in specific tissues. However, despite many scaffold designs, challenges were still encountered and will be discussed in the second part to this literature overview.

Literature review

Part 2: Evaluation of past and present SERMs

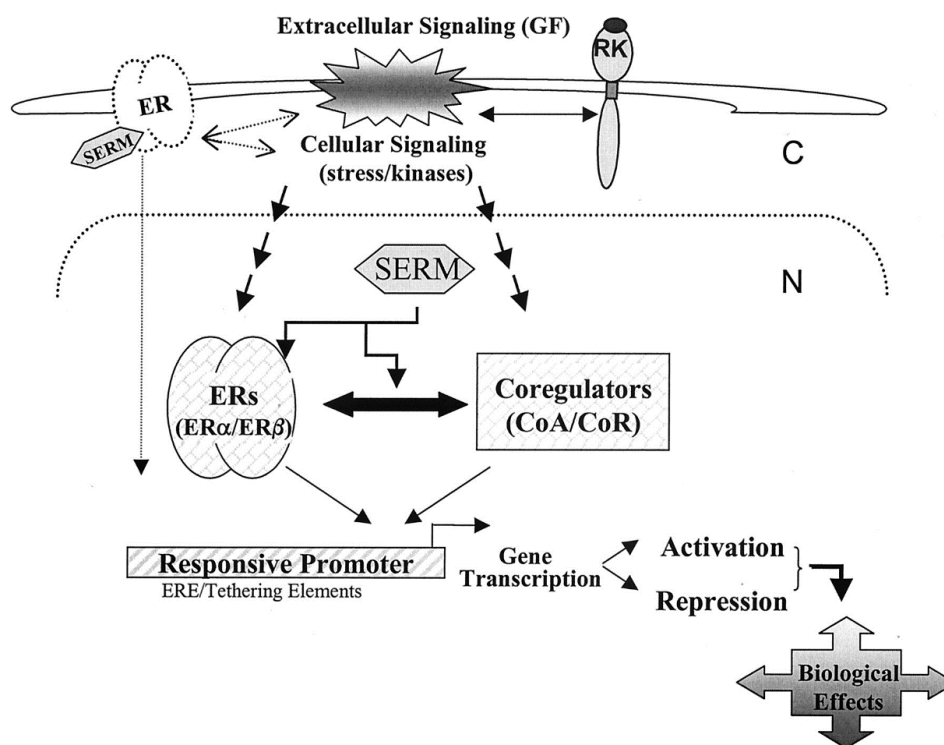
This subsection to the literature review discusses the development and relevance of the designed SERM molecules. A brief overview elaborates on the victories and challenges associated with exploration of varied scaffolds during the search for an ideal SERM. The metabolic pathways undergone by SERM molecules, their metabolites and their relation to the adverse effects experienced by the patients undergoing therapeutic treatment with them will also be reviewed briefly. In concluding the literature review, a description into the motivation behind the structural design, scaffold use, the aryl groups incorporated, and general research objectives targeted by this research will be presented.

2.5 Synthetic ligands and selectively mediating estrogenic gene transcription

As previously discussed, E2's vital role in the development and maintenance of the body, specifically sustaining overall health by its tissue specific gene transcription has been established.⁷ Since both E2 and ER have been implicated in tumour growth, the need to selectively orchestrate gene transcription has emerged.^{13,19,21} Primarily, women suffering from breast cancer have been treated by forms of hormonal therapy, but once it was realized that hormones (estrogen) encouraged tumour growth, antiestrogens were introduced. The implementation of antiestrogens was aimed toward locking the receptor/s in an inactive state thus, preventing any gene transcription. However it was soon realized that a cascade of negative health effects were experienced by the women undergoing this therapeutic strategy.⁴⁸ These adverse effects included ailments such as: the deterioration in skeletal health, the central nervous system, the reproductive system, as well as the development of cardiovascular diseases.^{16,42} In addressing these issues, the need of estrogen was substantiated leading to the realization of the need for synthetic estrogenic ligands. These ligands would need to selectively modulate gene transcription targeted at specific tissues. This class of synthetic ligands are known as selective estrogen receptor modulators (SERMs). The term describes their behaviour as estrogenic agonists in some tissues (such as skeletal, liver and the cardiovascular systems) and as antagonists in other tissues (such as mammary glands, uterus and the brain).⁷⁰ Current SERMs include a range of structurally diverse compounds, in which the steroidal skeleton of estrogen is absent.

2.6 The general SERM binding interaction mechanism

The unique pharmacology presented by SERMs allow for the agonistic and antagonistic behaviour within target estrogenic tissues. Apart from the classic ligand dependent transactivation mechanism for gene transcription, estrogens can mediate their transcription independently by many complex mechanisms previously summarized in Table 2.1. It was initially thought that SERMs occupied the LBD, blocking E2 access by locking the ER in an inactive state, and thus being unfavourable for the recruitment of coactivator proteins.^{23,42} However, contributions by Howell and co-workers reported that SERMs were able to bind with a lower affinity to the receptors in comparison to the endogenous ligand, and dissociate heat shock proteins (Hsp90).³² These Hsp90 are chaperone proteins, which assist in the folding of the dimerized ligand-ER complex, and the stabilization of proteins required for promoting tumour growth.⁶⁶



Scheme 2.5. Binding modes interaction by the SERM-ER bound complex.⁷¹ (Source: Diagram taken from the Schiff, R.; Massarweh, S.; Shou, J.; Osborne, C. K. *Clin. Cancer Res.* **2003**, 9, 447)

The SERM-ER complex undergoes homodimerization followed by its translocation into the nucleus, which triggers activation of AF-1 in the A/B-domains of the receptor, but not the E/F-domains (AF-2), generating a partial agonist.³² The transcription of estrogen responsive genes is therefore restricted by the inactive AF-2 domain. Inhibiting the

recruitment of coactivators, the AF-1 domain is thus available for activation.⁷¹ It can therefore be established that the SERM pharmacology is not only dependent on the ligand and receptor interaction, but includes the recruitment of coregulatory proteins illustrated in Scheme 2.5.

2.7 The gradual development of the SERM generations

As with numerous scientific developments, a prototype is initially established, to which further modifications are made to accomplish the ideal interaction. Likewise, since the development of the tamoxifen drug (the first generated SERM), new libraries of SERMs have been developed for enhancing the pharmacological profiles and reducing the adverse effects associated with previous generations of similar molecules. The developed generations of SERMs are arranged as 1st, 2nd, 3rd and 4th in the order of progression, in the establishment of more effective SERMs. The varied SERM generations are not designated according to their structural features, with each generation bearing slight structural variations from its predecessor, but possess distinct biological effects on targeted tissues.⁴⁸ It has been confirmed that exogenous ligand bound complexes adopt conformations required for the recruitment of coregulatory proteins that either enhance or retard a specified gene transcription.⁴²

2.8 First generation SERMs: Triphenylethylene analogues

The intended aim of the 1st generation of SERMs was for them to behave as antiestrogens. However, observing patients undergoing treatment with these SERMs proved otherwise.⁷² Displayed in Table 2.2, it was clear that the 1st generation of SERMs were good therapeutics for breast cancer treatment. However, apart from mimicking E2 in mammary glands, tamoxifen behaved agonistically in other tissues.^{22,32,48,73} The recognition of the tamoxifen-ER complex in specific tissues suggested that instead of it being an antiestrogen, it behaved as a SERM and it was soon reclassified as a SERM.⁷²

Table 2.2. Adverse effects observed in breast cancer patients undergoing hormonal mediated treatments.⁴⁶

Side Effects	Estrogen	Tamoxifen	Toremifene	Raloxifene
Hot flashes	–	+	+	+
Uterine bleeding	+	+	+	/
Endometrial cancer	+	+	?	/

Bone loss (in postmenopausal women)	+	+	/	+
Breast cancer	+	–	–	–
Serum lipids pattern	+	+	+	+
Venous thrombosis	+	+	+	+

+: refers to an increase in the mentioned side-effect.

–: refers a decrease in the mentioned side-effect.

?: refers to inconclusive results.

/: refers to no observed change in the mentioned side-effect.

2.8.1 Victories and challenges associated with tamoxifen

The 1st generation SERMs are the only class in which structural consistency was retained, as it was in this family of compounds where the triphenylethylene scaffold was used. This triphenylethylene skeleton was modified from the Stilbestrol (diphenylethylene) skeleton. During 1939 work reported by Lewis⁷⁴ suggested that similar estrogenic behaviour was observed when Stilbestrol was administered to a number of girls and women.^{74,75} It was initially developed for the treatment of endometrial irregularities in women and girls however, a vast number of side effects, where endometrial carcinomas in addition to cervical and vaginal abnormalities were experienced and was thus short lived.⁷⁵⁻⁷⁷ The first triphenylethylene molecule generated from the 1st generation SERM series, tamoxifen has been employed in clinical treatments for metastatic breast cancer since the early 1970's.^{32,48,70,72} Clinical drug trials have since indicated that tamoxifen had potential chemo preventative applications, particularly as a therapeutic agent in ER positive breast cancer cell lines.⁷² Tamoxifen not only showed promising results by reducing breast cancer in 16 – 49% of patients, but also that the incidence of ER positive breast cancer was reduced between 31 – 69%.^{48,72} With these results, it was understood that tamoxifen's mechanism of action involved blocking cancer cells in the G1 (growth) phase, where growth of these cells were inhibited.⁴⁸ Furthermore, it was observed that the bone mineral density in postmenopausal women was maintained, as well as producing decreased LDL cholesterol levels. Tamoxifen proved to be an estrogenic agonist in uterine cells and induced growth of endometrial cells, while displaying partial agonistic effects in skeletal maintenance and the cardiovascular system in postmenopausal women.⁷³

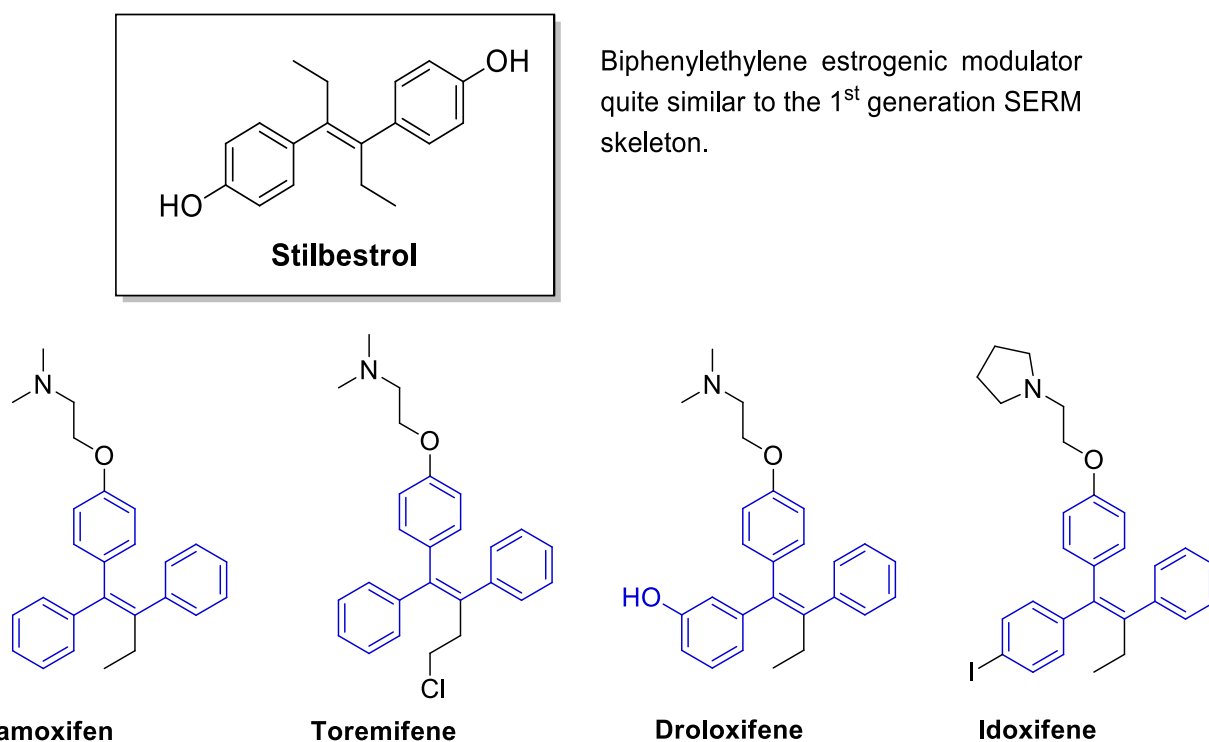


Figure 2.9. Evolutionary development of the triphenylethylene analogue.

Despite the successes obtained, tamoxifen has been associated with an increased risk in endometrial cancer,⁷² as well as having additional side effects listed in Table 2.2,^{70,72} which in themselves increase the risk of secondary health effects.^{48,70,72} It was later found that the long term use of tamoxifen resulted in resistance toward the drug, acquired by either the continual use or prior to use (the treatment was thus considered to be ineffective).²² Structural modifications to tamoxifen's triphenylethylene structure was explored with the objective being to limit the genotoxic effects associated with tamoxifen (which would further be elaborated on in later sections of the chapter).⁷⁰

2.8.2 The structural modification of tamoxifen to toremifene

The second triphenylethylene analogue, toremifene, was designed and targeted toward generating a molecule with reduced side effects compared to its predecessor tamoxifen. This triphenylethylene analogue included the introduction of a chloride atom on the ethylene chain, in Figure 2.9. Since the 1st generation SERMs possess a general scaffold, similar pharmacological profiles could be expected for the triphenylethylene analogues.^{48,70,72} As expected, toremifene displayed similar binding affinities toward ER α but also caused adverse effects.^{32,48} However, an increased rate of venous thromboembolism was observed, and despite a shared structural profile the toremifene analogue was less prone to the formation of genotoxic DNA adducts, previously observed for tamoxifen.^{48,70}

2.8.3 The triphenylethylene analogue: Droloxifene

Droloxifene was the third developed triphenylethylene analogue, targeted toward a more potent tamoxifen derivative with less side effects.

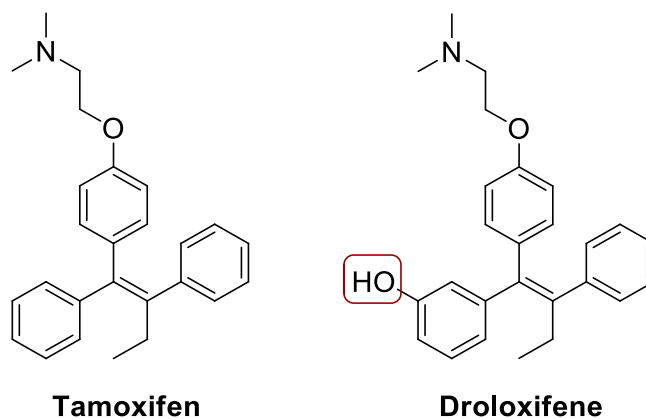


Figure 2.10. Derivatization of tamoxifen, providing the droloxifene analogue.

Shown in Figure 2.10, the new compound included a hydroxyl group on one of the phenyl rings. This significant change resulted in a molecule, which displayed an ER binding affinity 10 – 60 times greater, in addition to the absence of the genotoxic DNA adduct formation.^{48,70} The greater affinity observed toward ER α allowed droloxifene to be administered to patients with shorter dosing periods, and the compound displayed full ER α antagonistic behaviour in mammary glands with full ER α agonistic behaviour in skeletal tissue. An additional feature observed, was its inhibition of the insulin-like growth factor (IGF)-1,^{42,68} thus preventing the stimulation of E2 oncogene c-myc expression.^{48,68} Unfortunately, during phase III trials, droloxifene was found to be inferior upon comparison to tamoxifen.³² Additional side effects included hot flashes, nausea, fatigue, headaches, back pain and dyspnea, which brought an end to further developments on droloxifene, thus paving the way for structural improvements in developing a more effective triphenylethylene analogue.⁴⁸

2.8.4 The triphenylethylene analogue: Idoxifene

The structural modifications used to generate idoxifene, involved substitution of the hydroxyl motif by an iodine atom with the replacement of the dimethyl group on the side chain by a pyrrolidino-group (Figure 2.11).⁴⁸

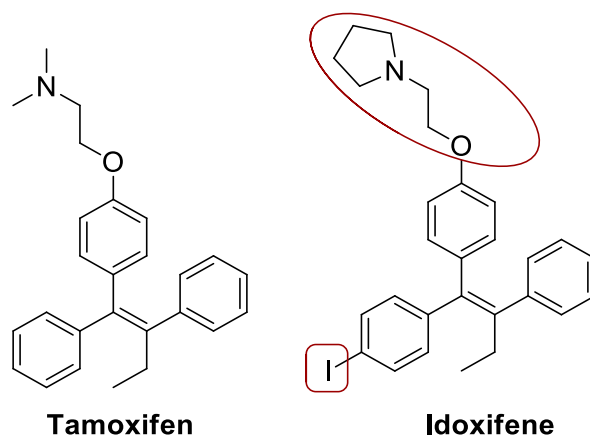


Figure 2.11. Derivatization of tamoxifen, providing the idoxifene analogue.

Idoxifene possessed an antiestrogenic ability comparable to tamoxifen but without the formation of hepatocarcinogenic effects previously observed in rat cell models with tamoxifen.⁷⁰ This analogue proved to be metabolically more stable and the associated slower metabolism resulted in a longer half-life when compared to tamoxifen. The idoxifene analogue presented an overall reduction in tumour size with good efficacy toward breast cancer cell lines. In addition, limited agonistic activity was observed in endometrium cells, thus lowering the potential risk of uterine cancer development post-treatment. Unfortunately, phase I and II drug trials showed no real significant advantages upon comparison of idoxifene with tamoxifen. These results led to the termination of further synthesis of the triphenylethylene-based analogues.^{32,46,47,52}

2.9 Second generation SERMs: Benzothiophene analogues

The development of 2nd generation SERMs was steered toward increasing potency, and the elimination of side effects associated with the 1st generation. Diverting from the triphenylethylene skeleton, a benzothiophene skeleton was adopted as the scaffold for the 2nd generation SERM analogues (in Figure 2.12).⁷⁸ Raloxifene was the first 2nd generation SERM developed for the treatment of breast cancer cell lines, but showed no therapeutic value when used by patients who developed resistance toward tamoxifen.⁴⁸ Unlike tamoxifen, it however proved to be effective in terms of preventing the development of endometrial cancer and possessed less thromboembolic effects.⁴⁸ Raloxifene showed ER agonistic effects in skeletal tissues and the cardiovascular system,⁷³ with antagonistic behaviour observed in the uterus and mammary glands.^{72,79} Despite its failure as a breast cancer therapeutic, this drug also proved to be an effective pre-treatment for breast cancer and a treatment for osteoporosis in postmenopausal women.⁴⁸

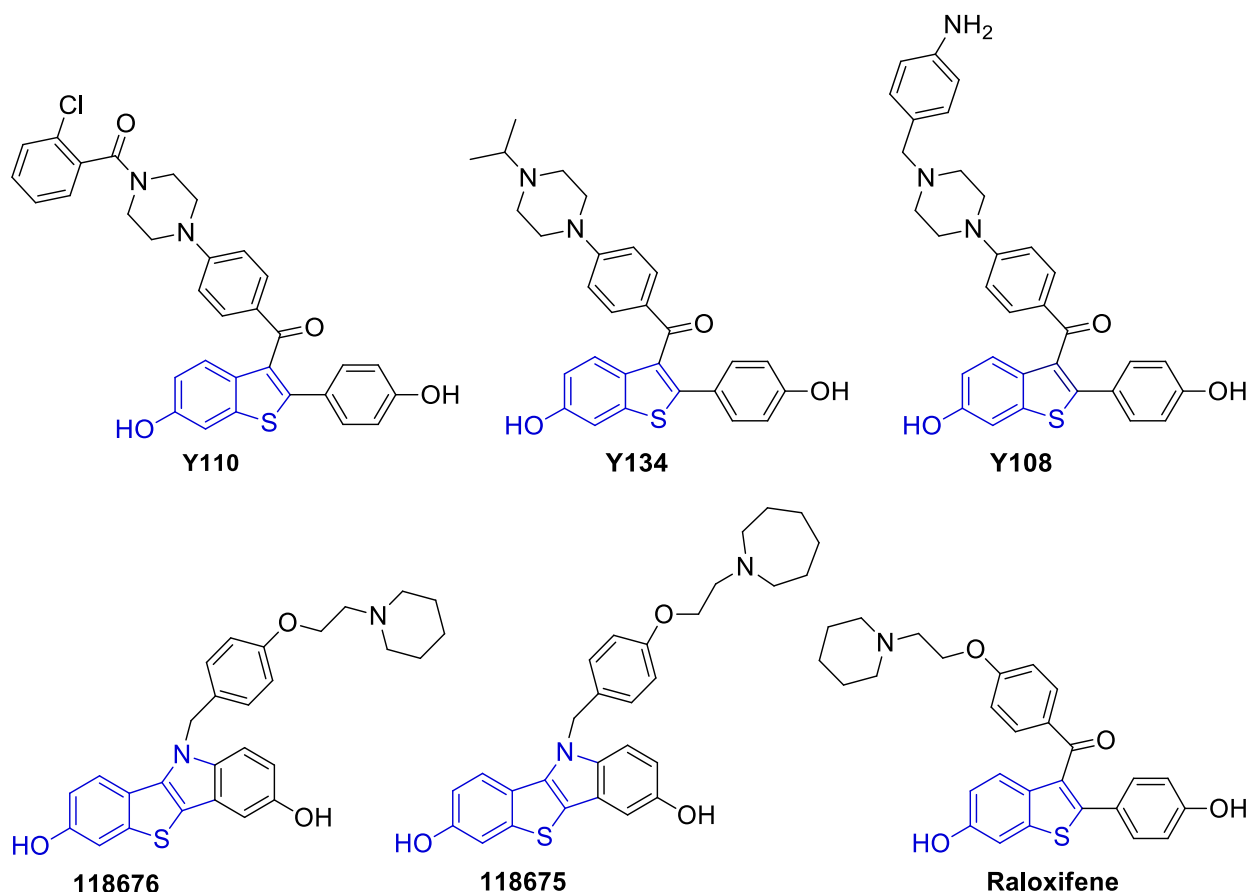


Figure 2.12. Evolutionary design of the benzothiophene analogues.

Studies of tamoxifen and raloxifene (STAR),³² demonstrated that raloxifene showed a 78% effectivity upon comparison to tamoxifen.⁴⁷ However, side effects such as hot flashes, an increased risk in blood clot formation and potential drug resistance associated with tamoxifen, were also experienced with raloxifene.^{48,70} Not much literature has been published on the additional analogues (**Y110**, **Y134**, **Y108**, **118676** and **118675**) in Figure 2.12. However, studies by Ning and co-workers established that **Y134** showed a 2-fold improvement in mammary gland efficacy when compared to raloxifene, but no significant improvements were observed for the **Y110**, **Y108**, **118676** and **118675** analogues, and further investigation into these compounds was soon abandoned.⁷⁹ Regardless of minor improvements, no significant pharmacological value was observed and no further investigations into 2nd generation SERMs were pursued.

2.10 Third generation SERMs

Unlike the 1st and 2nd generation SERMs, the 3rd generation differs significantly with a few fairly diverse range of structural features. The only common feature was that all 3rd generation SERM analogues contained three phenyl rings (Figure 2.13).

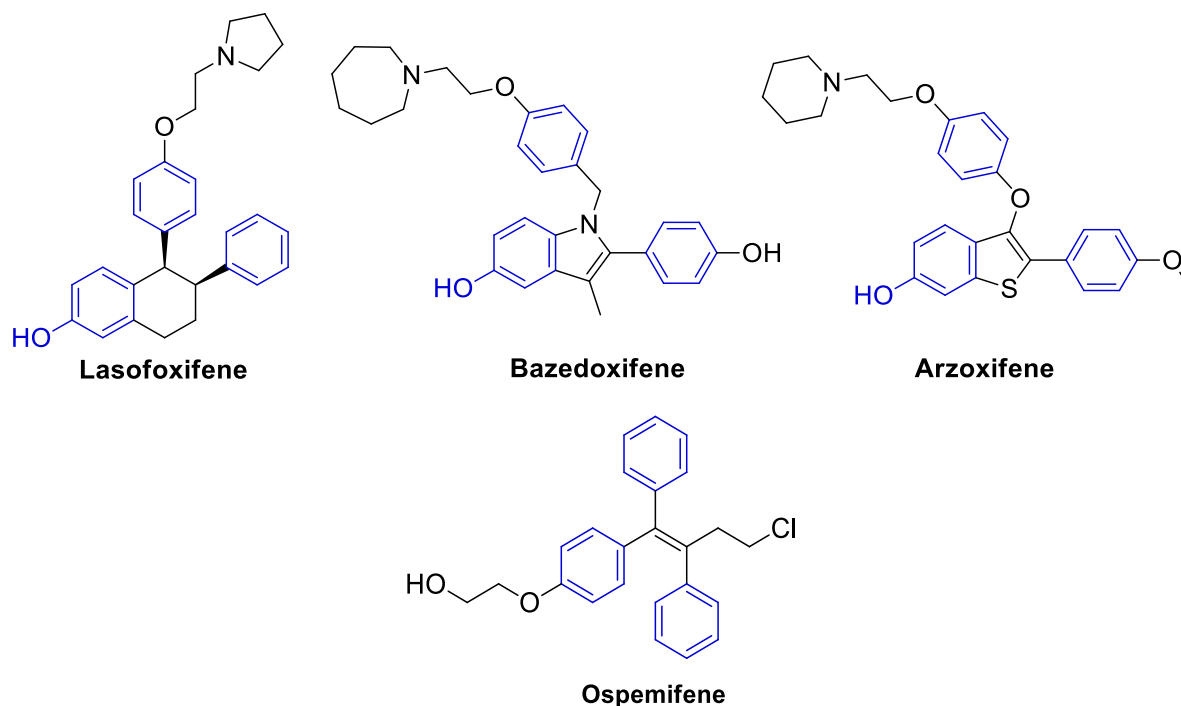


Figure 2.13. Evolution in the design of the 3rd generation SERM analogues.

The major driving force for the development of 3rd generation SERMs, was to establish a pharmaceutical containing the auspicious qualities of raloxifene, while decreasing adverse effects such as reduce LDL cholesterol serum levels and hot flashes. The most advanced 3rd generation SERMs included the molecules lasofoxifene and bazedoxifene, which were able to complete registration trials.²²

2.10.1 Redemption of the benzothiophene scaffold with the development of arzoxifene

The benzothiophene skeleton was recruited as the scaffold for the arzoxifene (**LY353381**) molecule. The arzoxifene structure resembled that of the earlier developed raloxifene but included derivations where the carbonyl linker was replaced with an ether linkage and a masked hydroxyl motif (as illustrated in Figure 2.14). Since raloxifene failed as a therapeutic towards metastatic breast cancer, the arzoxifene analogue was introduced, providing further

evidence supporting the claim that the benzothiophene core was a viable candidate for therapeutic agents treating metastatic breast cancer.^{32,48}

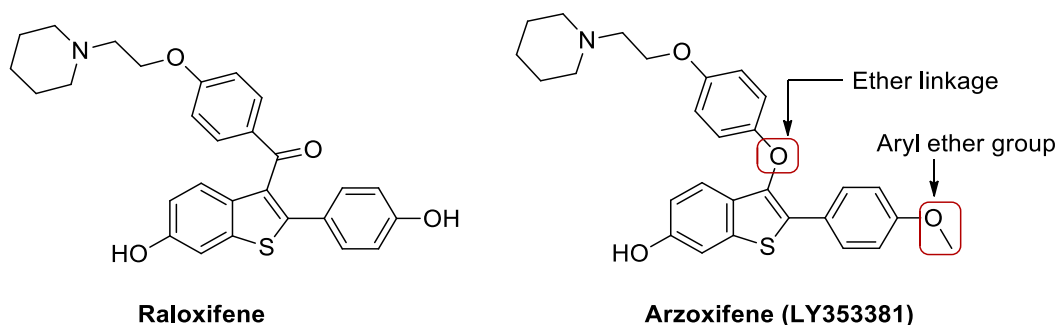


Figure 2.14. Comparison between the 2nd generation raloxifene and the 3rd generation arzoxifene.

Thankfully, the structural modifications significantly improved the pharmacological profile of arzoxifene when compared to raloxifene.³² These structural derivations provided a molecule with greater bioavailability, increased antiestrogenic activity and an increased binding affinity toward the ER α subtype (unlike raloxifene).³² In addition, arzoxifene demonstrated its ability to inhibit estrogenic agonistic effects in the uterus and endometrial cell growth, suggesting its application as a therapeutic for endometrial cancer.^{32,48} As observed with the triphenylethylene analogues, structural similarities resulted in a similar side-effect profile, which was observed for arzoxifene (experienced for raloxifene). The major side effects observed during these trials included hot flashes, nausea, cutaneous infection, neuromotor toxicity and weight gain.^{22,48,80} Additional side effects reported by Maximov and co-workers, further included cholecystitis, increased pulmonary complications and chronic obstructive pulmonary disease.²² Arzoxifene met its primary objective, by reducing vertebral fractures and breast cancer in postmenopausal women, but improvements on the non-vertebral fractures, cardiovascular and cognitive functioning were not obtained. Despite its valuable contribution in the treatment of breast cancer, when compared to tamoxifen, it was considered inferior and further developments on the arzoxifene analogue were discontinued.^{22,32,48}

2.10.2 Redemption of the triphenylethylene analogue with the development of ospemifene

With the development of each SERM generation, exploring past structural features has commonly been revisited, with ospemifene again making use of the triphenylethylene skeleton (previously used in 1st generation SERMs in Figure 2.15). Upon reviewing

tamoxifen metabolites, an interesting metabolite displayed weak antiestrogen activity, thus inspiring the ospemifene structural design.²² Ospemifene was found to bind with both ER-subtypes, but a greater affinity was exhibited toward the ER α . Its estrogenic effects were observed in skeletal tissue, displaying the ability to prevent bone loss and increase skeletal strength in the neck, lumbar and femoral vertebrae.²²

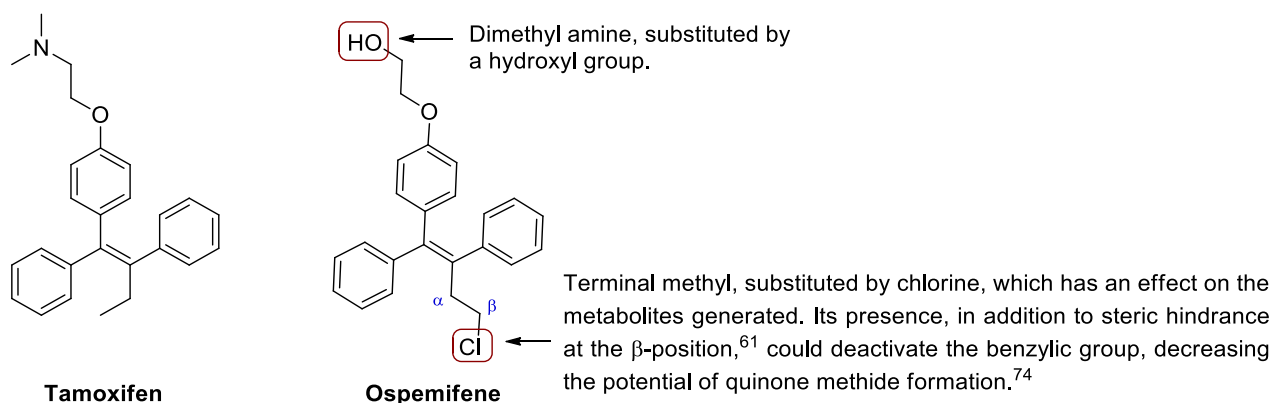


Figure 2.15. Triphenylethylene-based analogues 3rd generation SERMs.

Additionally, ospemifene showed weak antagonistic activity in the uterus and preserved endometrium activity. No genotoxicity was experienced, and the drug was well accepted, with headaches being the more commonly experienced side effect (with neutral effects on hot flashes).²² In subsequent studies, ospemifene has displayed a similar breast chemo preventative profile to toremifene and raloxifene.^{22,72}

2.10.3 The naphthalene analogue: Lasofoxifene

As mentioned, the 3rd generation of SERMs were developed to improve on the 1st and 2nd generations by reducing side effects associated with their applications. Lasofoxifene (shown in Figure 2.13) was developed using the tetrahydronaphthalene skeleton, which showed an affinity toward both ER-subtypes. This 3rd generation SERM behaved agonistically in skeletal tissue and antagonistically in the breast and uterine tissues.^{48,72} Lasofoxifene was found to behave similarly to raloxifene, with pharmacological outcomes that included the maintenance of femoral bone mineral density, the inhibition of osteoclastogenesis, with reduction in bone turn-over, thus preventing bone loss during preclinical studies.^{22,72,81} A decrease in bone turn-over markers, coronary heart disease, serum lipid levels and endometrium hypertrophy were revealed during osteoporosis prevention and lipid lowering (OPAL) and postmenopausal evaluation with the reduction of risk with lasofoxifene (PEARL) studies.^{48,72,82}

2.10.4 The indole analogue: Bazedoxifene

Bazedoxifene (in Figure 2.13) is an indole-based analogue developed as a preventative measure and a treatment for osteoporosis in postmenopausal women or used collectively with estrogens in treating menopausal symptoms. The drug demonstrated improved vasomotor activity during phase III clinical drug trials when compared to the 1st and 2nd generation SERMs.⁷² Like lasofoxifene, it has shown a great affinity toward both ER-subtypes with greater affinity been shown toward the ER α .²² Bazedoxifene was found to be the second most active compound clinically utilized in the 3rd generation series of compounds.²²

2.11 Fourth generation SERMs: Benzopyrans

The 4th generation SERMs were structurally based on the benzopyran skeleton also resembling the isoflavone structure of the phytoestrogen (see for instance the structure of genistein Figure 2.16).⁸³ EM-652 in Figure 2.16, has proved to be the more potent SERM inhibiting both ER-subtypes.⁷⁰ Binding of EM-652 with ER is significantly greater than that observed for E2, tamoxifen and raloxifene.³² The pro-drug EM-800, being potent by inhibiting E2-induced proliferation in breast cancer cells, prevented cardiovascular disease, bone loss, as well as the proliferation of estrogen-stimulated tumour xenographs in animal models.³² Additionally, it inhibited breast and endometrial cancer cell lines.⁷⁰

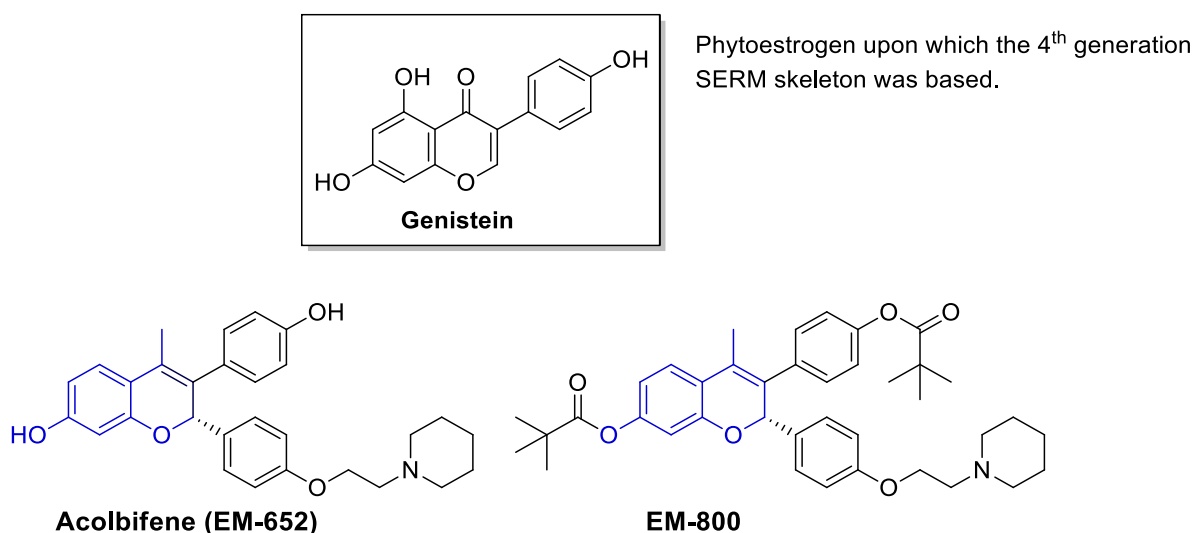


Figure 2.16. Phytoestrogen-like SERM analogues.

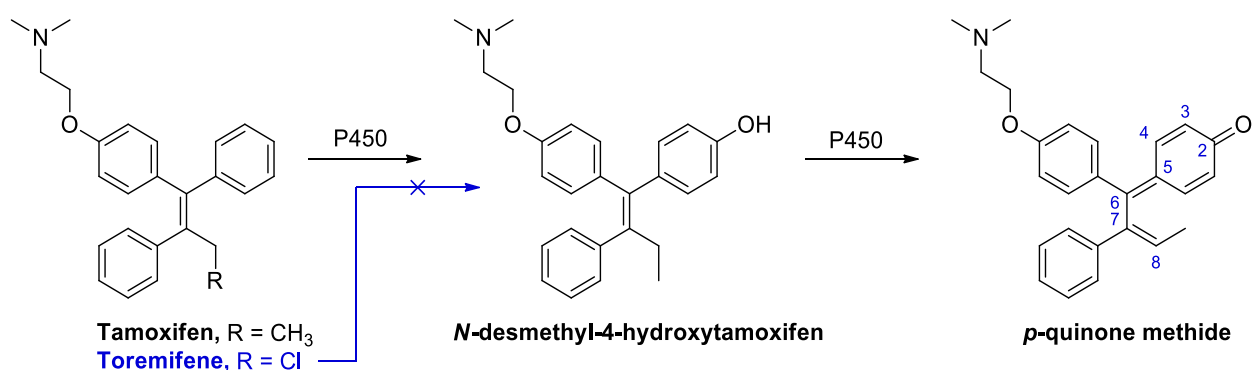
In summary, the ongoing development of SERMs has resulted in a better understanding of the biochemistry and biology of ERs. The significant improvements obtained in the field of ER targeted therapeutics, seen by the development of each new SERM generation.

2.12 The metabolic pathways undergone by SERMs

Briefly introduced in Chapter 1 section 1.3.1, was the metabolism of E2 and the potential contribution its metabolites exerted toward the development of carcinogenic cells.^{13,18,84} Some of these metabolic processes are also shared by SERMs.^{70,84} The metabolic substrates produced by estrogens and SERMs, not only alter the intensity of their action, but also the profile of their physiological effects in target tissues. This further contributes to the degree of toxicity associated with certain SERM compounds.^{13,84} There are at least four classes of electrophilic metabolites originating from the metabolic pathways undergone by the varied SERM molecules. The electrophilic metabolic substrates include carbocations, quinone methides, diquinone methides and *o*-quinones.^{70,84} The degree and concentration of these metabolites are dependent on the structure and reactivity of the SERM, as well as the class of CYP enzyme involved.^{70,84}

2.12.1 Metabolic pathways followed by the triphenylethylene analogues

The metabolism commonly observed in the triphenylethylene compounds includes a mechanism which involves the aromatic hydroxylation of tamoxifen at the 4-position by P450 (CYP2D6), giving the metabolite, *N*-desmethyl-4-hydroxytamoxifen, which is able to undergo further oxidation reactions forming the *p*-quinone methide metabolite in Scheme 2.6.^{70,84}



Scheme 2.6. The quinone methide biotransformation of the triphenylethylene analogue.

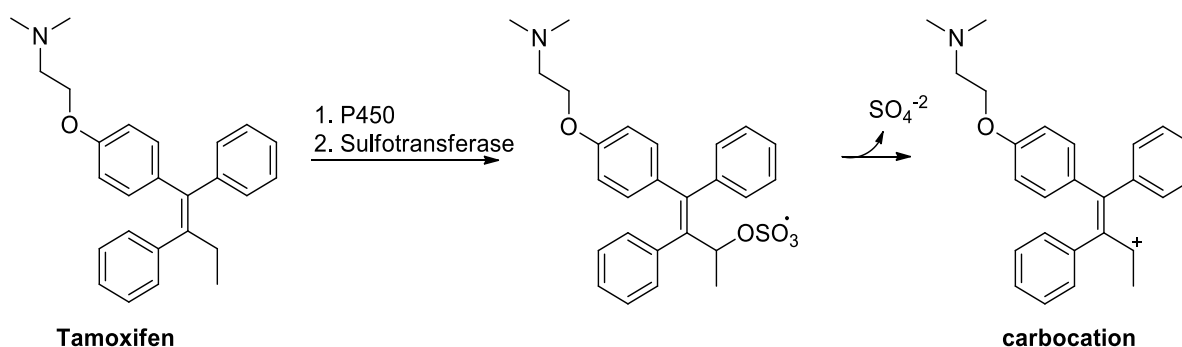
2.12.1.1 The quinone methide biotransformation

The *p*-quinone methide has a transient existence and rapidly reacts by a non-enzymatic 1,6-Michael addition reaction in biological systems, generating benzylic adducts. However, in the case of tamoxifen, the quinone methide's extended conjugation between the two phenyl rings and vinyl motif presents an unusually stable quinone methide, reported to form stable adducts with the exocyclic amine of deoxy guanosine *in vitro*, by way of a 1,8-Michael type addition (refer to the numbering in Scheme 2.6).⁸⁴

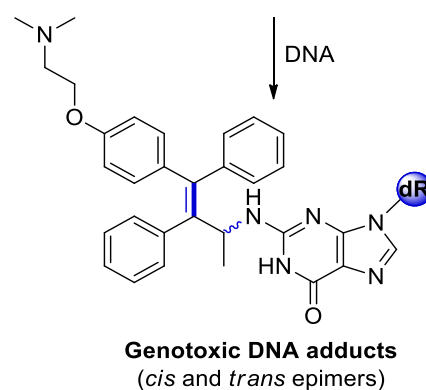
The toremifene analogue contains a β -chloro-substituent, which forms less DNA adducts than its predecessor. Reports by Dowers,⁷⁰ Bolton⁸⁴ and co-workers, suggests that the presence of the electron withdrawing chloride group, in addition to the steric hindrance at the β -position, could deactivate the benzylic group, thus decreasing the potential formation of the quinone methide metabolite. Reducing the formation of the quinone methide metabolite explains toremifene's inability to form the hepatocarcinogenic effects seen during rat model studies. Furthermore, Dowers and co-workers, suggest that lower concentrations of the quinone methide adducts were detected for the toremifene analogue.⁷⁰ Upon comparison to tamoxifen and droloxifene, the toremifene's adduct concentration was considered insignificant, with no DNA adducts reported for the idoxifene analogue.⁷⁰ It was however understood that the DNA adducts detected in women treated with tamoxifen were as a result of the carbocation biotransformation (discussed below).⁸⁴

2.12.1.2 The carbocation biotransformation

Formation of the carbocation metabolite is predominantly mediated by a specific CYP class (3A, 2D6, 2C9, 1A1, 1A2 and 1B), followed by *O*-sulfonation shown in Scheme 2.7.⁷⁰ The α -hydroxytamoxifen further reacts with the exocyclic amino group of the guanine in DNA forming two *cis* and *trans* epimers of the α -(*N*2-deoxyguanosyl)-tamoxifen.



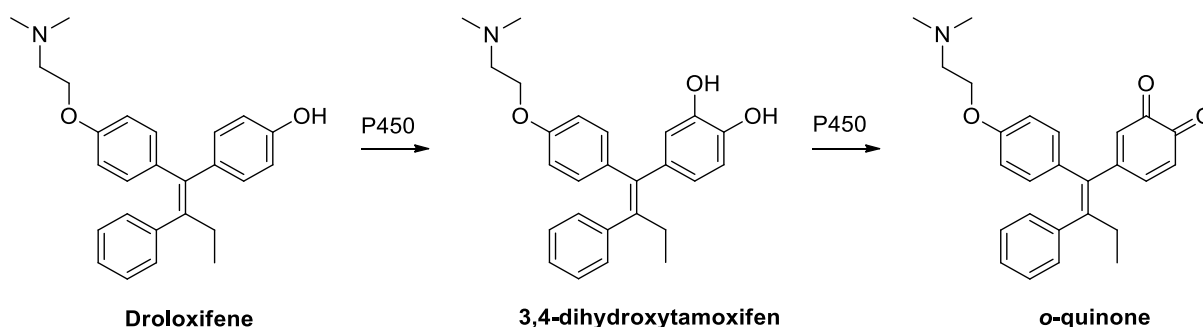
Sulfonation *viz.*, sulfotransferase
dR = DNA residue



Scheme 2.7. The carbocation biotransformation of tamoxifen.

2.12.1.3 The *o*-quinone biotransformation

Both droloxifene and the metabolite 3,4-dihydroxytamoxifen undergo oxidation by the CYP enzyme to form the corresponding *o*-quinone (Scheme 2.8).



Scheme 2.8. The *o*-quinone biotransformation of droloxifene.

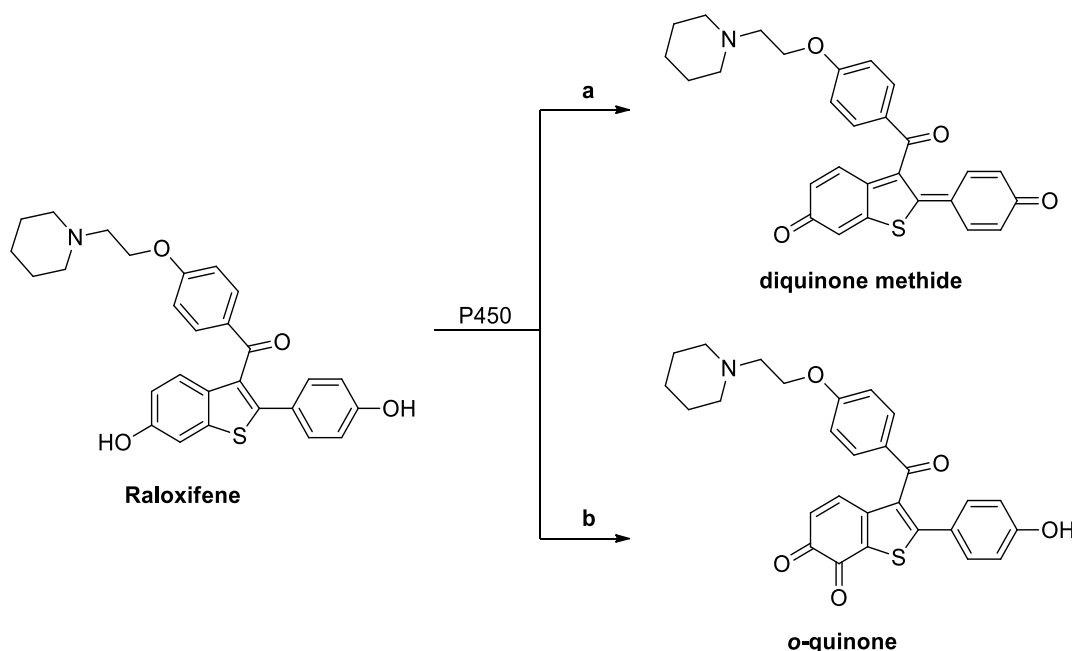
The intended catechol readily undergoes oxidization providing the *o*-quinone by a number of oxidative enzymes, metal ions, and in some cases molecular oxygen. The possibility that alkylation/oxidation of the cellular macromolecules provided by tamoxifen *o*-quinone could contribute to the toxic effects of tamoxifen has been muted.⁷⁰

2.12.2 Metabolic pathways followed by the benzothiophene analogues

The benzothiophene and benzopyran analogues have both demonstrated bioactivation to an electrophilic diquinone methide, potentially capable of reacting with cellular nucleophiles. Interestingly, this feature showed no known toxicities associated with the formation of the diquinone methide metabolite, since the drug's approval in 1997.^{70,84}

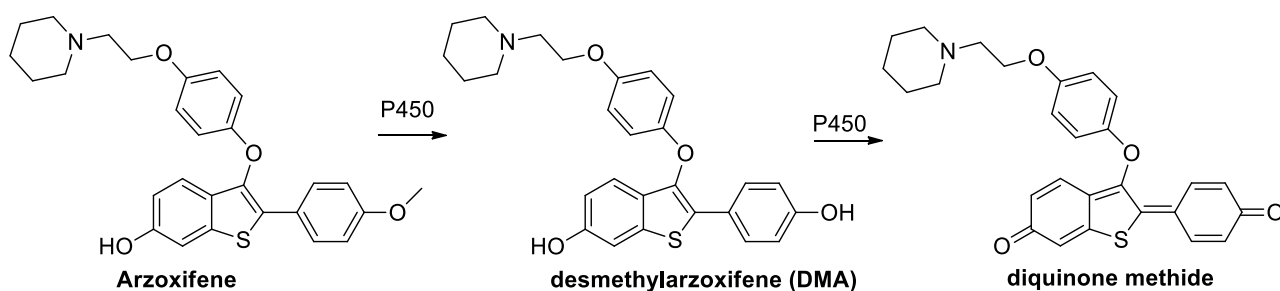
2.12.2.1 The diquinone methide biotransformation

It has been established that raloxifene undergoes bioactivation when forming electrophilic diquinone methide metabolites, with the minor *o*-quinone catalyzed by microsomes present within the rat and human liver (Scheme 2.9).^{70,84}



Scheme 2.9. The diquinone methide and *o*-quinone biotransformation adopted by raloxifene.

The diquinone methide metabolite is highly reactive, suggesting its ability to contribute toward the compound's cytotoxicity by *in vivo* alkylation of proteins.⁷⁰ Considering its transient nature, this reactive intermediate may result in a number of indiscriminate reactions with solvent molecules, glutathione (GSH) or non-critical proteins. Raloxifene and its diquinone methide metabolite has proven its ability to inhibit the inactivation mechanisms mediated by the enzymes CYP3A4 and CYP3A5.⁸⁴

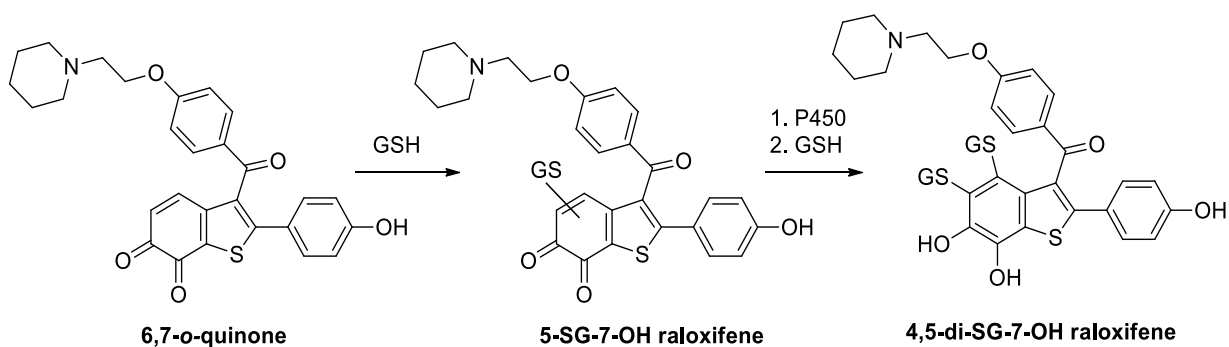


Scheme 2.10. The demethylation and diquinone methide biotransformation undergone by arzoxifene.

In addition, diquinone methide formation has also been observed as the major metabolite for the arzoxifene SERM and desmethylarzoxifene (DMA) metabolite. Reports by Bolton and co-workers, suggests that the formation of this diquinone methide metabolite can effectively be eliminated, while maintaining effective ER binding, by substitution of the 4'-hydroxyl group with a fluorine atom (i.e., 4'-F-desmethylarzoxifene).⁸⁴ This important observation proposes that the metabolism process could be manipulated by the introduction of certain heteroatoms onto the scaffold. The advantage would include maintaining the molecule's efficacy, whilst reducing the formation of its toxic metabolites. Arzoxifene is also demethylated by the oxidation with P450 providing the DMA metabolite (in Scheme 2.10), which is an inactive metabolite, that results in a more potent ligand for both ER-subtypes when compared to arzoxifene and raloxifene.⁸⁴ It is however unclear to quantify the amount of DMA formed from arzoxifene, since the DMA plasma concentration varies between women. As observed for the raloxifene SERM, DMA can undergo oxidation, providing the diquinone methide (a process mediated by microsomes present within the human or rat liver).⁸⁴

2.12.2.2 *o*-quinone methide biotransformation of Raloxifene

Raloxifene is known to undergo oxidation forming the highly active *o*-quinone by way of hepatomicrosomes, observed within human and rat biological models during clinical studies (Scheme 2.11).⁷⁰

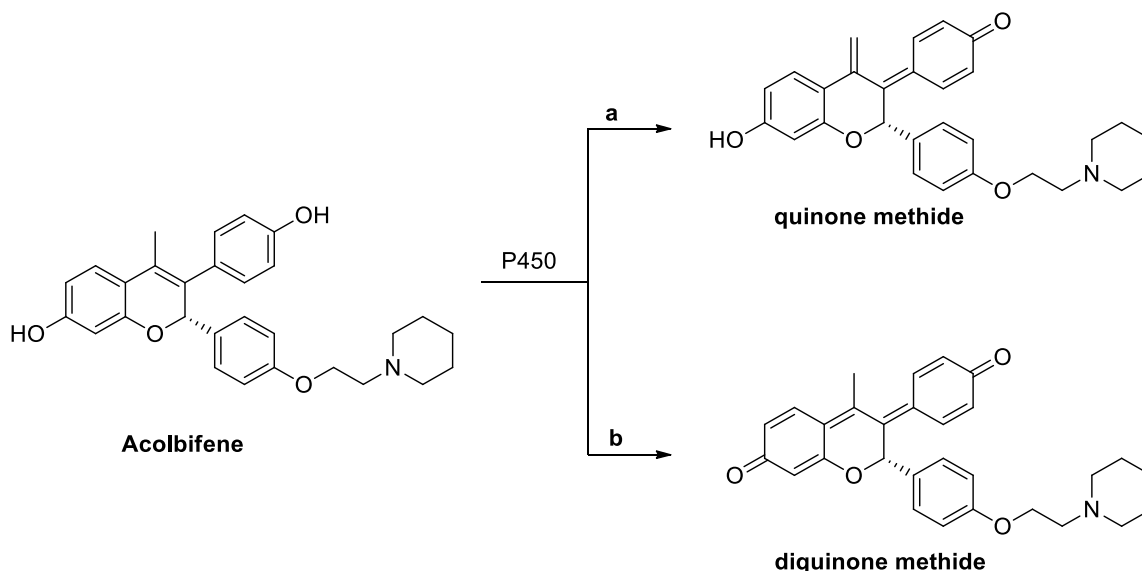


Scheme 2.11. The *o*-quinone methide metabolite formed from raloxifene's biotransformation.

The *o*-quinone metabolite can be trapped by the formation of a mono- and/or di-glutathione (GSH) conjugate (Scheme 2.11).^{70,85} Having a half-life of 67 minutes, the *o*-quinone is quite stable, suggesting that the metabolite can be considered as being toxic.⁸⁵ Fortunately, this metabolic pathway is a minor one, and is associated with insignificant concentrations and thus unable to cause toxicity.^{70,85}

2.12.3 Metabolic pathway followed by benzopyran analogues

Acolbifene (EM-652), as well as EM-800, are metabolized producing the respective quinone methide and diquinone methide metabolites, Scheme 2.12. These intermediates are good for Michael-type reactions with nucleophiles.



Scheme 2.12. Metabolic pathways under taken by the benzopyran analogue.

2.12.3.1 The quinone methide biotransformation

The quinone methide metabolite results from the oxidation of the C17 methyl group of EM-652 (Scheme 2.12) and has a half-life of 32 seconds under physiological conditions. This is a considerably shorter half-life than that observed for the 4-hydroxytamoxifen quinone methide (which is 3 hours). This suggests that the acolbifene and EM-800 quinone methide metabolite forms a stable electrophilic intermediate. The quinone methide metabolite readily undergoes reactions with GSH and deoxy nucleosides, resulting in the formation of stable DNA adducts, which eventually lead to DNA damage.⁷⁰

2.12.3.2 The diquinone methide biotransformation

Oxidation involving both phenolic substituents on the benzopyran scaffolds, easily provides the diquinone methide metabolites (Scheme 2.12). As described by Dowers and co-workers, the classical protocol for the quinone methide formation, which undergoes reactions with the GSH resulting in the formation of five mono-GSH and di-GSH conjugates.⁷⁰ Formation of the acolbifene and EM-800 quinone methide metabolites thus present a major toxic pathway, relative to the diquinone methide.^{13,70} Additional information

gained from studies focused on SERMs and in particular, their oxidized metabolites, which has broadened our understanding of the varied tissue specific biochemical responses. In certain cases, the metabolite results in the formation of radicals providing a substrate, which forms stable DNA adducts and results in oxidative DNA damage.^{13,70} In addition, the formation of unstable adducts can result in the mutation and depurination of the nucleic base, damaging the DNA sequence contributing to the toxicity associated with a few of the SERM molecules.⁷⁰

2.13 Drug discovery and its development rooted from natural products

Newman and Cragg,⁸⁶ in addition to Harvey and co-workers,⁸⁷ have highlighted that natural products derived from medicinal plants, have extensively been used as a guide in the synthesis of novel compounds making valuable contributions in terms of physiological and pharmacological applications. The isolation and characterization of these natural products has allowed chemists to identify biologically active compounds and extrapolate their contributions to pharmacokinetic activities. A broad class of chemical compounds such as alkaloids, saponins, tannins, flavonoids, steroids and terpenes are but a few general functionalized compound classes that have been isolated from medicinal plants.⁸⁸ Comprehensive investigative screening processes on medicinal plant species over time, has resulted in establishing general pharmacological profiles associated with identification of the class of bioactive chemical compounds present within them.⁸⁹ The identification of these bioactive compounds, in combination with technology (such as current computational software) has allowed studies of these bioactive compounds, to further understand and predict their biochemical reactivity. This has additionally led to the derivatizing of bioactive natural products geared toward enhancing the positive biological effects, while diminishing any adverse effects associated with these compounds.

2.14 The tetrahydroisoquinoline alkaloids: Natural and synthetic substrates

Interestingly, the alkaloid class of compounds has been identified as comprising biologically active compounds and has contributed to a broad range of pharmacological activities. Alkaloids are nitrogen-containing organic compounds, many of which have been medicinally employed as hormone, allelopathic, psychotropic, circulatory and respiratory therapeutic agents.⁹⁰ A specific THIQ alkaloid identified and isolated from the Animalia kingdom, namely from *Ecteinascidia turbinata*⁹¹ as reported by Wright and co-workers, has demonstrated interesting antitumor and antibiotic pharmacological properties.^{92,93} In terms

of structure, the THIQ core can be described as a phenyl–piperidine fused ring system as depicted in Figure 2.18.

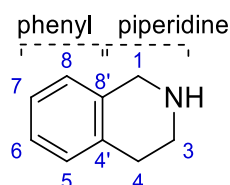
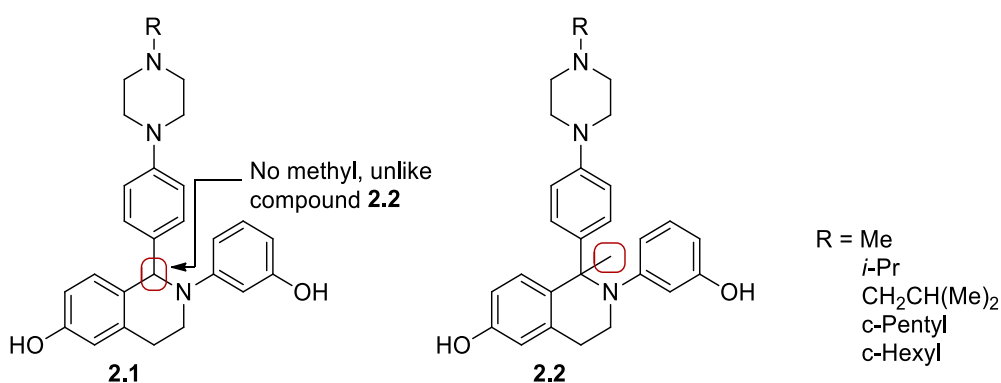


Figure 2.18. Tetrahydroisoquinoline core structure.

This privileged THIQ core has since gained a rich history and a broad spectrum of biological applications.^{5,39,40,51,93-100} Interesting work, initially driven by the Novartis company and co-workers,¹ found that the THIQ scaffold could be utilized as a structural motif which exhibited estrogenic modulator activity. At the time, this was quite advantageous since SERM research was striving towards generating new scaffolds able to address the challenges associated with the earlier developed SERM generations (refer to sections 2.7 – 2.11).⁴⁶ This concept was further explored by a number of groups, and valuable input by Renaud,^{4,39} Chesworth¹ and co-workers additionally provided new libraries of THIQ-based compounds **2.1** – **2.4** (Figure 2.19). It should be noted that analogue libraries (**2.1** and **2.2**), designed and developed by Renaud and co-workers, contain structural similarities to a well-known SERM namely lasofoxifene.^{4,39} Furthermore, THIQ-analogues **2.3** and **2.4**, designed by Chesworth and co-workers, were inspired by the tetrahydronaphthalene skeleton of the lasofoxifene SERM.¹



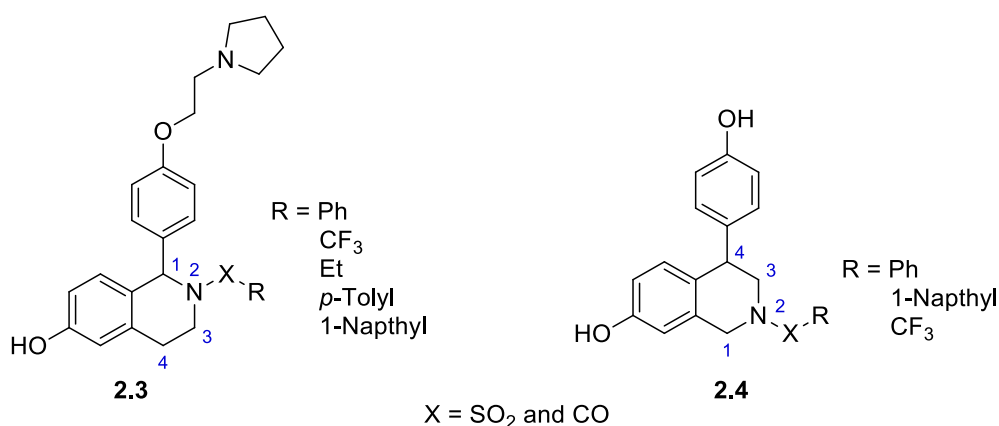


Figure 2.19. List of THIQ analogues generated by the independent research contributions by Renaud and Chesworth.^{1,4,39}

A few of the analogues listed in Figure 2.19 demonstrated improved ER α/β selectivity with a modest improvement observed upon comparison to lasofoxifene.^{1,39} Further exploration into the earlier developed SERMs by Lin and co-workers,⁵¹ focussed on generating antiestrogenic compounds by also employing the THIQ scaffold illustrated in Figure 2.20.

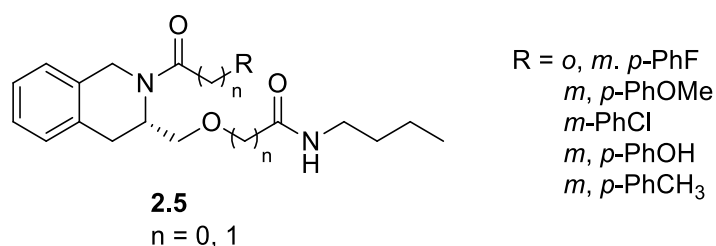


Figure 2.20. Antiestrogen compounds generated by Lin and co-workers.⁵¹

Upon comparison of compound **2.5** and its analogues in Figure 2.20 to tamoxifen, the compound **2.5** and its analogues where $n = 0$, $R = m\text{-PhOH}$, proved to be pure antiestrogens with an improved ER binding affinity being observed.⁵¹ Interestingly, the proliferation of ER positive breast cancer cell lines were selectively inhibited, but no inhibition was observed in the ER negative breast cancer cell lines.⁵¹ Apart from generating an antiestrogen, preventing adverse effects such as increased venous thrombosis, endometrial cancer and uterine bleeding, all previously associated with the 1st generation tamoxifen, illustrate why the diversion from antiestrogens to SERMs is essential.⁴⁶

These intriguing results linked to the incorporation of the THIQ scaffold attracted the attention of a number of scientific groups, including Brunsveld, ourselves and co-workers⁴⁰ who focussed their design and synthesis on small THIQ frameworks as potential ER

modulators. It was found that the THIQ molecules **2.6** and **2.7** showed moderate selectivity toward the ER β subtype and that this interaction was substituent dependent (Figure 2.21).

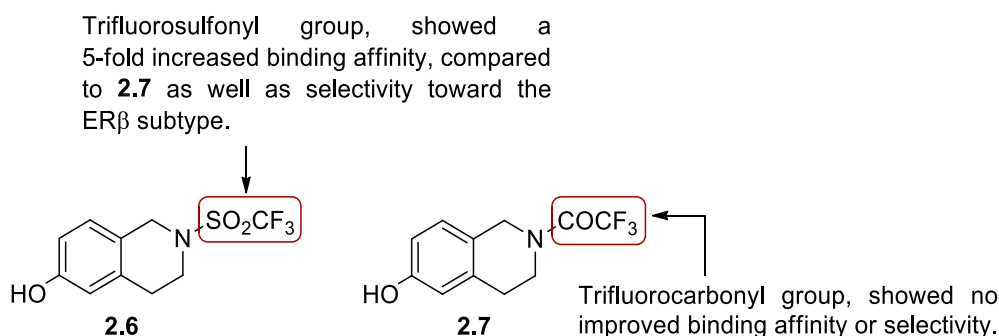
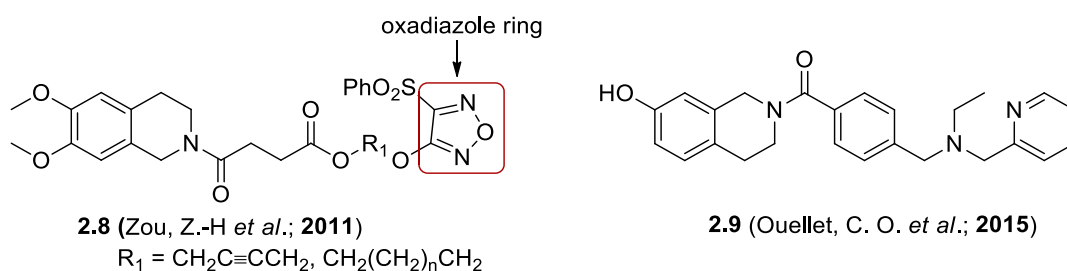


Figure 2.21. General scaffold employed by the research of Brunsveld and co-workers.⁴⁰

The trifluoromethyl carbamide moiety on the THIQ's *N*-phenyl ring, *viz.*, **2.7** (in Figure 2.21), revealed no selectivity or improved binding toward the ER-subtypes when compared to compound **2.6**; however, upon the incorporation of a trifluoromethyl sulfonamide moiety *viz.*, **2.6**, an improved 5-fold binding affinity was observed toward the ER β subtype.⁴⁰ Furthermore, work by Ouellet and co-workers focussed on generating a nonsteroidal sulfamoylated THIQ-based compound **2.9**, which showed the mitogenic inhibition of E2 in both MCF7 and T-47D cancer cell lines (Figure 2.22).⁹⁴ Similarly, Scott and co-workers employed the THIQ skeleton (which showed some structural equivalence to the compounds generated by Chesworth and Renaud), targeting and successfully generating compounds **2.10** and **2.11** to selectively downregulate ER antagonistically (Figure 2.22).¹⁰¹ Apart from this, Zhou and co-workers took a different approach, where the THIQ scaffold included the incorporation of furoxan-based nitric-oxide releasing derivatives **2.8** (Figure 2.22), which were synthesized and evaluated for their application in anticancer and multidrug resistant (MDR) reversal properties.¹⁰² The analogues **2.8** (in Figure 2.22) were compared to the therapeutic agent Adriamycin and performed reasonably well with a lower cytotoxicity, in addition to being a potent MDR reversal agent when tested against K562 and A02 cell lines.¹⁰²



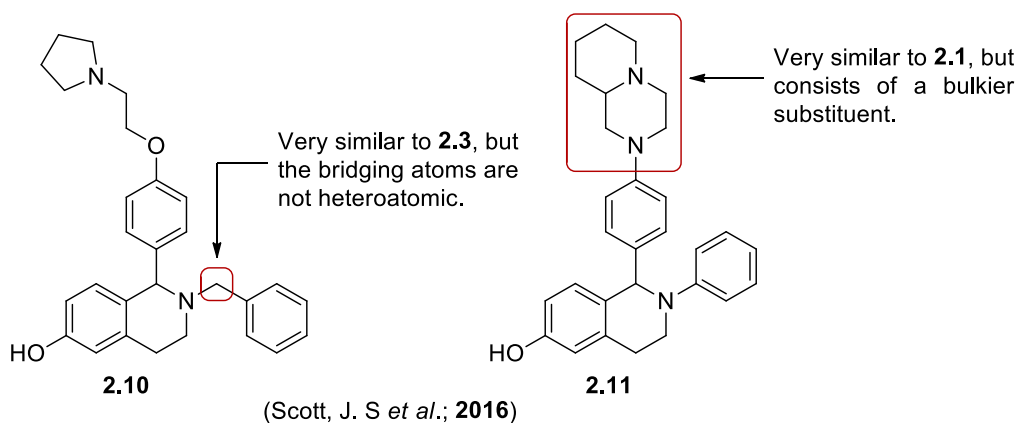


Figure 2.22. Compounds where THIQ designed scaffolds (reported by Zou,¹⁰² Ouellet,⁹⁴ and Scott¹⁰¹ and co-workers) were adopted as potential cancer therapeutic agents.

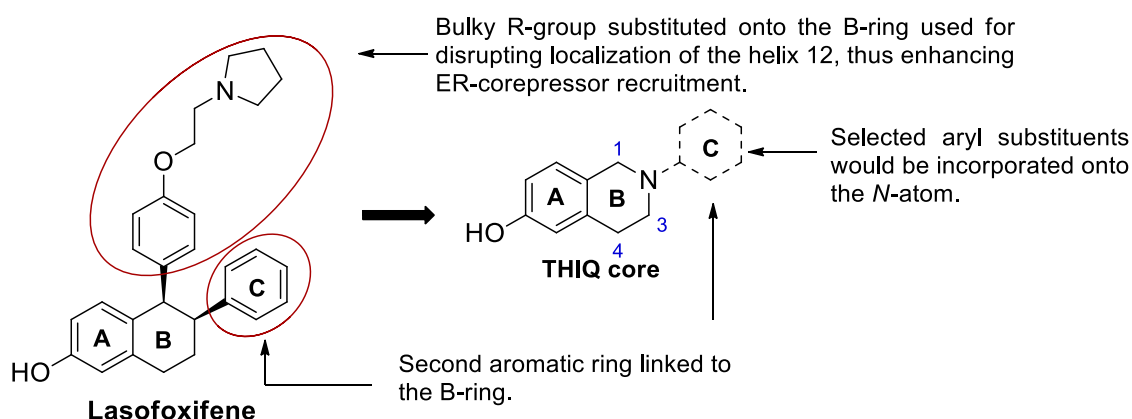
As previously mentioned in section 2.1, ERs are broadly distributed throughout the body with numerous overlapping functions and control vital pharmacological processes in the body.¹⁶ Bearing this in mind, it is clear that small molecules containing the THIQ skeleton can potentially aid in targeting therapeutic ailments such as Parkinson's disease, HIV/AIDs, antibacterials, antiinflammatories and antivirals.^{99,102-104} Conversely, reports by Surh,⁹¹ Abe³ and co-workers, suggest that the oxidized metabolites formed by THIQ analogues (namely tetrahydropapaverolines) have also demonstrated neurotoxic activity, as well as contribute to the development of potential Parkinson's disease therapeutics.^{3,91}

With its accomplishments, the THIQ scaffold has gained much attention as is evident from the literature sources provided since 1990 to date, and structures based on this motif have established its ability to behave as a SERM. Selectivity toward a specific ER subtype is essential for the inhibition of the estrogen positive breast cancer cell lines, which can be accomplished by the manipulation of the size, as well as the introduction of functional groups that may induce selectivity as reported by Brunsveld and co-workers.⁴⁰ In addition to the pharmacological properties described above, the estrogenic modulation activity presented by the THIQ scaffold has drawn our interest in the incorporation of its structural design and its relevance for this study.

2.15 Major research objectives of this project

The THIQ skeleton has proved its ability to underpin a treasure trove of structurally diverse natural products and synthetic drugs, which exhibit a series of biological and pharmaceutical activity. This has been demonstrated by its affinity for estrogenic modulation, further enhancing its applications.^{1-3,5,51,95,96,105-107} Molecules with the ability to induce or inhibit

estrogenic responses add value as biochemical tools and candidates for drug discovery, especially when treating estrogen related ailments.¹⁰⁸



Scheme 2.13. Lasofoxifene and THIQ scaffold.

With this in mind, the THIQ skeleton was selected as the most appropriate scaffold for developing a library of small THIQ-based molecules all designed according to rationalizing the structural profile of the previously mentioned compounds *viz.*, **2.1 – 2.11** in combination with molecular modeling (by making use of Schrodinger and Acclerys Discovery Studio software). Since ER α has a slightly larger binding site, larger ligands can more easily be accommodated by the α -receptor and conversely smaller ligands could be better accommodated by the β -receptor. The use of computational chemistry has further facilitated an enhanced understanding of the drug-ER interaction process and recognition sites, which could potentially enhance the desired drug interaction.⁵⁵ Structurally, most non-steroid estrogen receptor modulators, including agonists and antagonists contain three major components *viz.*, a) a core scaffold that mimics the A-phenolic moiety, b) B-rings of estrogen and a second aromatic C-ring directly connected to the B-ring of the core scaffold, and c) an antiestrogenic side chain that is substituted onto the B-ring of the core scaffold allowing torsional freedom (which can interrupt the localization of the helix 12, refer to Scheme 2.13). Chesworth and co-workers¹ revealed that the tetrahydronaphthalene skeleton of the well-known SERM lasofoxifene is structurally similar to that of the THIQ skeleton. Their findings suggested an improved activity provided by the N-atom on the ring (of the THIQ scaffold in Scheme 2.13) upon comparison to lasofoxifene and supports the incorporation of this scaffold.^{1,39,109}

The major objective of the project is to design and synthesize three small libraries of potentially active compounds based on small THIQ molecules and determine their

estrogenic structure–activity relationship. With this in mind, it was decided to employ the THIQ skeleton as the chemical core scaffold since it accommodates the requirements for non–steroid estrogen receptors as previously described. Furthermore, the presence of the *N*–atom on the THIQ skeleton would allow for the incorporation of relevant substituents (able to undergo hydrogen bond interactions). Heterocyclic structures belong to one of the most important classes of compounds in medicinal chemistry and have the ability to partake in a broad range of reactions providing valuable starting materials for broadening synthetic libraries.^{110,111} Heterocyclic systems form an essential component in our body’s functioning and their biological importance is displayed by the functioning of various vitamins, enzymes, co–enzymes, nucleic acids and neurotransmitter’s in the body.¹¹² In an attempt to take advantage of these heteroaryl systems, the thiazole ring structure was introduced onto our scaffold. Additionally, the incorporation of haloaryls would be expected to afford π –stacking interactions with one of the target residues, His475.⁵⁵ Literature discussed in section 2.12 (referring to SERM metabolic pathways), has shown that halogenated aromatic groups have less tendency of forming metabolites, which could further result in less toxic DNA adducts.

Three small libraries were designed to establish three important interactions required for mimicking key interactions with the ER.

- a) Size and selectivity. Since ER α possesses a slightly larger binding cavity than the ER β subtype, it is able to accommodate larger ligands. We aim to explore the limitations presented by steric bulk, by introducing R–groups onto the 4–position of the THIQ ring.
- b) Flexibility. This is a vital requirement for estrogenic ligand receptor interactions. Allosteric conformations need a certain degree of torsional freedom to generate a topographical surface suitable for recruiting of coregulators responsible for enhancing or repressing estrogenic gene transcription.
- c) Amino acid residues. A number of residues reside within the binding cavity of these receptors. However, only a few recognized key residues are targeted in the design of our small molecule. The aim is targeted toward key interactions with these residues, by including electron donor/acceptor functional groups onto our structural design. These functional groups could potentially generate distinguishable properties such as improving receptor specificity or enhancing (as well as diminishing) targeted interactions within a specific binding cavity.

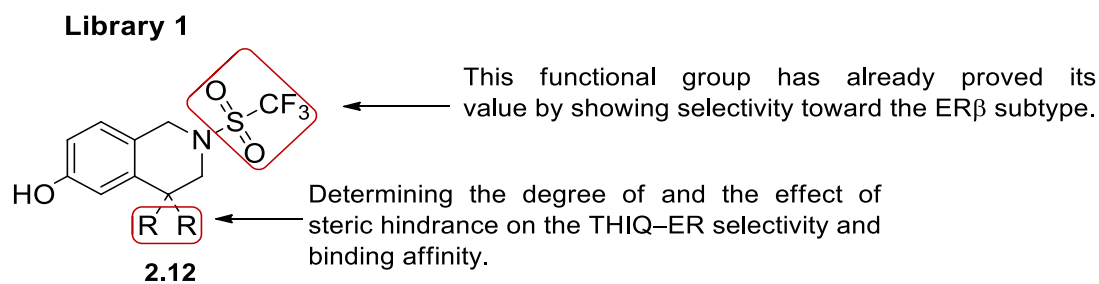


Figure 2.23. The general use of the THIQ scaffold, for further investigations into the work by Brunsveld.⁴⁰

In order to achieve and evaluate the three requirements *vide supra*, for the successful selectivity toward the ER β investigation into the structure-activity relationship, the proposed libraries of compounds were decided upon as illustrated in Figure 2.23 – 2.25 (compounds **2.12** – **2.17**). The first library (Library 1), was designed based on the work reported by Brunsveld.⁴⁰ The general scaffold **2.12** (R = H), showed selectivity toward the ER β with a 5-fold improved binding affinity. The aim of this library was to determine how increasing the molecule's steric bulk on the lower rim would either enhance or repress the activity, as well as determine size limitations, which could be accommodated by the receptor.

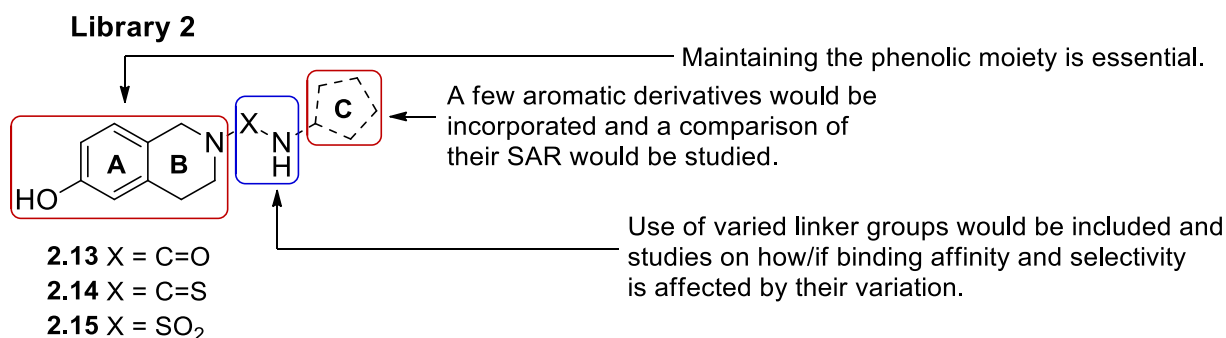


Figure 2.24. The THIQ analogues designed with the incorporation of a 2-atom spacer and various aryl groups.

The second library (Library 2) incorporates three varied linker groups aimed at facilitating the torsional freedom required for the conformational changes upon binding with the receptor (illustrated in Figure 2.24). By varying the linker groups, the urea, thiourea and sulfonyl urea motifs (compounds **2.13** – **2.15**) it is believed that this could also potentially facilitate proton donor/acceptor properties and thus influence their effects on the residues within the binding site.

Library 3

The absence of linker groups would determine its importance upon comparison to **2.13–2.15**.

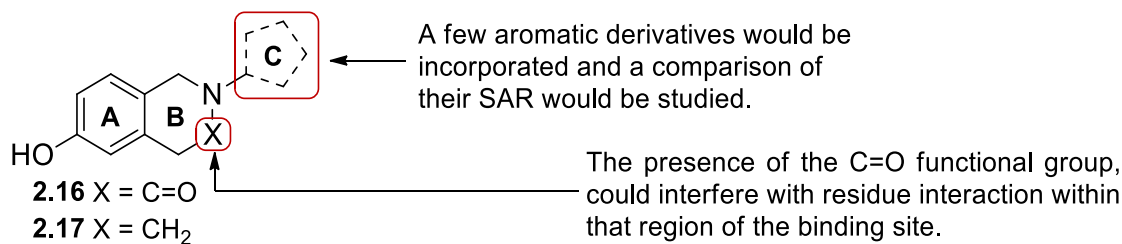


Figure 2.25. The THIQ scaffold without the 2-atom bridge maintaining the aryl groups.

The third library (Library 3) consists of an architecture similar to that of Library 2 but excluding linker groups and with the general structure displayed by compound **2.16** and **2.17** (in Figure 2.25). The aim here would be to determine the degree of torsional freedom required to support the conformations needed for binding interactions with the desired receptors. Additionally, the absence of the linker groups would allow one to determine whether their presence affects the selectivity toward the receptors or binding affinity.

Chapter 3

Synthesis of THIQ analogues

This chapter includes the synthetic routes considered for the synthesis of 6-methoxy-1,2,3,4-tetrahydroisoquinoline hydrochloride and its derivatives. The THIQ hydrochloride salt is a valuable substrate which plays a major role in several synthetic protocols and will be seen throughout this dissertation. This chapter further describes the methods employed for the synthesis of Library 1, which was generated to establish the effect of strategically placed steric bulk on the biochemical interactions of the synthetic ligand with the ER.

3.1 Introduction

Many tetrahydroisoquinoline (THIQ)-based derivatives have been established as pharmaceuticals,^{1-3,40,95,96,105-107} including compounds with antitumor, antibiotic, antimicrobial and cytotoxic applications, with their estrogenic activity being of interest in this thesis.¹¹³⁻¹¹⁵ The link which has been established between estrogen and mammary tumors and the development of THIQ-based SERMs further enhanced our interest into the THIQ core (see introductory section 2.15). The major aim of this series of compounds was directed toward mammary gland malignancies being the initial target cells. In 2004, Chesworth and co-workers illustrated structural similarities between the tetrahydronaphthalene ring system in lasofoxifene **3.1** and the THIQ core (Figure 3.1).¹ Lasofoxifene **3.1** is an estrogen modulator developed for the treatment of estrogen positive breast cancer, with the aim being to alleviate or significantly reduce side effects initially associated with the 1st and 2nd generation SERMs.^{22,83} According to the work by Renaud, Chesworth and co-workers, lasofoxifene-based THIQ analogues **3.2** – **3.9** have in fact displayed an improved antagonistic/agonistic estrogenic modulation.³⁹

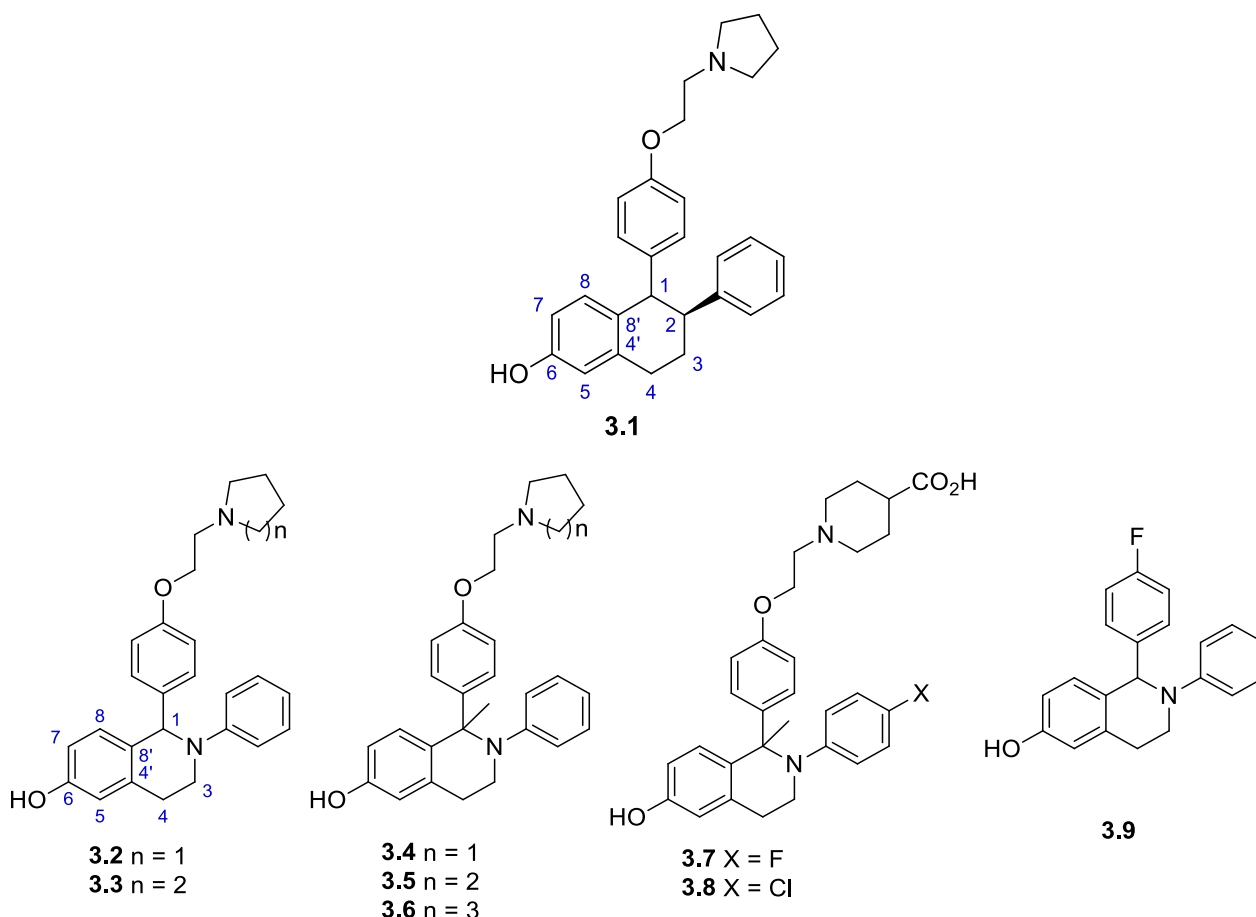


Figure 3.1. Compounds presenting ER binding capabilities and their inhibition of MCF7 cell proliferation.³⁹

Chesworth's work further suggested that the substitution on the *N*-atom of the THIQ scaffold (**3.2** – **3.9**) was responsible for the enhanced bioactivity. Previous studies on THIQ analogues, where substituted C1 and C3 derivatives showed selectivity toward both ERs, with a greater selectivity shown toward ER α binding (which is not further elaborated in this dissertation).^{1,39,51,100} Selectivity being challenging for the different ERs is associated with the shared homology between the DNA binding domains. Each binding domain contains amino acid residues within proximity of the ligand bound receptor, which plays a key role in establishing selectivity for a specific ER α / β isoform. Amino acid residues Leu384 and Met421 present within the ER α binding site are replaced by Ile373 and Met336 respectively, in the ER β 's binding site.⁵⁴ Apart from this feature, a slightly larger binding site is associated with the ER α binding site, which thus accommodates bulkier synthetic ligands, a common feature associated with the earlier developed SERMs. These minor variations within the binding site have been shown to be sufficient for distinguishing varied binding affinities and gene transcription with the ERs.^{6,54,58}

Reports from several research groups such as Brunsveld,⁴⁰ Renaud,^{4,39} Chesworth¹ and co-workers, to mention but a few, have described the estrogenic activity associated with the THIQ scaffold, which has enabled further study of the substrate as a potential drug for the treatment of breast cancer.⁴⁰ Since the functionalization of positions C1 and C3 adjacent to N2 on the ring has previously been explored, *we intend to focus our attention on substituting the 4-position and studying this effect of the activity of these analogues.*

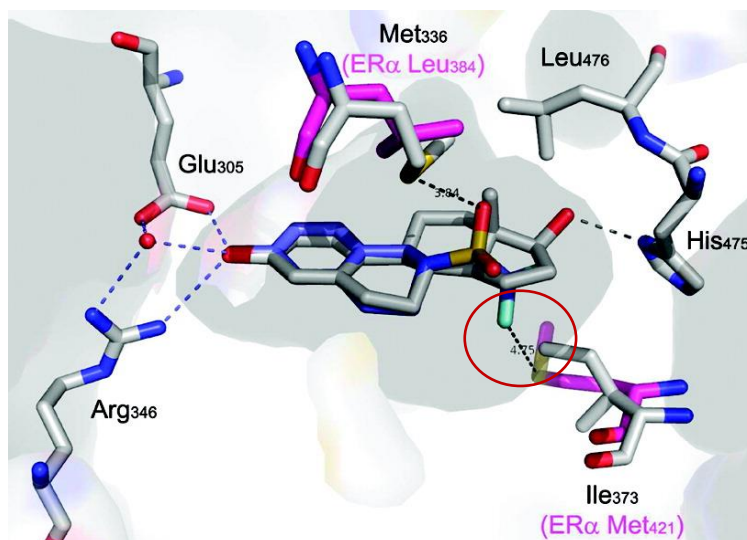


Figure 3.2. Proposed interaction between methionine residue 421 and the sulfonamide in the ER α binding site responsible for giving rise to ER β selectivity.⁴⁰

Work previously investigated by Brunsveld and co-workers, and in collaboration with our group, included the design and identification of small THIQ molecules as novel agonistic ER ligands that showed selectivity toward the ER β subtype.⁴⁰ The trifluoromethylsulfonamide THIQ analogue designed in this study led to a 5-fold increased selectivity for the ER β . This selectivity was associated with the repulsion experienced between the fluorine-atoms on the trifluoromethylsulfonamide moiety with the Met421 residue positioned in the same region within the ER α 's binding site, as confirmed by the crystal structure depicted in Figure 3.2.⁴⁰

As described in sections 2.10 and 2.11, the 3rd and 4th generation SERMs demonstrated greater selectivity toward the ER β subtype.^{48,58,70,72} Freedman's contribution towards understanding the estrogenic modes of binding proposed that, when looking at binding of the receptors with their endogenous ligand (E2), structural modifications projecting above the plane of the molecule promoted a greater ER α affinity, whereas modifications resulting in groups projecting below the plane of the molecule introduced a greater affinity toward ER β binding.⁵⁸ This was specifically demonstrated by the two SERMs lasofoxifene and

acolbifene (EM-652) (in Figure 3.3). These findings have been further confirmed by a computational analysis implemented by Zheng and co-workers.⁵⁴ Zheng's investigation confirmed that modifications to the lower region of the THIQ (synthetic ligand) enhanced interaction with the Ile373 residue situated in the binding pocket of the ER β , which is absent in the ER α binding pocket.⁵⁴ Thus, a further objective of this study was to determine the (i) pharmacological relevance, (ii) effect of size, and (iii) how the selectivity would be affected by adding steric bulk onto the C4-position of the THIQ scaffold (in Figure 3.3).

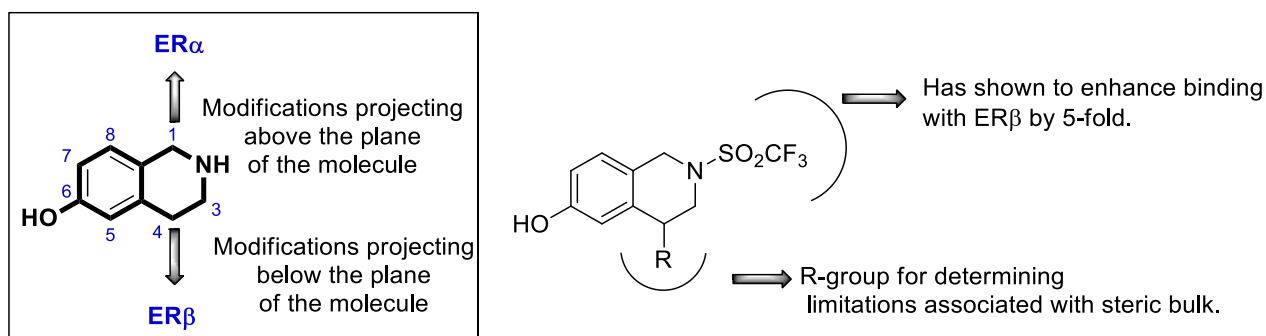


Figure 3.3. Structural enhancements on the THIQ scaffold to be investigated in this project.

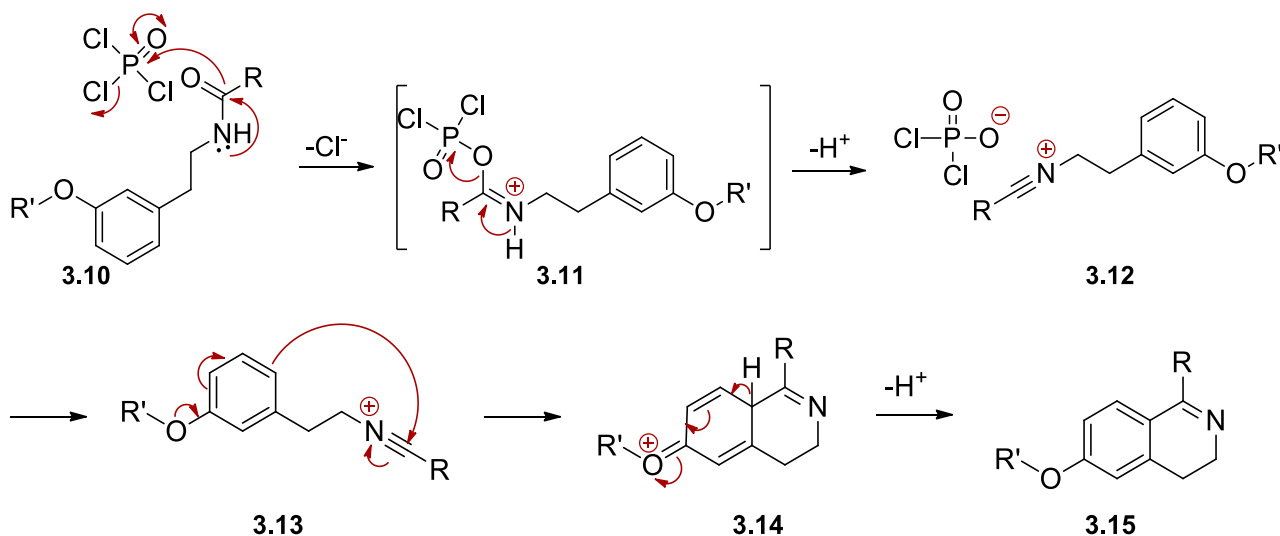
Further expanding Brunsveld's work, the intention was to investigate any enhanced structure-activity relationship upon sterically bulking up alkyl groups attached at C4-position of the THIQ scaffold.

3.2 Background chemistry on tetrahydroisoquinoline syntheses

The THIQ core may be synthesized by, amongst other methods, any of the three well documented protocols, *viz.* (a) Bischler-Napieralski, (b) Pictet-Spengler condensation or (c) Pomeranz-Fritsch reactions, as shown in Schemes 3.1 – 3.4.

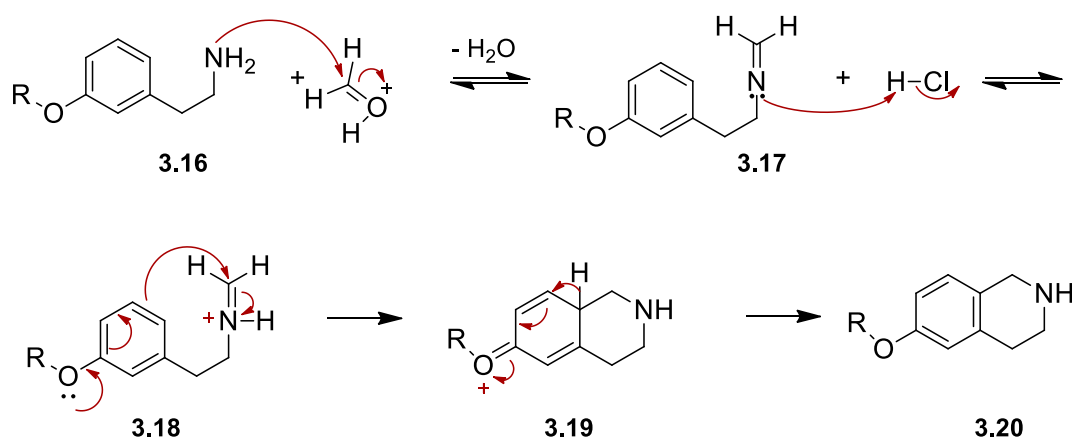
For the Bischler-Napieralski reaction, a procedure described by Wang and co-workers included the treatment of phenoxy amide **3.10** with dehydrating agents such as P₂O₅ or POCl₃ under acidic conditions, affords the 3,4-dihydro-isoquinoline **3.15**.¹¹⁶ In terms of the proposed mechanism, it is accepted that the nucleophilic attack of the amide oxygen on the dehydrating agent forms the imidoyl chloride **3.11** as a highly reactive intermediate, which transforms itself into the nitrilium salt **3.12**. An intramolecular electrophilic aromatic substitution *para* to the OR'-group of the phenolic moiety in **3.13** forms the bicyclic intermediate **3.14**, which rapidly aromatizes to give the 3,4-dihydro-isoquinoline **3.15** in Scheme 3.1.¹¹⁷ The presence of electron-donating groups on the phenyl ethyl amides is

known to increase the electron density on the aryl nucleus and consequently influences the regioselectivity, as well as the reaction rate.



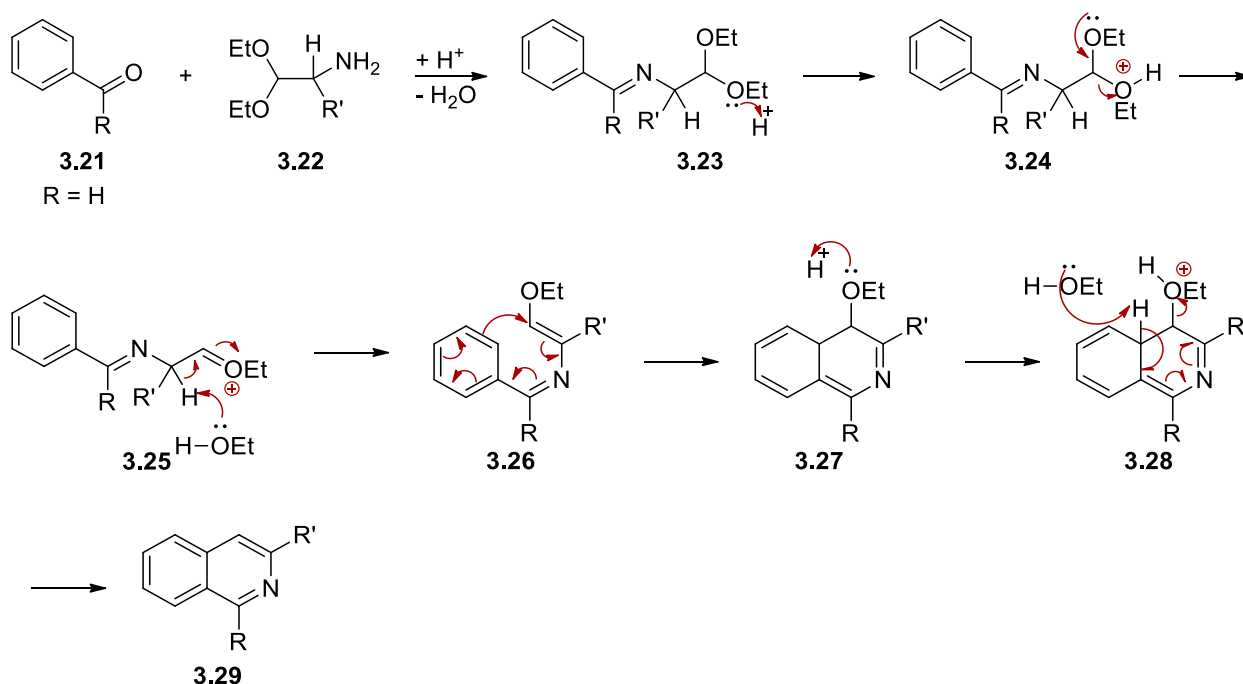
Scheme 3.1. The accepted mechanism for the Bischler–Napieralski reaction.¹¹⁷

In much the same way as the Bischler–Napieralski reaction, it is clear that electron-donating groups on the aryl ring are also an essential pre-requisite to drive the electrophilic aromatic substitution in the Pictet–Spengler reaction, as shown in Scheme 3.2. The Pictet–Spengler method employs a typical phenolic ethyl amine *viz.*, **3.16**, which when treated with an aldehyde or ketone under acidic conditions forms an enamine **3.17**, which upon protonation produces the enaminium salt **3.18**. An intramolecular cyclization then follows generating the THIQ analogue **3.20** by an electrophilic substitution onto the aryl ring again *para* to the alkoxy substituent by way of **3.19** (Scheme 3.2).^{117,118}



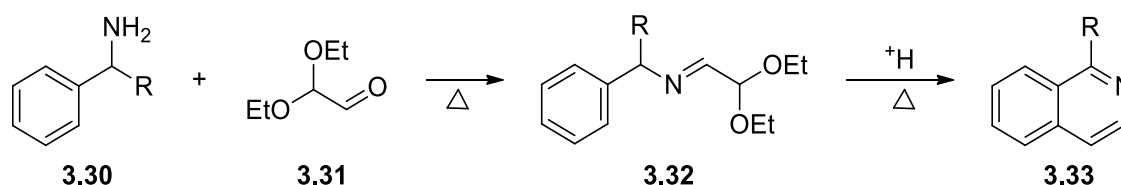
Scheme 3.2. The Pictet–Spengler reaction.¹¹⁸

In the Pomeranz–Fritsch cyclization, the reaction is initiated by condensation between the aryl aldehyde **3.21** with a 2-aminoacetal **3.22** to afford the aldimine **3.23**. Subjecting **3.23** to strong acidic conditions results in the protonation of the ethoxy (OEt) group of the acetal **3.24**, followed by the loss of EtOH to generate the intermediate **3.25**, which under the acidic conditions forms the unsaturated compound **3.27**. Further transformation of compound **3.27** provides the isoquinoline **3.29** and upon further hydrogenation substituted variants of the analogue **3.20** would then be accessible.¹¹⁷



Scheme 3.3. The accepted mechanism for the Pomeranz–Fritsch cyclization.¹¹⁷

Regarding the latter protocol, there is a well-known variation of the Pomeranz–Fritsch cyclization known as the Schlitter–Müller condensation reaction. In this case, the isoquinoline analogue **3.33**, having a single substituent at C1, may be produced by condensation of the aryl amine **3.30** with an aldehyde acetal *viz.* **3.31**, under acidic conditions as shown in Scheme 3.4.¹¹⁷



Scheme 3.4. The Schlitter–Müller condensation.¹¹⁷

3.3 Synthesis of the 2-[(trifluoromethyl)sulfonyl]-1,2,3,4-tetrahydroisoquinolin-6-ol

Considering the above synthetic options for constructing the THIQ scaffold, it appeared that the Bischler–Napieralski reaction is used mainly for the introduction of substituents onto the C1-position *viz.*, **3.15**, the Pictet–Spengler reaction is used for producing the general THIQ scaffold *viz.*, **3.20**, while the Pomeranz–Fritsch reaction introduces substituents onto the C1 and C3 positions *viz.*, **3.29** (in Figure 3.4). However, when implementing the Pictet–Spengler conditions on substrate **3.16**, activation of the C5- and C9-position by the methoxy electron-donating group, could result in two possible products, **3.20** (being the preferred and major product), as well as **3.20a**. Since **3.20** was a valuable intermediate, as will be seen in the following chapters, it was consequently decided that a modified Pictet–Spengler protocol, a method described by Zhong and co-workers, would be implemented to create a library of compounds containing the general structure **3.20**.¹¹⁹

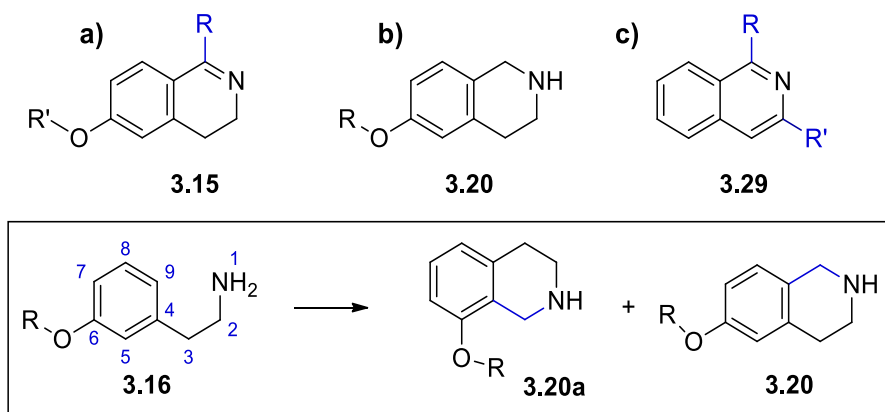


Figure 3.4. General structures from the **a**) Bischler–Napieralski **3.15**, **b**) Pictet–Spengler **3.20** and **c**) Pomeranz–Fritsch **3.29** reaction protocols.

The THIQ scaffold was thus synthesized starting from 2-(3-methoxyphenylethyl)amine **3.35** (refer to Scheme 3.5) where the amine heteroatom would present the desired opportunity for derivatization of the *N*-atom to generate a library of THIQ analogues based on the reference structure **3.34** in Figure 3.5.

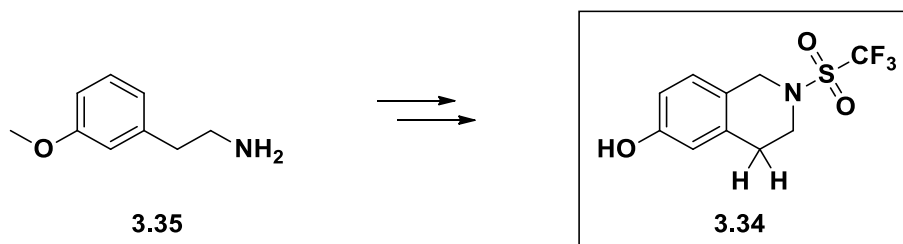
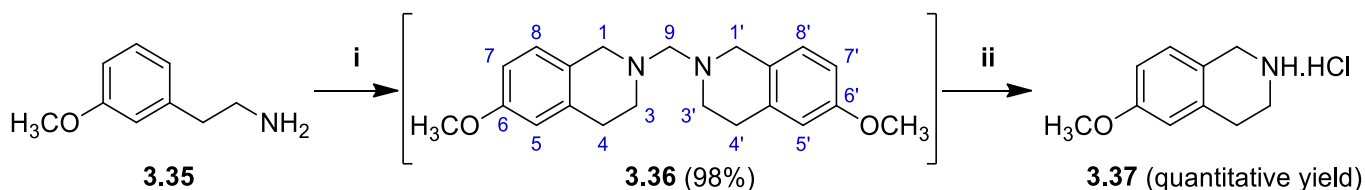


Figure 3.5. THIQ scaffold modified by the substitution of trifluoromethyl group.

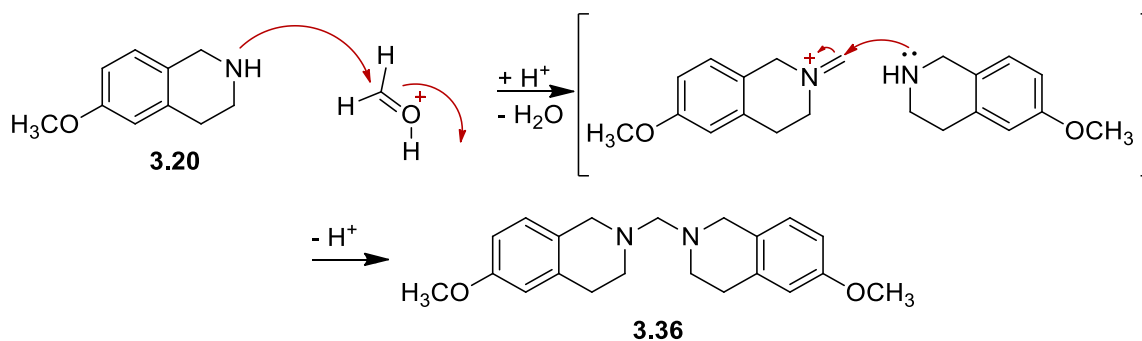
3.3.1 Synthesis of the 6-methoxy-1,2,3,4-tetrahydroisoquinoline hydrochloride salt

For the synthesis of 2-[(trifluoromethyl)sulfonyl]-1,2,3,4-tetrahydroisoquinolin-6-ol **3.34**, the employment of a modified Pictet–Spengler protocol was considered to be viable, which thus formed the basis of the current approach as illustrated by the first step shown in Scheme 3.5.



Scheme 3.5. Reagents and conditions described by Zhong and co-workers:¹¹⁹ (i) 37% CH₂O, 1 N HCl, 60 °C, 4 h; (ii) HCl, IPA, RT, 18 h.

We used a procedure reported by Zhong and co-workers, in the first two steps for the preparation of the desired THIQ scaffold which was closely followed in this work.¹¹⁹ This method included starting from commercially available 2-(3-methoxyphenyl)ethan-1-amine **3.35** and formaldehyde, which would result in the formylation of the terminal amine under acidic conditions to form a Schiff–base–type intermediate. However, under these conditions the dimeric intermediate **3.36** was produced (Scheme 3.5). The aminor dimer **3.36**, being polar, simply precipitated out of the aqueous solution as a white solid, which was filtered and allowed to air dry. The structure of **3.36** was confirmed by ¹H-NMR spectroscopy, in which the protons of the methylene bridge (C9) appeared as a singlet at δ 3.26, integrating for 2-protons. Relative to these methylene protons there was a doubling of all proton integrations for the aromatic signals, as well as the methoxy groups, which supported the assigned dimeric structure of intermediate **3.36**, and corresponded well to the reported literature values.¹¹⁹ It is believed that initially the Pictet–Spengler product **3.20** is formed as illustrated in Scheme 3.2, but that in the presence of excess formaldehyde, a Mannich–type reaction proceeds through an intermediate imine forming the dimer **3.36** (Scheme 3.6).

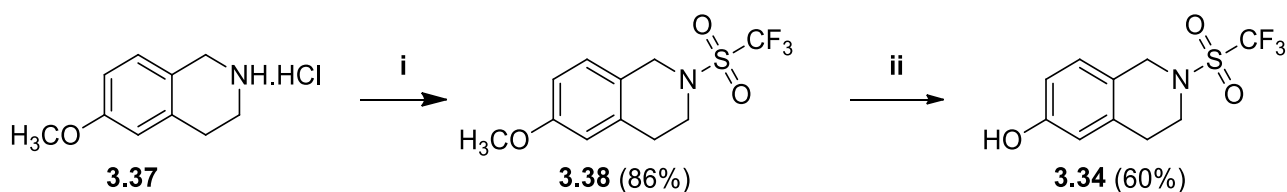


Scheme 3.6. The abbreviated mechanism for the formation of dimer **3.36**.

With the amination dimer **3.36** in hand, it was suspended in isopropyl alcohol (IPA) and upon treatment with a strong acid (HCl) under stirring for 18 hours at room temperature, it cleaved to give the THIQ hydrochloride salt **3.37**. This compound was isolated by trituration with methyl tertiary butyl ether (MTBE) and continuous stirring for a further 4 hours, resulting in the formation of a dense white mixture. The reaction mixture was then cooled to 0 °C and filtered using vacuum filtration, whilst washing with a 1:1 ratio of IPA/MTBE. An important factor to note was that the use of diethyl ether or petroleum ether as solvent, resulted in no precipitation. No further purification was required and the product **3.37** was isolated in good yields of 70 – 90% as a white amorphous solid. The structural integrity of compound **3.37** was confirmed by ¹H-NMR spectroscopy. The absence of the methylene bridge, originally at δ 3.26, was supplemented by a new signal *viz.*, a broad downfield 2-proton singlet at δ 9.47 [for the protonated NH (HCl) functionality]. Compound **3.37** was a valuable intermediate in a number of synthetic strategies employed in this project and represents an essential scaffold, upon which a number of derivatives were synthesized to produce the library of compounds needed for the study. Maintaining the masked hydroxyl as a methyl ether throughout all synthetic procedures was essential, mainly to avoid possible side reactions with the phenolic hydroxyl group.

3.3.2 Synthesis of the trifluoromethyl sulfonamide **3.34**

Introduction of the trifluoromethyl sulfonyl moiety was performed onto the basic THIQ scaffold by following a protocol described by the Brunsveld and van Otterlo groups. The THIQ scaffold formed an essential synthetic component for generating the molecule (**3.34**) previously shown to display moderate selectivity for one specific receptor (ER β) isoform.⁴⁰



Scheme 3.7. Reagents and conditions: (i) Et_3N , Tf_2O , CH_2Cl_2 , 5 h; (ii) BBr_3 , CH_2Cl_2 , -60°C , overnight.

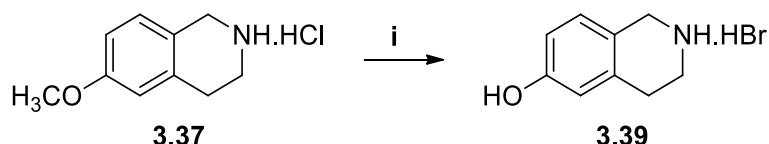
According to a procedure described by Bailey and co-workers,¹²⁰ treatment of **3.37** with triflic anhydride was performed under basic conditions (triethylamine) with stirring at room temperature for 3 hours. This was followed by concentration under reduced pressure, which afforded a brown residue which was purified by column chromatography to obtain product **3.38** as an orange oil in an 86% yield. The successful production of product **3.38**, was confirmed by ^1H - and ^{13}C -NMR spectroscopy. The most vital variation observed between the ^1H -NMR spectra of **3.37** and **3.38** was the absence of the amine (NH) signal at δ 9.47 from the former, indicating the successful replacement of NH by the triflate group forming the trifluorosulfonamide.

3.3.4 Demethylation of the aryl methyl ether

As mentioned before, the hydroxyl motif was masked as the methyl ether throughout the previous synthetic procedures. Despite the amine presenting a more nucleophilic nucleus to that of the hydroxyl motif, the potential of side reactions occurring at the hydroxyl group was still a possibility and it was considered wise that in order to avoid this, the hydroxyl motif be retained in the masked form. The phenolic group makes a valuable contribution toward binding in small molecule-large biomolecule systems, presenting an anchoring/binding site for a number of residues.^{24,53} Thus, the final requirement in the synthesis of reference compound **3.34** entailed the demethylation of the aryl methyl ether **3.38**. Aryl methyl ethers are usually cleaved under fairly harsh conditions such as Lewis acids and strong acids,¹¹⁹ for long periods of time and at high temperatures. The introduction of functional groups onto the scaffold generates a number of additional reactive sites, which could enhance the compound's sensitivity toward harsh conditions, and which could potentially cleave or hydrolyse these functional groups under these conditions.

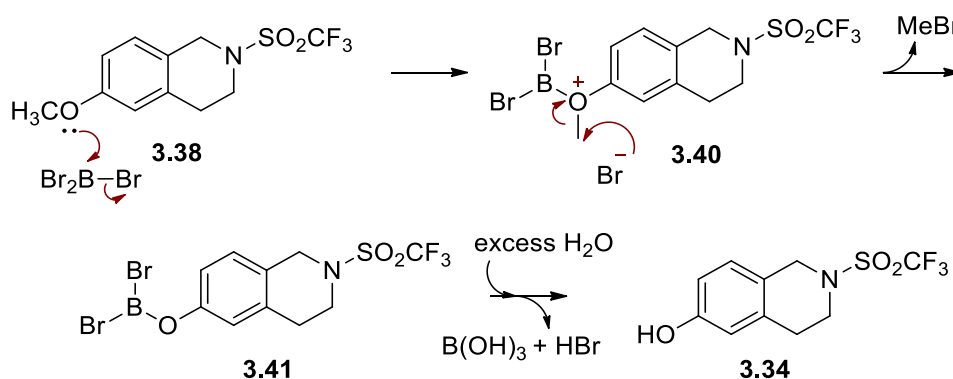
The general reaction procedure described by Brunsveld and co-workers,⁴⁰ as illustrated in Scheme 3.8, was employed to establish the best practice as a demethylation technique (using aqueous HBr), but unfortunately the yields associated with this method were not reproducible, since it relies on the precipitation of the product.⁴⁰ Monitoring the progress of

the reaction was also rather problematic since it involved proceeding from one salt to another, in which the R_f values remained in the region of almost zero and the spots thus remaining on the baseline. Yields for the reactions attempted ranged from 40 – 70%. Product formation for compound **3.39** was confirmed by use of $^1\text{H-NMR}$ spectroscopy, where the methoxy signal previously observed at δ 3.71 for compound **3.37** was absent. This method required patience in waiting for the product to crystallize from the mother liquor without the assurance of complete crystallization.



Scheme 3.8. Reagents and conditions described by Brunsveld, L. *et al* for demethylation: (i) 47% HBr stirred at 105 °C for 18 h.

Despite the above-mentioned challenges associated with Scheme 3.8, the introduction of additional functionalities on the *N*-atom of the THIQ nucleus, *viz.*, compound **3.38** necessitated that a milder approach be considered. To this end, a procedure described by McOmie and co-workers was utilized,¹²¹ where the aryl methyl ether **3.38** was dissolved in CH_2Cl_2 and cooled to $-40\text{ }^\circ\text{C}$, to which three equivalents (per methyl ether) of boron tribromide (BBr_3) in CH_2Cl_2 was slowly added (refer to Scheme 3.9). A temperature of $-40\text{ }^\circ\text{C}$ was maintained for 1 hour, followed by stirring at room temperature for 4 hours, which gave complete conversion to afford the 6-hydroxyl THIQ analogue **3.34**. The reaction conditions employed were found to be efficient and clean, providing product **3.34** in a moderate yield of 60% as a thick brown oil after purification by column chromatography. The proposed mechanism for the demethylation is given in Scheme 3.9.

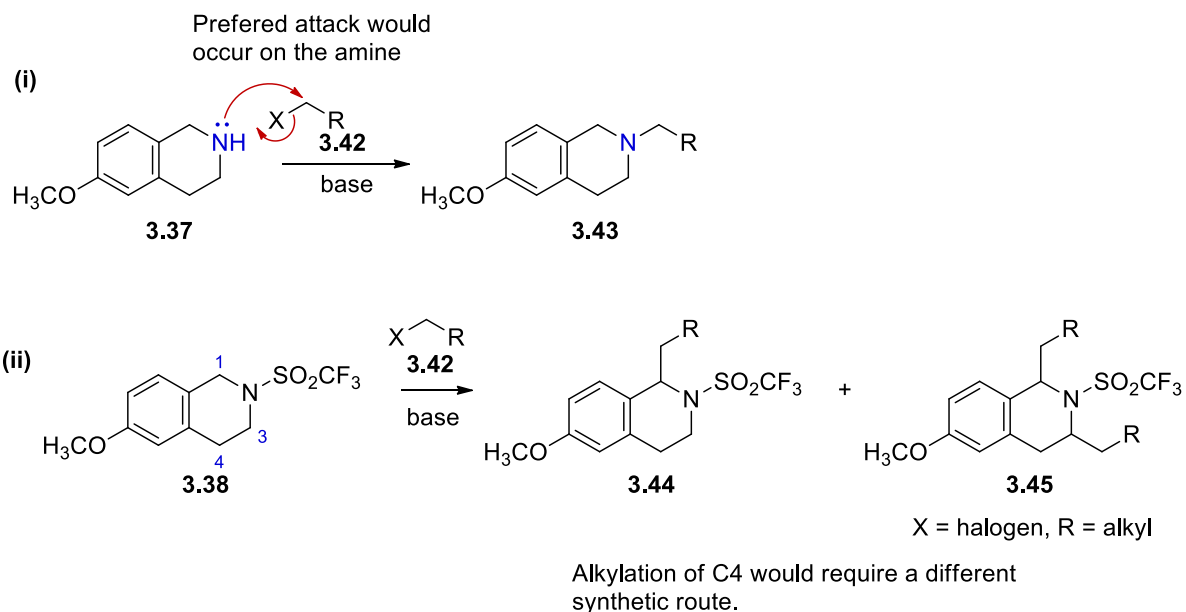


Scheme 3.9. A proposed mechanism for the aryl methyl ether demethylation.

Methyl bromide, being a gas and one of the side products, was easily liberated from the reaction mixture upon reaching room temperature and a water work-up generated HBr *in situ*, affording the acid required for protonation of the alkoxy ion generated. Excess boron species was hydrolysed in water giving boronic acid and HBr, which was readily abstracted into the aqueous layer, affording **3.34** upon further extraction with EtOAc. The impurities easily dissolved into the water layer, which meant that no further purification was required unless for the removal of unreacted material. ¹H-NMR spectroscopy confirmed the absence of the methyl ether signal previously found at δ 3.74, thus confirming the successful demethylation. In addition, the ¹³C-NMR spectrum in certain cases clearly demonstrated coupling interaction between the C-atom of the triflic motif and the adjacent F-atoms providing a quartet signal at δ 121.97 and δ 118.75 ($J = 241.5$ Hz, CF₃) to further substantiate the presence of the *N*-sulfonation (SO₂CF₃).

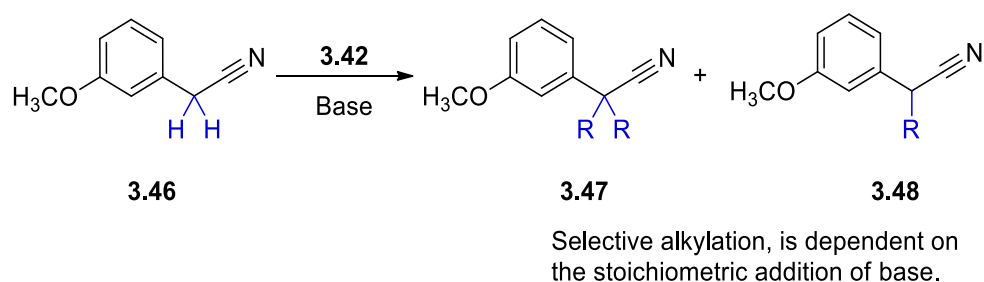
3.4 The synthesis of the C4 analogues 3.49

With the successful synthesis of reference compound **3.34**, synthesis of its C4 alkylated derivatives were explored. The C4 analogues were generated to provide an understanding of the limitations steric bulk would present in the binding pocket. It was considered that the introduction of a R-group at the C4-position of the reference compound **3.34**, by way of an alkylative approach in the presence of the amine or trifluorosulfonamide functionality was not possible for the following reasons: (i) amines (**3.37**) are excellent nucleophiles for substitution reactions involving halogenated alkanes and (ii) upon protection of the nitrogen giving the sulfonamide compound **3.38**, the more reactive positions are the α -carbons adjacent to the *N*-atom with C1 being the more preferred position (being adjacent to the aryl ring), followed possibly by the C3-position (Scheme 3.10).



Scheme 3.10. Preferred positions for C-alkylation on the general THIQ scaffold.

A known suitable strategy for alkylating the C4-position required a different protocol described by Melvin and co-workers,¹²² involving the use of 2-(3-methoxyphenyl)acetonitrile **3.46** as the initial substrate. The selective α -alkylation, controlled by reaction conditions, may then effectively be employed to synthesize either the di- or monoalkylated derivatives **3.47** and **3.48** respectively, as illustrated in Scheme 3.11. It is thus important to realize that we deemed it necessary to introduce the alkylations very early in the synthetic sequence. The advantage being control, but with the disadvantage that it would not allow for a divergent functionalization strategy later.



Scheme 3.11. Chemoselective alkylation of 2-(3-methoxyphenyl)acetonitrile with haloalkyls (**3.42**) under alkaline conditions.

The above reasoning was that after alkylation, reduction of the nitrile **3.47** would give the corresponding amines and thus act as starting materials for the Pictet–Spengler protocol previously illustrated in Scheme 3.2, to afford a library of THIQ analogues **3.49** (in Figure

3.6). A reference compound **3.34** (where, R = H) already in hand would be used for the purpose of comparing its biochemical effect to that of the various **3.49a – d** analogues.

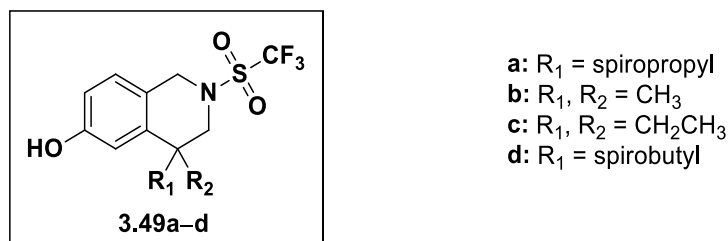
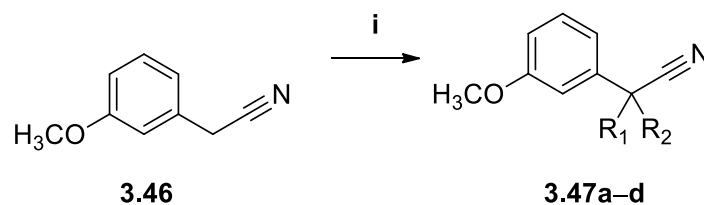


Figure 3.6. Target 4-alkylated 2-[(trifluoromethyl)sulfonyl]-1,2,3,4-tetrahydroisoquinolin-6-ol analogues.

3.4.1 Synthetic protocol for alkylation of 2-(3-methoxyphenyl)acetonitrile

To this end, commercially available 2-(3-methoxyphenyl)acetonitrile **3.46** was treated with 60% NaH at 0 °C under anhydrous conditions in DMF, by employing a modified protocol described by Melvin and co-workers.¹²² The suspension was allowed to warm to room temperature and then treated with the desired haloalkanes under the conditions illustrated in Table 3.1. Upon treatment with the dihalogenated alkanes 1,2-dibromoethane and 1,3-dibromopropane it was found that 1 equivalent of halogenated species afforded low yields (40%) of the desired products. However, the addition of an excess of the halogenated species resulted in even lower yields and in some cases no product at all. This was confirmed by a multiple number of spots on the TLC. Once isolated it was confirmed that the monoalkylated species was formed. It was subsequently found that by modifying the stoichiometric ratio of dibrominated alkane to 1.10 – 1.20 equivalents, much improved yields ranging between 81 – 86% were obtained. The products were isolated after work-up and readily purified by column chromatography. Compound **3.47a** was isolated as an oil and its structural integrity confirmed by ¹H-NMR spectroscopy. The presence of two 2-proton multiplets at δ 1.40 and δ 1.71 supported the cyclopropyl formation. The presence of the cyclobutyl moiety of **3.47d**, resulted in a more complex ¹H-NMR spectrum comprising a number of multiplets between δ 2.07 – 2.89 integrating for 6-protons, which to an extent could be explained by the conformational lability of the cyclobutyl ring. Apart from the spirocyclic compounds **3.47a** and **3.47d**, the dialkylation only required a slight variation in the previously applied parameters.

Table 3.1. Diverse alkylation of 2-(3-methoxyphenyl)acetonitrile.

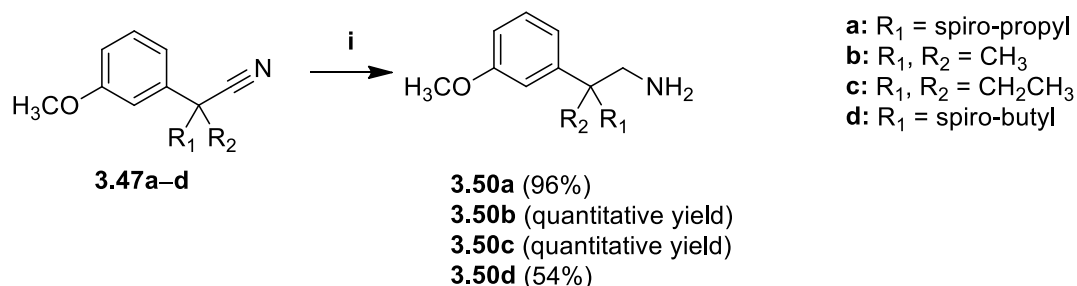
Entry	Substrate	Haloalkane	Product	Yield (%)
1	3.46			86
2	3.46			Quantitative
3	3.46			77
4	3.46			81

Reaction conditions described by Melvin and co-workers¹²² for alkylation of **3.46**: (i) DMF at RT, ^aNaH (8.0 equiv), haloalkane (4.0 equiv); ^bNaH (8.0 equiv), haloalkane (1.1 equiv).

Upon treatment of **3.46** in the NaH/DMF suspension with 2 equivalents of the monohaloalkanes *viz.*, iodomethane (MeI) and bromoethane (EtBr), multiple products were formed, as illustrated by their reaction TLC profiles. The multiple spots no doubt represented the monoalkylated product, dialkylated product and/or unreacted starting material. The reaction conditions were thus optimized, and it was determined that a large excess of haloalkane was required to give the dialkylated species. The products **3.47b** and **3.47c** were isolated and purified by column chromatography in good yields, as shown in Table 3.1. Once again, assignment of the structures for these compounds was confirmed by ¹H- and ¹³C-NMR spectroscopy. For example, compound **3.47b** was isolated in a quantitative yield as a colourless oil. An intense 6-proton singlet at δ 1.67 indicated the presence of the two equivalent methyl groups. Compound **3.47c** was also isolated as an oil in 77% yield and was identified by a 6-proton triplet at δ 0.88 and a 4-proton multiplet centred at δ 1.92, indicative of the diethyl alkyl side chains.

3.4.2 Reduction of nitriles **3.46a – d** to amines **3.47a – d**

Having the various alkylated nitriles **3.47a – d** in hand, reduction of the nitrile functionality was next investigated as shown (in Scheme 3.12).



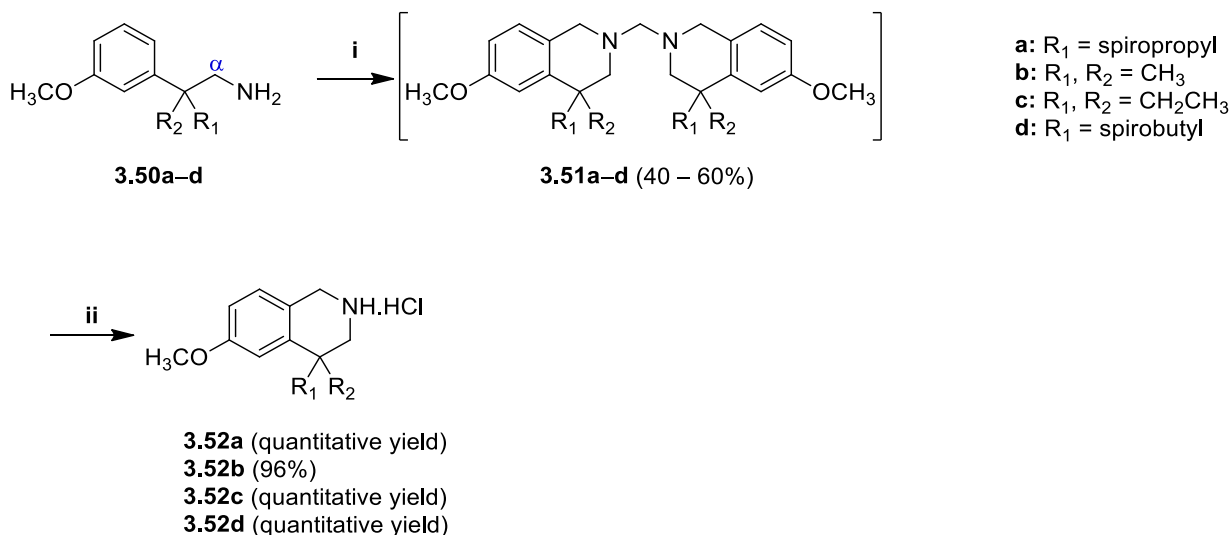
Scheme 3.12. Reagents and conditions for the reduction of nitriles: (i) AlH₂Cl, THF under reflux for 5 h.¹²³

Reduction of the nitrile group was naturally necessary for the all-important Pictet–Spengler ring closing condensation, being an essential element in the synthetic strategy of this THIQ protocol formation. The nitrile analogues **3.47a – d** were efficiently reduced to their corresponding amines (in Scheme 3.12) by following a procedure described by Nystrom,¹²³ Davis¹²⁴ and co-workers. Treatment of **3.47c – d** with monochloroalane (AlH₂Cl), prepared *in situ* from a 1:1 mixture of LiAlH₄/AlCl₃ in THF at 0 °C resulting in a grey suspension. The suspension was warmed to room temperature and stirred for 15 minutes, after which it was once again cooled to 0 °C, to which a mixture of **3.47a – d** in THF was slowly added. Upon consumption of **3.47a – d** (confirmed by TLC monitoring), the products were isolated in good yields after column chromatographic purification. The structures of products **3.50a – d**, in which all had an additional methylene group and an amine functional group, were confirmed by ¹H- and ¹³C-NMR spectroscopy. Thus, a 2-proton singlet found at δ 2.77 – 2.86 confirmed the presence of the new methylene group, while the absence of the nitrile motif with the carbon signal previously found at δ 120.2 in the ¹³C-NMR spectrum, further supported the successful reactions.

3.4.3 Synthesis of the THIQ salts **3.52a – d**

Amines **3.50a – d** were treated under similar Pictet–Spengler conditions as previously described for compound **3.35** (in Scheme 3.13). Thus amines **3.50a – d** were treated with 37% formaldehyde in the presence of 1 N HCl at 60 °C for 4 hours. The reaction mixtures were cooled to 0 °C and basified with NaOH. It was found that under these small-scale reaction conditions no precipitant was formed and thus an EtOAc extraction was required

for the isolation of product. Increasing the scale of the reaction still did not afford a solid precipitate, but instead gave a sticky gum-like residue after filtration. Unlike for the compound **3.36**, the yields were not very good giving products ranging in yields of between 40 – 60%. In addition, purification of the intermediates was not effective, and it was decided to use the crude material in the next reaction step.



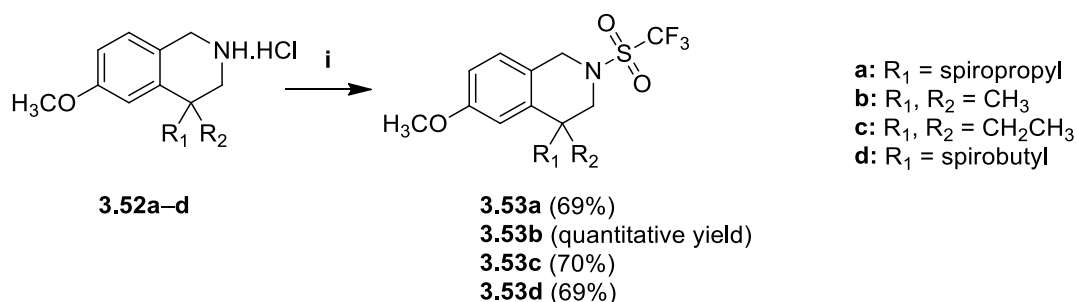
Scheme 3.13. Reagents and conditions for generating the THIQ salts: (i) 37% CH₂O, 1 N HCl, 60 °C, 4 h; (ii) HCl, IPA, RT, 18 h.

However, it should be noted that the ¹H-NMR spectra of all crude intermediates showed the presence of the key signal for the methylene bridge protons for compounds **3.51a – d**. The gum-like residues **3.51a – d** were next suspended in IPA, to which the HCl was added and stirred overnight at room temperature. Formation of the hydrochloride salts **3.52a – d** then proceeded, followed by MTBE addition (in Scheme 3.13). The reaction mixtures were cooled to 0 °C for 3 hours to enhance precipitation and the products **3.52a – d** were isolated in good to quantitative yields by filtration. The ¹H-NMR spectra of these compounds confirmed product formation by the presence of a broad 2-proton downfield singlet at δ 9.78 – 9.62 for the protonated amine (NH₂Cl). An intense 2-proton singlet in the region of δ 4.25 – 4.11 was also illustrative of the aryl α-methylene group.

3.4.4 Synthesis of the trifluoromethyl sulfonamide analogues

To allow for the biochemical comparison of the THIQ scaffolds containing sterically demanding groups on the C4-position it was now necessary to convert them into their respective trifluorosulfonamide to allow for comparison with compound **3.34** designed and tested in the Brunsveld and van Otterlo study.⁴⁰ To this end, a similar synthetic pathway

employed for the synthesis of compound **3.38** was followed in the synthesis of compounds **3.53a – d** as illustrated in Scheme 3.14.

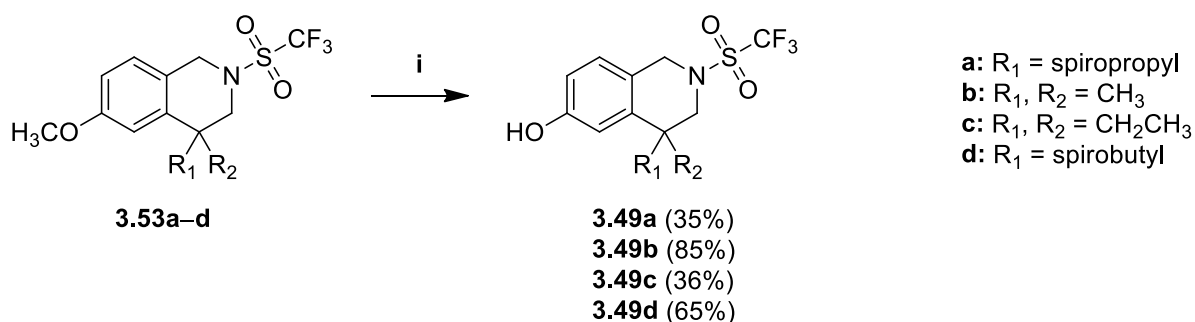


Scheme 3.14. Reagents and conditions for the synthesis of trifluorosulfonamide: (i) Et₃N, Tf₂O in CH₂Cl₂, RT, 5 h.¹⁰²

A general procedure described by Bailey and co-workers¹²⁰ was followed, where hydrochloride salts **3.52a – d** and Et₃N dissolved in anhydrous CH₂Cl₂, were combined. The reaction mixture was then cooled to –40 °C, to which triflic anhydride was slowly added over a 15-minute period. The progress of the reaction was monitored using TLC, which indicated consumption of starting materials **3.52a – d**, between 4 – 6 hours depending on the substrate. After a work-up, brown coloured residues were obtained, which were further purified by column chromatography to give the products **3.53a – d** as thick oil-like substances in good yields ranging between 69 – 86%. ¹H- and ¹³C-NMR spectroscopy were employed for confirmation of the structures of compounds **3.53a – d**. The ¹H-NMR spectra were very useful in this regard, since the absence of the amine (N–H) signal previously noted at δ 9.73 – 9.62 for compounds **3.53a – d** was absent. Additionally, positive electron spray time of flight mass spectrometry (ESI⁺ TOF MS) was employed to confirm the successful *N*-sulfonation of the precursors **3.52a – d** to give sulfonamides **3.53a – d**. Compound **3.53a** did not appear very stable with multiple spots being observed after column chromatography. These multiple spots were isolated in trace amounts and further spectroscopy to confirm their structure was not attempted. The expected structure was further confirmed by a reasonably good ¹H-NMR spectrum, but it should be noted that the calculated monoisotopic mass of **3.53a** was (C₁₃H₁₄F₃NO₃S) 322.0680, while the experimental monoisotopic mass was found to be 290.2690. The calculated monoisotopic mass for **3.53c** (C₁₅H₂₀F₃NO₃S) was 350.1038; with the experimental monoisotopic mass being 350.1046 and thus corresponded well. Finally, compound **3.53d**, had a calculated monoisotopic mass of (C₁₄H₁₆F₃NO₃S) 336.0837 and was found to correspond well with the experimental monoisotopic mass of 336.1977.

3.4.5 Demethylation of aryl methyl ethers **3.53a – d**

The final step in the synthesis of the first target library was the demethylation of sulfonamides **3.53a – d**. With the sulfonamides in hand, and using the established protocol described by McOmie and co-workers,¹²¹ the aryl methyl ethers **3.53a – d** were dissolved in CH₂Cl₂ and cooled to -40 °C as illustrated in Scheme 3.15. A solution of BBr₃ in CH₂Cl₂ was then slowly added to the cooled solution of the sulfonamides, which resulted in orange coloured solutions. The reaction mixtures were stirred at room temperature overnight to afford the demethylated products as oils after work-up, all in poor to reasonable yields (in Scheme 3.15).



Scheme 3.15. Reagents and conditions for demethylation: (i) BBr₃, CH₂Cl₂, -60 °C, overnight.⁴⁰

The phenolic products **3.49b – d** had their structures confirmed by ¹H-NMR spectroscopy, in which it was noted that the intense 3-proton methoxy singlet, previously present in the δ 3.00 – 4.00 aliphatic region, was absent. Product was obtained for compound **3.49a** but found to be unstable and soon decomposed. Decomposition of compound **3.49a** was confirmed by a second ¹H-NMR spectrum which showed no product after another round of column chromatography. It is proposed that the strain introduced by the cyclopropyl group resulted in an unstable THIQ scaffold which readily decomposed on silica gel during purification. For compounds **3.49b** a broad singlet at δ 4.89 was indicative of the phenol hydroxyl group, which was also observed for compound **3.49d** at δ 4.99. However, no broad singlet was observed for compound **3.49c**, and product structure was further confirmed by the use of mass spectrometry. The calculated monoisotopic mass (C₁₄H₁₈F₃NO₃S) 336.0881 for **3.49c** corresponded exactly with the experimental monoisotopic mass obtained at 336.0881.

3.5 Summary and concluding remarks

Synthesis of the general THIQ scaffold **3.37** was successful by following a procedure described by Zhong and co-workers.¹¹⁹ This procedure included the synthesis of the amination dimer **3.36** obtained in quantitative yield, which was later cleaved under strong acidic conditions to provide the THIQ hydrochloride salt **3.37**. Under general Pictet–Spengler conditions, multiple products such as **3.20** and **3.20a** were obtained, but implementation of the method described by Zhong resulted in quantitative yields. Since the compound **3.37** was required in large quantities, the modified protocol seemed viable and was thus employed. The THIQ analogues **3.53a – d** were efficiently synthesized by alkylating the 2-(3-methoxyphenyl) acetonitrile **3.46** with a few selected haloalkanes under alkaline conditions. The nitrile group in compounds **3.46a – d** were readily reduced by use of monochloroalane providing product in excellent yields, which produced the amines required for cyclization under the conditions described by Zhong and co-workers.¹¹⁹ Demethylation of the products **3.53a – d** were successfully accomplished upon treatment with BBr₃. In our hands, the highly strained spirocyclopropyl analogue **3.53a** however, proved problematic with multiple spots being observed on the TLC after purification and thus a lower yield of product was isolated which soon decomposed. As for the rest of the THIQ compounds **3.53b – d**, the products were obtained in acceptable yields that could be utilized in further biochemical testing.

Chapter 4

Investigation of linker group effects on the THIQ analogues

The literature reviewed in Chapter 2, section 2.14, introduced a few research objectives for the design of compounds able to meet certain criteria, which would potentially allow a small library of synthetic compounds to mimic the E2 ligand. In chapter 3 the first objective was met, where investigations into the effect of steric hindrance at the C4-position was evaluated by bulking up the lower rim of the THIQ scaffold using various alkyl groups. The second objective required a library of compounds to investigate and determine the degree of flexibility required for potentially determining its structural effect on allosteric conformations and/or binding with ER. Chapter 4 would thus include the design and synthesis of these compounds described for Library 2 to meet or determine the criteria associated with flexibility. This included the structural extension of the THIQ core by the incorporation of varied amide-type derivatives onto the amine group of the THIQ scaffold. Additionally, the amide-type derivatives (and their terminal functional groups) would also provide a moiety allowing for the easy substitution by a number of phenyl groups onto the molecule. Variation of the amide derivatives would be essential in determining the structure-activity relationships they also presented toward generating selectivity for certain residue interactions. In addition to linker groups, the phenyl groups incorporated onto the amide functional group are geared toward further enhancing potential target interactions with the His475 residue.

4.1 Initial motivation for the design of the second library

Efforts by Brunsveld and co-workers have provided evidence that the 2-[(trifluoromethyl)sulfonyl]-1,2,3,4-tetrahydroisoquinolin-6-ol analogues illustrated in Figure 4.1, showed modest selectivity toward the ER β nuclear receptor,⁴⁰ meeting one of the desired objectives, that of selectivity. Selectivity toward the β -receptor is essential since reports by Kang *et al.*,²¹ Yagar *et al.*¹⁸ and Russo *et al.*¹⁹ have indicated that activation of the α -receptor played a significant role in the proliferation of cancer within reproductive tissues.^{13,18,19,21,46} Despite the minor advancement in selectivity generated by the small THIQ molecules generated by Brunsveld and co-workers,⁴⁰ their second objective, which required extension of the THIQ analogue toward the His475 residue, was not achieved.

CHAPTER 4 | Investigation of linker group effects on the THIQ analogues

Further extrapolation of Brunsveld's work, led to the THIQ scaffold being used as a starting point, followed by functionalization of the amine being employed to influence the selectivity toward the ER-subtypes.⁴⁰ Brunsveld reported that the incorporation of the trifluoromethyl sulfonamide moiety on compound **4.1** enhanced both the activity as well as selectivity, and showed that incorporation of the trifluoromethyl carboamide moiety on compound **4.2** resulted in no comparative improvement.⁴⁰



Figure 4.1. Compound scaffolds reported by Brunsveld and co-workers.⁴⁰

These findings continued to stimulate our interest to design and synthesize a new small library of THIQ analogues to primarily maintain key hydrogen bond interactions observed for the natural ligand (E2, in Figure 4.2), as well as to provide a certain degree of flexibility required during the allosteric conformational changes, which occur in the nuclear receptor.

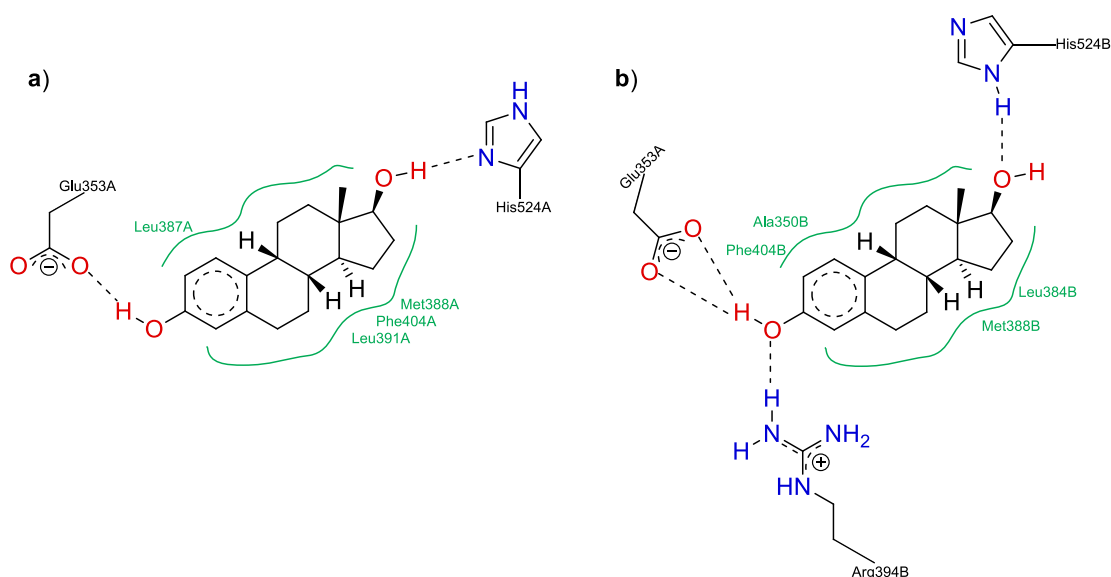


Figure 4.2. Estradiol's general binding properties are illustrated within the receptors binding cavity taken from the PDB website. Frame **a**) Shows that the residues (Glu353 and His524) interact with E2 as proton acceptors (a base), and in frame **b**) the Arg394 and His524 behave as proton donors (acids) and Glu353 as a base with E2.

For the purpose of comparison, four different linker groups were considered, which would potentially provide the conformational adaptations usually facilitated by the C- and D-rings

CHAPTER 4 | Investigation of linker group effects on the THIQ analogues

of E2, as well as accommodate electrostatic requirements, such as the protic and/or van der Waals interactions, required for mediating valuable protein interactions with target residues within the receptors active binding site. The intended design included the THIQ skeleton illustrated in Figure 4.3, where the Ar-substituents would consist of heteroaryls, *viz.*, thiazoles and substituted aromatic rings. In theory, the THIQ amine group should provide an easy point for functionalization, where a two-atom linker group *viz.*, peptidyl, carboamide, thiocarbamide and sulfonamide (in Figure 4.3) would be incorporated.

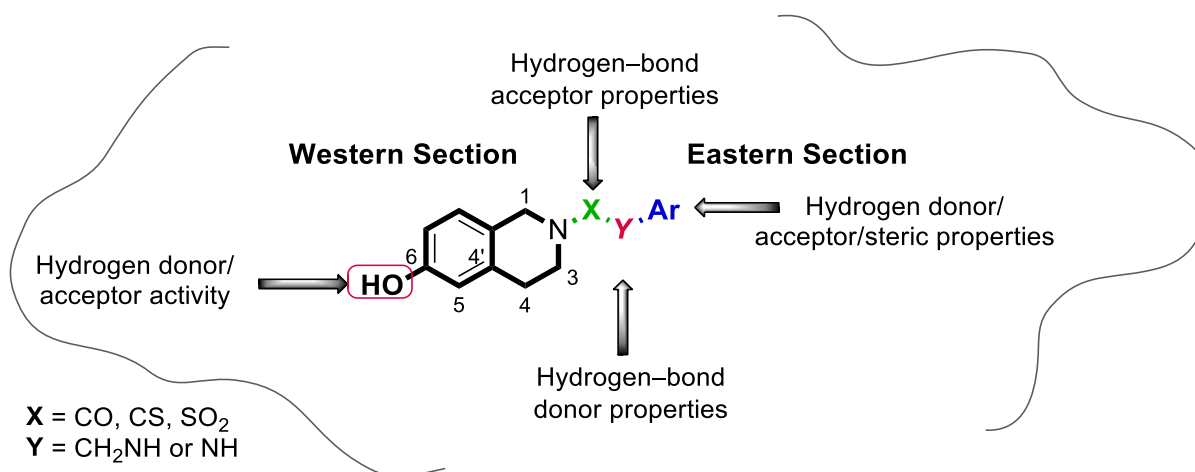


Figure 4.3. Structural design of the THIQ analogues containing the diverse linker groups.

Since the biological world does not function independently, as clearly demonstrated by the versatility associated with the binding ability of the ER,⁶ small changes brought about on a synthetic ligand could significantly influence the residue's response within the active site to the newly introduced functionalities such as those proposed in Figure 4.3. The western section of the molecule would be comprised of the 6-hydroxy-THIQ moiety, essential for mimicking the A- and B-rings of E2.^{1,39,40} On the other hand, the heteroatoms on the linker groups would serve as hydrogen bond donors/acceptors, as well as participate in dipole interactions with target residues present within the receptor's binding cavity.¹²⁵⁻¹²⁷ Introduction of the linker group (X) in Figure 4.3, could also potentially enhance or reduce certain interactions within the receptor binding cavity, hopefully providing selectivity toward a specific receptor subtype observed in the work of Brunsveld, *et al.*⁴⁰ The possibility of conformational flexibility provided by the linker groups would be a requirement to further accommodate allosteric configurations experienced by the ligand upon binding within the receptor and promote target protein interactions with desired neighbouring residues.¹²⁷

CHAPTER 4 | Investigation of linker group effects on the THIQ analogues

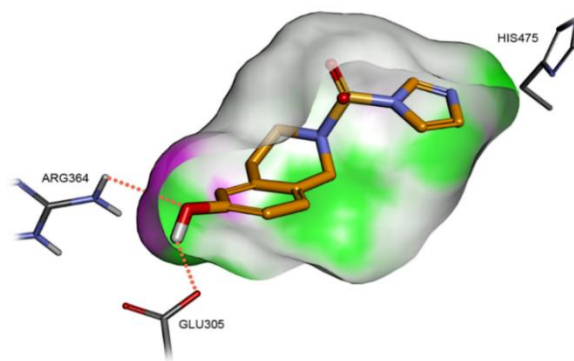


Figure 4.4. A generic structure designed with Acclerys Discovery studio software displaying the intended interaction of the western and eastern section of the synthetic ligand within the receptors active site.

Computational docking studies using Schrodinger and Acclerys Discovery Studio software were employed for the design and prediction of the physiological behaviour that the THIQ analogues would present within the receptors binding pocket as illustrated in Figure 4.4.

Interestingly, recent work reported by Redda and co-workers,⁹⁸ described compounds with similar structural architectures (as shown in Figure 4.5). These compounds included the incorporation of a two spaced hydrazine linker group (compounds **4.4** – **4.7** shown in Figure 4.5) which displayed effective anti-breast cancer properties.^{2,98} The following compounds, **4.4** – **4.7**, with IC₅₀ values at the ng/mL scale had an improved anti-proliferative activity against the human ER⁺ (MCF7) breast cancer, ER⁻ (MDA-MB-231) breast cancer and Ishikawa (endometrial cancer) cell lines, upon comparison to the well-known drug tamoxifen **4.3**, initially developed as a treatment for breast cancer.²

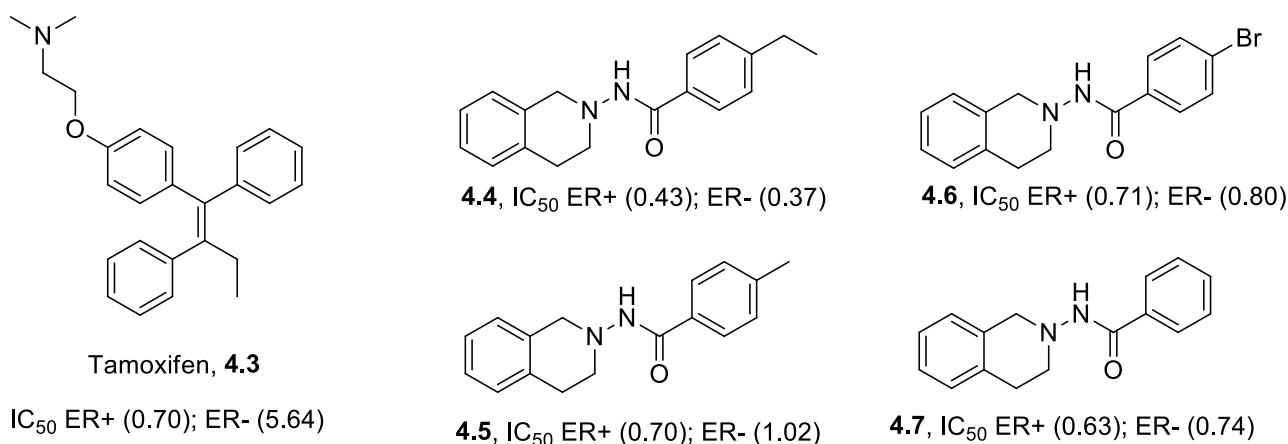


Figure 4.5. Compounds **4.4** – **4.7** with an improved structure-activity relationship relative to compound **4.3**.⁹⁸ The values in brackets represent the IC₅₀ values reported by Redda and co-workers.

CHAPTER 4 | Investigation of linker group effects on the THIQ analogues

The hydrazine (N–NHC=O) structural linker group used in Redda's compounds (Figure 4.5), adopt a planar conformation rendering restrictive conformations for the ligand within the binding site (Figure 4.6), yet still managing favourable inhibition.² Despite this, the excellent results obtained by compounds **4.4** – **4.7** were surprising, since these structures also lack the phenolic functional group considered as being essential for providing favourable interactions with in the ER binding site described in Figure 4.6.⁵²

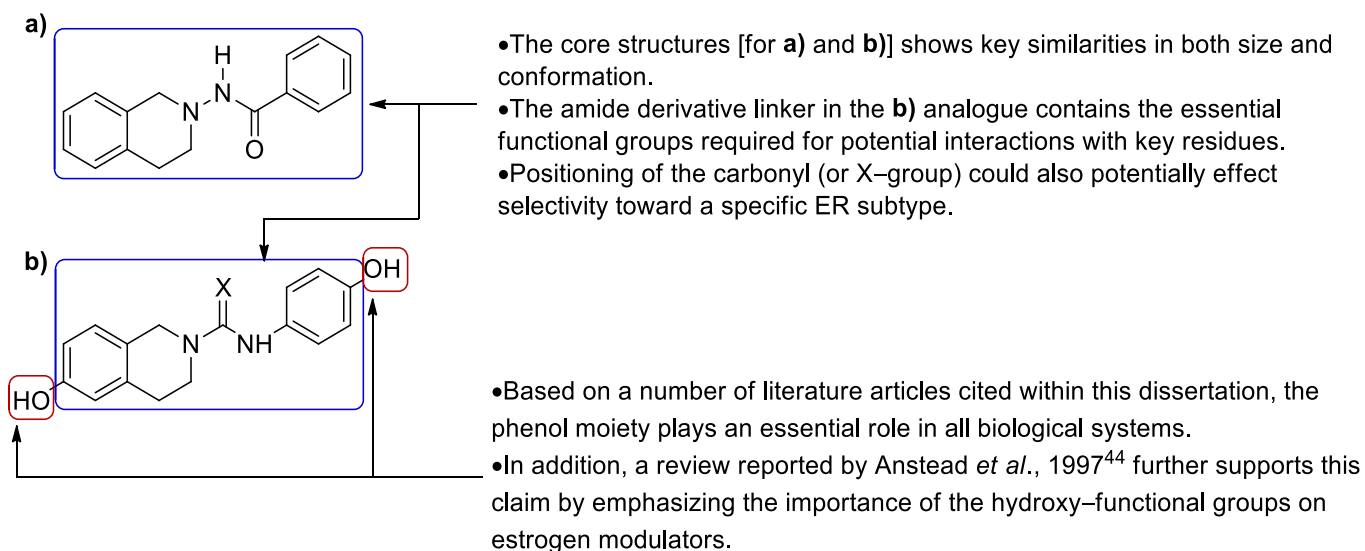


Figure 4.6. Frame **a**) refers to the structural design Redda's compounds contain; frame **b**) relates to the structural design we aim to generate.⁹⁸

The valuable information obtained from Redda and co-workers concerning maintained activity, prompted our further exploration in generating the proposed library of compounds containing amide derivatized linker groups.⁹⁸ The main objective of these amide linked compounds, would be targeted toward enhancing our compound's ability to extend within the hydrophobic cavity, while at the same time potentially showing preferential selectivity toward the ER β subtype.

4.2 The synthesis of 1,2,3,4–tetrahydroisoquinolin–6–ol peptidyl–linked analogues

The initial library generated and presented within this chapter included the introduction of a peptidyl linker group. Unpublished work generated by previous group members, namely Thomas Xhurdebise and Hassam Mohammad, forms the foundation of this synthetic strategy. The idea was to generate a library of small molecules that included the THIQ core designs **4.8** and **4.9** as illustrated in Figure.4.7. These compounds were generated to contain acyl chains forming the derivatized analogues of **4.8** and **4.9**, in order to extend

CHAPTER 4 | Investigation of linker group effects on the THIQ analogues

these compounds toward the His475 residue, by mimicking the 5-membered ring of E2. It was later determined with the use of computational docking studies, that this ultimately ineffective binding was due to the increased torsional freedom provided by the acyl chain, thus limiting the molecules ability to interact with desired residues, as well as successfully dock within the binding cavity. The valuable results obtained from analogues the **4.8** and **4.9** presented the foundation, upon which the libraries discussed in this chapter were constructed.

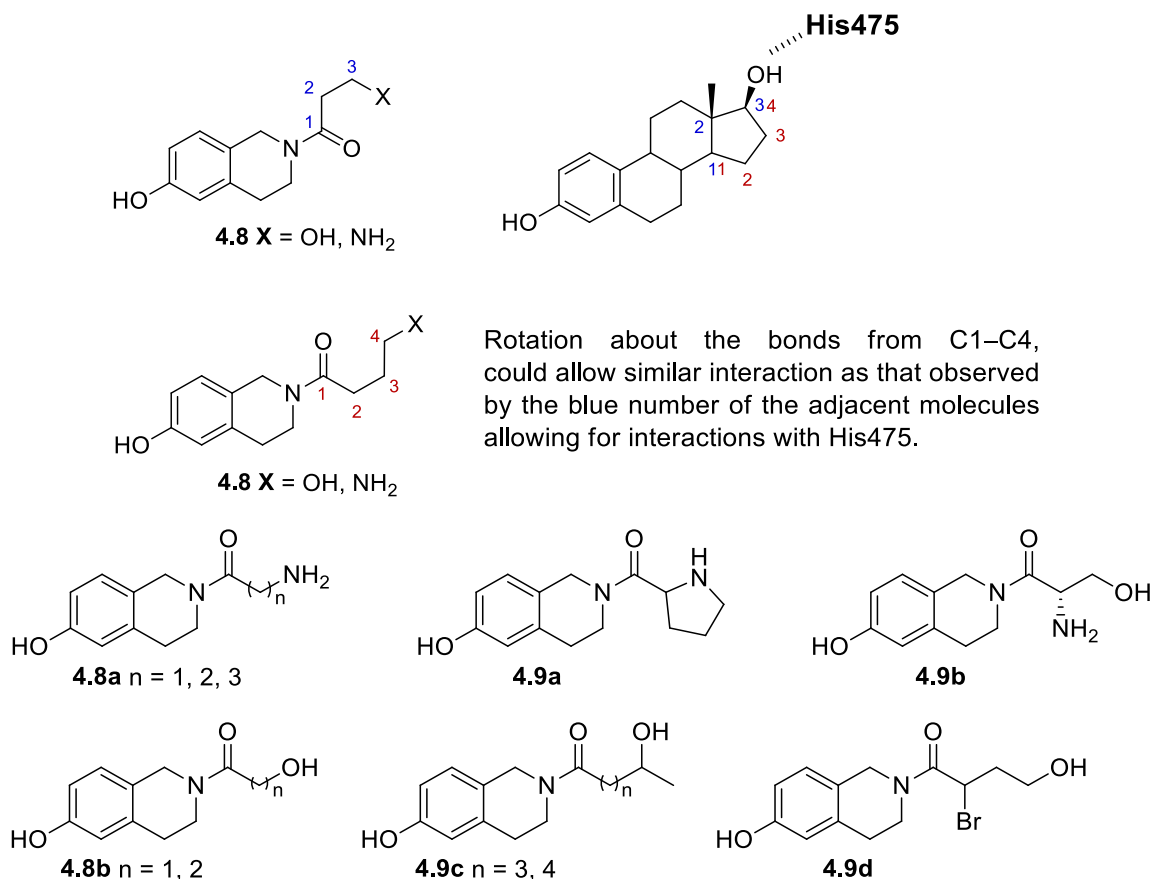
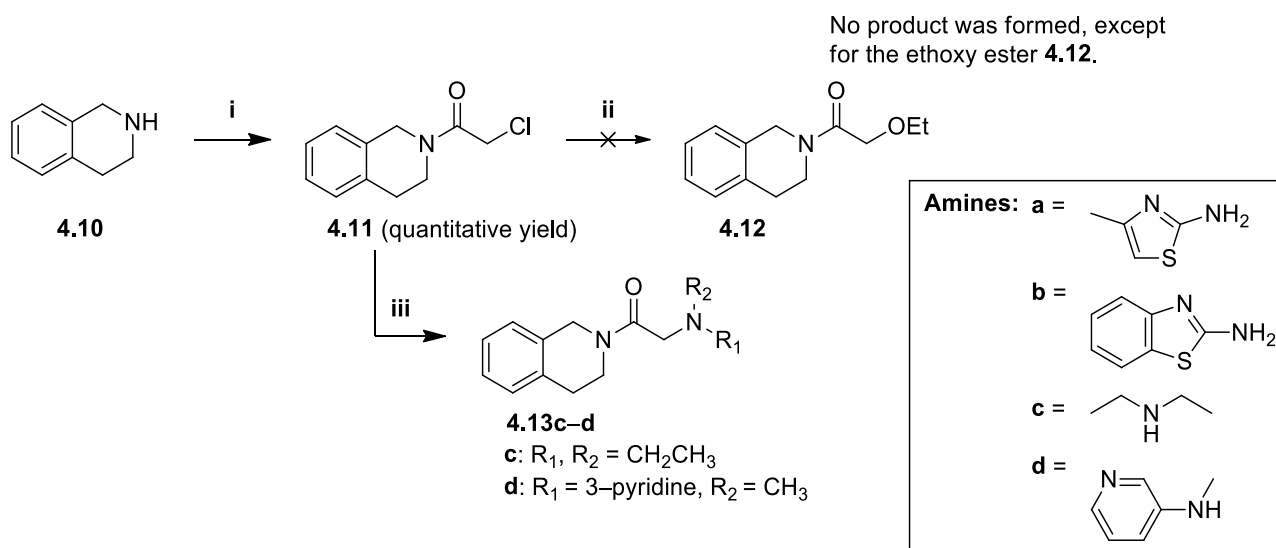


Figure 4.7. Compounds structurally designed to extend toward the His475 residue.

Our new structural modifications to compounds **4.8** and **4.9** included maintaining the peptidyl moiety from the initial library in Figure 4.7 but exchanged the terminal alcohol and heteroaryl amine groups as demonstrated in Scheme 4.1.

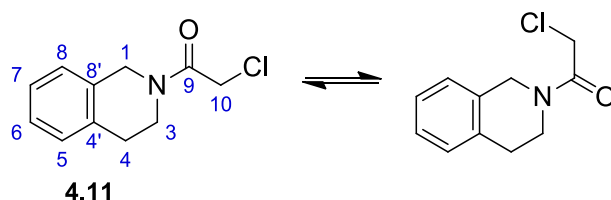
CHAPTER 4 | Investigation of linker group effects on the THIQ analogues



Scheme 4.1. Reagents and conditions: (i) DIPEA, chloroacetyl chloride, CH_2Cl_2 ; (ii) amines (**a** and **b**), K_2CO_3 , EtOH under reflux; (iii) amines (**c** and **d**), K_2CO_3 , EtOH under reflux.

In generating analogues of compounds **4.13**, the general THIQ scaffold **4.10** was employed for optimization of reaction conditions so as to not lose the valuable 6-methoxy-1,2,3,4-tetrahydroisoquinoline hydrochloride salt (utilized in the previous chapter). The initial step required the synthesis of the carbamoyl chloride **4.11** in Scheme 4.1. The THIQ substrate **4.10** was treated with chloroacetyl chloride under basic conditions using Hünig's base and readily afforded the chloroacetamide **4.11** in quantitative yield. Upon use of ^1H - and ^{13}C -NMR spectroscopy, characterization of compound **4.11** provided an interesting spectrum, as amide rotamers were observed for compound **4.11**. Not surprisingly, the rotamers resulted from the two conformations attributed to the two main conformations taken on by the amide moiety (see Scheme 4.2). The ^{13}C -NMR spectrum also showed that the carbon atoms experienced different chemical environments, resulting in a doubling of the resonating signals. In this regard, signals in the ^{13}C -NMR spectrum were split, providing two signals at δ 28.08 and δ 29.20 representing the C4 signal. The resonance signals observed at δ 40.44 and δ 41.19 were indicative of the methylene signal for C10, while the signals at δ 43.73, δ 44.67 and δ 47.64 were representative of the C3 and C1. The four aryl carbons (C5 – C8) were represented by doubling up of signals giving a total of eight signals at δ 125.91 (C7') and δ 126.52 (C7), δ 127.06 (C8') and δ 128.25 (C8), δ 128.76 (C6') and δ 131.82 (C6), with δ 132.42 (C5') and δ 133.56 for (C5) in the aromatic region. Only one quaternary carbon was observed at δ 134.51 (C4' and C8') for the carbonyl motif, clearly evident by the chemical shift observed at δ 165.48.

CHAPTER 4 | Investigation of linker group effects on the THIQ analogues

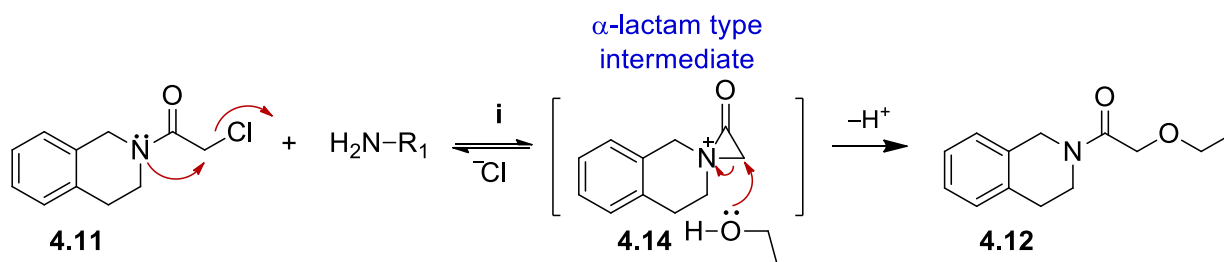


Scheme 4.2. Tautomeric conformations adopted by compound **4.11**.

With chloroacetamide **4.11** in hand, it was then treated under Schotten–Baumann conditions and reacted with primary amines (**a** and **b**) with the aim of achieving our first desired products **4.13**. However, coupling of **4.11** with primary amines (**a** and **b**) instead provided compound **4.12**. Work reported by Lippa and co-workers,¹²⁸ provided an explanation for this challenge described in Scheme 4.3. This could further be explained by the nucleophilic competition between the amine and the ethanol solvent, the latter which proved a more effective nucleophile under the reaction conditions in Scheme 4.3. Another issue might have been that the initial amines chosen were not nucleophilic due to conjugation of the amine lone pairs.

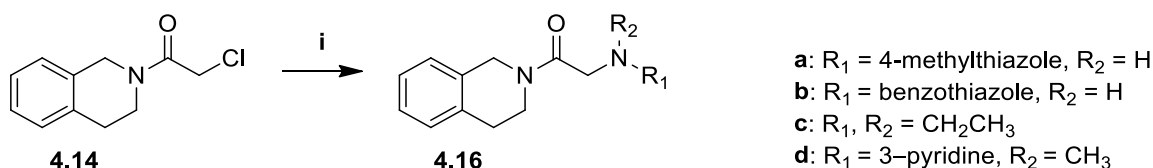
Surprisingly, upon reacting the chloroacetamide **4.11** with other secondary amines (**c** and **d**) product formation was achieved within acceptable to good yield under similar conditions. One may therefore conclude that failure to synthesise the desired product from amines (**a** and **b**) was due to the weaker nucleophilic character of the heteroaryl amines compared to the ethanol group. The explanation for failing to obtain product when using amines (**a** and **b**) was explained mechanistically in a report by Lippa and co-workers,¹²⁸ who postulated the formation of very electrophilic highly-strained α -lactam **4.14** intermediate (in Scheme 4.3). In the presence of a relatively more abundant nucleophile, ring-opening of the α -lactam occurred in this case the ethanol group providing the ether product **4.12**. Unfortunately, the heteroaryl primary amines of interest were found not to be sufficiently nucleophilic. It was furthermore found that performing the reactions in a non-polar solvent led to the recovery of compound **4.11**. Table 4.1 demonstrates, the various conditions applied to resolve the unwanted formation of compound **4.12**, unfortunately with mixed success.

CHAPTER 4 | Investigation of linker group effects on the THIQ analogues



Scheme 4.3. Reagents and conditions described by Lippa and co-workers: i) K_2CO_3 , amines (**a** and **b**), EtOH under reflux. Lippa and co-workers proposed mechanistic pathway explaining the formation of the undesired ether product.¹²⁸

Table 4.1a. Reagents and conditions for the peptidyl linker synthesis.



Entry	Substrate	Amine	Product	Yield (%)
1	4.11	2-amino-4-methylthiazole ^a	4.13a	0
2	4.11	2-amino-4-methylthiazole ^b	4.13a	0
3	4.11	2-amino-4-methylthiazole ^c	4.13a	0
4	4.11	diethylamine ^a	4.13c	78
5	4.11	<i>N</i> -methyl pyridin-3-amine ^a	4.13d	25

Reaction conditions:(i) ^aheated at 80 °C in EtOH; ^bat RT in EtOH; ^cheated at 70 °C in THF.

In an effort to obtain product, the following reaction conditions listed in Table 4.1 were attempted. As displayed by entries 1 – 3, despite the use of varied parameters such as the absence of base, variation of solvents and heat, failed to produce product, with starting material only being recovered, for entry 3. However, entries 4 and 5 proved to be successful with product being obtained in good to reasonable yields. In the second half of Table 4.1b, the chloroacetamides of amines **a** and **b** were treated under Schotten–Baumann conditions with the THIQ **4.10** scaffold. Shown by entry 1, success was obtained when using the 4-methylthiazole chloroacetamide **4.15a**, but no product was obtained for compound **4.15b**.

CHAPTER 4 | Investigation of linker group effects on the THIQ analogues

Table 4.1b. Reagents and conditions for the peptidyl linker synthesis with two thiazole analogues.

Entry	Substrate	Amine	Product	Yield (%)
1	4.15a	THIQ	4.16	37
2	4.15b	THIQ	4.16	0

Reaction conditions:(i) Heated at 115 °C in PhCH₃.

Not being able to successfully generate the peptidyl-linked compounds with our desired amines, further work on the peptidyl linker groups was abandoned, and our focus was shifted to other amide derivatized linker groups. Upon reviewing the literature, the urea group proved to show great promise considering its use, ranging from cosmetic, medicinal and industrial applications.¹²⁹ This information led to the consideration of the urea group (essentially a modified amide), as the next sequence of linker groups.

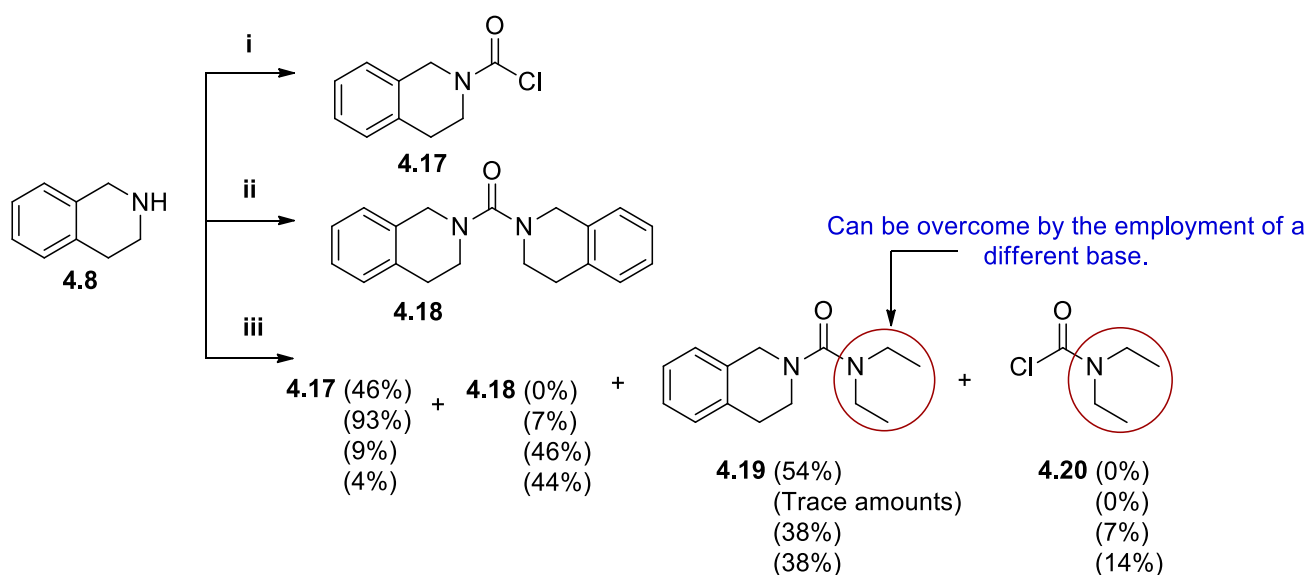
4.3 The synthesis of 1,2,3,4-tetrahydroisoquinolin-6-ol urea-linked analogues

The urea motif occupies a prominent position in both pharmaceutical and industrial uses, demonstrated by its extensive applications.¹²⁹ Substituted ureas have previously been employed agriculturally as plant growth regulators, pesticides and herbicides. In addition, their medicinal applications include being used as part of tranquilizing agents, anticonvulsants and for compounds used for the treatment of cardiac and respiratory diseases.¹²⁹ They have further been incorporated in cosmetics to improve their value as dermatological applications for immune regulators, dyeing agents and in modified cellulose fibres.¹²⁹ Lastly, industrial applications include their use as part of thermal stabilizers in the production of synthetic rubbers.¹²⁹ The broad applications associated with the urea motif establishes its ability to participate in a number of interesting reactions and for the interest of this project, we aimed to take advantage of this versatile functional group at a molecular level.

Synthesis of the carbamoyl moiety has been explored since 1848 as reported by Würtz and many others.^{127,129,130} As a result, a number of efficient routes have been developed for the synthesis of this fascinating carbamoyl moiety.¹¹³ As illustrated in Scheme 4.4, carbamoyl

CHAPTER 4 | Investigation of linker group effects on the THIQ analogues

chlorides have been used in popular synthetic strategies for generating the urea moiety, which was the basis of interest to this work. However, a number of limitations have been associated with this protocol.¹¹³ Only a few carbamoyl chlorides are commercially available and their employment in a general synthetic strategy toward urea's include the use of primary or secondary amines in the presence of hazardous reagents such as phosgene or bis(trichloromethyl)carbonate (BTC), thus limiting its general usage.^{113,131} In addition, carbamoyl chlorides are highly reactive species, illustrated by the number of side products generated with their use in the synthesis of ureas in Scheme 4.4. As described by Lemoucheux *et al.*,¹¹³ in this strategy THIQ **4.8** was treated under a range of conditions shown in the legend for Scheme 4.4. Apart from the dimerized product *viz.*, **4.18** (conditions for ii), the carbamoyl chloride showed reactivity toward the amine base (conditions for iii), which resulted in the formation of compounds **4.17**, **4.18**, the unsymmetrical urea **4.19** and carbamoyl chloride **4.20**. Carbamoyl chlorides are also prone to undergo hydrolysis, providing the corresponding carboxylic acids, which prevents long term storage and consequently requires careful handling under atmospheric conditions.¹³¹ In conclusion, the reactivity associated with the carbamoyl chlorides limit their application as a substrate for our intended strategy. The corresponding carboxylic acid could be formed by hydrolysis of the carbamoyl chloride **4.17**. However, as previously mentioned, synthesis of **4.17** is associated with a few difficulties and was thus not considered as a suitable protocol for the synthesis of the urea linker groups.



Scheme 4.4. Described by Lemoucheux *et al.*, reagents and conditions for chloroacylation: (i) Excess COCl_2 , PhCH_3 , RT; (ii) $^{13}\text{C}[\text{OCl}]_2$, THF, -78°C ; (iii) COCl_2 or BTC, Et_3N , CH_2Cl_2 .¹¹³

CHAPTER 4 | Investigation of linker group effects on the THIQ analogues

4.3.1 Coupling agents used for the synthesis of urea bonds

Apart from the carbamoyl chloride synthon used in generating a urea motif, many coupling agents are available for application, under which activated carboxylic acids can easily undergo aminolysis for the formation of the urea moiety. These coupling agents are divided into classes depending on their structural architecture. The first developed coupling agents shown in Figure 4.8, *viz.*, the carbodiimides, were used since 1955 for the coupling of carboxylic acids with amines.¹³²

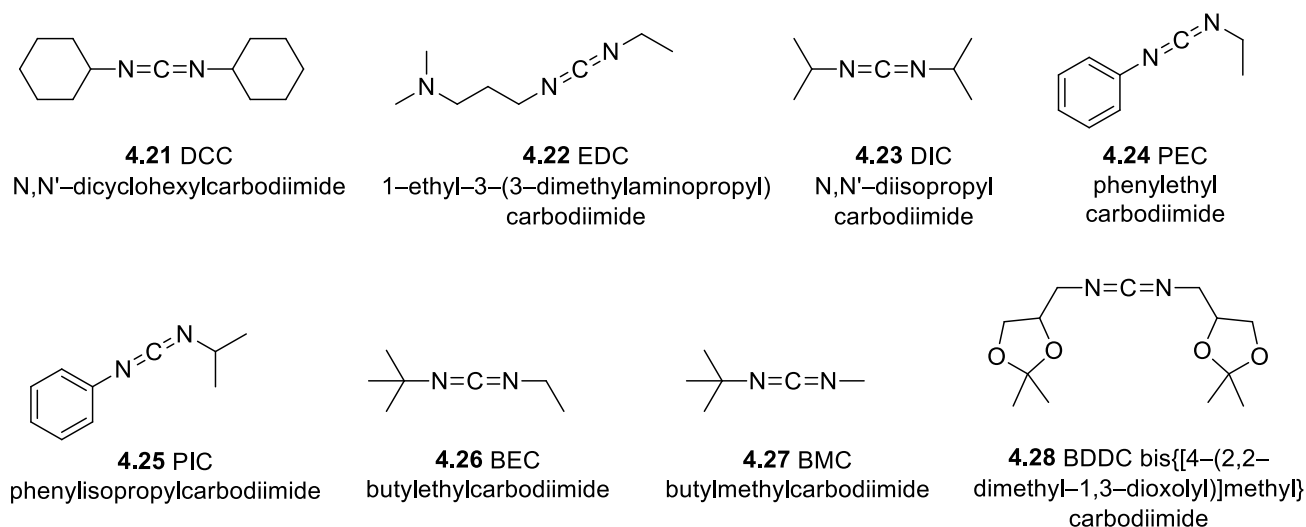
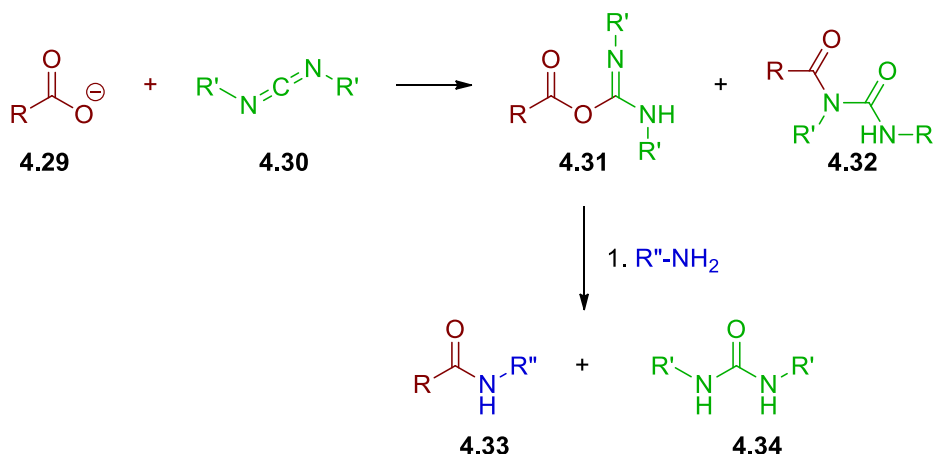


Figure 4.8. Popular carbodiimide coupling reagents as reported in a review by Valeur and co-workers.¹³²

A major advantage when using carbodiimides as coupling agents includes mild reaction conditions resulting in enhanced peptide formation.¹²⁷ However, a drawback associated with this class of coupling agent is that a portion of the carboxylic acid **4.29** is sacrificed by the formation of by-products *viz.*, compound **4.32** and the symmetrical urea **4.34**, with the remainder efficiently being converted into product **4.33** in Scheme 4.5.^{127,132-134}



Scheme 4.5. By-products generated from the carbodiimide coupling procedure.

CHAPTER 4 | Investigation of linker group effects on the THIQ analogues

The second class of coupling agents include those that incorporate the benzotriazole scaffold, as shown in Figure 4.9. The very effective Castro's reagent, benzotriazolyl-*N*-oxytrisdimethyl amino phosphonium hexafluorophosphate (BOP, **4.35**), was developed in the early 1970's, but despite its efficiency its utilization was short-lived due to the hazardous hexamethyl phosphoric triamide (HMPA) intermediate generated during its synthetic pathway.¹²⁷ For this reason, it was soon replaced by PyBOP **4.36**, which displayed a better conversion with increased efficiency during aminolysis.^{127,132,134}

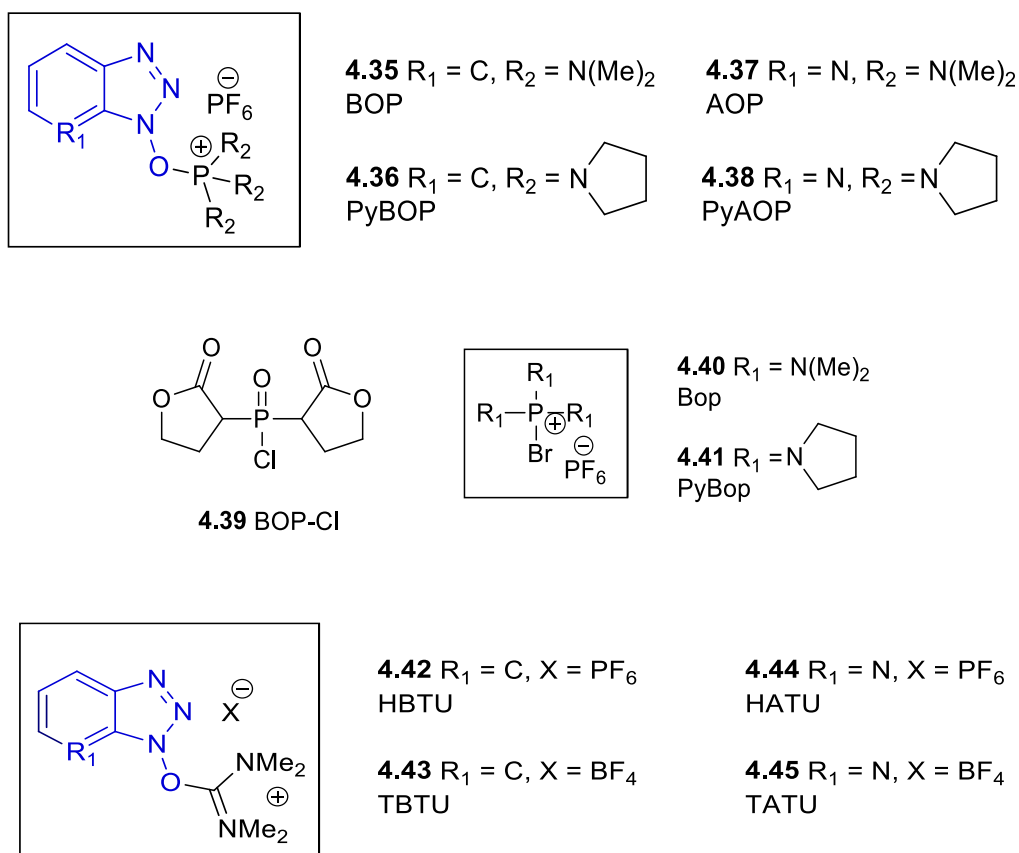
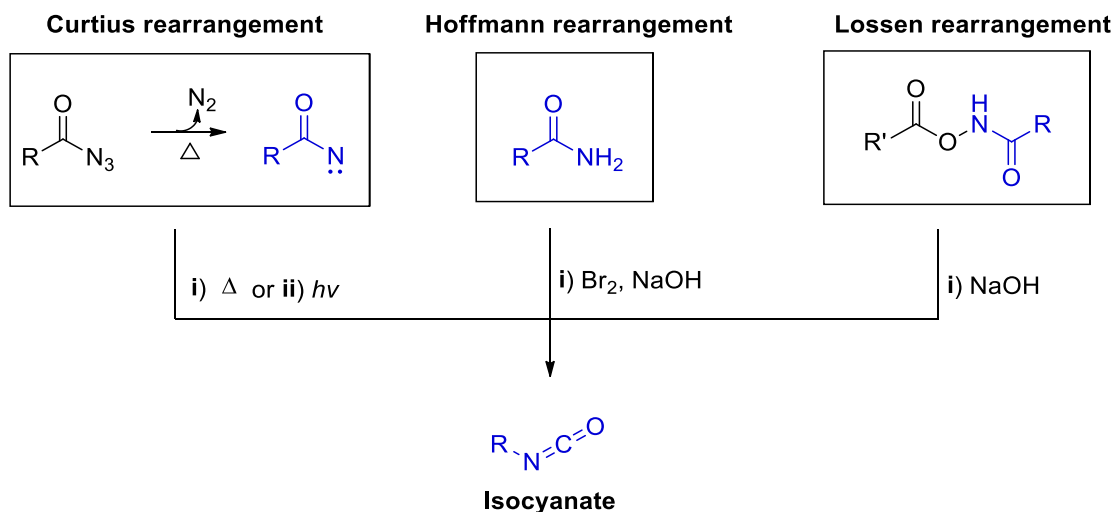


Figure 4.9. Commonly used coupling agents as described in a review by Valeur and co-workers,¹³² phosphonium salts (**4.35** – **4.41**) and uronium salts (**4.42** – **4.45**).

4.3.2 Isocyanates as an intermediate towards the urea moiety

The urea moiety may also be generated from an isocyanate intermediate. Isocyanates are easily prepared from a number of well-known rearrangement reactions (see Scheme 4.6), and thus with the desired isocyanate in hand, it could easily be reacted with the intended amine (i.e. a THIQ analogue) to deliver the corresponding urea moiety.

CHAPTER 4 | Investigation of linker group effects on the THIQ analogues



Scheme 4.6. Isocyanate synthesis by way of rearrangement reactions.

As illustrated in Scheme 4.6, isocyanates can efficiently be provided from the Curtius rearrangement, which involves the degradation of acyl azides, usually catalyzed by photochemical or thermal stimuli. Secondly, starting from an amide substrate, the Hoffmann rearrangement proceeds by using strong alkaline conditions, in addition to bromine, thus providing the isocyanate. Lastly, an isocyanate can also be generated from an acetamide rearrangement under strong basic conditions, a procedure known as the Lossens rearrangement.^{130,135} Reactivity associated with isocyanate intermediates unfortunately limit their use. For example, the presence of moisture easily causes the isocyanate to revert to its corresponding amine with concomitant liberation of carbon dioxide.

Batey and co-workers¹³⁶ reported on the synthesis of a carbamoyl chloride equivalent, where the corresponding carbamoyl imidazole and carbamoyl imidazolium carbocation in Figure 4.10 of our intended substrates, could easily undergo nucleophilic substitution to provide the corresponding urea moiety.

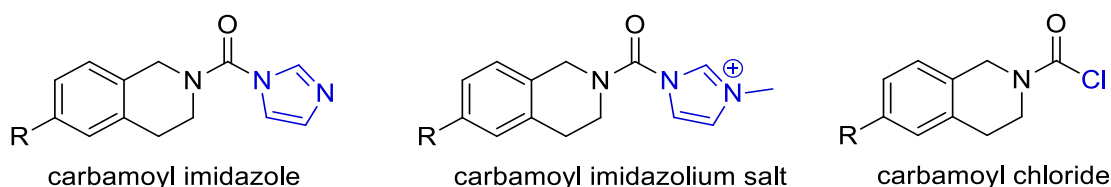


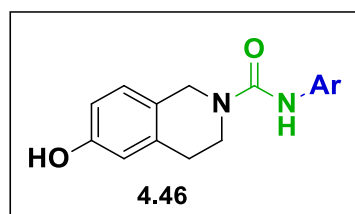
Figure 4.10. Least to most reactive carbamoyl chloride/equivalent species.¹³¹

CHAPTER 4 | Investigation of linker group effects on the THIQ analogues

The work reported by Batey¹³⁶ was further elaborated on in research reported by Grzyb,¹³¹ Padiya,¹³⁷ Sumathi¹³⁸ and co-workers and was thus the synthetic pathway chosen for the synthesis of the THIQ-urea linked analogues.

4.3.3 Carbamoyl transfer agents for the synthesis of THIQ-urea analogues

As illustrated in Figure 4.11, the scope of the intended library of urea linkers was limited to coupling of the THIQ scaffold with a number of primary and secondary amines. It was initially intended to incorporate heteroaryls such as triazole and tetrazole-type ring systems. However, due to numerous failed reactions on the model THIQ substrate, these were discarded as possibilities. An interesting and important feature associated with the urea linker previously reported by Benbrook and co-workers,¹³⁹ which further prompted our interest, was the fact that the lone pair of electrons of the carbonyl group occurs in the same plane and forms angles of 120° with the carbon, thus providing a potentially improved hydrogen bond interaction with any biological receptor. Despite the ability for carbonyl groups to undergo hydrogen bond interactions at angles of between 115° and 180°, the hydrogen bond interaction was shown to be greater when an angle of 120° was formed, an advantageous feature common to the urea moiety.^{55,139} The next sections will discuss the synthesis of compounds **4.46a – i**.



Ar = **a:** 4-methylthiazole
b: 5-nitrothiazole
c: 4-anisole
d: 3-chlorophenyl
e: 3-fluorophenyl
f: 4-chlorophenyl
g: 4-fluorophenyl
h: morpholine
i: piperazine

Figure 4.11. Targeted THIQ-urea-linked analogues.

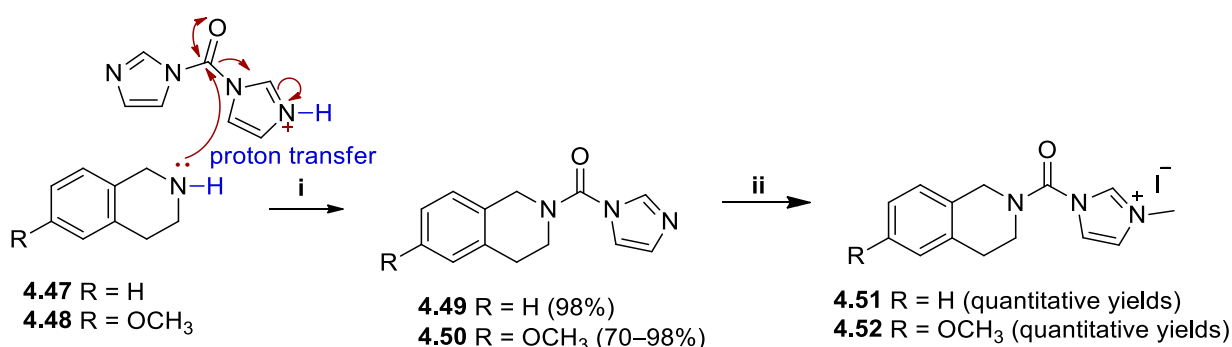
4.3.3.1 Synthesis of the THIQ-carbamoyl imidazolium iodide salt

The library of THIQ analogues in Figure 4.11 were obtained after several optimization reactions, in which modelled reaction parameters were employed using THIQ **4.47**, prior to following the reaction sequence described in Scheme 4.7. The more expensive, but essential precursor **4.48**, was synthesized *via* a three-step protocol, previously discussed in Chapter 3. The value associated with compound **4.48** is essentially linked to its masked phenol, an important requirement for proton donor properties needed for mimicking the A-ring in E2. Potential competition between the reactivity of HN⁻ and the HO⁻ in the starting

CHAPTER 4 | Investigation of linker group effects on the THIQ analogues

material, **4.48**, required that the phenol be masked as the aryl methyl ether throughout the synthetic protocol.

The reagent 1,1'-carbonyldiimidazole (CDI) is commonly used for coupling reactions between amines (and/or alcohols) with carboxylic acids.^{129,133,140} Grzyb and co-workers described and reported the use of CDI as an interesting carbamoyl transfer agent, and in our hands its use in the synthesis of compounds **4.49** and **4.50** gave excellent yields.¹³¹ The reaction was efficient in displacing one imidazole ring and displayed a great tolerance to an array of solvents *viz.*, THF, CH₂Cl₂ and CH₃CN.



Scheme 4.7. Synthesis of the THIQ carbamoyl imidazolium iodide salts. Reagents and conditions: (i) CDI, K₂CO₃, CH₃CN, RT, overnight; (ii) CH₃I, CH₃CN, RT, 6 h.

Initially, compound **4.47** was employed to investigate the reaction parameters required for the optimized yield of **4.48**. Compound **4.47** afforded **4.49** in excellent yields, and not surprisingly, reaction compound **4.48** with CDI afforded **4.50**, also in reasonably good yield. Better yields for **4.50** were expected, since **4.48** was expected to be more nucleophilic due to the methyl ether electron-donating group on the aromatic ring. The THIQ carbamoyl imidazoles **4.49** and **4.50** were purified by way of column chromatography and their structures elucidated by ¹H-NMR spectroscopy. The structural architecture of compound **4.49** displayed a 6-proton complex multiplet at δ 7.21 – 7.01, in addition to a 1-proton aromatic doublet observed at δ 7.86. The successful synthesis of compound **4.50** was supported by among other signals, a few key signals such as the three 1-proton doublet signals at δ 7.86, δ 7.20 and δ 6.95 confirming the incorporation of the imidazole ring, and by a 5-proton multiplet of overlapping signals between δ 3.78 – 3.67 (OCH₃ and CH₂ groups) confirming the incorporation of the THIQ moiety. Additionally, ¹³C-NMR spectroscopy was employed for the identification of the carbonyl functional group, which in compound **4.49** was found at δ 151.22 (C=O) and at δ 159.00 for compound **4.50**. Unlike the corresponding

CHAPTER 4 | Investigation of linker group effects on the THIQ analogues

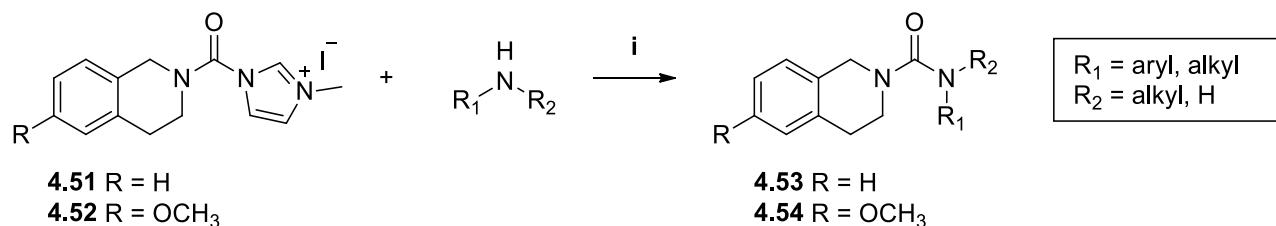
carbamoyl chloride, the carbamoyl imidazoles **4.49** and **4.50** were found to be a lot more stable under atmospheric conditions and could also be stored for extensive periods at low temperatures (refrigeration at $-16\text{ }^{\circ}\text{C}$).

Reacting compound **4.49** and **4.50** with a range of amines (**a** and **c**) proved to be unfruitful and gave no products, even under reflux, with only starting material and amine reagents being recovered. This illustrated the need for the imidazole ring to be activated, thus allowing for its easier displacement. Fortunately, this was easily achieved by methylation of the imidazole moiety of compounds **4.49** and **4.50**, thereby transforming them into more effective leaving groups, and enabling substitution on the substrates **4.51** and **4.52**. Synthesis of the THIQ carbamoyl imidazolium iodide salts **4.51** and **4.52** was affected by treatment of **4.49** and **4.50** with iodomethane. This activation of the imidazole ring was necessary for its efficient displacement by the varied selected primary and secondary amines as described in literature.^{131,140} Methylation of the imidazole ring occurred at a rapid rate with concomitant precipitation of the salt from the reaction mixture. No further purification was required and the salt, products **4.51** and **4.52**, were obtained by the removal of solvent and excess MeI under reduced pressure. Structural confirmation of compounds **4.51** and **4.52** was provided by the additional methyl signal observed in the ^1H - and ^{13}C -NMR spectra. Apart from an increased reactivity, compounds **4.51** and **4.52** were still stable enough to be handled under atmospheric conditions and could be stored for long periods of time (months) in the refrigerator at $-16\text{ }^{\circ}\text{C}$.

4.3.3.2 Coupling of THIQ-carbamoyl imidazolium iodide salt with amines

Optimization of reaction conditions were effected by employing the sacrificial compound **4.51** prior to using **4.52**. As previously mentioned, displacement of the imidazole ring had earlier failed, which necessitated use of the activated carbamoyl imidazolium iodide salts **4.51** and **4.52**. These were subsequently reacted with the primary amines (2-amino-4-methylthiazole, 2-amino-5-nitrothiazole, haloanilines and anisidine) and secondary amines (morpholine and piperazine), which unfortunately gave poor yields. However, Grzyb and co-workers overcame this problem by pre-treatment of the amines with base prior to the addition of salts **4.51** and **4.52**, which further improved yields.¹³¹ When applying these conditions to the current substrates, improved yields were obtained as illustrated in Table 4.2.

CHAPTER 4 | Investigation of linker group effects on the THIQ analogues

Table 4.2. Results and conditions for the procedures followed in Scheme 4.4.

Entry	Substrate	Nucleophile	Product	Yield (%)
1	4.51	2-amino-4-methylthiazole ^a	4.53a	37 – 57
2	4.52	2-amino-4-methylthiazole ^a	4.54a	92
3	4.52	2-amino-5-nitrothiazole ^b	4.54b	74
4	4.52	4-anisidine ^c	4.54c	67 – 98
5	4.52	3-chloroaniline ^c	4.54d	86
6	4.52	3-fluoroaniline ^c	4.54e	70
7	4.52	4-chloroaniline ^c	4.54f	44
8	4.52	4-fluoroaniline ^c	4.54g	81
9	4.52	morpholine ^b	4.54h	Quantitative
10	4.52	piperazine ^b	4.54i	Trace amounts

Reagents and conditions described by Grzyb and co-workers:¹³¹ (i) THIQ salt (1.1 equiv), amine (1.0 equiv). ^aEt₃N (2.0 equiv), CH₃CN at RT, overnight; ^bCs₂CO₃ (3.0 equiv), CH₃CN at RT, overnight; ^c*n*BuLi (3.0 equiv), THF at –78 °C – RT, overnight.

CHAPTER 4 | Investigation of linker group effects on the THIQ analogues

Displacement of the imidazolium salt **4.51** and **4.52** with 2-amino-4-methylthiazole was successful and the desired products were obtained in moderate to excellent yields, as illustrated in Table 4.2. Substrate **4.52** in entry 2, showed improved yield when compared to the displacement of the imidazolium moiety in comparison to **4.51**. The structure of **4.53a** and **4.54a** were determined using $^1\text{H-NMR}$ spectroscopy, the spectra of which contained a 3-proton singlet upfield at δ 2.26 (for **4.53a**) and δ 2.27 (**4.54a**) indicative of the methyl present on the thiazole ring. However, reaction of **4.52** with 4-anisidine and 2-amino-5-nitrothiazole under similar conditions resulted in no product being formed. In an effort to improve on this, initial deprotonation with *n*BuLi was employed for these aromatic amines, which resulted in an improved yield for the amines (**c – g**). In contrast, treatment of **4.52** with *n*BuLi to 2-amino-5-nitrothiazole resulted in multiple spots on TLC, indicating either the decomposition of the substrate or multiple by-product formation. Evaluation of a number of bases eventually led to the pre-treatment of 2-amino-5-nitrothiazole with either K_2CO_3 or Cs_2CO_3 , which consequently provided products in good yield. As illustrated in entry 3, gentle heating (at 40°C) was required for the delivery of product in good yield. In general, the unreacted amine and product displayed a slight difference in their R_f values, making column chromatography a rather challenging process. This was overcome by partitioning the reaction mixture between EtOAc and an aqueous 1 M HCl solution, which removed any excess amine as its water-soluble salt prior to purification by column chromatography.

Upon comparison of the $^1\text{H-NMR}$ spectra of **4.52** with **4.54b** it was evident that the imidazole ring was absent. However, the $^1\text{H-}$ and $^{13}\text{C-NMR}$ spectra were insufficient for an unambiguous confirmation of the product **4.54b** since the NMR spectrum displayed only an indistinctive signal for the thiazole aromatic proton. Heteronuclear single quantum correlation (HSQC) spectroscopy, as well as TOF MS, were consequently employed to support the assigned structure of product **4.54b**. A 1-proton singlet observed downfield at δ 8.58 confirmed the presence of the thiazole proton, as well as the broad singlet observed at δ 12.17 which indicated the presence of an amine (NH). The assigned structure was further supported by four clearly assigned signals observed in the aromatic region of the $^{13}\text{C-NMR}$ spectrum at δ 165.54 (*thiazole-ArCNO*₂), δ 157.90 (*ArCOMe*), δ 154.54 (*C=O*), and δ 142.10 (*ArCNH*), present in compound **4.54b**, in addition to the expected carbons of the THIQ skeleton.

CHAPTER 4 | Investigation of linker group effects on the THIQ analogues

Entries 4 – 8, reflect the efficient substitution of the imidazolium iodide salt **4.52** by amines (**c – g**) affording **4.54c – g**, which were successfully obtained after the use of the most efficient conditions, which included stirring at $-60\text{ }^{\circ}\text{C}$ for 3 hours prior to the addition of **4.52**. The nucleophile used in entry 4, as expected, allowed good to excellent displacement of the imidazolium salt, with the product **4.54c** being obtained in good yield. Inspection of the $^1\text{H-NMR}$ spectrum for the product **4.54c** indicated a complex 2-proton multiplet between δ 7.30 – 7.14, a 1-proton signal at δ 6.99, and a 4-proton multiplet at δ 6.84 – 6.60, illustrative of the presence of two substituted aromatic rings and a broad 1-proton singlet at δ 6.32 for the amine (NH). Key signals observed in the aliphatic region included an intense singlet at δ 4.52, a 6-proton signals at δ 3.73 indicative of the two methoxy-groups and two 2-proton triplets representing the methylene groups of the THIQ moiety.

However, it was noted that those reactions involving the haloanilines (**d – g**) in entries 5 – 8, required longer reaction times, in addition to increased amounts of *n*BuLi. On the other hand, the 3-haloanilines (entries 5 and 6) proved to be much more convenient to work with than the 4-haloanilines (entries 7 and 8), which required more extensive reaction times. The halogen-substituent on the aniline plays a role in deactivation of both *ortho* and *para* positions of the aryl ring by an inductive effect, thus making it a weaker nucleophile requiring more time for the successful displacement of the imidazolium iodide salt moiety (products were obtained in moderate to poor yields observed for entries 7 and 8). The 3-haloanilines proved to be sufficiently nucleophilic and product was obtained in good yields (entries 5 and 6) in Table 4.2. Products **4.54d** and **4.54e** as expected, demonstrated similar $^1\text{H-NMR}$ spectra profiles in the aromatic region with a 1-proton doublet of doublets at δ 7.47 (haloaryl moiety of the compound) for **4.54d** and at δ 7.38 – 7.18 (haloaryl moiety of the compound) for **4.54e**. Two 2-proton multiplets between δ 7.31 – 7.07 (haloaryl moiety of the compound) and δ 7.06 – 6.90 (haloaryl moiety of the compound) for **4.54d**, while comparable signals between δ 7.09 – 7.03 (haloaryl moiety of the compound) were observed for **4.54e**. Lastly, a 3-proton multiplet between δ 6.85 – 6.61 (for the THIQ-moiety) for **4.54d** and δ 6.80 – 6.70 (for the THIQ-moiety) for **4.54e** confirmed the successful incorporation of the haloaryl substituents (**d** and **e**). However, in the $^{13}\text{C-NMR}$ spectra, these two molecules were easily differentiated by a complex signal pattern in the aromatic region, as a result of the doubling of signals attributed to the C-F coupling observed for compound **4.54e**. In addition, ESI⁺ TOF MS for the protonated molecular ion ($[\text{M}+\text{H}]^+$; m/z) 317.1052 was found to correspond well to the calculated monoisotopic mass of 317.1057 of $\text{C}_{17}\text{H}_{17}\text{ClN}_2\text{O}_2$ for **4.54d**, and of

CHAPTER 4 | Investigation of linker group effects on the THIQ analogues

301.1356 was calculated for C₁₇H₁₇N₂O₂ and found to be 301.1356 for **4.54e**, further supporting product formation.

Similarly, compounds **4.54f** and **4.54g** displayed common features in both their ¹H-NMR spectral profiles. Formation of compound **4.54f** was confirmed by a 4-proton multiplet between δ 7.40 – 7.19, a 1-proton doublet at δ 7.06 and a 2-proton multiplet between δ 6.88 – 6.65 ascribed to the aromatic protons for both the THIQ, as well as the haloaryl moiety. Additionally, a 1-proton broad singlet (NH, amine) at δ 6.45 confirmed product **4.54f** formation. Compound **4.54g** formation was substantiated by a 2-proton multiplet between δ 7.38 – 7.28, a 3-proton multiplet between δ 7.10 – 6.91, a 2-proton multiplet between δ 6.83 – 6.68, accounting for the overlapping aromatic protons for both the THIQ and haloaryl moieties. Additionally, a 1-proton broad singlet at δ 6.43 provided evidence of the amine functional group.

Entry 9 describes the reaction between morpholine and **4.52** under the alkaline conditions, whilst stirring at room temperature in CH₂Cl₂, to afford a quantitative yield for **4.54h**. In this case, upon comparison of the spectral information obtained for the starting material **4.52**, variation in the aliphatic region confirmed product formation. ¹H-NMR spectroscopy depicted two new 4-proton multiplets at δ 3.74 – 3.53 and δ 3.29 – 3.13, indicative of the methylene groups on the morpholine moiety of compound **4.54h**. It was disappointing however, to note that the reaction between piperazine and **4.52** gave no identifiable product (entry 10).

4.4 The synthesis of 1,2,3,4-tetrahydroisoquinolin-6-yl thiourea-linked analogues

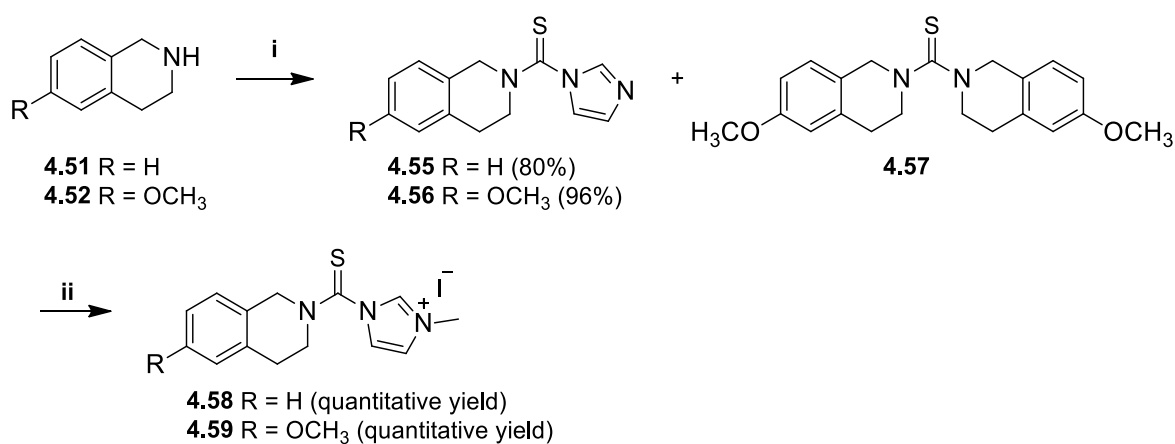
The second linker introduced involved the thiocarbonyl system, for which a number of methods reported by Katritzky and co-workers was consulted.¹⁴¹ These methods included the use of thioacylating agents such as thiophosgene,¹⁴¹ carbon disulfide^{114,115,142-145} and 1,1'-thiocarbonyldiimidazole (TCDI),¹³¹ all being reported for the synthesis of thiourea and thioamide moieties.¹⁴¹ Apart from thioacylation, the alternatives to achieving the same objective included the use of thionating agents, in which conversion of carbonyls into their corresponding thiocarbonyls with the use of sulfur dihydride, phosphorous pentasulfide and Lawesson's reagent among others, are important.¹⁴¹ However, since the results obtained in Table 4.2 illustrated that CDI was an effective carbamoyl transfer agent, the corresponding 1,1'-thiocarbonyldiimidazole (TCDI) was investigated for generating the intended

CHAPTER 4 | Investigation of linker group effects on the THIQ analogues

thiocarbonyl linker.¹³¹ For the purposes of comparison, it was considered that generating a library reflecting a variety of linker groups would empirically establish whether these groups could affect hydrogen bond interactions and/or affect the selectivity within the ER-binding pocket, especially since the thiocarbonyl motif has been quite pronounced in pharmaceutical applications.^{125,126} As with the carbonyl species, it was reported by Benbrook and co-workers¹⁴⁶ that this feature could be attributed to the C–S bond containing a more pronounced lone pair forming a 105° angle in molecules contain a thiocarbonyl functional group, *viz.*, R₂C=S, and being different to the angles between 130° and 180° calculated for thiourea systems, which had proved less suitable for facilitating effective hydrogen bonding.¹³⁹

4.4.1 Synthesis of THIQ–thiocarbamoyl imidazolium iodide salt

In Scheme 4.8 it is shown how the THIQ–thiocarbamoyl imidazoles **4.55** and **4.56** were prepared in reasonable yield, namely by treatment of compounds **4.51** and **4.52** with TCDI respectively. Surprisingly, treatment of **4.52** with TCDI gave in addition to product **4.56**, the unexpected dimer **4.57**, albeit in a low yield of 4%, not observed in the synthesis of **4.55**.



Scheme 4.8. Synthesis of the THIQ–thiocarbamoyl imidazolium iodide salts. Reagents and conditions: (i) TCDI, K₂CO₃, CH₃CN, 5 °C, overnight; (ii) CH₃I, CH₃CN, RT, overnight.

Dimerization resulting in the formation of **4.57** was not reported by Grzyb and co-workers,¹³¹ but was easily avoided by the introduction of an excess of solvent and by conducting the reaction at lower temperatures (0 °C), while adding **4.52** portion-wise over 2 hour-periods. Confirmation of the structure of products **4.55** and **4.56** by ¹H-NMR spectroscopy was as follows: two 1-proton multiplets at δ 7.92 – 7.83, δ 7.26 – 7.19, and a 1-proton doublet of doublets at δ 7.08 (*J* = 1.4 and 0.9 Hz) indicated the incorporation of the imidazole moiety. Furthermore, ¹³C-NMR spectroscopy confirmed the presence of the expected thiocarbonyl

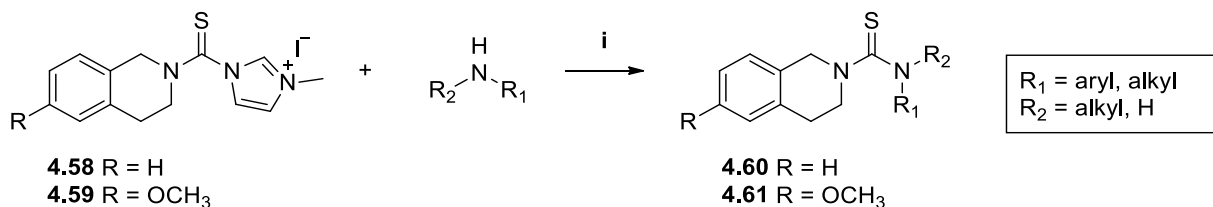
CHAPTER 4 | Investigation of linker group effects on the THIQ analogues

(C=S) moiety signal observed at δ 178.24. Subsequent alkylation of THIQ–thiocarbamoyl imidazoles **4.55** and **4.56** was cleanly achieved upon treatment with iodomethane at room temperature. No precipitant was observed in this case. However, monitoring the progress of the reaction by TLC indicated the consumption of both **4.55** and **4.56** starting materials. The product **4.58** obtained was a brown foam upon removal of solvent under reduced pressure and the $^1\text{H-NMR}$ spectrum for **4.58** displayed a 3-proton singlet at δ 3.77 indicating the presence of the newly incorporated methyl group. However, the analogue **4.59** proved to be too hygroscopic for isolation and characterization and consequently, a one-pot protocol was pursued for the subsequent reactions. It was noted that after storage of compound **4.59** at low temperatures and upon exposure to atmospheric conditions the foam-like material transformed into a sticky state which made its handling very onerous.

4.4.2 Coupling of THIQ–thiocarbamoyl imidazolium iodide salt with amines

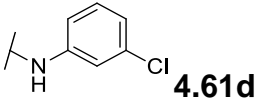
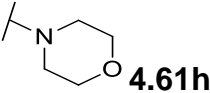
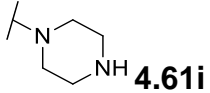
With compounds **4.58** and **4.59** in hand, the initial displacement of the imidazolium moiety was optimized using the model compound **4.58**. Once the best yields were obtained, **4.59** reacted in the same way but gave quite variable yields of product, as described in Table 4.3.

Table 4.3. Results and conditions for the procedures followed in Scheme 4.4.



Entry	Substrate	Nucleophile	Product	Yield (%)
1	4.58	2-amino-4-methylthiazole ^a	 4.60a	40
2	4.59	2-amino-4-methylthiazole ^a	 4.61a	80
3	4.59	2-amino-5-nitrothiazole ^b	 4.61b	7
4	4.59	4-anisidine ^{a-c}	 4.61c	17

CHAPTER 4 | Investigation of linker group effects on the THIQ analogues

5	4.59	3-chloroaniline ^{a,c}		Dimer 4.57 was obtained in 35%
6	4.59	morpholine ^b		64
7	4.59	piperazine ^b		Trace amount

Reagents and conditions described by Grzyb and co-workers: (i) THIQ salt (1.1 equiv), amine (1.0 equiv). ^aEt₃N (2.0 equiv), CH₃CN at RT, overnight; ^bCs₂CO₃ (3.0 equiv), CH₃CN at RT, overnight; ^c*n*BuLi (3.0 equiv), THF at RT, overnight.

Entry 2 demonstrates the successful displacement of the imidazolium moiety in **4.59** by 2-amino-4-methylthiazole to yield **4.61a** (80%). As previously observed in Table 4.2, the aryl methyl ether **4.59** resulted in better reactivity relative to **4.58**, which resulted in a lower yield of **4.60a** (40%). Progress of the reactions were monitored by TLC and despite longer reaction times and subsequent heating, no improvement on the 80% yield was observed for **4.61a**. An acidic work-up procedure was implemented for the removal of excess amine followed by purification with column chromatography, which afforded product as an oil in good yield. The ¹H-NMR spectrum showed the presence of a 3-proton singlet at δ 2.16 and a 1-proton singlet at δ 6.30, both being characteristic of the methyl group and the heteroaryl hydrogen of the thiazole moiety on compound **4.61a**, confirming product formation. Initially, no product was obtained (shown by entries 3 and 4) when similar conditions as for entries 1 and 2 were applied to the 2-amino-5-nitrothiazole and 4-anisidine starting materials. To improve product formation, pre-treatment of amines (**b** and **c**) by evaluating a few bases such as *n*BuLi, NaH and K₂CO₃ were investigated, unfortunately without any real change in product formation. In contrast to the carbamoyl linker, working with the thiocarbamoyl moiety proved to be more challenging than expected. It was clear that the replacement of the oxygen atom (C=O) with the sulfur atom (C=S), significantly affected the electrophilic centre (^{δ+}C=^{δ-}S) resulting in a decreased electrophilicity thus requiring better nucleophiles to allow the displacement of the imidazolium iodide salt moiety reported by Grzyb and co-workers.¹³¹ This was explained by the less efficient S_{3p}-C_{2p}π-orbital overlap in the thiocarbonyl (C=S) bond relative to the O_{2p}-C_{2p}π-bond and thus rendering a less polarized and more inert thiocarbonyl species.¹³¹

CHAPTER 4 | Investigation of linker group effects on the THIQ analogues

At the very best, only poor yields of product were obtained in Table 4.3 for entries 3 and 4. One obvious remedy for this conundrum would be the use of better nucleophiles. However, replacement of our current amines was not feasible since the synthesis of this library (containing varied linker groups) was to establish the influence of the substituent patterns on the potency and selectivity of these compounds provided by the varied linker groups within the receptors binding cavity. Achieving this, allowed only one variable *viz.*, the linker group, and thus amines (**a** – **g**) had to remain constant. Further investigation into the generation of thiourea substituents was thus explored by further studies of current literature.

4.4.3 Isothiocyanate to the rescue: Generating thiocarbamoyl analogues

Perusal of the literature resulted in the consideration of using isothiocyanates as a precursor toward our synthetic target. Use of isothiocyanates upon treatment with amines to readily form thioureas has been reported by Grzyb and co-workers, as well as by Berglund *et al.*^{126,130,133} Initial attempts by us at generating the isocyanate failed despite using a number of varied parameters.^{130,135} The problems associated with the synthesis of the isocyanates led to a degree of uncertainty as to whether the synthesis of isothiocyanates as an intermediate toward generating the thiourea bond should even be considered. Surprisingly, the isothiocyanate analogue proved to be much more stable and selective in comparison to the corresponding isocyanate.

This observation was explained by the different phases in which the p-orbitals exist as illustrated in Figure 4.12 (frame a and frame b). In the isocyanate molecule (in Figure 4.12, frame a) all the LUMO p-orbitals are in phase, thus making electron transfer from the nitrogen to the carbon and oxygen viable and thus generating a good electrophile, easily attacked by a nucleophile. In contrast, for the isothiocyanate molecule (in Figure 4.12, frame b), the p-orbitals are out of phase making the electron transfer by the nitrogen to the sulfur less likely. In addition to the electron donation, resonance of the isothiocyanate further results in the carbon being less polarized and making the isothiocyanate less sensitive to moisture in contrast to that previously experienced with the isocyanate species. These findings necessitated further exploration into employing the isothiocyanate as a synthon in the synthesis of our thiourea linkers.

CHAPTER 4 | Investigation of linker group effects on the THIQ analogues

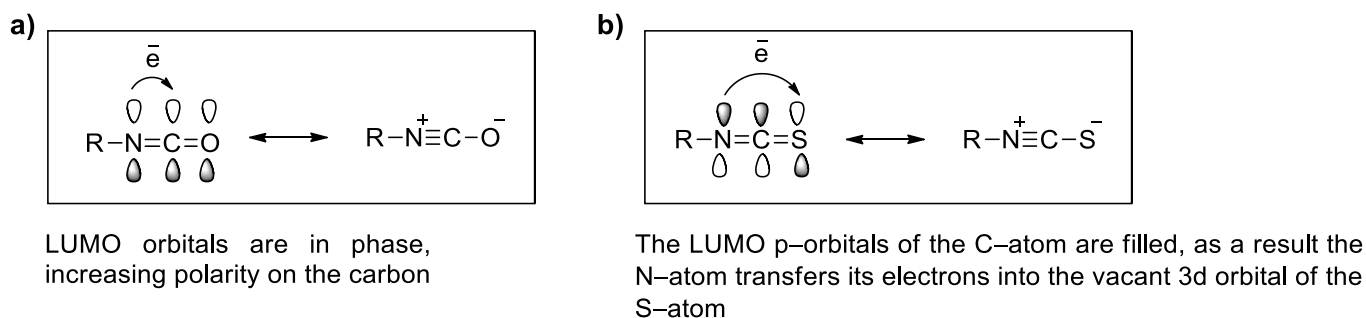
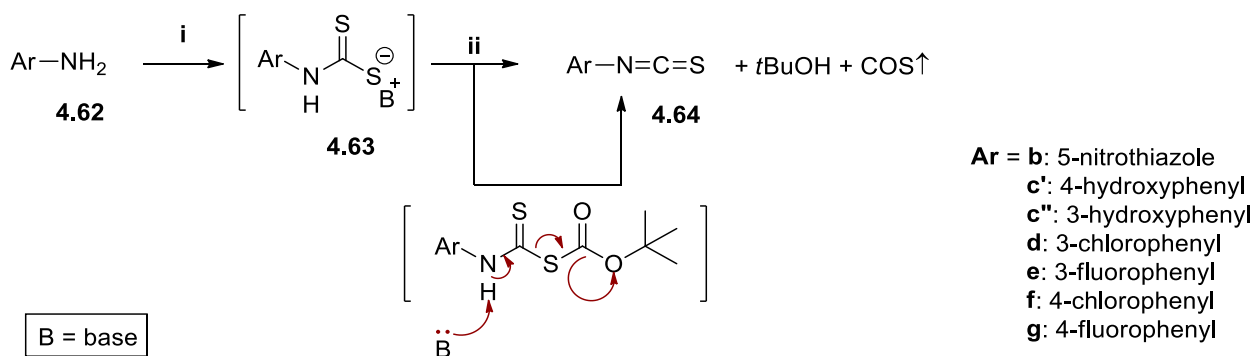


Figure 4.12. Frame a) Isocyanate, and frame b) Isothiocyanate.

4.4.3.1 Synthesis of isothiocyanate analogues

As previously mentioned, the isothiocyanate is another valuable reaction intermediate used for the synthesis of thiourea motifs. It was obtained upon treatment of the respective amines (**b – g**) with an excess of carbon disulfide under basic conditions (as shown in the Scheme associated with Table 4.4).

Table 4.4. Results obtained, and reaction conditions employed.

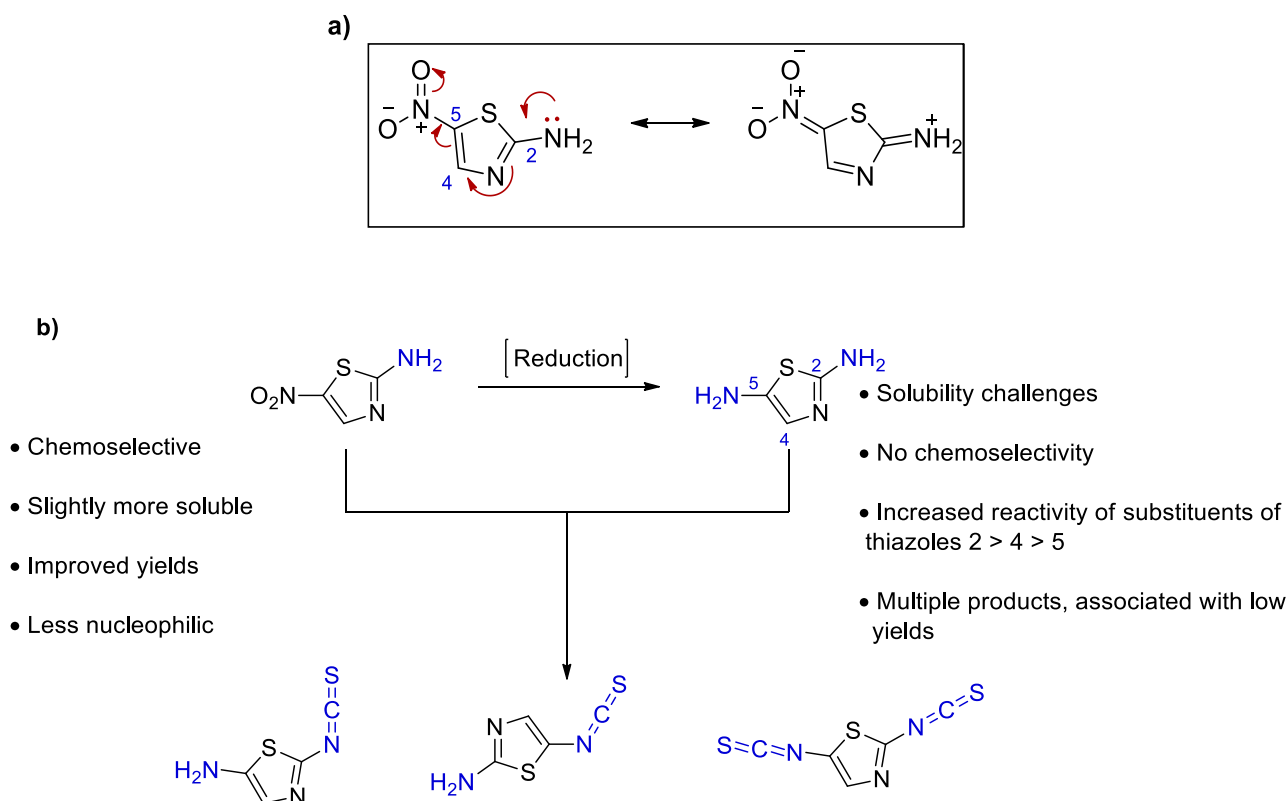


Entry	Substrate	Base	Desulfurylating agent	Reaction time (h)	4.64 Yield (%)
1	4.62b	NaH, THF	Boc ₂ O, DMAP	36	Trace amounts
2	4.62c'	Et ₃ N, EtOH	Boc ₂ O, DMAP	1.5	68
3	4.62c''	Et ₃ N, EtOH	Boc ₂ O, DMAP	1.5	77
4	4.62d	NaH, THF	TsCl	48	34
5	4.62e	NaH, THF	TsCl	48	85
6	4.62f	NaH, THF	TsCl	48	77
7	4.62g	NaH, THF	TsCl	48	36

Reaction conditions: (i) base (1.2 equiv), CS₂ (5.0 equiv); (ii) desulfurating agents.

CHAPTER 4 | Investigation of linker group effects on the THIQ analogues

Compound **4.61a** was successfully synthesized in respectable yields of 80% (see Table 4.3) using **4.59** and there was no need for synthesizing the corresponding isothiocyanate of 2-amino-4-methylthiazole. In Table 4.4 (entry 1), no product was obtained for amine **4.62b**. Despite changing parameters, *viz.*, base and solvent, no product was isolated. Failure associated with amine **4.62b** to react may be associated with its electron deficient amine due to resonance effects operating in the 2-amino-5-nitrothiazole (shown in Scheme 4.9a). The strong inductive and resonance effects associated with the nitro group would result in the lone pair of electrons of the 2-position amino moiety being less available for donation due to them being conjugated into the nitro group at the C5-position and thus not reactive enough toward the carbon disulfide. To improve the nucleophilicity of the amine functionality, reduction of the nitro-group would transform it into a better electron-donating group and thus improve the reactivity/nucleophilic character of the amine. However, upon consideration, the possibility that this procedure might lead to the formation of multiple products convinced us that this approach would not be a viable route (see Scheme 4.9b).



Scheme 4.9. Proposed resonance structures for 2-amino-5-nitrothiazole **4.62b**.

Entries 2 and 3 from Table 4.4 illustrate a method described by Munch and co-workers,¹¹⁴ where amines (**4.62c'** and **4.62c''**) were dissolved in EtOH under basic conditions, and to

CHAPTER 4 | Investigation of linker group effects on the THIQ analogues

which an excess of carbon disulfide was then added. It was fortunate that the latter two phenols did not show any chemo selectivity issues in the reaction and thus saved a demethylation step which would have been required if anisole was used as the amine. The reaction was efficient, with short reaction times, and provided isocyanate product in moderate yields. Precipitation of the intermediate salt **4.63** occurred within 30 minutes, confirmed completion of the reaction. Formation of products **4.64c'** and **4.63c''** was achieved upon separate treatment of intermediates **4.63c'** and **4.63c''** with di-*tert*-butyl dicarbonate (Boc₂O), catalyzed by the addition of 4-dimethyl aminopyridine (DMAP), which was required for accelerating the desulfurylation of the dithiocarbamate **4.63** intermediate to provide the isothiocyanate **4.64**.

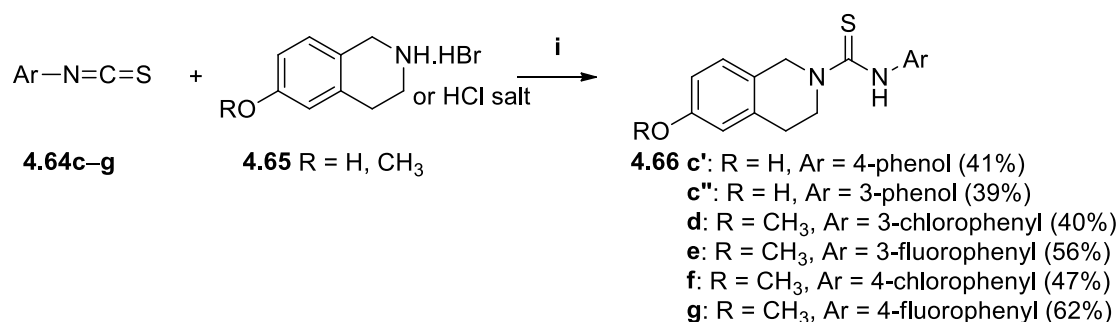
Apart from the use of Boc₂O, desulfurylation could additionally be effected by a) use of tosyl chloride as described in a method reported by Wong and Dolman,¹⁴⁵ b) 1,1'-(ethane-1,2-diyl) dipyridinium bistribromide (EDPBT) as reported by Yella and co-workers,¹⁴² c) triphosgene as reported by Chaskar and co-workers¹⁴⁴ or d) thiophosgene and 2,4,6-trichloro-1,3,5-triazine (TCT).^{114,115,142-145} However, these methods frequently result in the formation of many by-products, as well as require tedious work-up procedures for quenching the harsh reagents (*viz.*, thiophosgene or phosgene) by acidification or basification (TCT), followed by purification with column chromatography which could be time consuming. The employment of Boc₂O as the desulfurylation agent generated by-products such as carbonyl sulfide (COS) which could easily be eliminated as a gas, while the Et₃N, *t*BuOH and EtOH were efficiently removed under reduced pressure with no further purification being needed (as illustrated in the scheme of Table 4.4). Unfortunately, this method was only successfully executed with the amines **4.62c'** and **4.62c''** containing electron-donating substituents. Unlike with **4.62c'** and **4.62c''**, much longer reaction times and stronger bases were required to obtain products **4.64d – g**. For this reason, the method reported by Wong and Dolman¹⁴⁵ was implemented which included the use of tosyl chloride. The use of tosyl chloride in entries 4 – 7 indicated good results, but were not very reproducible with variable yields being obtained.¹⁴⁵

For entries 4 – 7, the haloanilines (**d – g**) were treated with three equivalents of NaH in THF and left to stir at room temperature for 4 hours. During this time, multiple colour changes were observed with the chloroaniline species (**4.62d** and **4.62f**) going from a black to a bright green coloured mixture and the fluoroaniline species (**4.62e** and **4.62g**) from a white to a bright purple coloured mixture. Once the later colour change occurred the reaction mixture

CHAPTER 4 | Investigation of linker group effects on the THIQ analogues

remained this colour (indicating the complete deprotonation), and to which carbon disulfide (CS₂) was added, affording an orange coloured mixture containing the dithiocarbamate salt **4.63**. Despite the addition of extra CS₂ and NaH, and even with reaction times exceeding 48 hours, no complete or improved conversion of starting material was observed. However, compound **4.64e**, initially obtained in 35% yield, was the only case which showed an improved yield of product upon the addition of extra base and CS₂, since after a further 24-hour stirring period an 85% yield of **4.64e** was obtained (entry 5, in Table 4.4). With the electron-rich amines (**4.62c'** and **4.62c''**), use of Boc₂O as a desulfurylating agent proved successful, but this was not the case when applied to the electron poor amines (**4.62d – g**), where the only products obtained after purification were the *tert*-butyl carbonate protected amines. Despite longer reaction times, for entries 4 – 7 the tosyl group was easily substituted by the more resonance stabilized intermediate system. The tosyl moiety thus provided an excellent leaving group, with products **4.64d – g** obtained in poor to moderate yields after purification (as illustrated by entries 4 – 7 in Table 4.4).

With the isothiocyanates **4.64** in hand, they were treated with the THIQ hydrochloride or hydrobromide salt **4.65** under basic conditions, to provide a small library of products **4.66**, generally in moderate yields, as shown in Scheme 4.10.



Scheme 4.10. Formation of the thiourea analogues. Reagents and conditions: (i) Et₃N in CH₃CN under reflux.

The THIQ-based compounds **4.66** share significantly similar key signals in the aliphatic region for both ¹H- and ¹³C-NMR spectral information of the THIQ moiety. For this reason, the NMR spectra described below will focus on the aromatic region for compounds **4.66c – g**, in order to avoid too much repetition. Remarkable and interesting disparities were observed in the aromatic region of the ¹H-NMR spectra of products **4.66c – g**. The spectrum of the 4-hydroxy-analogue **4.66c'** showed a 4-proton arrangement of doublets at δ 7.06 – 7.94 for the 4-hydroxyphenyl moiety, in addition to a 3-proton multiplet observed at δ 6.64

CHAPTER 4 | Investigation of linker group effects on the THIQ analogues

– 6.59 for the THIQ aromatic moiety. On the other hand, the spectrum for the 3-hydroxy-analogue **4.66c''** displayed two 1-proton multiplets at δ 7.44 – 7.29 and δ 7.16 – 7.02 (overlapping aromatic protons from both the THIQ moiety and the phenol moiety). In addition, a 2-proton complex multiplet between δ 7.16 – 7.00 and a 3-proton multiplet between δ 6.71 – 6.53, indicative of the THIQ moiety, made up the rest of the spectrum for compound **4.66c''**. Upon comparison to the THIQ hydrochloride salt **4.65** precursor, the spectroscopic data obtained for compounds **4.66d** and **4.66f** contained an additional set of aromatic proton resonances. This was attributed to the successful incorporation of the isothiocyanatochlorobenzene portion of compound **4.66d**. Three 2-proton multiplets were observed between δ 7.30 – 7.21 (6-protons), a 4-proton multiplet at δ 7.19 – 7.00 and a 2-proton multiplet between δ 6.86 – 6.68, supporting the successful synthesis of **4.66d**. The structural characterization of **4.66f** was evident from a 2-proton multiplet at δ 7.25; a 3-proton multiplet at δ 7.06, with an additional 2-proton multiplet between δ 6.86 – 6.70 attributed to the overlapping aromatic protons of both the THIQ and chlorophenyl moiety. Apart from the ^1H -NMR spectra, ^{13}C -NMR spectroscopy was employed for the identification of the thiocarbonyl (C=S) group at δ 183.20 (for **4.66d**) and δ 182.52 (for **4.66f**), further confirming product formation.

A similar NMR spectroscopic profile was also shared by compounds **4.66e** and **4.66g** in the aliphatic region, including a few key signals confirming the incorporation of the THIQ-moiety. However, compounds **4.66e** and **4.66g** could be differentiated by their ^1H NMR spectroscopic J -values, and the aromatic profile in frame a and frame b in Figure 4.13.

CHAPTER 4 | Investigation of linker group effects on the THIQ analogues

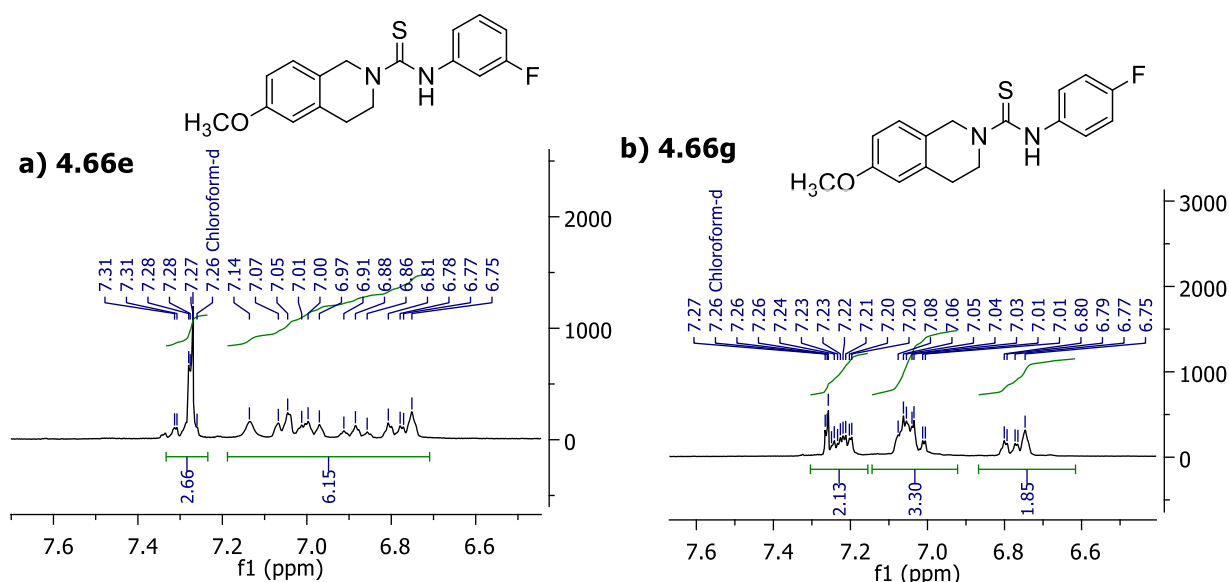


Figure 4.13. Portions of the aromatic ¹H-NMR spectra for compounds **4.66e** and **4.66g**.

Figure 4.13 frame a, shows the overlapping aromatic signals for the THIQ and 3-fluorophenyl moieties of compound **4.66e**, two sets of multiplets between the regions δ 7.31 – 7.26 and δ 7.14 – 6.75. Frame b, represents the overlapping signals associated with the THIQ and 4-fluorophenyl moiety of compound **4.66g**.

4.5 The synthesis of 1,2,3,4-tetrahydroisoquinolin-6-yl sulfonylurea-linked analogues

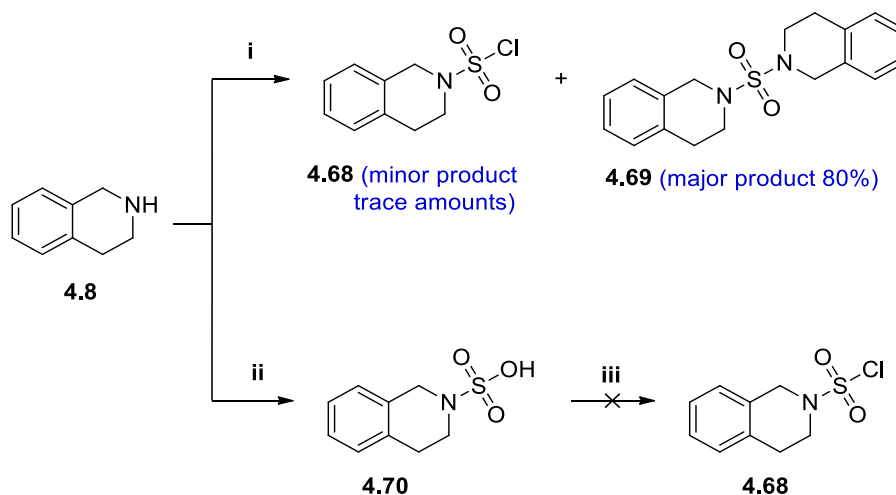
4.5.1 Evaluation of protocols developed for the synthesis of the sulfonyl amide moiety

One of the main goals of the current work was to generate varied linkers on the THIQ scaffold. To achieve this, an effective strategy for generating a library with a sulfonyl urea linker formed an essential part of the project.

However, as previously described with the carbamoyl chloride analogues, only a limited number of sulfonyl chlorides are commercially available, and consequently a synthetic protocol for their preparation would be desired. However, as with the carbamoyl chlorides, the corresponding sulfonyl chlorides were found to be too reactive, placing a serious limitation on their synthesis. As illustrated by Scheme 4.11, employing conditions (i) for sulfonyl chlorination, resulted in several problems being encountered, the major one being the synthesis of the unwanted dimer **4.69**. Attempts at varying the conditions, *viz.*, order of

CHAPTER 4 | Investigation of linker group effects on the THIQ analogues

addition, concentration, as well as the rate of addition of amine **4.8** to sulfuryl chloride and temperature variation, yielded either very little or no product **4.68**. Confirmation of the unwanted product **4.69** was provided by both ESI⁺ TOF MS, as well as ¹H-NMR spectroscopy. Conditions used in method ii were employed to generate the sulfonic acid **4.70** to avoid dimerization. However, treatment of **4.70** with a variety of chlorinating agents all led to the formation of a brown residue whose ¹H-NMR spectrum was devoid of aryl hydrogen signals.

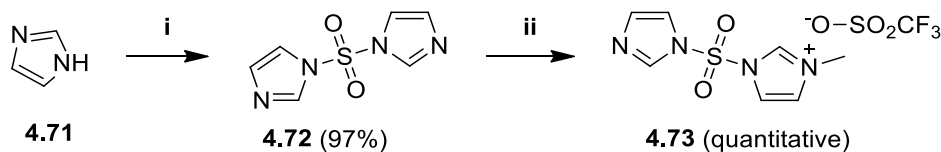


Scheme 4.11. Reagents and conditions for sulfonyl chlorination: (i) SO₂Cl₂, CH₂Cl₂, -78 °C; (ii) SO₃HCl, CH₂Cl₂, 0 °C; (iii) SOCl₂ or C(COCl)₂ or POCl₃, CH₂Cl₂, 0 °C.

This result suggested that substrate **4.70** decomposed quite easily. This once again led to the use of a sulfonyl equivalent of the CDI transfer agent, prepared by means of the method described in Scheme 4.12.

4.5.2 Synthesis of 1,1'-sulfonylbis(1*H*-imidazolium) triflate salt

Investigations into the literature suggested that, 1,1'-sulfonylbis(1*H*-imidazolium) triflate salt chemistry associated with the imidazolium triflate salt **4.73** could offer alternative solutions to form CDI analogues.¹⁴⁰



Scheme 4.12. Reagents and conditions: (i) SO₂Cl₂, CH₂Cl₂, 0 °C, overnight; (ii) CH₃OTf, CH₂Cl₂, 0 °C, 6 h.

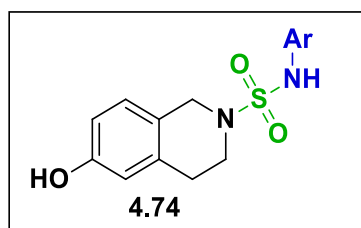
CHAPTER 4 | Investigation of linker group effects on the THIQ analogues

Thus synthesis of compound **4.72** was efficiently undertaken, following a procedure previously described by Cívicos and co-workers,¹⁴⁷ involving the slow addition of sulfonyl chloride to a solution of imidazole **4.71** in CH₂Cl₂ at low temperatures, as illustrated in Scheme 4.12. The low temperature (0 °C) was maintained for 5 hours during which formation of a dense white precipitant confirmed the complete consumption of imidazole. The white precipitant (salt) was filtered and the eluent partitioned between water and CH₂Cl₂, giving product **4.72** in good yields ranging from 60 – 97%.

The structure of compound **4.72** was confirmed using ¹H-NMR spectroscopy, which confirmed the presence of three 1-proton singlets at δ 8.02, δ 7.28 and δ 7.14, that corresponded well with the values reported in the literature.¹⁴⁰ However, unlike CDI and TCDI, no substitution reactions were possible with **4.72** in our hands. Despite the pre-treatment regime of the THIQ amine **4.8** with base, or heating, no sulfonamide linker was obtained. Consequently, sulfone **4.72** was treated with methyl triflate at low temperatures, which generated the 1,1'-sulfonylbis(1*H*-imidazolium) salt **4.73**. The integrity of **4.73** was confirmed by ¹H-NMR spectroscopy, in which an intense 3-proton singlet was observed upfield at δ 3.87, indicative of the successful methylation of the one imidazole moiety. Additionally, the chemical shifts observed in the aromatic region seemed more complex compared to the precursor, due to the asymmetric structure generated by the incorporation of the methyl group. Pleasingly, both ¹H- and ¹³C-NMR spectra for **4.73** corresponded well with the reported literature values described by Beaudoin and co-workers.¹⁴⁰

Preparation of the THIQ analogues **4.74** shown in Figure 4.14 were next undertaken, in which **4.73** upon treatment with the THIQ hydrochloride salt would provide the THIQ sulfonyl imidazole intermediate. The subsequent reactions included methylation of the THIQ sulfonyl imidazole moiety group, which would then be methylated providing the activated imidazolium triflate salt, for undergoing treatment with amines (**a – h**) to generate the sulfonyl analogues **4.74** in Figure 4.14.

CHAPTER 4 | Investigation of linker group effects on the THIQ analogues

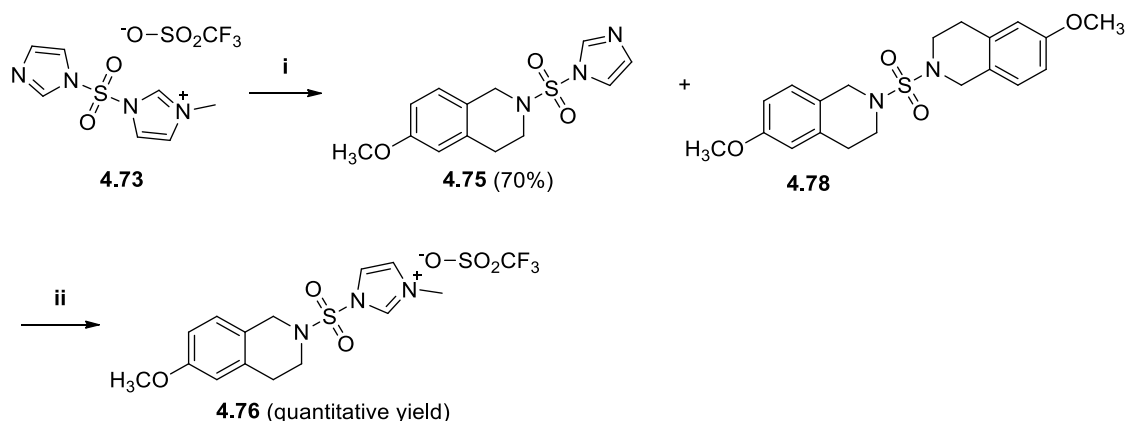


- Ar =** a: 4-methylthiazole
 b: 5-nitrothiazole
 c: 4-anisole
 d: 3-chlorophenyl
 e: 3-fluorophenyl
 f: 4-chlorophenyl
 g: 4-fluorophenyl
 h: morpholine

Figure 4.14. Intended structures for the sulfonyl urea linked library.

4.5.3 Synthesis of 1-[[6-methoxy-3,4-dihydroisoquinolin-2(1*H*)-yl]sulfonyl]-3-methyl-1*H*-imidazol-3-ium triflate salt

Neutralization by pre-treatment of the 6-methoxy-1,2,3,4-tetrahydroisoquinoline hydrochloride salt **4.51** with base, prior to addition of the sulfonyl imidazolium triflate salt **4.73** was essential for improving on the homogeneity of the reaction (see Scheme 4.13). The reaction mixture was stirred at room temperature overnight to afford compound **4.75** in good yield. However, as previously observed in the TCDI reactions, caution had to be taken, since the dimer **4.78** was also obtained in minor amounts. ^1H - and ^{13}C -NMR spectroscopy was employed for confirmation of compound **4.75** and allowed characterization by the key identifiable structural features associated with the THIQ skeleton. Two 2-proton triplets (indicative of the methylene groups at C3 and C4) were found at δ 2.85 and δ 3.48, together with an intense 3-proton singlet at δ 3.74 (OCH_3) and a 2-proton singlet at δ 4.33 (ArCH_2N) which confirmed the presence of the THIQ moiety. Further signals observed were the three 1-proton singlets at δ 7.91, δ 7.23 and δ 7.08 ascribed to the imidazole ring. The THIQ sulfonyl imidazole-analogue **4.75**, was next converted into its corresponding imidazolium triflate salt **4.76** upon treatment with methyl triflate at low temperature, to give the final triflate salt **4.76** in quantitative yield as a white solid.



Scheme 4.13. Synthesis of the THIQ-sulfonyl imidazolium triflate salt. Reagents and conditions: (i) **4.39**, K_2CO_3 , CH_2Cl_2 , RT, overnight; (ii) CH_3OTf , CH_2Cl_2 , 0°C , 6 h.

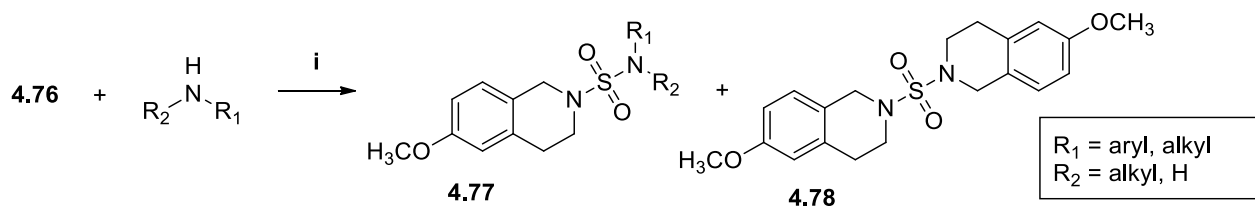
CHAPTER 4 | Investigation of linker group effects on the THIQ analogues

Compound **4.76** proved to be hygroscopic, which complicated its handling under atmospheric conditions. These findings resulted in the synthetic procedure described by Beaudoin and co-workers being modified to a one-pot procedure, in which the amine was directly added to **4.76** without prior isolation.¹⁴⁰ Product **4.76** formation was elucidated from its ¹H-NMR spectrum by the presence of an overlapping 5-proton multiplet between δ 3.86 – 3.74 (CH₃ and CH₂ groups) indicating the presence of the THIQ moiety. Additionally, the aromatic protons of the imidazolium moiety appeared as 1-proton doublets ($J = 3.0$ Hz) at δ 9.59, δ 8.02 and δ 7.70 for all three protons.

4.5.4 Coupling of the THIQ-sulfonyl imidazolium triflate salt **4.76** with amines

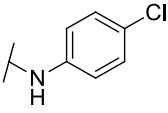
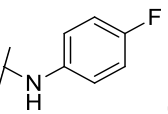
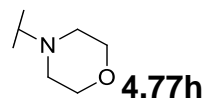
The hygroscopic nature of the compound **4.76** made handling very challenging. Compound **4.76** was thus generated, followed by solvent removal under reduced pressure to provide a residue. This residue was then placed under a vacuum followed by backfilling with nitrogen, and finally by addition of the respective amines (**a – h**) as illustrated in Table 4.5.

Table 4.5. Reaction conditions applied in the synthesizing sulfonamide linked analogues.



Entry	Substrate	Nucleophile	Product	4.77 Yield (%)
1	4.76	2-amino-4-methylthiazole a	No product but 4.78 was obtained.	Dimer 60
2	4.76	4-anisidine ^b	 4.77c	87
3	4.76	3-chloroaniline	 4.77d	40
4	4.76	3-fluoroaniline	 4.77e	46

CHAPTER 4 | Investigation of linker group effects on the THIQ analogues

5	4.76	4-chloroaniline		54
6	4.76	4-fluoroaniline		94
7	4.76	Morpholine		70

Reagents and conditions described by Beaudoin and co-workers:¹⁴⁰ (i) **4.76** (1.1 equiv), amine (1.0 equiv). ^aEt₃N (2.0 equiv), CH₃CN at 80 °C, overnight; ^bK₂CO₃ (2.0 equiv), CH₃CN at RT, overnight; ^cCs₂CO₃ (3.0 equiv), CH₃CN at 80 °C, overnight.

The synthesis of compounds **4.77c – h** essentially followed a similar method to that employed for the urea analogues. It should be noted that there is a paucity of literature for the synthetic design of unsymmetrical sulfonyl urea analogues. Other popular methods for synthesis of the sulfonyl urea motif, includes oxidation of a sulfur-bridge to afford the desired sulfonamide (SO₂NH) moiety. However, work described by Cívicos,¹⁴⁷ Beaudoin¹⁴⁰ and co-workers included the substitution of the imidazolium triflate salt with primary and secondary amines, thereby providing asymmetric sulfonyl ureas. The results reported in Table 4.5, were obtained by making use of a synthetic protocol similar to that described by Beaudoin and co-workers.¹⁴⁰ However, it was necessary to modify the earlier developed parameters to achieve satisfactory results.

Entry 1 in Table 4.5, demonstrated that the product obtained by treatment of the sulfonyl imidazolium triflate salt with the primary amine **a** (2-amino-4-methylthiazole), was the unwanted dimer **4.78**. Considering the lability displayed by **4.76**, the procedure was repeated at lower temperatures. It was found that at room temperature no reaction occurred with amine **a**, and **4.76** was recovered unchanged with no product formation. Optimization by investigating a variety of bases, solvents and temperatures, produced no product when trying to couple the **4.76** with the thiazole amine. The aminothiazole proved to be too weak a nucleophile, which caused the focus being shifted to coupling between amines (**c – h**) with compound **4.76**. Entry 2 illustrates **4.77c** being isolated in good yield (87%) when the reaction mixture was stirred at room temperature overnight. However, heating only led to formation of dimer **4.78** in a 70% yield. Furthermore, compound **4.77c** was isolated as a brown oil and its structure confirmed by use of ¹H-NMR spectroscopy. As observed with the former carbonyl and thiocarbonyl coupled compounds (**4.54**, **4.61** and **4.66**), the

CHAPTER 4 | Investigation of linker group effects on the THIQ analogues

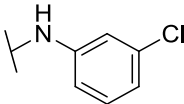
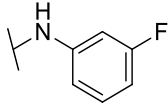
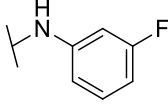
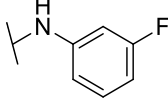
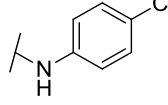
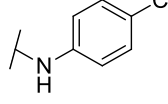
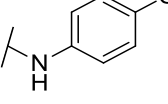
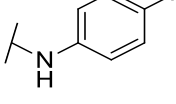
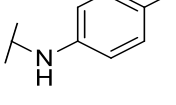
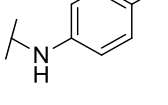
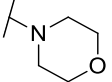
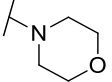
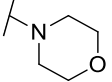
sulfonamide analogue displayed a similar $^1\text{H-NMR}$ spectral profile. The presence of the THIQ moiety was confirmed by the two 2-proton triplets observed at δ 2.82 and δ 3.63 indicative of the two methylene groups. Additionally, an intense 6-proton signal at δ 3.73 (2 x OCH_3), an intense 2-proton singlet at δ 4.52 (ArCH_2N), two multiplets at δ 6.60 and δ 6.84, a 1-proton singlet at δ 6.99 and a 2-proton multiplet at δ 7.14 – 7.30 (2-protons) provided sufficient confirmation to the ascribed structure of the product **4.77c**. HRMS ESI^+ was further employed which provided a molar mass m/z $[\text{M}+\text{H}]^+$ of 349.1207 that corresponded well with the calculated value 349.1177.

Surprisingly, in order to obtain products **4.77d – g** room temperature proved to be insufficient. Upon coupling the haloanilines with compounds **4.76**, no strong base was necessary, but heating at $80\text{ }^\circ\text{C}$ provided the products in moderate to good yields as shown in Table 4.5. When being stirred at room temperature all reagents were recovered unchanged. As previously described, product structures were confirmed by $^1\text{H-}$ and $^{13}\text{C-NMR}$ spectroscopy. The THIQ moiety was easily confirmed by the general profile presented by the aliphatic region of the NMR spectral data. Use of ESI^+ TOF MS was employed to further confirm product formation, in which the calculated monoisotopic masses of the compounds **4.77d – g** corresponded well with the experimental values (see experimental section for more details).

4.6 Deprotection of aryl methyl ethers

The various linker groups displayed different stabilities toward demethylating protocols and reagents. A common problem associated with general compounds **4.79** was their solubility before and especially after deprotection of the aryl methyl ether functional group. Thus, a few methods were evaluated in Table 4.6 for obtaining demethylated products in good yield. A preferable method included one in which no water work-up would be required. In entries 1, 2 and 5, the use of boron tribromide (BBr_3) proved to be compatible with a range of functional groups. Despite its tolerance, the reagent had the tendency of coordinating to additional functional groups and was thus required in a large excess for effecting a successful demethylation of the aromatic methyl ether groups. Demethylation was efficient with the reaction being complete within 6 hours. Problems were however encountered during the aqueous work-up procedure. An aqueous work-up procedure was essential for hydrolysing the excess BBr_3 , as well as to promote the *in situ* HBr formation required for the protonation of the alkoxide to form the phenol group. Extraction of the phenolic products

CHAPTER 4 | Investigation of linker group effects on the THIQ analogues

9	4.77d^a	SO ₂	Me		34
10	4.54e^b	CO	Me		35
11	4.64e^b	CS	Me		0
12	4.77e^a	SO ₂	Me		10
13	4.54f^b	CO	Me		50
14	4.64f^{a, b}	CS	Me		44
15	4.77f^a	SO ₂	Me		41
16	4.54g^b	CO	Me		2
17	4.64g^{a, b}	CS	Me		0
18	4.77g^a	SO ₂	Me		33
19	4.54h^c	CO	Bn		79
20	4.64h^b	CS	Me		20
21	4.77h^b	SO ₂	Me		25

Reagents and conditions: (i) THIQ salt (1.1 equiv), amine (1.0 equiv). ^aBBr₃ (10.0 equiv), CH₂Cl₂ at 0 °C, 24 – 48 hours; ^bAll₃ (5.0 equiv), PhCH₃/PhH at 40 – 110 °C, 24 – 48 hours; ^cPd/C, H₂, EtOH at 40 °C, overnight.

CHAPTER 4 | Investigation of linker group effects on the THIQ analogues

It was found that despite the use of BBr_3 or aluminium triiodide (AlI_3), certain products were inaccessible (mostly C=S linked entries 3, 4, 8, 11 and 17). The reactions (entries 3 and 4), were monitored with TLC which indicated multiple spots and thus formation of a number of compounds or the decomposition of the product. Isolation of these compounds resulted in even more spots with yields too low for analytical evaluation. However, for entries 8, 11 and 17, the TLC indicated the complete conversion of starting material to products **4.80d – g**. Despite this, when purifying the crude residue through a small plug of silica gel, no product was obtained. TLC monitoring presented evidence of decomposition, where the initial single spot now presented multiple spots. Purification was attempted using a plug of activated aluminium oxide. However, this did not solve the problem and unfortunately no product was obtained.

After a number of trial reactions, AlI_3 proved to be the best demethylating protocol for the carbonyl ureas **4.54**, as shown in entries 7, 10, 13, 16, 20 and 21. The AlI_3 was prepared by treatment of suspended Al-filings with iodine, followed by heating under reflux for 2 hours in toluene.⁹³ The reaction mixture was cooled, to which the ureas **4.54d – g**, **4.64h** and **4.77h** were then added. When left at room temperature no reaction occurred, but with heating at 60 °C for 24 – 48 hours, product in poor to moderate yields became obtainable. Strangely, while TLC monitoring of the reaction mixture indicated complete conversion, during purification products were only obtained in low yields. Apart from the sulfonyl urea **4.77c** (entry 6), the AlI_3 reaction conditions proved to be too harsh. Even with mild heating at 40 °C, no reaction proceeded when applied to sulfonyl ureas (**4.77d – g**). The products of entries 9, 12, 15 and 18 were then demethylated using BBr_3 as the demethylating agent. Despite the poor yields obtained for compounds **4.74d – g** enough product was obtained for characterization, as well as for the required biological testing.

Unlike most of the reactions reported in Table 4.6, which were associated with solubility problems, as a precaution the hydroxyl group of the compound **4.54h** was protected by conversion to a benzylic group using a benzyl chloride. The deprotection protocol required for substrate **4.54h** has advantages since it eliminates (i) the aqueous work-up, (ii) filtration of the heterogeneous catalyst (10% Pd/C) gives less impurities and (iii) solubility would not be a problem since the reaction would be performed in a polar solvent (EtOH). For entry 19, good yields were obtained when compound **4.54h** was dissolved in EtOH, to which the 10% Pd/C catalyst was added and stirred at 40 °C. Unfortunately, this method could not be applied to any of the sulfur containing compounds, since these have been well-known for poisoning

CHAPTER 4 | Investigation of linker group effects on the THIQ analogues

metal catalysts. Although the benzyl group proved to be the best protecting group experiencing very little challenge during the deprotection to generate the hydroxyl moiety, it was thus not a general method to be adopted.

4.7 Summary and concluding remarks

Three urea-linked THIQ molecules were synthesized using a general procedure, in which CDI-type equivalent reagents were used (in Figure 4.15). The imidazole behaved as an excellent leaving group, providing a near perfect transfer agent. However, removal of the second imidazole moiety was only achieved by initial methylation forming the imidazolium salts **4.82a – c**, followed by displacement of the imidazolium portion with the THIQ hydrochloride salt (shown in Figure 4.15).

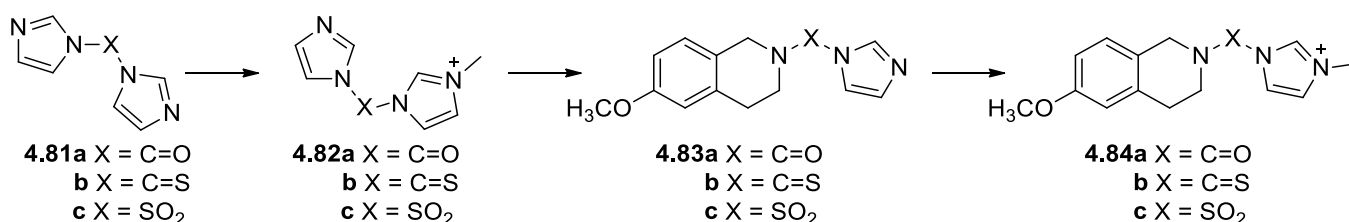


Figure 4.15. General protocol for synthesis of the THIQ imidazolium salt **4.84**.

Compounds **4.83a** and **4.83c** were obtained in reasonable yields; however, the synthesis of compound **4.83b** required much lower temperatures and the reaction mixture was diluted to avoid formation of the dimer **4.57**. Treatment of compounds **4.83a** and **4.83b** with methyl iodide provided the imidazolium iodide salts **4.84a** and **b**. Compound **4.83c** was however treated with methyl triflate to yield the sulfomoyl imidazolium triflate salt **4.84c**. Once compound **4.84** was in hand, it was treated with a few selected amines (**a – g**) under conditions previously described in earlier sections of the chapter to afford the pivotal, precursor **4.54**, **4.61**, **4.64** and **4.77** for target compounds **4.46**, **4.74** and **4.80**. However, in the case of **4.84b** substitution with the haloanilines, using the *n*BuLi was not as successful and synthesis of the haloisothiocyanates were synthesized.

The thiourea-linked THIQ analogues (**4.66c – g**) were synthesized in good yields, by heating the THIQ salt **4.65** with the isothiocyanate (**4.64d – g**) under alkaline conditions. One of the challenges associated with this method, was the poor reproducibility when synthesizing the isothiocyanate. Demethylation of the thiourea linked compounds **4.66d – g** also proved to be quite challenging with either no or very poor yields of product being

CHAPTER 4 | Investigation of linker group effects on the THIQ analogues

obtained. Due to time restraints, no further attempts to demethylate compounds **4.66d – g** were pursued. Despite the unsuccessful demethylation of the thiourea species, both the carbonyl and sulfonyl urea compounds were successfully demethylated in satisfactory yields and products are shown in Table 4.6.

Chapter 5

Isochromanone: A surprisingly valuable intermediate

The final library, library 3, in which the THIQ analogues do not contain the two-atom linkers previously discussed for library 2 (Chapter 4) is presented here. A broad range of synthetic approaches were trialled for this library of compounds which eventually led to a procedure including the condensation reaction between the isochromanone intermediate and a few selected primary amine aryls, which provided the desired target compounds. These compounds were specifically designed to compare their structure-activity relationship to that of the THIQ urea-linked analogues generated in library 2.

5.1 Introduction

As mentioned in earlier chapters, THIQs are important synthetic targets because of their potent pharmacological properties.^{1,95,96,107} Members of this family displayed improved antagonistic/agonistic estrogen modulation upon comparison to a well-known SERM, lasofoxifene discussed in Chapter 3.¹ This resulted in the designing of a library of compounds which contained the THIQ skeleton with varied linker groups having heteroaryl substituents intended for mimicking the estradiol D-ring interactions, within the ER binding pocket described for Library 1. A similar set of compounds designed by Redda *et al.* indicated that with a two-atom linker their compounds were able to demonstrate positive anti-proliferative results when tested against three different cancer cell lines.⁹⁸ These encouragingly positive results indicated that despite our initial computational docking study predictions, such relatively large compounds were able to successfully enter the binding pocket of the ER and interact with targeted residues. Apart from Redda's work, the docking studies generated some uncertainty in how compounds containing a linker group could behave within the binding pocket of the ER (Figure 5.1, frame a). To test this theory, modification in the THIQ series was included, whereby the linker unit was absent, to determine the structure-activity relationship between the compound in Figure 5.1 shown in frame a and frame b. Thus, an alternative approach was followed by eliminating the linker group, whilst maintaining the western and eastern sections of the compounds in this library (Figure 5.1, frame b).

CHAPTER 5 | Isochromanone: A surprisingly valuable intermediate

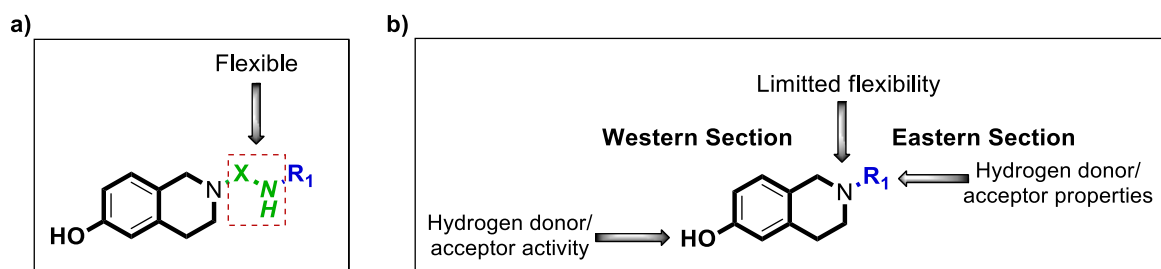


Figure 5.1. a) Library 2, THIQ linker analogues, b) Library 3, THIQ analogues without linker groups.

The envisaged new library was hoped to correspond quite well with E2 (the natural ligand), upon overlaying the desired analogues as illustrated in Figure 5.2 with the endogenous ligand in modelling. The docking studies indicated numerous promising binding interactions within the binding pocket and it was thus decided to proceed with the synthesis of a small library of THIQ analogues **5.1**.

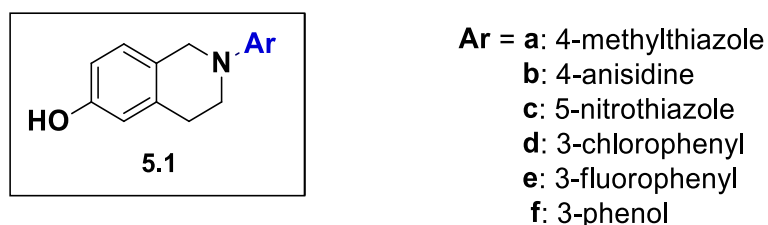


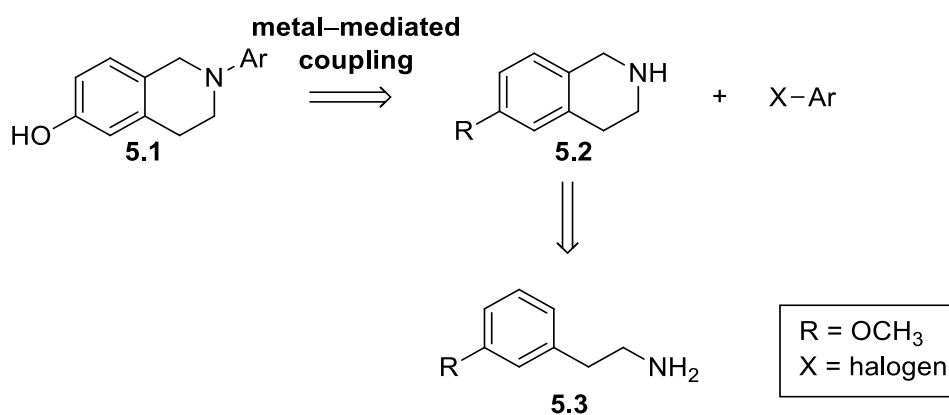
Figure 5.2. Library of isoquinolines possessing no linker groups.

Due to the structure–activity relationship studies for library 2 and library 3 the Ar–groups were to remain constant. The choice of aryl groups were determined by suggestions from Dowers,⁷⁰ Bolton⁸⁴ and co-workers, who proposed that the use of halogenated aromatic groups resulted *in vivo* in the generation of fewer metabolites, and less toxic DNA adducts. The toxic adducts were generated from aromatic methoxy and hydroxy functional groups during the analysis of their synthetic ligands for ERs, and therefore encouraged our use of haloaryl compounds for this study.

5.2 Retrosynthetic analysis 1: Metal–mediated coupling protocol for synthesizing THIQ analogues

In considering potential methods for construction of the target compounds (Figure 5.2), upon reviewing literature by Monnier and co-workers, a retrosynthetic analysis suggested that metal–mediated C–N bond formation could be employed as a good protocol for obtaining the various products depicted in the retrosynthetic Scheme 5.1.¹⁴⁸

CHAPTER 5 | Isochromanone: A surprisingly valuable intermediate



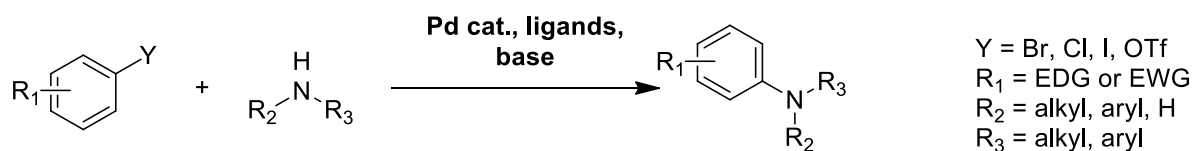
Scheme 5.1. Potential retrosynthetic route to the synthesis of the tetrahydroisoquinoline library.

The starting material, *viz.* the aryl ethyl amine **5.3**, has the required electron-donating group in the *meta*-position in order to promote a Pictet–Spengler reaction to form THIQ **5.2**, which would then be treated with a metal catalyst and various halogenated aryl substrates to afford the intended target compounds **5.1** (Scheme 5.1).

The development of protocols for C–C bond formation has seen some major innovative successes. Among these are well-known chemical procedures such as the Ullmann, Suzuki, Stille, and Negishi coupling reactions, described by Romero and co-workers in a review.¹⁴⁹ Despite significant improvements in the scope of C–C cross coupling methodologies for aryl–heteroaryl ring couplings, the C–N bond formation scope has been fairly limited.¹⁵⁰ These methods included the commonly used metal-mediated techniques such as the Buchwald–Hartwig,^{150–152} Chan–Lam¹⁵³ and Ullmann condensation^{148,154,155} type reactions depicted in Schemes 5.2 – 5.4.

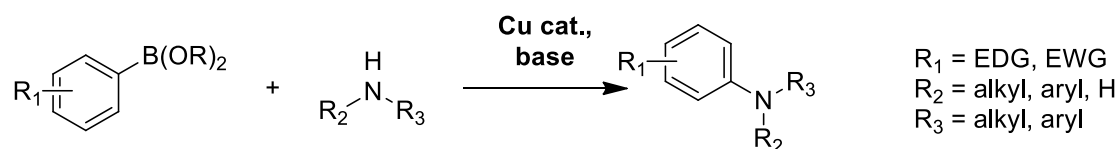
The Buchwald–Hartwig coupling reaction includes the use of palladium (Pd) catalysts with a broad range of ligands reviewed by Pujol and co-workers, which can be rather expensive.¹⁴⁹ Upon consulting the literature it was noted that under these reaction conditions led to the successful coupling of *N*-based substrates with varied aryl groups. However, literature supporting our initially intended heteroaryls THIQ coupling could not be found for the desired library to be synthesized.¹⁵⁶

CHAPTER 5 | Isochromanone: A surprisingly valuable intermediate



Scheme 5.2. A modified representation of the Buchwald–Hartwig coupling reaction as reported by Fischer and Koenig.¹⁵⁶

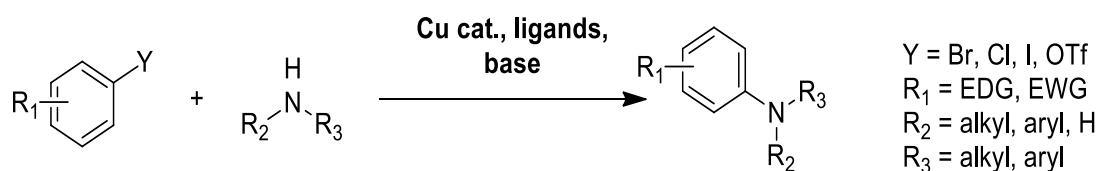
The Chan–Lam coupling is catalyzed by a copper^{II} species by the oxidative coupling of boronic acid substrates with a heteroaryl substrate to afford products with the desired C–N bond.¹⁵⁶ However, the Chan–Lam coupling reaction is limited to the use of boronic acids or boronic esters and is associated with long reaction times as reported by Rao *et al.*¹⁵³ In addition, a relatively limited number of commercial boronic acids are available and they can be expensive. Upon reviewing literature, it was found that synthetic procedures used for the coupling of secondary amines with boronic acids could generate our heteroaryls. However, it was found that the use of substrates such as the amine (THIQ) with heteroaryls (**a** – 2-bromothiazole, **b** – 4-bromothiazole and **c** – bromobenzene) were not that successful and were frequently associated with very low yields.^{148,149,153-155} As a result, this synthetic route was not considered as a possible protocol for the synthesis of our intended target molecules.



Scheme 5.3. A modified representation of the Chan–Lam coupling reaction as reported by Rao and Wu.¹⁵³

The Ullmann condensation reaction involves substitution reactions with a nucleophilic (heteroatoms such as NH, OH and SH groups) substrate with a haloaryl species where either a Cu^I or Cu^{II} species is employed as the catalyst.¹⁵⁵ There are a few advantages associated with the application of the Ullmann condensation protocol *viz.*, it is less toxic in terms of side products produced and utilizes less expensive reagents. However, like the Chan–Lam protocol, it is also associated with long reaction times and high temperatures, thus limiting its applications. A number of mechanistic pathways discussed in the literature explain the traditional Ullmann–type reactions broadly described in Scheme 5.5.^{4,98,101,149}

CHAPTER 5 | Isochromanone: A surprisingly valuable intermediate



Scheme 5.4. A modified representation of the Ullmann condensation reaction as reported by Sambiagio *et al.*¹⁵⁴

An interesting review by de Vries and co-workers, describes the Ullmann-type reactions being composed of four possible steps demonstrated in Scheme 5.5. The first route is described by method A in the diagram and involves the oxidative addition of the aromatic halide by Cu^I, resulting in the formation of a Cu^{III} intermediate formation. The Cu^{III} intermediate was initially questioned, but further investigations led to the idea being supported by many other researchers.¹⁵⁵ The second step, for method A, involves the coupled product and regeneration of the catalyst. Two possible protocols *viz.*, single electron transfer (SET) or halide transfer of the aryl radical intermediate, were the described processes responsible for the product formation and catalyst regeneration. Metals and organometallics have been accepted as compounds able to facilitate electron transfers (for instance, unimolecular radical nucleophilic substitution reactions). Initially, the role of free radicals in recovery of the catalyst was proposed by Waters in 1937. Valuable experimental contributions by Russel, Kornblum, Bunnet and Kochi provided further support to this claim, as described in Sperotto's review.¹⁵⁵ The results provided evidence supporting the presence of aryl radical anions in the mechanistic cycle, with the unimolecular radical nucleophilic substitution being accepted. The Cu^I Nu thus behaves as the coupling agent and the Cu coordinates to the ArX *via* a 4-centred intermediate, orientated accordingly to the partial charges of the Cu (δ⁺) and halide (δ⁻) species. Polarization of the carbon-halide bond then generates a partial positive charge on the formed *ipso*-carbon and assists in the substitution of the nucleophile, providing the free Cu species, as demonstrated in Scheme 5.5.

CHAPTER 5 | Isochromanone: A surprisingly valuable intermediate

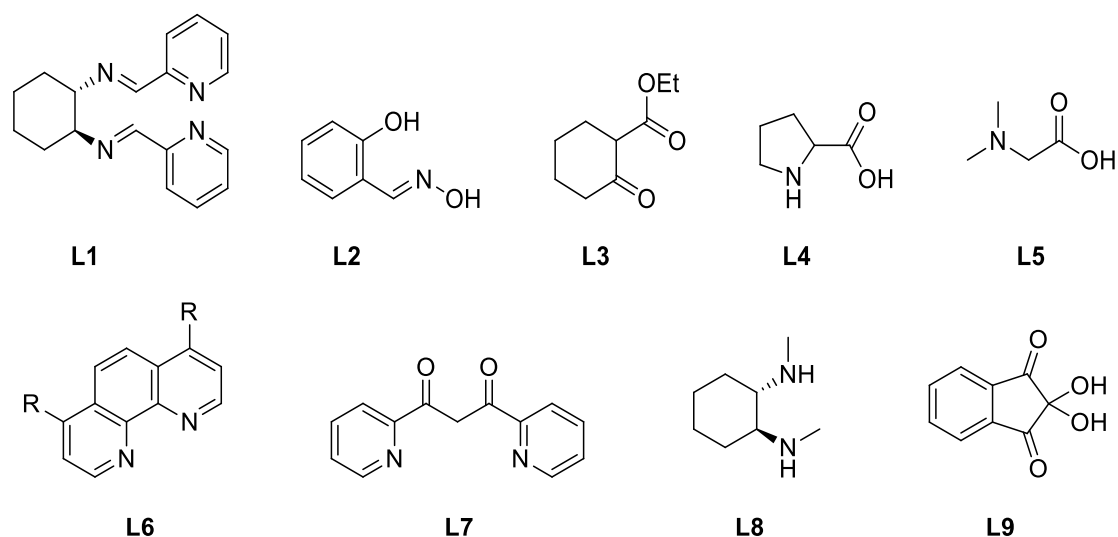


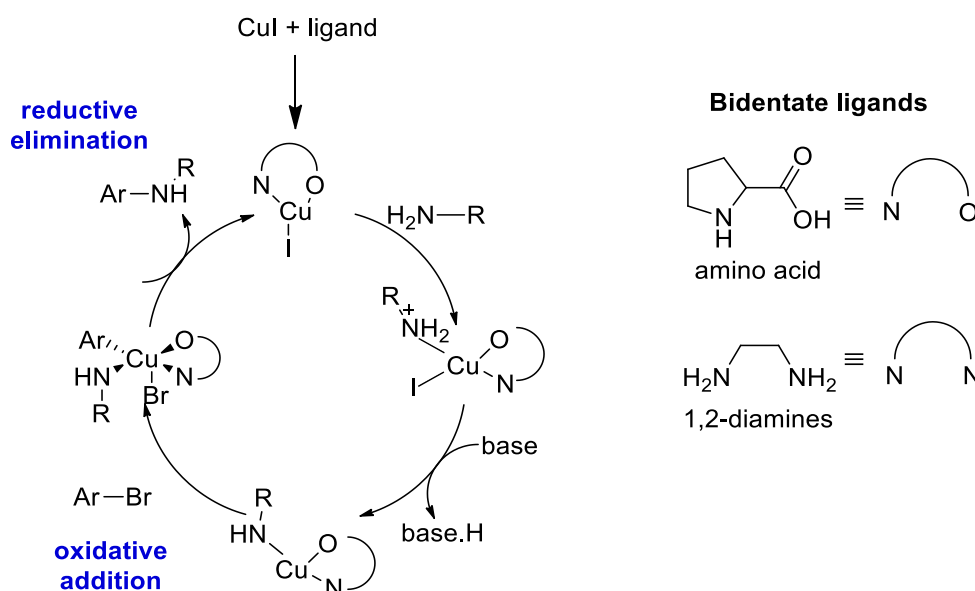
Figure 5.3. Ligands (**L1** – **L9**) used in Ullmann–type reactions developed by Buchwald¹⁵⁰ and Ma as reported in a review by Taillefer *et al.*¹⁴⁸

Research by Bethel described in Sperotto’s review, reported that the reaction rate was not just dependant on ligand inclusion, but also on the nature of the leaving group X (I>Br>Cl). This work further reported that *N*-deuteration produced a small kinetic isotopic effect, which did not affect product ratio, and that deuteration of the α -carbon of the amine gave an increase in formation of the aminated product.¹⁵⁵ Work by both Ma,¹⁵⁷ Taillefer¹⁴⁸ and co-workers proved that the use of bidentate ligands, such as amino acids and diamines, enhanced product formation and gave higher yields at lower temperatures with shorter reaction times. The work by Taillefer *et al.*¹⁴⁸ included the screening of a number of ligands containing an imine group, in addition to the oxygen or nitrogen sites enabling Cu coordination (Figure 5.3).

The oxygen and nitrogen donor groups on the ligand are believed to promote the oxidative addition by the transfer of electrons to afford either the Cu^I species, or by stabilizing the Cu^{III} intermediate species shown in Scheme 5.6. Ma and co-workers¹⁵⁷ further focused on the use of amino acids as ligands, establishing (L)-proline (**L4**) as a superior ligand for Ullmann–type reactions.¹⁴⁸ Apart from these investigations, Buchwald and co-workers¹⁵⁰⁻¹⁵² reported that 1,2-diamines (**L6** and **L8**) also proved to be highly efficient ligands for the coupling of aryl bromides with various nitrogen–based nucleophiles (Figure 5.3). Apart from the few ligands illustrated in Figure 5.3, many others have been screened. For the purpose of this work, the ligands **L4** (L-proline) and 1,2-diamine (ethylene diamine) were available. Since Buchwald and co-workers¹⁵² reported that **L8** (with a saturated bond system) was able to efficiently couple compounds usually coupled under Pd-catalyzed conditions,

CHAPTER 5 | Isochromanone: A surprisingly valuable intermediate

ethylene diamine (being available in the department) was employed to determine its efficiency in comparison to **L4**. Independent work by Surry *et al.*¹⁵² established that in a Cu-catalyzed arylation ethylene/cyclohexane diamine was an effective ligand (shown in Scheme 5.6). These researchers found that even the replacement of the methyl groups on **L8** with hydrogen did not limit product formation. The presence of the methyl groups on **L8** gave improved reaction rates, while larger substituents slowed the rate of the coupling reaction. Apart from ligand introduction, the use of various bases *viz.*, K_2CO_3 , K_3PO_4 , Cs_2CO_3 and $NaOtBu$,^{148,154,155,157} were shown to further improve the yield by improving the solubility of reagents. In addition, Ma and co-workers reported that additional coordination with the phosphate group could be responsible for the improved yield when using the base K_3PO_4 .¹⁵⁷



Scheme 5.6. A modified representation of bidentate ligands used in Ullmann reactions, and the proposed mechanisms, as described by de Vries *et al.*¹⁵⁵

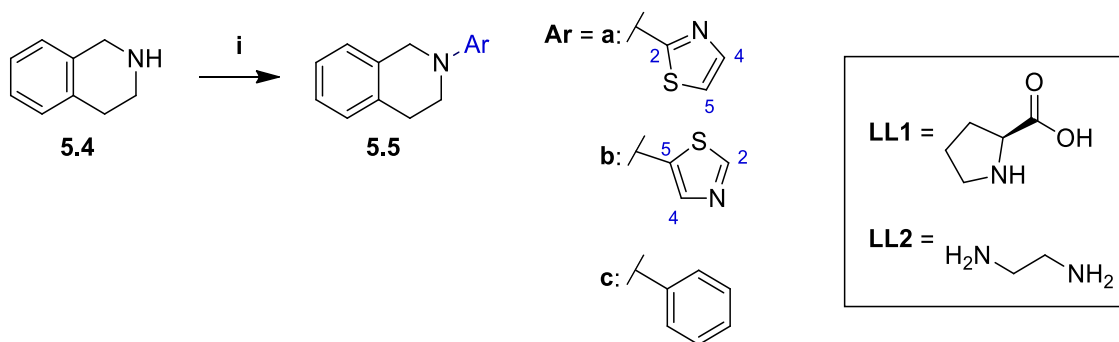
5.2.1 Investigation toward the feasibility of Ullmann condensation for synthesizing *N*-aromatic THIQ analogues

With the convenience of reagents such as CuI, L-proline, 1,2-diamine, K_2CO_3 and K_3PO_4 in hand, the synthetic procedure followed was similar to that described by Ma¹⁵⁷ and Buchwald.¹⁵⁰ The substrates utilized in Buchwald's work included *N*-heterocycles and this offered a procedure promising for the reagents and substrates at hand for the synthesis of the intended target molecule **5.1**. For the purposes of optimizing reaction conditions, a model substrate **5.4** was employed to be used with the readily available aryl bromides in Table 5.1. Interestingly, the thiazole chemistry described by Ganapathi and co-author reported that

CHAPTER 5 | Isochromanone: A surprisingly valuable intermediate

thiazoles containing a halogen at the C2-position are able to undergo a nucleophilic substitution reaction.¹⁵⁸ Entry 1, in Table 5.1 illustrates a substitution reaction protocol in the absence of the ligand and catalyst, in which a low yield of **5.5a** was obtained. According to a protocol described by Klapars *et al.*, addition of CuI was included; however, an insignificant improvement in the yield was obtained (5%), shown by entry 2. Despite a number of varied reaction conditions, which included different CuI loadings, ranging from catalytic to stoichiometric amounts, as well as elevated temperatures of up to 120 °C, no improvement in the yield of **5.5a** was observed. Work described by Ganapathi and co-author suggests that the chloride or bromide halogens present on the 5- and 4-position of the thiazole proved to be on the more unreactive position, thus better yields for entries 3, 4 and 5 were not expected.¹⁵⁸ Entry 4 illustrates that with both ligand and catalyst, product was achieved, but only in poor yields.

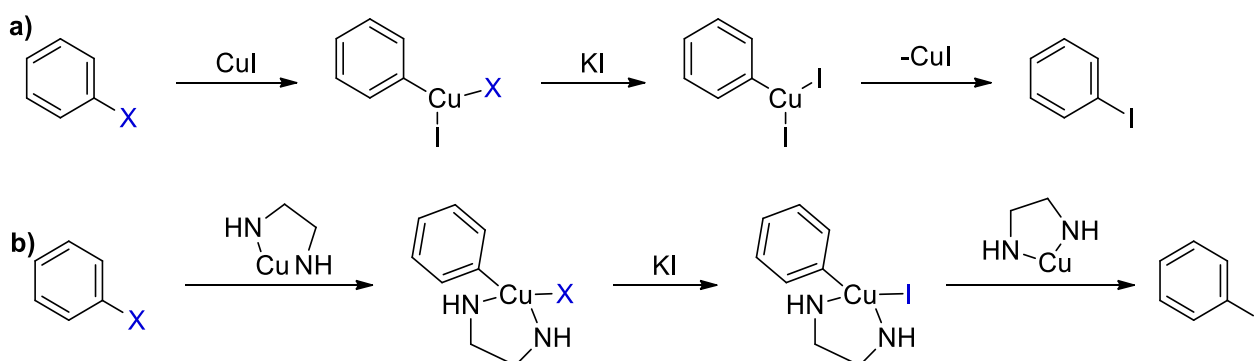
Table 5.1. Cu-mediated arylation of THIQ.



Entry	Substrate	Ligand	CuI (equiv)	Base	Product	Yield (%)
1	2-bromothiazole ^a	/	/	Et ₃ N	5.5a	18
2	2-bromothiazole ^a	LL1	10 mol% – 1 mol	K ₃ PO ₄	5.5a	23
3	5-bromothiazole ^a	/	10 mol% – 1 mol	K ₂ CO ₃	5.5b	0
4	5-bromothiazole ^a	LL1	10 mol% – 1 mol	K ₃ PO ₄	5.5b	9
5	5-bromothiazole ^a	LL2	10 mol% – 3 mol	K ₃ PO ₄	5.5b	0
6	bromobenzene ^b	LL1	10 mol% – 0.5 mol	K ₃ PO ₄	5.5c	60

Reagents and conditions described by Klapars *et al.*¹⁵⁰: (i) Heteroaryl bromide (1.2 equiv), amine (1.0 equiv) and base (2.0 equiv). ^aDMF at 110 °C, overnight; ^bDMSO at 150 °C, 15 min.

In an effort to improve on the yield, the thiazole was treated with KI to affect a Cu^I-catalyzed aromatic Finkelstein-type halogen exchange reaction *in situ* described by Klapars *et al.*¹⁵⁰ Thus, treatment of the thiazole with an excess of CuI, KI and 1,2-diamine led to the formation of 5-iodothiazole (as per a procedure described by de Vries and co-workers).¹⁵⁵ It has been reported that the iodoaryl species performed optimally upon comparison to their corresponding bromo- and chloroaryl species^{148,154,155} and excess CuI and ethylene diamine was required to mediate the halogen exchange illustrated in Scheme 5.7.



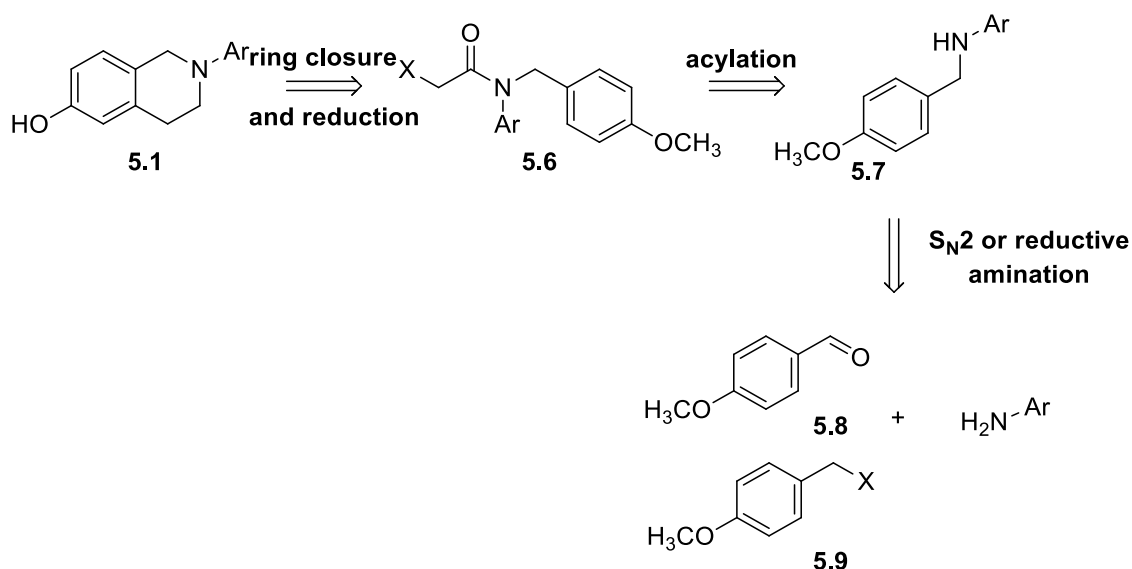
Scheme 5.7. Copper-catalyzed aromatic Finkelstein-type reaction **a)** in the absence of a ligand and **b)** aided by a ligand.¹⁵⁰

In contrast to results reported in literature, in our hands compound **5.5b** was not formed. It was then decided to model the protocol on a known substrate (in entry 6). Similar conditions as applied to entries 2 and 4 were adopted in entry 6 in DMSO, which afforded product **5.5c** in reasonable yields. These results suggested that the unsuccessful reactions were associated with the reactivity of the thiazole substrate and not the reaction protocol *per se*. Despite low yields, L-proline (**LL1**) was the only ligand for which product was obtained. The low yields obtained in Table 5.1 resulted in the investigation taking on a different approach for the synthesis of THIQ analogues (as shown in Figure 5.2).

5.3 Retrosynthetic analysis 2: Intramolecular cyclization as an approach to synthesizing THIQ analogues

In this approach, the focus was to employ a S_N2 substitution and/or implement reductive amination for generating the desired intermediates **5.6**, which were required for the synthesis of the desired target molecule analogues as illustrated in Scheme 5.8.

CHAPTER 5 | Isochromanone: A surprisingly valuable intermediate

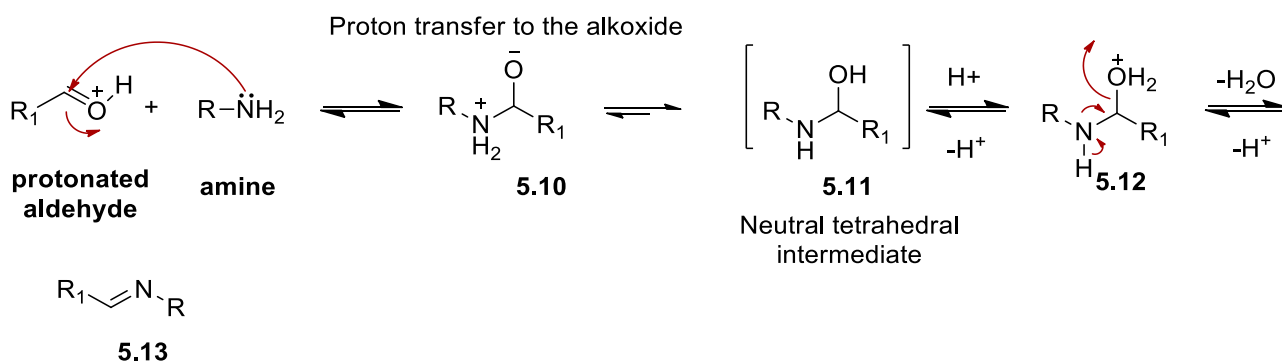


Scheme 5.8. The Friedel–Crafts approach to the synthesis of THIQ analogues.

Reductive amination between **5.8** with the aryl amine or a S_N2 substitution reaction between the aryl amine with the substituted benzyl halide **5.9** would result in formation of compound **5.7**. Acylation of amine **5.7**, followed by an intramolecular Friedel–Crafts (F–C) cyclization would then afford the target compound **5.1** after complete reduction of the keto group (Scheme 5.8).

5.3.1 Reductive amination reactions

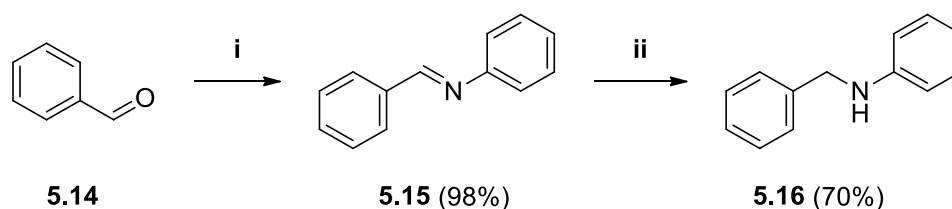
The reductive amination protocol presented a “greener” approach with water being the major by-product, in addition to the absence of expensive ligands or metals required for this synthetic strategy. Reductive amination involves the initial formation of a Schiff base intermediate **5.13**, shown in Scheme 5.9, by the condensation of an aldehyde with a primary amine and involves the proposed intermediates **5.10** – **5.12**.



Scheme 5.9. A general reaction mechanistic scheme proposed for the imine formation as described by Qin and co-workers.¹⁵⁹

CHAPTER 5 | Isochromanone: A surprisingly valuable intermediate

The classical approach described by Qin and co-workers included the azeotropic removal of water using a Dean–Stark apparatus.¹⁵⁹ Elimination of water is essential, since conversion of the amine to the imine **5.13** is a reversible process. An interesting two reviews by da Silva,¹⁶⁰ Qin¹⁵⁹ and co-workers reported that the aid of acids (such as mineral, organic or Lewis acids) and dehydrating agents (like molecular sieves or MgSO_4) greatly accelerated reactions, affording the desired imine **5.13** under milder conditions. By employing known chemistry and implementing a procedure described by Wei and co-workers,¹⁶¹ a model reaction was explored, in which benzaldehyde and aniline were condensed to optimize reaction conditions suitable for the intended substrate and subsequent reactions. One method tried included a mixture of benzaldehyde **5.14** and aniline which were heated at 60°C in EtOH with acetic acid catalyzing the removal of water, as illustrated in Scheme 5.10.



Scheme 5.10. Reagents and conditions for reductive amination: (i) aniline, $\text{Mg}(\text{ClO}_4)_3$, MgSO_4 , CH_3CHCl_2 (1,2-dichloroethane), 60°C , 5 h; (ii) NaBH_4 , EtOH, RT, overnight.

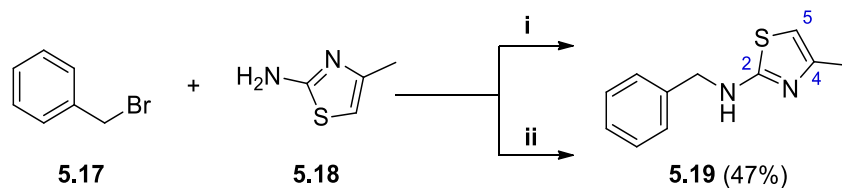
The reaction's progress was monitored every hour using TLC for determining the complete consumption of reagents. However, despite overnight stirring, the reaction did not proceed to completion. Failing to obtain a high yield of product for this protocol, a method described by Kang *et al.*¹⁶² was explored, where triflic acid was introduced as an alternative catalyst, but still no improvement in the formation of **5.15** was observed. Failure to obtain complete conversion was explained by the grade of the EtOH used, as the presence of any additional water favoured the reverse reaction resulting in unreacted starting material being recovered. Thus, EtOH was replaced by benzene as solvent and triflic acid was used as the catalyst and the reaction mixture was heated to 60°C . However, the yields obtained were still unsatisfactory with incomplete conversion. The incomplete conversion made purification very challenging since the product and reagents moved with similar R_f -values. Finally, 1,2-dichloroethane was chosen as solvent in addition to the Lewis acid catalyst $\text{Mg}(\text{ClO}_4)_3$ and heating at 60°C which afforded product **5.15** in a 53% yield. Furthermore, the stoichiometric addition of anhydrous MgSO_4 to the reaction mixture gave product in quantitative yield within 3 hours. As illustrated in Scheme 5.9, with the nature of the reaction being sensitive to water, no work-up procedures were implemented. The reaction mixture was thus concentrated to

CHAPTER 5 | Isochromanone: A surprisingly valuable intermediate

dryness, followed by a general reduction commonly used in Schiff base chemistry.¹⁶²⁻¹⁶⁴ To this end, after treatment with NaBH₄ in EtOH, the amine **5.16** was produced in a 70% yield and its structure was confirmed by ¹H-NMR spectroscopy. A complex 7-proton multiplet in the aromatic region observed between δ 7.48 – 7.02, with an additional 3-proton multiplet between δ 6.79 – 6.55, were indicative of the two benzene rings. A broad 1-proton singlet observed in the aliphatic region at δ 4.03 (NH), with the benzylic methylene group observed at δ 4.34, further confirmed product formation.

5.3.2 Nucleophilic substitution reactions

In order to reduce the number of reaction steps, S_N2 substitution was initially considered. This required the implementation of a protocol described by Kim and co-workers,¹⁶⁵ where benzyl bromide **5.17** and amine **5.18** were allowed to react in the presence of Cs₂CO₃ and heated under reflux in DMF (parameters for condition i).^{164,165} The reaction mixture was stirred and heated for 24 hours and longer. However, in our hands the maximum yield obtained was only 34%.



Scheme 5.11. Reagents and conditions for Ullmann reaction: (i) Cs₂CO₃, DMF, 80 °C, overnight; (ii) L-proline, CuI, Cs₂CO₃, DMF, 80 °C, overnight.

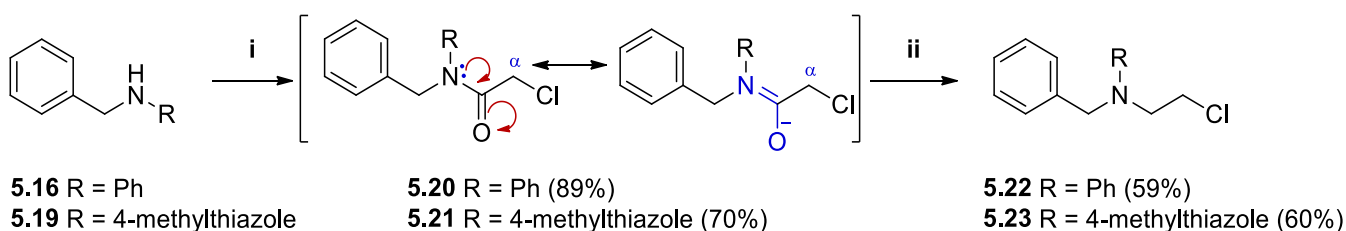
Observations made from the Ullmann condensation-type chemistry previously discussed (in Table 5.1), indicated that a slight improvement in yield would be possible upon coupling the halogenated species with aryl amines and applying Cu as a catalyst. Subsequent addition of catalytic amounts of CuI and L-proline to the reaction mixture resulted in a moderate improvement, with the yield increased to 47% for compound **5.19** (in Scheme 5.11). ¹H-NMR spectroscopy was employed for elucidating the structure of compound **5.19**. What appeared to be rotamers were observed for the benzylic CH₂ group of **5.19**. The aromatic region showed a 5-proton complex multiplet between δ 7.54 – 6.89. In addition, a 1-proton singlet at δ 6.42 was assigned to H5 of the thiazole ring. Upon close inspection, the methylene chemical shift, usually observed as an intense 2-proton singlet, was represented by two sets of multiplets at δ 5.29 and δ 5.16. In addition, the intense 3-proton singlet normally observed for the methyl group at δ 2.51 – 2.05 was in this case observed

CHAPTER 5 | Isochromanone: A surprisingly valuable intermediate

as a 3-proton multiplet and not a singlet as expected. Furthermore, it was found that in ESI⁺ TOF MS, presented an experimental monoisotopic mass of 205.0793 for C₁₁H₁₂N₂S being obtained, which corresponded well with the calculated mass of 205.0755.

5.3.3 Acylation of secondary amines

Addition of the alkyl group onto the side chain nitrogen of the side chain was essential for facilitation of the envisaged F–C ring closure. Due to the propensity of amines to undergo multiple alkylations providing the quarternized amine, α -chloroacetanilides **5.20** and **5.21** were pursued (Scheme 5.12) circumventing quaternization. The shared electron density across the amide bond generates a resonance stabilized moiety preventing a second acylation. Thus, acylated compounds **5.20** and **5.21** would be subsequently reduced to afford the desired alkylated products, *viz.* compounds **5.22** and **5.23**, hopefully in reasonable yields.



Scheme 5.12. Reagents and conditions: (i) chloroacetyl chloride, DIPEA, CH₂Cl₂, RT, 6 – 18 h; (ii) LiAlH₄/AlCl₃ (1:1), THF, 70 °C, 5 h.

To this end, using a general procedure described by Velavan and co-workers,¹³⁸ compounds **5.16** and **5.19** in CH₂Cl₂, were subsequently separately cooled to 0 °C. DIPEA was added to render the reaction mixture basic and this was followed by the slow addition of the acylating agent. The reaction mixture was then stirred at room temperature for 6 hours to afford the acylated compounds **5.20** and **5.21**. ¹H-NMR spectroscopy confirmed product formation for structures **5.20** and **5.21**, where an additional methylene signal observed at δ 4.92 for **5.20** indicated the successful acylation. Compound **5.21** was confirmed by the absence of rotamers previously observed for **5.19**; additionally, the methylene signal represented by a singlet at δ 5.18 was observed for **5.21**, further confirming product formation. Amides are considered to be rather stable, due to the presence of their delocalized electrons across the amide bond and they were thus reduced with a metal hydride affording the haloalkyl chain to accommodate the subsequent reactions. Reduction was effected by a procedure described by Nystrom,¹²³ Davis¹²⁴ and co-workers, which involved treatment of the acylated compounds **5.20** and **5.21** with the monochloroalane

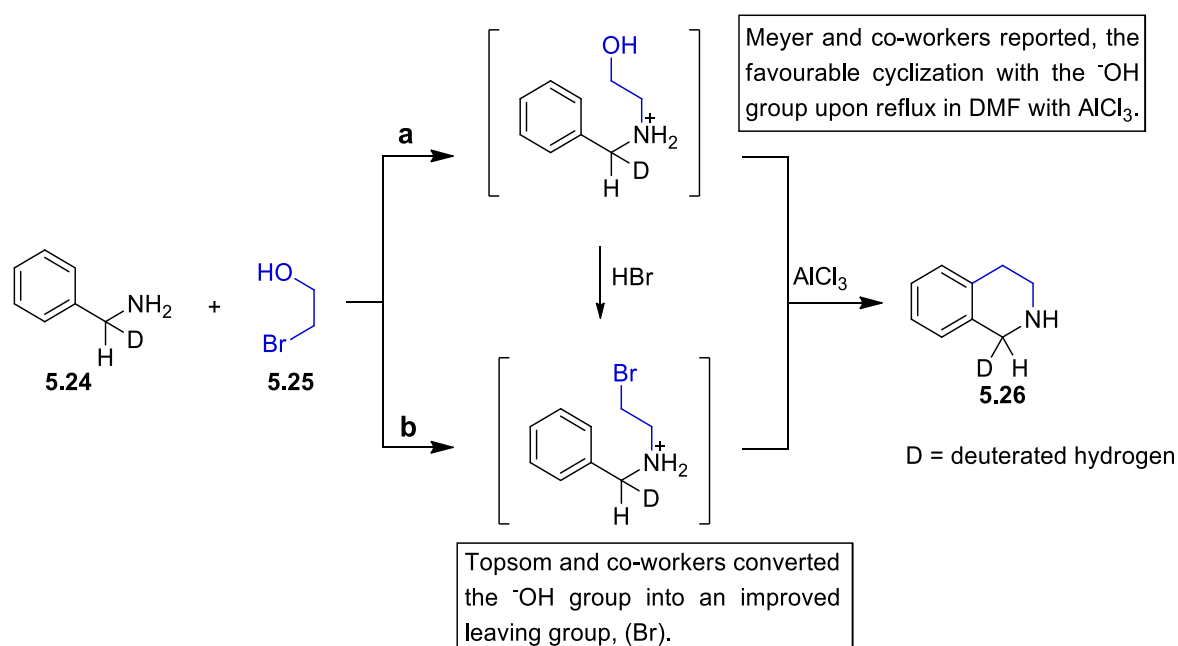
CHAPTER 5 | Isochromanone: A surprisingly valuable intermediate

generated *in situ* from a 1:1 mixture of $\text{AlCl}_3/\text{LiAlH}_4$. The reaction mixtures were heated under reflux for 4 hours, efficiently giving products **5.22** and **5.23** in reasonable yield after work-up.

5.3.4 Intramolecular Friedel–Crafts cyclization reactions

With the successful alkylated amines **5.22** and **5.23** in hand, subsequent reactions could resume for facilitating the intramolecular F–C cyclization to afford the THIQ analogues.¹⁶⁶ Work reported by Meyer and Turner,¹⁶⁷ inspired the use of the intramolecular F–C cyclization protocol. Apart from the work implemented by Topsom,¹⁶⁸ upon reviewing the literature several other publications prompted our further investigation into the use of the F–C intramolecular cyclization as a synthetic route toward our target compound **5.1**.¹⁶⁷⁻¹⁶⁹

The cyclization protocol described by Meyer and Turner, included the use of deuteriobenzylamine **5.24**, which upon treatment with 2-bromoethanol in the presence of AlCl_3 , coordinated with the hydroxyl functionality and facilitated the cyclization that provided the deuteriotetrahydroisoquinoline **5.26** (seen in Scheme 5.13).¹⁶⁷

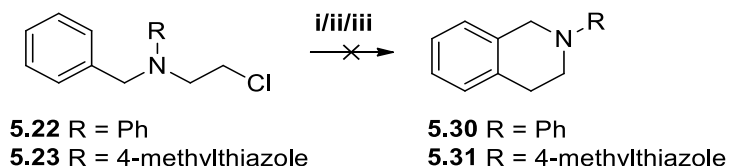


Scheme 5.13. Successful F–C intramolecular cyclization reported by the independent work of Topsom,¹⁶⁸ Meyers¹⁷⁰ and co-workers.

The work reported by Topsom and co-workers however, included the hydroxyl functionality being converted into an improved leaving group for further promotion of the electrophilic substitution.¹⁶⁸ Surprisingly, the F–C intramolecular cyclization was able to occur in the

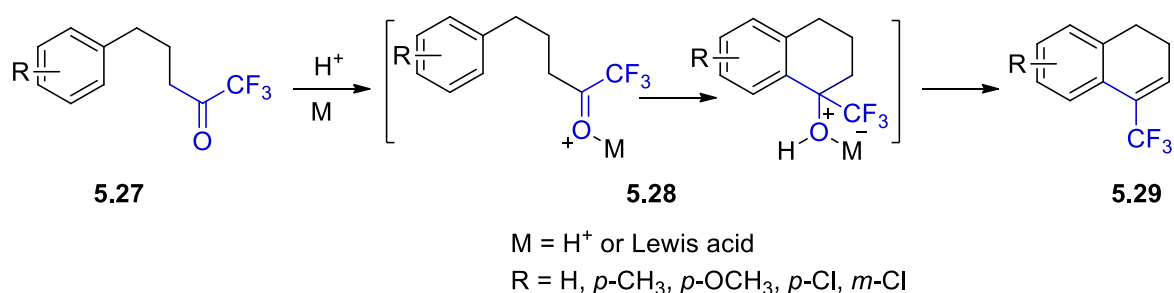
CHAPTER 5 | Isochromanone: A surprisingly valuable intermediate

absence of an electron-rich aryl system, but unfortunately any yields were unreported. Upon comparison, compound **5.22** should provide similar reactive possibilities to the resulting **b** route intermediate in Scheme 5.13. This method allowed for the optimization of the protocol, using the tetrahydroisoquinoline model scaffold **5.22** (Scheme 5.14) prior to implementing the synthetic strategy on our valuable substrate containing the *meta* methoxy-substituent.



Scheme 5.14. Reagents and conditions for the attempted intramolecular F-C cyclization: (i) AlCl_3 , CH_2Cl_2 , RT, overnight; (ii) SnCl_4 , CH_2Cl_2 , RT, overnight; (iii) SnCl_4 , PhNO_2 , RT – 150 °C, overnight.

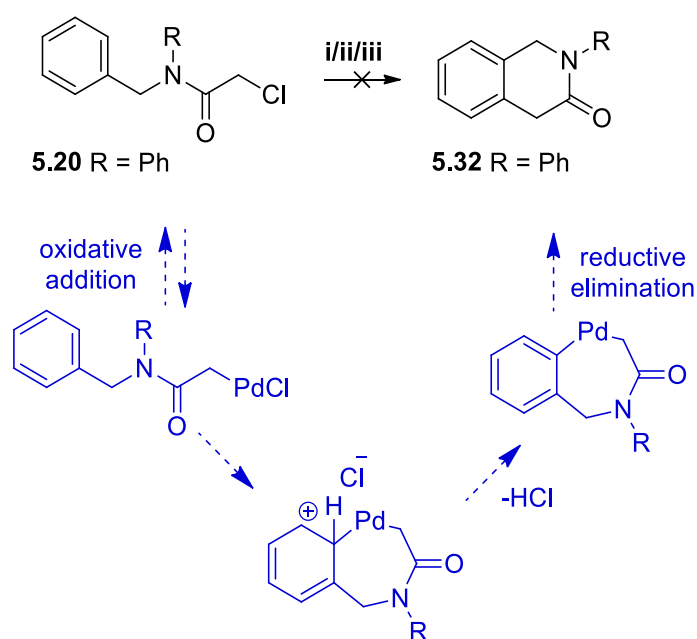
However, in our hands no product was isolated, despite the use of various metal chlorides commonly used for facilitating the F-C ring-closing reactions. Failure to obtain the cyclized product **5.30** with various acid catalysts was believed to result from the aromatic ring being too unreactive shown in Scheme 5.14. During the monitoring of the reaction's progress with TLC, it appeared that a reaction had occurred; however, the difference in R_f values presented by the product and starting material could be clearly be differentiated by the complexation of the acid catalyst with substrates **5.22** and **5.23**. $^1\text{H-NMR}$ spectroscopy applied to the “products” yielded inconclusive results with no variation in chemical shifts to confirm product formation. The absence of product was confirmed using ESI^+ TOF MS, in which the monoisotopic mass confirmed the presence of only the starting material being present. Apart from the advancements achieved by Meyers and Dickman, it was established that the cyclization was also Lewis acid-dependent and that even in the absence of an electron-donating group on the aryl ring, product could be obtained as illustrated in Scheme 5.15 by the work reported by Charpentier-Morize and co-workers.¹⁷¹



Scheme 5.15. The successful intramolecular F-C cyclization reported by Charpentier-Morize and co-workers.¹⁷¹

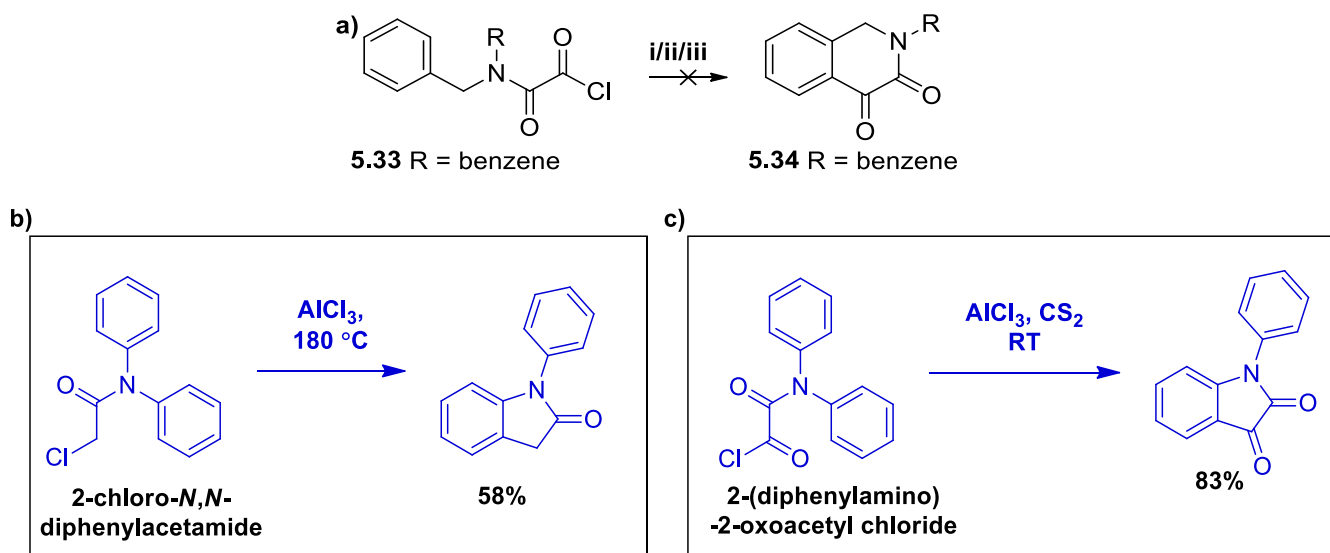
CHAPTER 5 | Isochromanone: A surprisingly valuable intermediate

However, the acylium ion intermediate **5.28** and the electron-withdrawal caused by the terminal trifluoro carbonyl increases polarization of the C=O bond ($\delta^+C-O\delta^-$), thereby lowering the HOMO-LUMO energy gap to favour cyclization. This work included the screening of several mineral acids and Lewis acids *viz.*, ZnCl₂, SnCl₄, FeCl₃, CF₃CO₂H, H₂SO₄, TiF₄, SbF₅, AlCl₃ and TiCl₄ with no product observed when ZnCl₂ and SnCl₄ were implemented.¹⁷¹ Cyclization of several compounds containing the general formula **5.27** illustrated the successful cyclization depicted in Scheme 5.15. It was suggested that the successful ring closure could be attributed to the presence of the electrophilic terminal -COCF₃ group (favouring the acylium ion formation), which mediated the ring-closure, aided by activation promoted by complexation of the Lewis acid. A general literature procedure, where two commonly used Lewis acids (AlCl₃ and SnCl₄) were employed, was attempted on compound **5.20**, but failed (Scheme 5.16). Failure to obtain the desired product **5.32** using the procedure described by Charpentier-Morize and co-workers on our substrates was frustrating since enough literature evidence was found to support this type of reaction.¹⁷¹ This led to making small protocol changes to redress this failure.



Scheme 5.16. Reagents and conditions for intramolecular F-C cyclization: (i) AlCl₃, CH₂Cl₂, overnight; (ii) SnCl₄, CH₂Cl₂, overnight; (iii) SnCl₄, PhNO₂, RT – 150 °C, 48 h. The blue schematic is a representation of an alternate protocol, employed by Buchwald and co-workers,¹⁵¹ where yield could be obtained using a Pd-catalyzed reaction promoting cyclization of the α -chloroacetanilide.

CHAPTER 5 | Isochromanone: A surprisingly valuable intermediate



Scheme 5.17. Reagents and conditions for intramolecular F–C cyclization: (i) AlCl_3 , CH_2Cl_2 , 48 h; (ii) SnCl_4 , CH_2Cl_2 , 48 h; (iii) SnCl_4 , PhNO_2 , RT – 150 °C, 48 h.

Despite failure in our hands to successfully cyclize **5.20**, a protocol employed by Shindikar and co-workers illustrated that at higher temperatures (180 °C) and with AlCl_3 they were able to obtain product (in a reasonable yield of 58%) from the cyclization of 2-chloro-*N,N*-diphenylacetamide illustrated in Scheme 5.17 b and c.¹⁶⁹ A final attempt towards the desired cyclization thus involved the use of compound **5.33** (Scheme 5.17 a). The intention was to generate a more reactive species based on the work described by Shindikar and co-workers who reported higher yields being obtained upon comparison of the cyclization when using 2-(diphenylamino)-2-oxoacetyl chloride as it gave the corresponding product in 83% yield, to that of 58% yield on cyclization with 2-chloro-*N,N*-diphenylacetamide in Scheme 5.17.¹⁶⁹ However, it is important to note that this reaction worked well for generating the indole substrate, but unfortunately not for the isoquinoline scaffold when tried in our hands. The varied use of Lewis acids such as AlCl_3 and SnCl_4 provided no positive results. In addition, temperature variations by the use of low boiling point solvent (CH_2Cl_2) and a high boiling point solvent such as nitrobenzene were employed. The synthetic problems experienced during this reaction procedure could perhaps have been overcome by the use of aryl substrates containing electron-donating groups compatible with the Lewis acids utilized in the synthetic procedure with much higher temperatures.^{41,151,169} Reports by Spangler and co-workers indicate that the presence of an electron-donating substituent on the aryl ring would further enhance the electron density required to improve the propensity for the intramolecular cyclization.¹⁷²

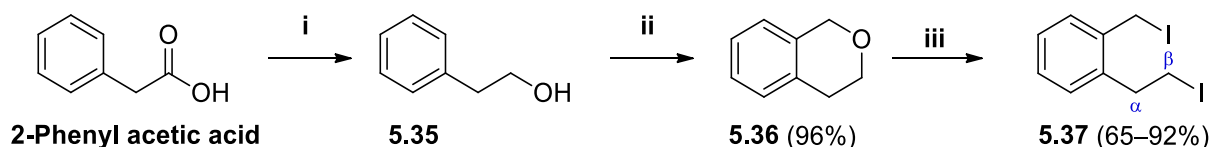
5.4 Isochroman: A valuable intermediate for the synthesis of THIQ analogues

With no successful results obtained from the F–C intramolecular cyclization, literature was again reviewed and focus was placed on the work reported by Ma and co-workers.¹⁷³ This work introduced the concept where an isochroman motif would be used as a key intermediate in the synthesis of the THIQ skeleton. This prompted our interest in further exploring the isochroman as a valuable intermediate toward generating our target compounds with a general structure as **5.1**.



5.4.1 Synthesis of THIQ analogues from an isochroman

In order to avoid the loss of the valuable aryl methyl ether substrate, it was not initially used and conditions for the isochroman work was primarily optimized starting from the commercially available 2-phenyl acetic acid as the model substrate. Generating the isochroman scaffolds required a number of reaction steps initiated from phenyl acetic acid. 2-Phenyl acetic acid was first reduced by a well-known procedure described by Chapman and co-workers,¹⁷⁴ whereby treatment of the 2-phenyl acetic acid with LiAlH₄ in THF afforded the corresponding alcohol, **5.35** in good yield (Scheme 5.18). A ¹H-NMR spectrum confirmed the successful reduction, as evident by the presence of two 2-proton triplets at δ 3.81 and δ 2.85 in the aliphatic region, as expected for the CH₂CH₂ fragment and corresponding well with the reported literature values.¹⁷³

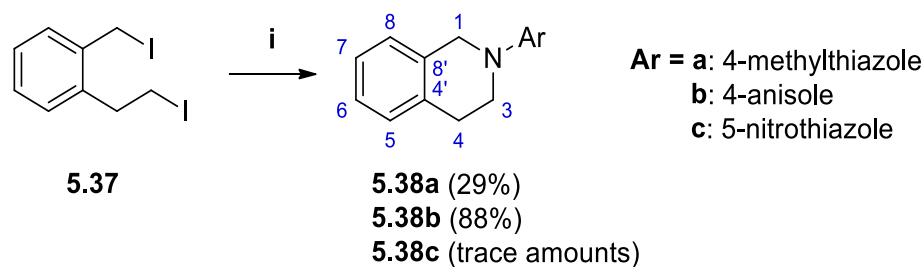


Scheme 5.18. Reagents and conditions: (i) LiAlH₄, THF; (ii) CH₂O, HCl, PCl₃, 4 h; (iii) HI, reflux, overnight.

A procedure described by Deady and co-workers was then implemented where cyclization of the alcohol **5.35** with paraformaldehyde under acidic conditions generated the isochroman **5.36** in 96% yield.¹⁶⁸ Furthermore, addition of PCl₃ accelerated the elimination of water and provided isochroman **5.36** in good yields. Confirmation of the product was obtained by comparison of the ¹H-NMR spectrum obtained experimentally, to that reported in the literature.¹⁶⁸ Compound **5.36** displayed a 3-proton multiplet between δ 7.23 – 7.17 and a 1-proton multiplet between δ 7.05 – 7.02, in addition to an intense 2-proton singlet at δ 4.83 for the Ar-CH₂-O protons. Synthesis of the 1-(2-iodoethyl)-2-(iodomethyl)benzene **5.37** was performed by following a procedure described by Ma and co-workers,¹⁷³ where heating

CHAPTER 5 | Isochromanone: A surprisingly valuable intermediate

5.36 under reflux in excess HI for 3 hours in a darkened environment afforded the ring-opened diiodinated compound **5.37** as an oil in good yield. Furthermore, $^1\text{H-NMR}$ spectroscopy identified this product. Iodination was evident by the different chemical shifts produced by the protons on the α - and β -carbons situated on the iodoethyl chain *viz.*, a 2-proton multiplet at δ 3.51 – 3.39 (α -CH₂) and a 2-proton multiplet at δ 3.28 (β -CH₂), confirming the successful ring opening and iodination of **5.36**. The diiodinated substrate **5.37** provided an interesting precursor for the synthesis for a number of different THIQ analogues by varying the added amines in the THIQ cyclization event (shown in Scheme 5.19).



Scheme 5.19. Reagents and conditions for S_N2 substitution reactions described by Ma and co-workers:¹⁷³ (i) Primary amines (**a – c**), NaHCO₃, H₂O, SDS, reflux, 4 h.

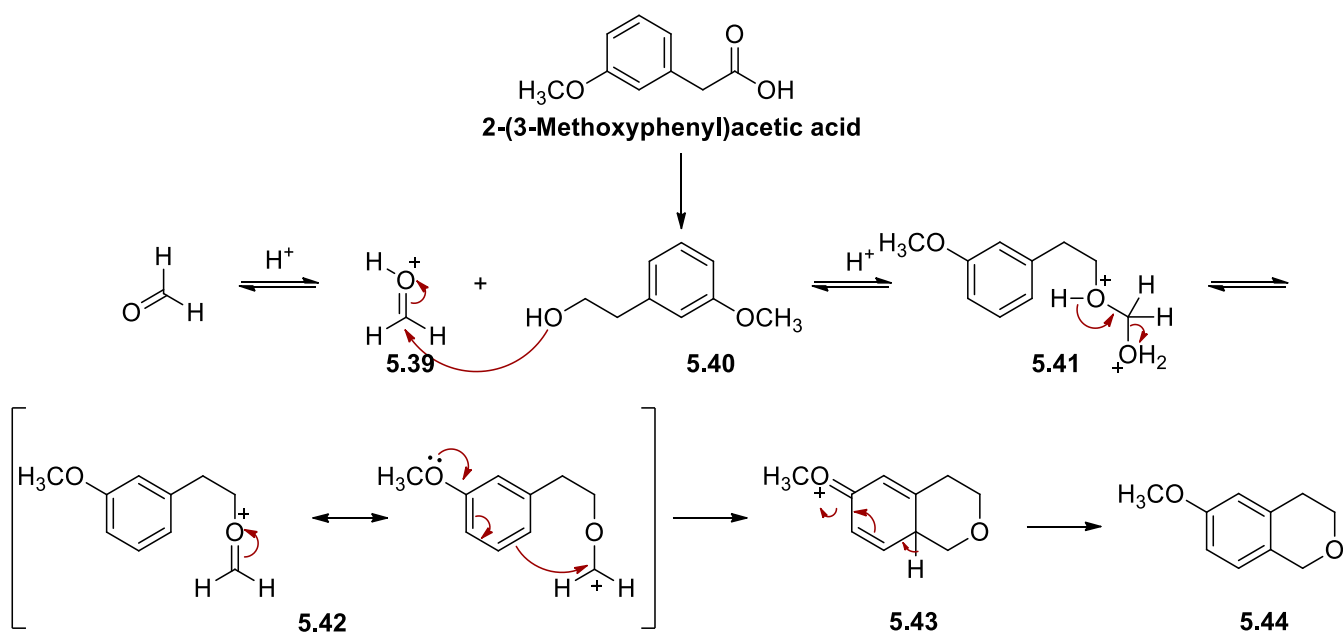
Amines (**a – c**) were chosen in accordance with the intended amines for generating the THIQ analogues **5.1**, as well as to determine their compatibility under the reaction conditions applied. Thus, two THIQ analogues (**5.38a – b**) were successfully synthesized by the nucleophilic substitution of **5.37** with the various primary amines listed in Scheme 5.19. The reaction conditions included a procedure described by Ma and co-workers,¹⁷³ using a weak base NaHCO₃, which resulted in the formation of a number of inorganic by-products (such as NaI, H₂O and CO₂) thus decreasing the number of impurities. The amphiphile sodium *N*-dodecyl sulfate (SDS) was employed for homogenizing the reaction mixture to further increase the reaction rate. The reaction conditions could easily be optimized by longer reaction times or pre-treatment of the amines with stronger bases, prior to their addition to the halogenated species **5.37**. The structure of product **5.38a** was confirmed by $^1\text{H-NMR}$ spectroscopy, illustrating the general THIQ skeleton. The key structural profile of the THIQ motif included a 4-proton multiplet between the δ 7.22 – 7.16, indicative of the aromatic protons H5 – H8. In addition, three 2-proton triplet signals were evident between δ 4.65 – 4.31 (H1), δ 3.76 – 3.46 (H4) and at δ 3.00 (H3). The individual analogues were further differentiated according to the structure of their incorporated amines. The key identifying components for the structure of compound **5.38a** was confirmed by the presence of a 3-proton singlet at δ 2.30 (*thiazole-CH*₃), in addition to a 1-proton singlet at δ 6.13

CHAPTER 5 | Isochromanone: A surprisingly valuable intermediate

(*thiazole*-ArCH). The successful synthesis of **5.38b** was confirmed by two 2-proton multiplets between δ 7.04 – 6.96 and δ 6.92 – 6.85, which were ascribed to the anisole portion of compound **5.38b**. Furthermore, a 3-proton singlet observed at δ 3.79 was indicative of the presence of the aromatic methyl ether protons. Unfortunately, no expected product by reaction with 5-nitrothiazole was isolated. Subsequently, the successes achieved from the illustration in Scheme 5.19, prompted us to go ahead with synthesis of the isochroman **5.44** by using the 3-methoxyphenyl ethanol substrate.

5.4.2 Synthesis of an isochroman analogue from 3-methoxyphenyl acetic acid

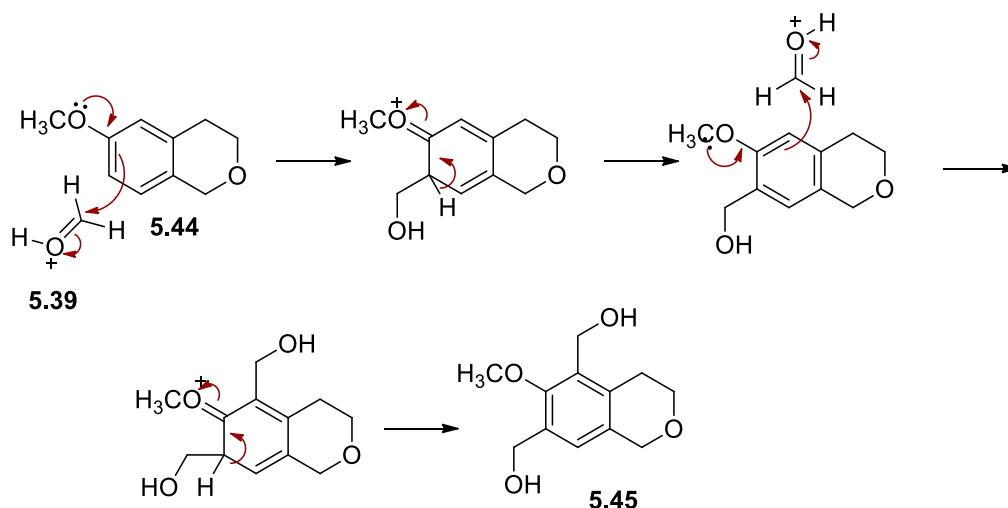
3-Methoxyphenyl ethanol **5.40** was efficiently obtained in quantitative yield by the reduction of the corresponding 3-methoxyphenyl acetic acid upon treatment with LiAlH_4 in THF, using a general procedure described by Chapman and co-workers.¹⁷⁴ The structure of product **5.40** was confirmed using $^1\text{H-NMR}$ spectroscopy, which illustrated the presence of two overlapping signals integrating for 5-protons at δ 3.81 – 3.62 (OCH_3 and CH_2), in addition to a second methylene triplet at δ 2.72, providing evidence of the successful carbonyl reduction. The next step involved the crucial cyclization of compound **5.40** to form the isochroman **5.44**, as illustrated in Scheme 5.20. An interesting review by Kaufman and Larghi,¹⁷⁵ reported that this reaction has previously been classified as a variation of the F-C alkylation, the Prins cyclization, the Mukaiyama reaction, as well as the *oxa*-Pictet-Spengler reaction. The mechanism for the reaction is shown below in Scheme 5.20.



Scheme 5.20. The proposed mechanism described by Kaufman and Larghi.¹⁷⁵ Reagents and conditions for the *oxa*-Pictet-Spengler cyclization of 2-(3-methoxyphenyl)ethanol: (i) CH_2O , HCl , PCl_3 , 4 h.

CHAPTER 5 | Isochromanone: A surprisingly valuable intermediate

As described by Deady and co-workers,¹⁶⁸ paraformaldehyde was treated with HCl and left to stir for 30 minutes allowing the formation of **5.39**.¹⁶⁸ Alcohol **5.40** was then added, generating the hemi acetal **5.41** in a process involving proton transfer. The reaction mixture was stirred for 2 hours after which PCl₃ was added. Addition of PCl₃ accelerated the removal of water by the *in-situ* formation of H₃PO₄ and HCl. The elimination of water was essential for generating two highly reactive intermediates *viz.*, **5.42**, which were required for the intramolecular electrophilic addition/cyclization to form the all-important substrate **5.44** *via* **5.43**. The reaction's progress was carefully monitored with TLC, which indicated the presence of three different compounds. The major compound isolated was not the desired product **5.44**, as demonstrated by ¹H-NMR spectroscopic investigations. Rather compound **5.45** (shown in Scheme 5.21) was obtained in an appreciable yield of 47% with the recovery of some starting material **5.40** (25%) and only trace amounts of product **5.44** (28%).



Scheme 5.21. Proposed mechanism for the formation of compound **5.45**.

The chemical shifts observed in the ¹H-NMR spectrum of **5.45** indicated that the ring closure was successful, namely the 2-proton triplets observed at δ 2.94 and δ 4.02, with an intense 3-proton singlet at δ 3.83 and a 2-proton singlet at δ 4.83 (see Figure 5.4). These are chemical shifts common to the isochroman skeleton as discussed for compound **5.36**. In addition to these signals, two further methylene signals at δ 4.62 and δ 4.56, together with a single 1-proton aromatic signal at δ 7.31 were observed. Based on this data, the structure assigned for the major compound was **5.45** in Figure 5.4. It can therefore be concluded that when using electron-rich aryl systems, they do not provide the predictable reactivity observed with the use of 2-phenylethanol (**5.35**).

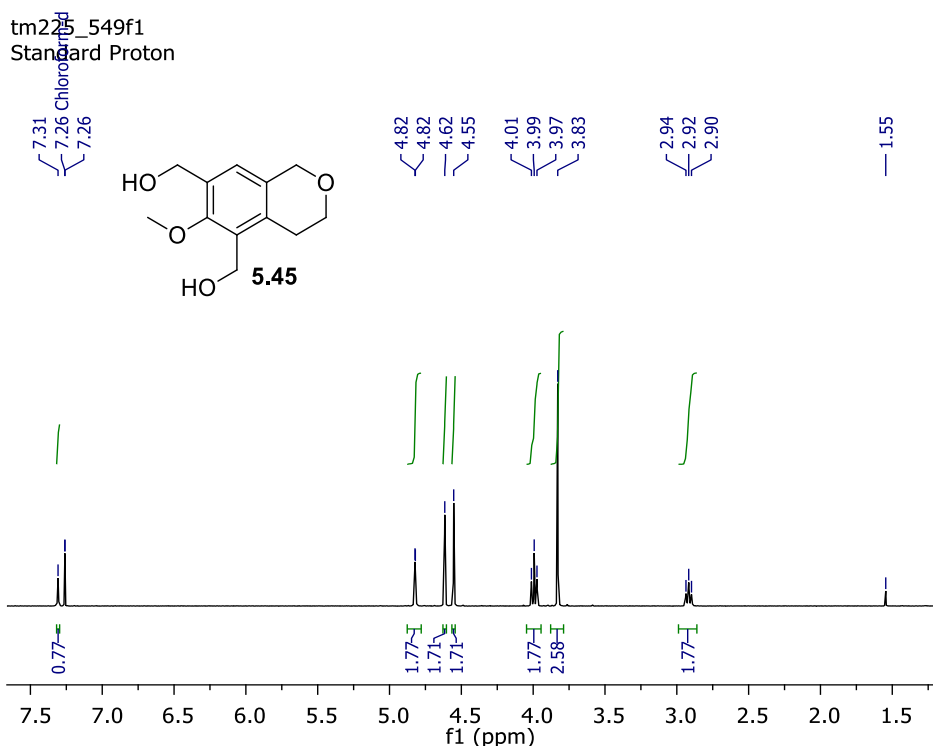
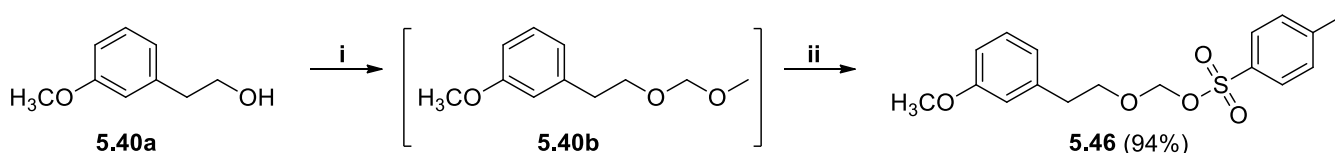
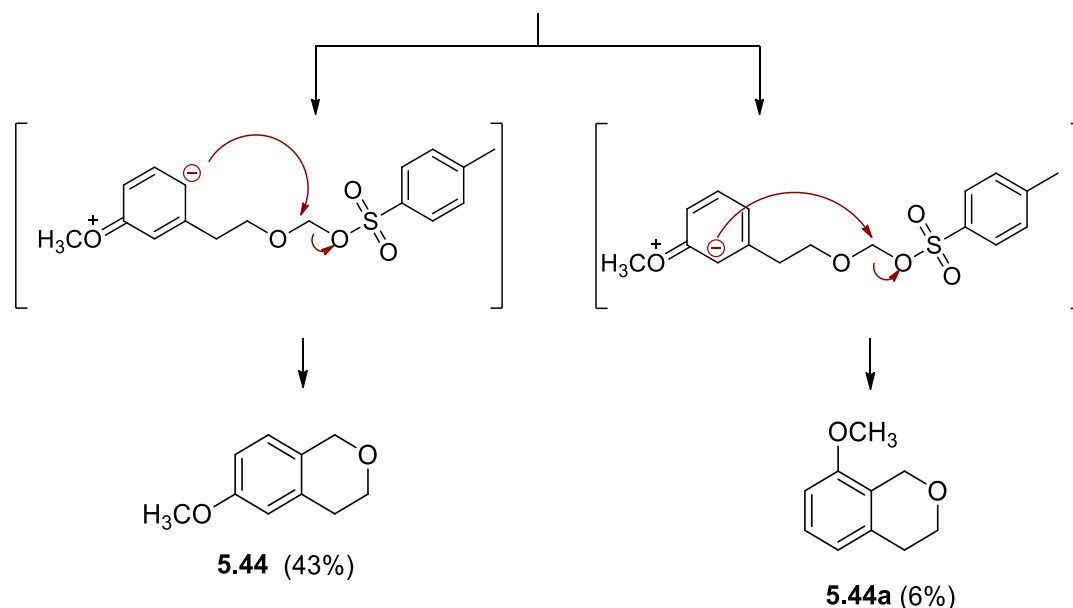


Figure 5.4. ^1H -NMR spectrum of undesired side product, compound **5.45**.

This result can be explained by the presence of the electron-donating methoxy group and its ability to activate both *ortho*- as well as *para*-positions, on the aryl ring. It is clear that the product **5.45** resulted from the excess paraformaldehyde added. However, even by adding only 1 mol of CH_2O , formation of very little desired product **5.44** (35% yield) was obtained (for discussion of characterization see later). Since the isochroman **5.44** was a valuable intermediate required for generating a number of substrates, a different protocol for generating product in improved yields was needed. The second approach involved an interesting method described by Taber and Raciti, which involved the synthesis of compound **5.46**.¹⁷⁶



CHAPTER 5 | Isochromanone: A surprisingly valuable intermediate



Scheme 5.22. Reagents and conditions for the cyclization described by Taber and Raciti:¹⁷⁶ (i) 60% NaH, MOMCl, THF, overnight; (ii) TsOH, PhCH₃, 80 °C, overnight.

Taber and Raciti described a two-step procedure in which chloromethyl methyl ether and NaH were used to convert compound **5.40a** into its corresponding MOM ether derivative.¹⁷⁶ Treatment of the intermediate **5.40b** with tosic acid generated **5.46**, a compound with an improved leaving group as illustrated in Scheme 5.22 and this intermediate underwent intramolecular cyclization to afford isochroman **5.44**. Despite the rather low yield of **5.44** (43%) obtained in our hands, 49% of the starting material **5.40a** was recovered, which could fortunately be recycled in the protocol for the further synthesis of **5.44**. Unfortunately, it should be noted that at higher temperatures (to try to improve the yield) multiple side products were formed. The structure of the major side product was confirmed using ¹H-NMR spectroscopy and was found to be **5.44a**. The only major differences in the spectra of **5.44** and **5.44a** were observed in the aromatic region, as illustrated in Figure 5.5.

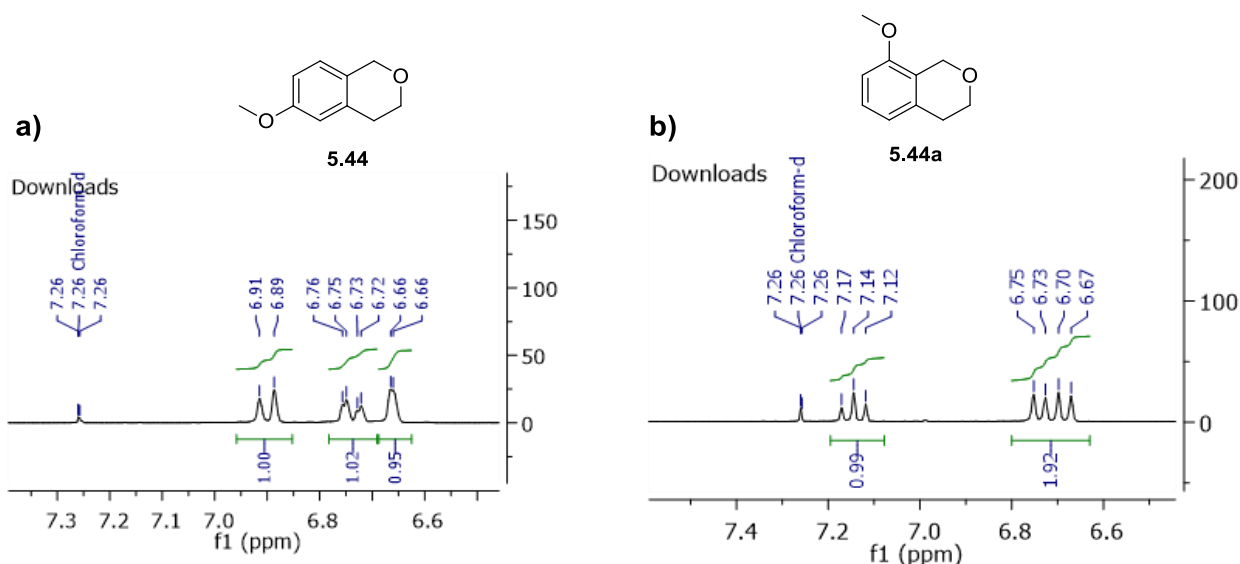


Figure 5.5. ¹H-NMR spectra of the aromatic regions for a) compound **5.44** and b) **5.44a**.

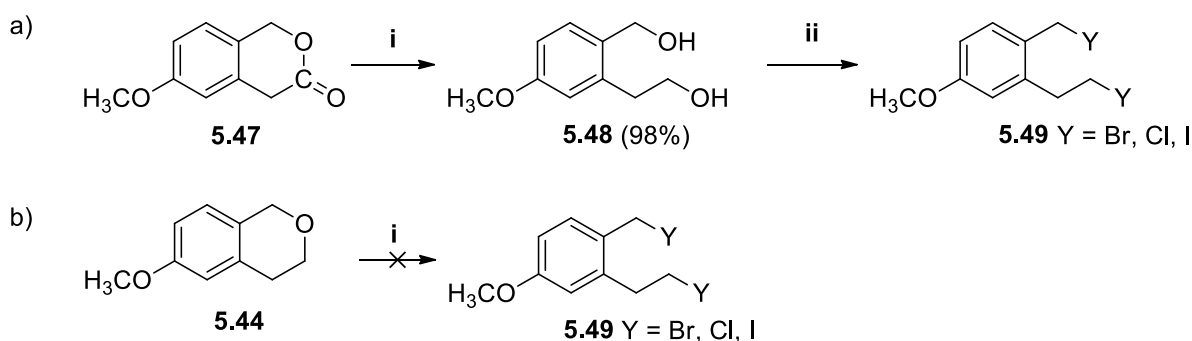
In compound **5.44** a doublet ($^3J = 8.4$ Hz) at δ 6.89, a multiplet at δ 6.72, as well as a multiplet at δ 6.66 each integrating for 1-proton, supported the assigned structure illustrated in Figure 5.5a. However, it is clear that the aromatic protons fit the classical 1,2,4 substitution pattern. In addition, the shielding effect resulted in the adjacent aromatic protons appearing marginally upfield. On the other hand, the *ortho*- and *para*-aromatic protons in compound **5.44a** appeared as a multiplet with overlapping signals between δ 6.75 – 6.67. A doublet of doublets, observed as a triplet, was observed for the *meta*-aromatic proton at δ 7.14 ($^3J = 7.9$ Hz).

5.4.3 Ring-opening and halogenation of the 6-methoxyisochroman

Ring-opening of the isochroman was considered as one of the crucial steps required for the synthesis of the THIQ analogues. However, ring-opening of **5.44** with the intent of generating a dihalogenated species was not successful, despite applying several varied procedures as described in Table 5.2. As a result, this led to the investigation of isochromanone **5.47**, which upon treatment with LiAlH₄ generated the diol species **5.48**. To this end, the use of a procedure described by Spangler and co-workers¹⁷² was applied for the synthesis of isochromanone **5.47**.¹⁷² This protocol involved the stirring of 3-methoxyphenyl acetic acid and 37% formaldehyde in acetic acid at room temperature for 5 days. It is important to note that the addition of excess formaldehyde, as well as introduction of heat, only led to the synthesis of several side products and thus the reaction was stirred at room temperature for an extensive time. After work-up, the product **5.47** was obtained as a white solid in moderate yields ranging between 45 – 70%. ¹H-NMR

CHAPTER 5 | Isochromanone: A surprisingly valuable intermediate

spectroscopy was employed to confirm the identity of compound **5.47**. A 2-proton singlet at δ 5.26, a 2-proton singlet at δ 3.68, a 3-proton singlet (OCH₃), as well as a singlet at δ 3.82 supported product formation upon comparison to the literature values.¹⁷⁶ Furthermore, treatment of **5.47** with LiAlH₄ afforded the diol **5.48** as a white solid in a 98% yield, as confirmed by ¹H-NMR spectroscopy. The unique chemical shifts observed for **5.48** were a 2-proton triplet at δ 2.86, overlapping signals of the methoxy and methylene hydroxyl between δ 3.83 – 3.78, in addition to an intense 2-proton singlet at δ 4.52 for the benzylic methylene hydroxyl group, which accounted for all the aliphatic substituents.



Scheme 5.23. Reagents and conditions: **a)** (i) LiAlH₄, THF, 60 °C, 4 h; (ii) Refer to Table 5.2 and **b)** (i) Refer to Table 5.2.

This next step entailed the double halogenation of diol **5.48** to generate the dihalogenated intermediate **5.49**, as depicted in Scheme 5.23. The intention was next to substitute the halo-analogues **5.49** with a variety of amines to afford the intended products illustrated by the model reaction described in Scheme 5.19. Whilst the ring-opening worked very well in providing **5.48**, formation of the desired products **5.49** remained elusive, despite the variation of a number of fine-tuned reaction parameters, such as halogenating agents and solvents, being attempted (see Tables 5.2).

Table 5.2. Halogenation protocols of diol **5.48**.

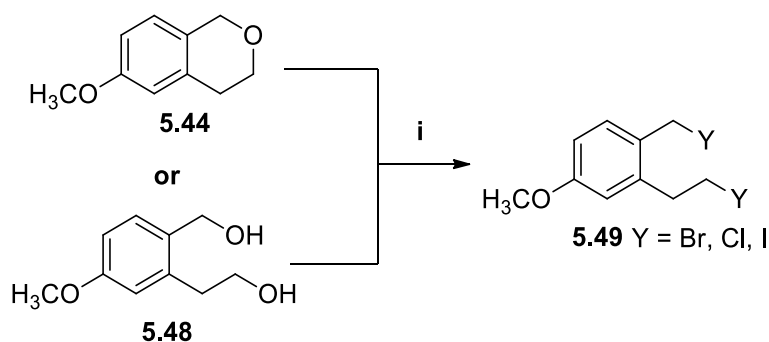


Table 5.2a.

Entry	Substrate	Halogen source	Conditions	5.49 Yield (%)
1	5.44	BBr ₃ , 3.0 equiv ¹⁷³	CH ₂ Cl ₂ at RT	0
2	5.44	HI, 10.0 equiv ¹⁶⁸	Neat under reflux	0

As shown in Table 5.2, entries 1 and 2 indicated that no product was obtained when attempting to halogenate and open the aliphatic ether ring **5.44** by treatment with strong acids. It was however, expected that multiple product formation could occur giving rise to the formation of a few compounds (**a** – **f**), as illustrated in Figure 5.6. It was also surmised that upon treatment of **5.48** with halogenating agents a similar product profile would be formed. However, these compounds **a** – **f**, were still considered valuable for two reasons: (i) if a monohalogenation occurred, the substrate could be recycled for a second halogenation, and (ii) as demethylation of the aryl methyl ether is considered a final step in our reaction sequence, it could thus be avoided by using the demethylated products **d** – **f**.

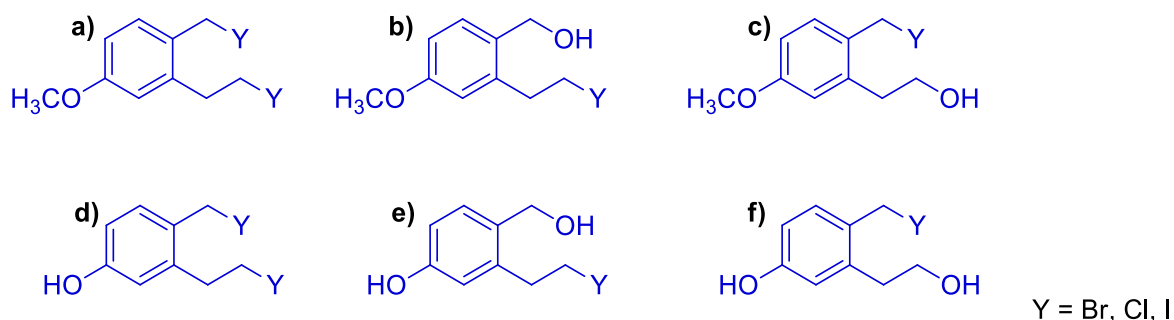


Figure 5.6. Possible mixture of products obtained upon halogenation.

Table 5.2b.

Entry	Substrate	Halogen source	Conditions	5.49 Yield (%)
1	5.48	ZnCl ₂ cat.; SOCl ₂ , 4.0 equiv ^{177,178}	Neat	0
2	5.48	PBr ₃ , 5.0 equiv ¹⁷⁹	PhCH ₃ /PhH under reflux	13
3	5.48	SOCl ₂ , 10.0 equiv ¹³⁶	CH ₃ CHCl ₂ (1,2-dichloroethane) at 60 °C	21 – 50

CHAPTER 5 | Isochromanone: A surprisingly valuable intermediate

However, upon treatment of **5.48** under the conditions listed in Table 5.2b, only trace amounts of mixtures were isolated, all comprising a number of products (by TLC). Evaluation of the aliphatic region of the NMR spectroscopic results for the isolated products provided evidence of numerous triplets indicative of multiple methylene groups, thus demonstrating the possible formation of numerous products. Separation of these compounds seemed futile, especially because of the low overall yield associated with each formed product.

The conditions employed for entry 2, were previously applied to the (3-methoxyphenyl) methanol scaffold for obtaining the monohalogenation providing product in quantitative yield, prior to dihalogenation of the diol **5.48**. This prompted the procedure to be used in entry 2. However, entry 2 in Table 5.2, gave poor conversion, with entry 5 affording the most dihalogenated product in a moderate yield. For the latter experiment, a protocol described by Batey and co-workers was explored.¹³⁶ Compound **5.48** was thus dissolved in CH₂Cl₂, cooled to 0 °C, to which SOCl₂ was added followed by overnight heating and TLC monitoring. Product formation was confirmed by ¹H-NMR spectroscopy, where two 2-proton triplets were observed at δ 3.94 and δ 2.84 with the methyl ether at δ 3.79. In spite of product formation, the poor yield mitigated against the continuation of this protocol. A number of varied reaction conditions, halogenating agents and solvents were investigated (see Table 5.2b) without being able to satisfactorily optimize product formation. This failure led to an alternative approach being considered.

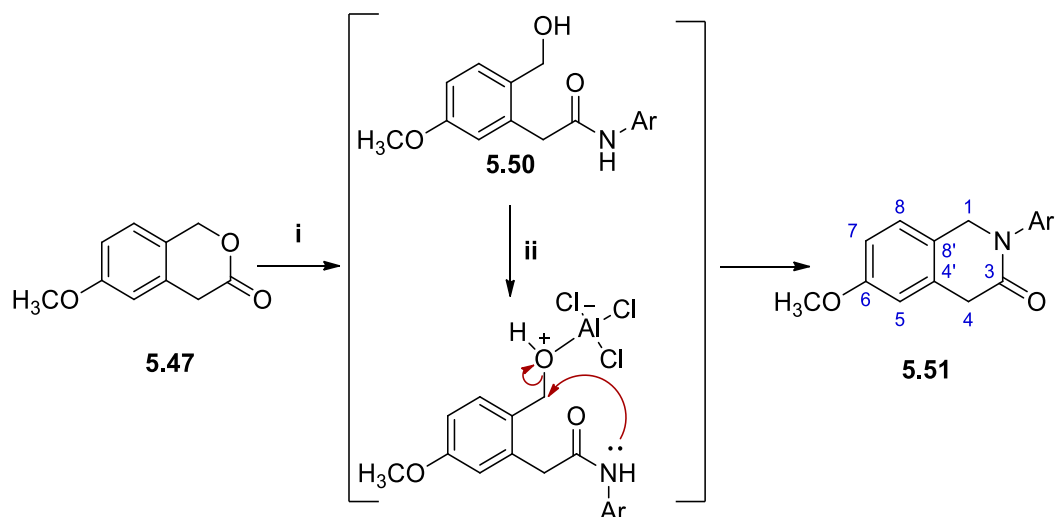
Table 5.2c.

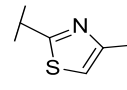
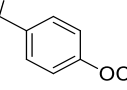
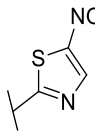
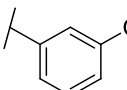
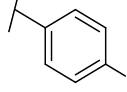
Entry	Substrate	Halogen source	Conditions	5.49 Yield (%)
1	5.48	HCl, 10.0 equiv ¹³⁷	Neat under reflux	0

5.5 Isochromanone as an intermediate toward the synthesis of THIQ analogues

Since the halogenation of compounds **5.48** was not an efficient route towards the synthesis of our target compounds, a different synthetic approach, employing starting material **5.47**, was explored. In this new approach, the use of amines (**a – g**) as reagents were used for delivering the required THIQ analogues, (**5.51a – g**) in Table 5.3.

CHAPTER 5 | Isochromanone: A surprisingly valuable intermediate

Table 5.3. Conditions employed for generating lactam analogues.

Entry	Nucleophile	Ar = Aryl group	5.51 Yield (%)
1	2-amino-4-methylthiazol e	 5.51a	35
2	4-anisidine	 5.51b	40
3	2-amino-5-nitrothiazole	 5.51c	15
4	3-chloroaniline	 5.51d	57
5	3-fluoroaniline	 5.51e	89
6	4-chloroaniline	 5.51f	37
7	4-fluoroaniline	 5.51g	29

Reagents and conditions for generating lactams **5.51**: (i) nucleophiles, 150 °C; (ii) AlCl_3 , 150 °C, neat without solvent.

Work by Chen and co-workers,¹⁸⁰ demonstrated that the isochromanone **5.47** was able to undergo condensation reactions with high boiling point amines under specific reaction conditions, thereby providing the lactam analogue such as **5.51**.¹⁸⁰ Thus compound **5.47** and the respective amines (nucleophiles) in Table 5.3 were heated together at 150 °C while

CHAPTER 5 | Isochromanone: A surprisingly valuable intermediate

stirring for 48 hours, producing a melt.¹⁸⁰ One would expect decomposition of the amine, especially with the extended time period of being exposed to such high temperatures. However, the use of conventional heat at 150 °C for 4 hours resulted in the recovery of reagents with no product formation, proving that longer reaction times were essential. The high temperatures were required to facilitate the ring opening, thereby generating the amido–alcohol intermediate **5.50**. The melt was then cooled to room temperature, followed by the addition of AlCl₃ in toluene for the facilitation of the ring–closing reaction leading to formation of the lactam analogue **5.51**. Exposure to the high temperatures was important for the removal of water, which further promoted ring closure. In this manner, compounds **5.51a** – **c** were obtained in low to moderate yields (15 – 40%). These reaction conditions could be improved by the use of excess amine, followed by shorter reaction times after the addition of AlCl₃.

Key structural features for compounds **5.51a** – **c** were the signal profiles generated by the ¹H–NMR spectra from the substituted heteroaryl groups (**a** – **c**). However, the structural profile of the THIQ motif was generally identified by a 2–proton singlet for the methylene bridge (H1), which appeared in the region of δ 5.38 – 4.76, in addition to a 5–proton multiplet resulting from the overlapping signals of the methylene group at H4 and the methoxy protons observed between δ 3.92 – 3.80. The individual structural characteristics associated with the **5.51** analogues were differentiated and identified by the unique signals observed in the aromatic region for each of the individual heteroaryl moieties incorporated. Apart from the absence of a methylene at C3, the carbonyl motif at C3 was identified in the ¹³C–NMR spectra by a signal resonating at approximately δ 170.00, which was observed for all the **5.51** analogues.

Compound **5.51a** was isolated as a white solid in 35% yield and its structure confirmed by ¹H–NMR spectroscopy. For example, an intense 3–proton singlet at δ 2.33 confirmed the presence of the thiazole’s methyl group. In comparison to the starting material **5.47**, an additional aromatic proton singlet was observed at δ 6.58, indicative of the thiazole’s single aromatic proton. Compound **5.51b** was isolated as a beige solid in 40% yield and its ¹H–NMR spectrum displayed a complex pattern in the aromatic region between δ 7.24 – 6.77 integrating for 7–protons, which confirmed the incorporation of the anisidine substituent, further supported by an intense 6–proton singlet at δ 3.81 indicative of the two methoxy moieties. Product **5.51c** was also confirmed by ¹H–NMR spectroscopy and isolated as an orange solid in only 15% yield. The only variation upon comparison of **5.51c** to **5.47**

CHAPTER 5 | Isochromanone: A surprisingly valuable intermediate

was the 1-proton singlet observed at δ 8.40 (*thiazole*-ArH). In addition to the ^1H and ^{13}C NMR spectroscopic data, ESI⁺ TOF MS data was implemented for all three products for final verification. An attempt to generate **5.51c** from a two-step reaction process to improve the yield involved the heating of the substrate **5.47** under reflux in THF with amine (**c**) followed by removal of the solvent and providing a solid residue. This residue was then heated for 24 hours under reflux in toluene with catalytic amounts of AlCl_3 being added. However, no product was obtained with this approach.

Entries 4, 5, 6 and 7 illustrate that products were formed in low to reasonable yields. The aniline nucleophiles used in these entries were liquid and thus added in excess, making TLC monitoring of the reaction's progression easier since no hard melt was formed. The structure of compound **5.51d** was elucidated by an 8-proton aromatic multiplet observed between δ 7.56 – 6.97 including the NH signal observed in the ^1H -NMR spectrum. Product formation of **5.51d** was further validated by use of ESI⁺ TOF MS where the protonated molecular ion ($[\text{M}+\text{H}]^+$; m/z) was found to have a monoisotopic mass of 288.0785, which corresponded well to the calculated monoisotopic mass for $\text{C}_{16}\text{H}_{14}\text{ClNO}_2$ being 288.0791 for **5.51d**. Confirmation of compound **5.51e** was established by use of ^1H -NMR spectroscopy, in which a 1-proton multiplet between δ 7.46 – 7.21, a 3-proton multiplet between δ 7.20 – 6.90, in addition to a 3-proton multiplet found between δ 6.88 – 6.78 indicated the presence of two separate aromatic moieties. Additionally, the ESI⁺ TOF MS confirmed the monoisotopic mass as being 272.1086 compared to that calculated for $\text{C}_{16}\text{H}_{14}\text{FNO}_2$, being 272.1087. Compounds **5.51f** and **5.51g** showed a similar aliphatic ^1H -NMR spectroscopic profile to that observed for the compounds **5.51d** and **5.51e**. However, their aromatic profiles differed quite significantly, and they could be differentiated by their coupling constants. Compound **5.51f** was elucidated by ^1H -NMR spectroscopy, in which a 4-proton multiplet between δ 7.39 – 7.28, a 1-proton multiplet between δ 7.12 – 7.09 were found, in addition to a 2-proton multiplet found between δ 6.82 – 6.78 indicative of the presence of two separate aromatic moieties. Additionally, a 5-proton multiplet between δ 7.47 – 7.23, and a 2-proton multiplet between δ 7.00 – 6.95 for compound **5.51g** indicated the presence of two separate aromatic moieties. Furthermore, all compounds therefore were verified by HRMS.

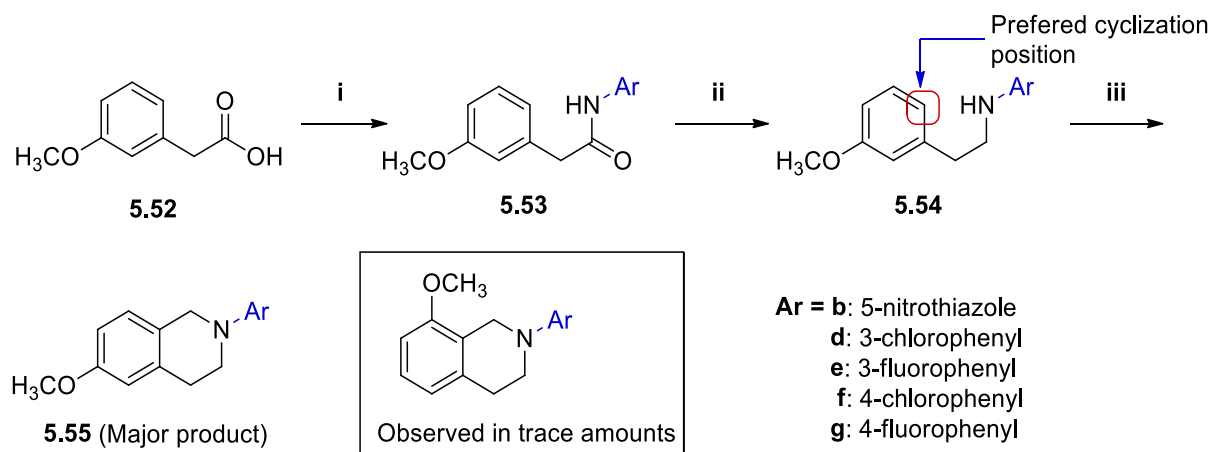
5.5.1 Synthesis of THIQ analogues promoted through coupling reactions

As shown in section 5.5, low yields were associated with the formation of most products (**5.51**) shown in Table 5.3. Despite the protocol described by Table 5.3, we would have preferred to reduce the carbonyl group. This method resulted in insufficient material for

CHAPTER 5 | Isochromanone: A surprisingly valuable intermediate

generating the analogues **5.55** and a different method was required. This led to the notion of employing an alternate method, involving the use of the Pictet–Spengler protocol shown in Scheme 5.24, for generating the THIQ analogue precursor for compounds **5.1** in an improved yield. Using this approach, the successful synthesis of product was established upon examination of the $^1\text{H-NMR}$ spectra, as well as mass spectrometry results.

In an initial attempt, 3-methoxyphenyl acetic acid **5.52** was converted into the acid chloride **5.53** upon treatment with thionyl chloride at 40 °C. Since the hydrolysis of this acyl chloride occurred quite readily, the reaction procedure was soon changed to take this into account by making use of coupling agents. As shown in Scheme 5.24, a method reported by Pelly and co-workers¹⁸¹ was employed where a cooled solution (0 °C) of amines (**b** and **d – g**) was dissolved in CH_2Cl_2 , to which catalytic amounts of DMAP were added for activation of the coupling agent *N,N'*-dicyclohexylcarbodiimide (DCC), were added to carboxylic acid **5.52**. The resulting reaction mixture was stirred at room temperature for 5 hours to ensure complete conversion of the amine to afford amide **5.53**, since they both possessed similar R_f values upon monitoring with TLC.



Scheme 5.24. Reagents and conditions described by Kano and co-workers:¹⁸² (i) amines (**b**, **d – g**), DCC, cat. DMAP, CH_2Cl_2 , RT, 5 h; (ii) $\text{LiAlH}_4/\text{AlCl}_3$, THF, overnight; (iii) CH_2O , formic acid, 80 °C, overnight.

Table 5.4. Results obtained for Scheme 5.24.

Entry	Amide 5.53 Yield (%)	Amine 5.54 Yield (%)	THIQ analogue 5.55 Yield (%)
1	5.53b (16)	5.54b (no product)	5.55b (no product)
2	5.53d (66)	5.54d (98)	5.55d (no product)
3	5.53e (94)	5.54e (73)	5.55e (75)
4	5.53f (87)	5.54f (88)	5.55f (83)
5	5.53g (56)	5.54g (75)	5.55g (98)

CHAPTER 5 | Isochromanone: A surprisingly valuable intermediate

Entry 1, suffered from a poor yield, which could be associated with the low solubility observed for amine **b** and poor nucleophilicity previously observed in earlier reactions. Despite the low yields associated with the generated amide **5.53b**, the overall yield was improved upon comparison to entry 3, Table 5.4. As illustrated in Table 5.4, it is clear that the general coupling reaction proceeded successfully providing the products **5.53d – g** in moderate to good yields. The general structural profile presented by products **5.53b** and **5.53d – g** was confirmed using $^1\text{H-NMR}$ spectroscopy which provided sufficient evidence of the amide, as well as the aromatic protons. The overlapping aromatic and amine signals were often observed as a multiplet and integrated for 9-protons between the region δ 7.51 – 6.80 indicative of the incorporated aryl motifs. Additionally, the methylene signal was observed as a 2-proton singlet between δ 3.71 – 3.69. The amide carbonyl's signal was confirmed and identified using $^{13}\text{C-NMR}$ spectroscopy. This signal was found to resonate between δ 169.00 – 171.00. In addition, ESI⁺ TOF MS further confirmed product formation by an increase in the monoisotopic mass of the products.

Reduction of the amides **5.53** was easily accomplished by gentle heating of the reaction mixture at 45 °C after treatment with monochloroalane in THF. Products **5.54d – g** were obtained in reasonable yields as illustrated in Table 5.4. Their structures shared a general $^1\text{H-NMR}$ spectroscopy profile and were confirmed by the identification of two 2-proton triplets observed upfield between δ 3.35 – 2.50, indicating the presence of two methylene groups. Absence of the carbonyl amide signal previously observed in the $^{13}\text{C-NMR}$ spectrum between δ 169.0 – 171.0, in addition to the new methylene signal resonating at approximately δ 35.0, further supported the structure of compounds **5.54**.

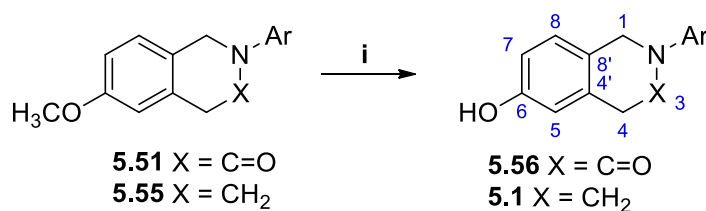
Work previously described by Kano and co-workers¹⁸² provided a procedure for the final step of the synthesis for cyclization of the amines **5.54d – g** by condensation with a mixture of paraformaldehyde in formic acid at 80 °C overnight.¹⁸² The reaction mixture was then cooled to room temperature, followed by neutralization using a saturated sodium bicarbonate solution at 0 °C. The mixture was subsequently extracted with EtOAc to afford products **5.55d – g** in good yield, with the added advantage being that no further purification required. The structures for products **5.55d – g**, were confirmed using $^1\text{H-NMR}$ spectroscopy, in which an intense 2-proton singlet observed between δ 4.00 – 4.50 demonstrated the presence of the newly formed methylene signals. The chloroaryl substituted compounds **5.55d** and **5.55f** in Table 5.5 were found to lack stability and soon

CHAPTER 5 | Isochromanone: A surprisingly valuable intermediate

decomposed. Decomposition of these compounds were confirmed by HRMS which showed the absence of their expected masses. Additional compounds such as **5.55a** in Table 5.5 (with an expected mass of 261.1062 and an experimental 261.1070), **5.55b** (with an expected mass of 270.1494 and an experimental 270.1494), **5.55e** (with an expected mass of 258.1294 and an experimental 258.1288) and **5.55g** (with an expected mass of 258.1249 and an experimental 258.1292) were however confirmed with HRMS.

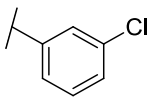
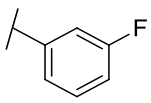
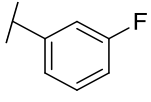
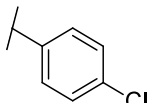
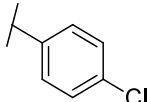
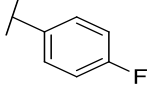
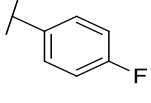
5.6 Demethylating routes toward obtaining 5.1 and 5.56 THIQ analogues

The importance related to the demethylation of the aryl methyl ether moiety has previously been mentioned, since the hydroxyl group is essential for the intermolecular binding interactions within the binding pocket of the ER receptor. Successful demethylation of compounds **5.51** (**a** and **c**) and **5.55** (**a** and **c**) was achieved using BBr_3 in a large excess for the efficient removal of the methyl group, thus generating the all-important phenol functionality.

Table 5.5. Reagents and conditions for the demethylation of **5.51** and **5.55**.

Entry	Substrate 5.51	X	Ar-Aryl group	Product	Yield (%)
1	5.51a^a	C=O		5.56a	45
2	5.55a^a	CH ₂		5.1a	45
3	5.51c^a	C=O		5.56c	78
4	5.55c^a	CH ₂		5.1c	38
5	5.51d^b	C=O		5.55d	57

CHAPTER 5 | Isochromanone: A surprisingly valuable intermediate

6	5.55d ^b	CH ₂		5.1d	Trace amounts. Not enough for NMR.
7	5.51e ^b	C=O		5.56e	89
8	5.55e ^b	CH ₂		5.1e	48
9	5.51f ^b	C=O		5.56f	Trace amounts. Not enough for NMR.
10	5.55f ^b	CH ₂		5.1f	58
11	5.51g ^b	C=O		5.56g	24
12	5.55g ^b	CH ₂		5.1g	55

Reagents and conditions for demethylation of methyl ether aryls: (i) **5.51** or **5.55**. ^aBBr₃ (10.0 equiv), CH₂Cl₂, 0 °C; ^bAlI₃ (5.0 equiv), PhCH₃/PhH

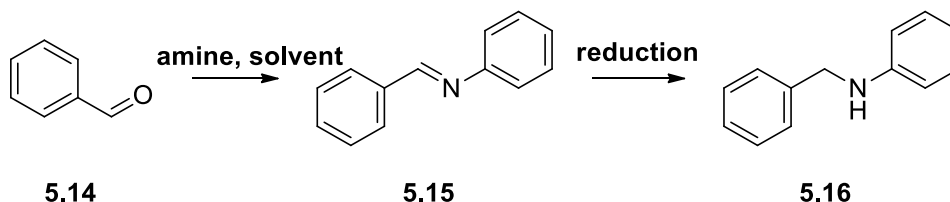
Reasonable yields of products were obtained (see Table 5.5). Confirmation of the structural integrity of **5.56a** and **5.56c** was confirmed by the absence of the intense singlet previously observed at δ 3.00 – 3.98 (OCH₃). Although not optimized, these experiments provided sufficient product for further modifications. Structural confirmation of products **5.56a**, **5.56c** – **g**, **5.1a** and **5.1c** – **g** was evident by ¹H- and ¹³C-NMR spectroscopy and mass spectrometry. The series of compounds **5.56a** and **5.56c** – **g**, were easily identified by the lactam skeleton which had a 2-proton singlet in the region of δ 3.50 – 3.90 for H₄, and a 2-proton singlet at δ 5.00 indicative of the H₁ methylene group, in addition to the aromatic signals. Apart from this, the structure of these products were confirmed by the absence of the methoxy previously observed in the δ 3.00 – 3.98 region. In addition, ESI⁺ TOF MS was employed, in which the monoisotopic mass was determined to further confirm product formation. Compounds **5.1a** and **5.1c** – **g** also presented a similar general spectral profile of **5.56** with two sets of 2-proton triplets found between δ 2.00 – 2.99 (H₄) and δ 3.00 – 3.70

CHAPTER 5 | Isochromanone: A surprisingly valuable intermediate

(H3). In addition, an intense 2-proton singlet at δ 4.00 – 5.00 (H1) and a complex aromatic region supported the formation of the desired product. Furthermore, absence of the methoxy signal, as well as the ESI⁺ TOF MS confirmed products **5.1a** and **5.1c – g**. Although not optimized, these experiments provided sufficient product for further biological screening.

5.7 Summary and concluding remarks

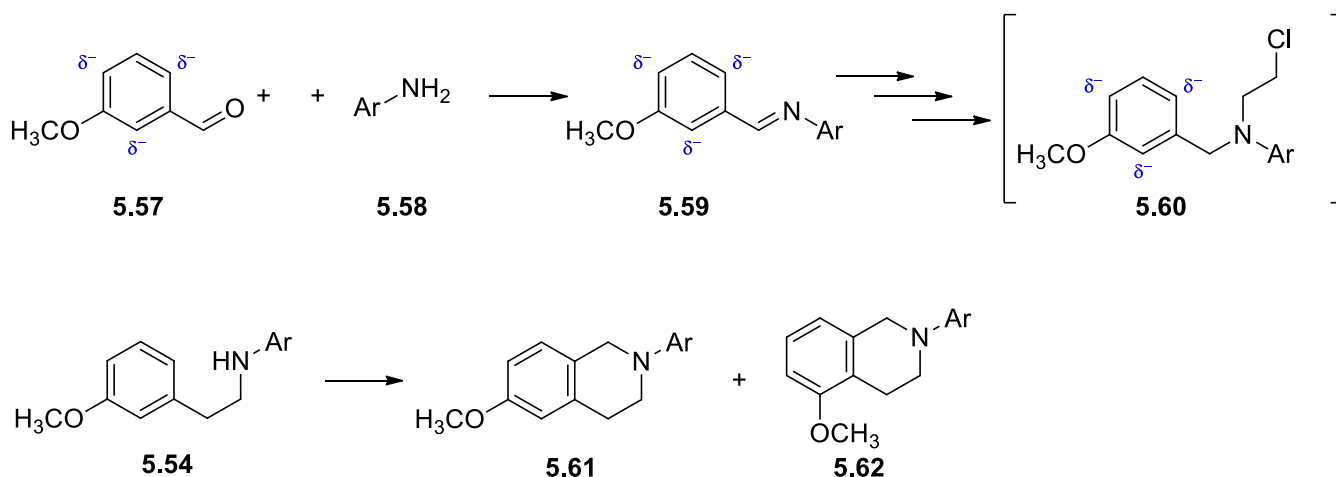
Synthesis of the THIQ analogues without linker groups proved quite challenging, despite the number of synthetic routes reported. The relevant synthetic routes to afford our target molecules included the use of Ullmann condensation reaction with our initial C-ring aryl groups (including heteroaryl systems). Coupling of the thiazoles (C-ring, heteroaryls) however failed. This issue was resolved by a method in which condensation between amines and aldehyde (**5.14**) formed a valuable Schiff base intermediate **5.15** shown in Scheme 5.25. This intermediate provided a substrate ready to undergo reduction, followed by an intramolecular F–C cyclization forming the THIQ analogue.



Scheme 5.25. A subsequent F–C cyclization reaction with amine **5.16** would provide the desired product.

It is unfortunate that none of these reactions were optimized using the **5.57** precursor (for synthesis of the Schiff base), since the presence of the electron-donating methyl ether group (see Figure 5.12) could have increased the electron density in the relative *ortho*- and *para*- positions, further improving reaction conditions for the F–C cyclization. However, cyclization could potentially occur at C4 or C2 of the aryl ring (depending on the specific functional groups on the aniline compound) providing a mixture of products. Thus, this approach was soon abandoned and synthesis of the isochroman molecule was pursued as an intermediate toward the THIQ analogue.

CHAPTER 5 | Isochromanone: A surprisingly valuable intermediate



Scheme 5.26. *m*-Anisaldehyde **5.57**, which could undergo F–C cyclization.

Synthesis of the isochroman intermediate **5.36** and the subsequent reactions leading to the THIQ analogue **5.38** were optimised using the substrate without a methyl ether group. Once optimized the actual reaction was done on compound **5.40**. However, it was found that the presence of the methyl ether moiety resulted in a number of unexpected products such as **5.45** and **5.44a**. Product **5.44** was eventually obtained in reasonable yield, but the subsequent reactions (ring opening and halogenation) provided multiple problems and product in very low yield. It was subsequently decided to generate the THIQ analogue by condensation between isochromanone **5.47** with a few selected amines (**a** – **f**). Products **5.51** were obtained in low yield, but in sufficient amounts for subsequent reactions. Compounds **5.51** were comparatively easily demethylated, albeit in low yields as a mixture of starting material **5.51** and product **5.56**. The THIQ analogues **5.1** were easily demethylated, but the final products were found to be relatively unstable and after storage gave spectra with additional $^1\text{H-NMR}$ signals clearly indicating the slow decomposition of these compounds.

Chapter 6

Computational and Biological evaluation of the THIQ analogues

The current study was aimed towards the generation of small compounds, with the potential to selectively bind with a greater affinity to the ER β subtype. Computational docking simulations done by Dr Stephen Pelly were initially trialled, where ligand efficiency scores of the synthesized compounds were generated for both ER α and ER β upon comparison to estradiol. Apart from computational analysis, with the successful synthesis, it was necessary to assess the bioactivity of the ability of the synthesized analogues of compounds **3.49b**, **3.49d** and **4.46h** (synthesis described in Chapters 3 – 5). For the biological assays, the EC₅₀ values were contributed by the valuable input of Prof Lech G. Milroy from the Technische Universiteit, Eindhoven, where the screening of some of these compounds **3.49** (discussed below) was carried out under the supervision of a PhD student in the Eindhoven group, Chan Vinh Lam. The remaining compounds (**4.46d**, **4.46f**, **4.46g**, **4.46h**, **4.66c'**, **4.66c''**, **4.74h**, **5.1a**, **5.1c**, **5.1f**, **5.1g**, **5.56a**, **5.56c**, **5.56e** and **5.56g**) were screened by the Council for Scientific and Industrial Research (CSIR) investigator, Dr Alex Alexandre, to determine their cellular anti-proliferation values.

6.1 Computational evaluation of the synthesized compounds

Computational molecular docking simulations have been used as an important tool to understand the biochemical pharmacological interactions between receptors and their ligands. Ever since the early 1980s, this technique has become increasingly important in the world of medicinal drug discovery.¹⁸³ The use of computational screening has permeated all aspects of drug discovery, frequently resulting in a more direct and rational medicinal chemical approach, with advantages such as low cost, time efficiency and effective screening of the designed compounds. Despite the value provided by virtual screening, reports by Carlson,¹⁸⁴ Schultes,¹⁸⁵ Friesner¹⁸⁶ and co-workers further indicate the need for additional improvements in this approach to optimize its application. Essentially, the aim of the computational docking study utilized in our work was to provide a prediction of the ligand-receptor complexed structures. This being a general method, it was employed for predicting the binding modes or ligand conformations required for designing a synthetic ligand with an

improved potency and selectivity for ERs. The virtual screening was targeted toward the design of an effective ligand, likely to bind with the ERs.^{183,186-188}

6.1.1 Ligand–ER efficiency docking results

Ligand efficiency is a measure of the binding affinity (as measured by the Glide XP score), divided by the molecular weight of the ligand. There are many ways to calculate ligand efficiency but in general it is some measure of the ligand's performance (be that docking score or, or binding energy), divided by its molecular weight).

Docking studies were achieved by primarily sampling conformations of compounds (**3.49**, **4.46**, **4.66**, **4.74**, **4.80**, **5.1** and **5.56**) in the active site of the protein (ER), followed by ranking these conformations *via* a scoring function shown in Table 6.1. Ideally, sampling algorithms should be able to reproduce the experimental binding mode, in this case with estradiol, and the scoring function should also rank it highest among all generated conformations. From this, a brief overview of the basic docking results are provided, as demonstrated in the tables and graphs below.^{183,187,188} It is important to note that a lower or more negative ligand efficiency score, demonstrates a better ligand binding interaction. To facilitate comparisons between THIQs with specialized structural features the various entries in Table 6.1 have been grouped according to the ligand efficiency scores obtained by the aryl substituted groups on the THIQ amine.

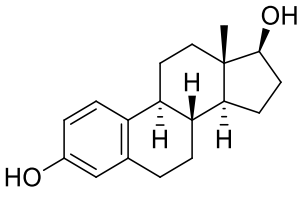
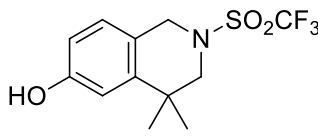
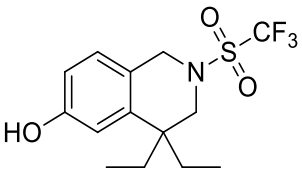
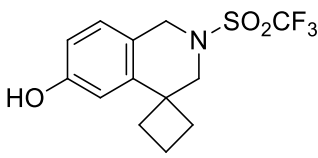
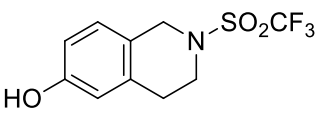
6.1.1.1 Computational results obtained for set 1 compounds

The compounds of set 1 consisted of trifluoromethylsulfone–decorated THIQs and included compounds **3.34**⁴⁰, **3.49b**, **3.49c** and **3.49d**. In terms of the molecular modelling, for ER α the reference **3.34** showed a ligand efficiency of -0.030 and -0.031 for ER β . As mentioned before, the research reported by Brunsveld *et al.*,⁴⁰ has shown that **3.34** had a 10–fold improved binding affinity for ER β when compared to estradiol, although this did not seem reflected in the ligand efficiency scores which were very similar. It should thus be realized that the computational results were unable to distinguish this subtle difference in **3.34**'s selectivity. Compounds **3.49b**, **3.49c** and **3.49d** were generated to explore the effect of the varied R–groups in the 4–position of the THIQ scaffold. However, in terms of molecular modelling compounds **3.49b**, **3.49c** and **3.49d** showed much lower ligand efficiency scores of -0.028 – -0.030 for ER α and -0.029 – -0.031 for ER β , as shown in Table 6.1. It should also be noted that all three ligands docked much less efficiently when compared to the -

CHAPTER 6 | Biological evaluation of the THIQ analogues

0.042 values obtained for the natural ligand estradiol in ER α and ER β). These results seemed to correlate well with the biological results discussed later in this chapter (6.2.1).

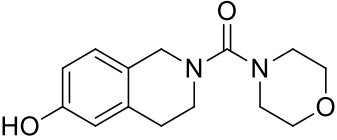
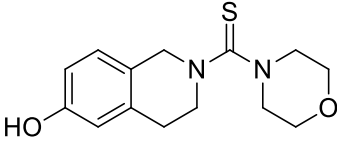
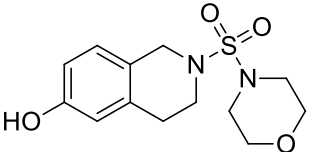
Table 6.1. Ligand efficiency scores obtained for compounds from set 1.

Entry	Compound	Structure	Ligand efficiency score α/β ER
	Estradiol		-0.042 (α)/-0.042 (β)
1	3.49b		-0.028 (α)/-0.029 (β)
2	3.49c		-0.028 (α)/-0.029 (β)
3	3.49d		-0.030 (α)/-0.029 (β)
4	3.34		-0.030 (α)/-0.031 (β)

6.1.1.2 Computational results obtained for set 2 compounds

The compounds described in Table 6.2 include the structures where the THIQ skeleton and the morpholine substituents were kept constant with varied linker groups between these moieties. Compound **4.46h** had a carbonyl linker (resulting in an overall urea functional group), **4.80h** had a thiocarbonyl linker (giving the thiourea functional group) and **4.74h** had a sulfone linker. The amide-linked **4.46h** and thioamide-linked **4.80h** compounds of set 2 showed the best efficiency scores with -0.036 for both ER α and ER β and **4.80h** showed an equal efficiency of -0.036 for both ERs. It should be noted that all of them were still quite far from the value of estradiol (-0.042).

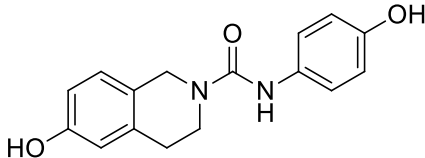
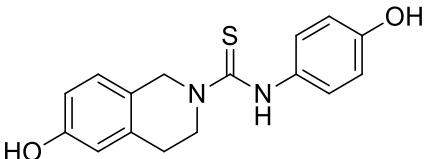
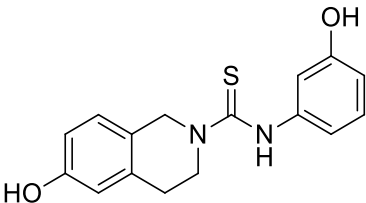
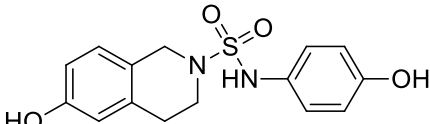
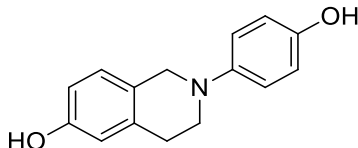
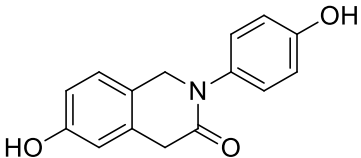
Table 6.2. Ligand efficiency scores obtained for compounds from set 2.

Entry	Compound	Structure	Ligand efficiency score	
			α	β ER
1	4.46h		-0.036	-0.035
2	4.80h		-0.036	-0.036
3	4.74h		-0.028	-0.028

6.1.1.3 Computational results obtained for set 3 compounds

The compounds in Table 6.3 from set 3, included a phenolic substituent with the THIQ skeleton remaining constant. Entries 1 – 4 contain varied linker groups, with compound **4.46c** possessing a carboamide linker (urea), compounds **4.66c'** and **4.66c''** the thioamide (thiourea) and **4.74c** the sulfonamide linker. Of these three compounds **4.66c''** showed the best score being -0.033 in the ER α and -0.032 for ER β . Compounds **4.46c**, **4.66c'** and **4.74c** showed similar scores within the range of -0.027 to -0.030 ligand efficiency toward both ERs. The remaining entries 5 and 6, for compounds **5.1c** and **5.56c** in set 3, with the phenol directly linked to the THIQ, showed improved ligand efficiency scores, with **5.1c** having a value of -0.037 for ER α and -0.038 for ER β . Of note was that compound **5.56c** (entry 6) had the best ligand efficiency scores for both ERs upon comparison to estradiol (-0.041/-0.042 versus -0.042 for ER).

Table 6.3. Ligand efficiency scores obtained for compounds from set 3.

Entry	Compound	Structure	Ligand efficiency score
			α/β ER
1	4.46c		-0.027 (α)/-0.030 (β)
2	4.66c'		-0.029 (α)/-0.030 (β)
3	4.66c''		-0.033 (α)/-0.032 (β)
4	4.74c		-0.027 (α)/-0.028 (β)
5	5.1c		-0.037 (α)/-0.038 (β)
6	5.56c		-0.041 (α)/-0.042 (β)

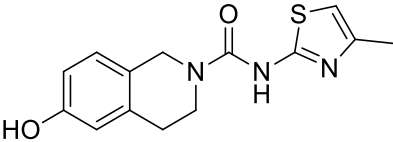
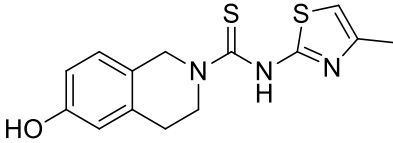
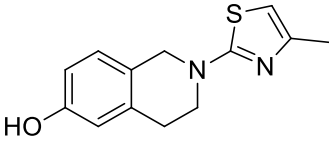
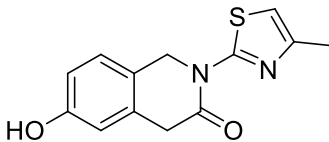
6.1.1.4 Computational results obtained for set 4 compounds

Compounds belonging to set 4 included the THIQ–skeleton with a thiazole substituent as invariables. The variable portion of set 4 compounds included different linker groups between the THIQ and thiazole moieties such as **4.46a** (containing the carbamide linker to form a urea), **4.80a** (the thioamide linker to form a thiourea), **5.1a** (no linker group) and **5.56a** where the linker group is absent and with a lactam group replacing the THIQ–skeleton in

CHAPTER 6 | Biological evaluation of the THIQ analogues

Table 6.4. The linker–group compounds in entries 1 and 2 (Table 6.4) showed poor ligand efficiency scores, with the amide **4.46a** proving to be the worst with a score of ~ -0.020 for both ERs. Entry 2 (**4.80a**), showed a slightly better score with a value of -0.031 observed for both ERs. The directly–linked compounds, **5.1a** and **5.56a** in entries 3 – 4, showed reasonable ligand efficiency scores with **5.1a** being -0.033 (for ER α), -0.034 (for ER β). Lastly for this set, compound **5.56a** showed an improved score of -0.035 for both ERs.

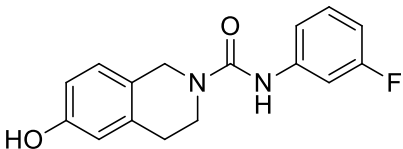
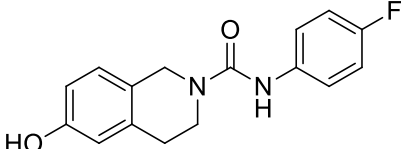
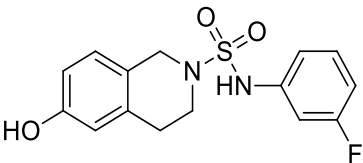
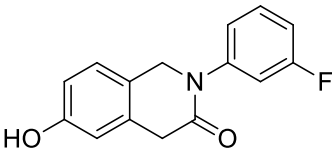
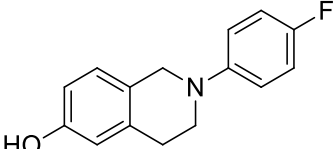
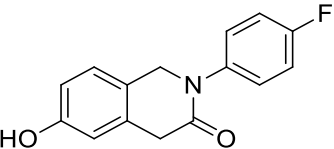
Table 6.4. Ligand efficiency scores obtained for compounds from set 4.

Entry	Compound	Structure	Ligand efficiency score	
			α	β ER
1	4.46a		-0.022	-0.023
2	4.80a		-0.031	-0.031
3	5.1a		-0.033	-0.034
4	5.56a		-0.035	-0.035

6.1.1.5 Computational results obtained for set 5 compounds

The compounds listed in Table 6.5 set 5, entries 1 – 3, contain the invariable fluoroaryl motif and the THIQ core. The compounds **4.46e**, **4.46g** and **4.74e** showed relatively poor scores (as shown in Table 6.5) upon comparison to estradiol or the non–linker–containing compounds in entries 4 – 6. The γ –lactam (**5.56e** and **5.56g**), in addition to the THIQ **5.1g**, showed better ligand efficiency scores upon comparison to the amide– and sulfonamide–linked fluoroaryl groups (**4.46e**, **4.46g** and **4.74e**).

Table 6.5. Ligand efficiency scores obtained for compounds from set 5.

Entry	Compound	Structure	Ligand efficiency score	
			α	β ER
1	4.46e		-0.027	(α)/-0.028 (β)
2	4.46g		-0.025	(α)/-0.029 (β)
3	4.74e		-0.031	(α)/-0.030 (β)
4	5.56e		-0.038	(α)/-0.036 (β)
5	5.1g		-0.037	(α)/-0.038 (β)
6	5.56g		-0.037	(α)/-0.038 (β)

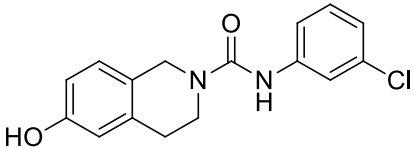
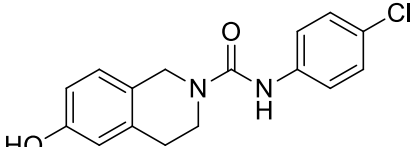
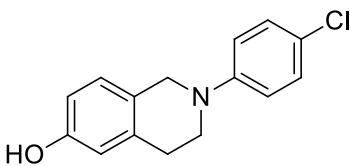
6.1.1.6 Computational results obtained for set 6 compounds

The compounds shown in set 6 (Table 6.6) includes variations on the THIQ portion, and the chloroaryl substituent linker by way of a carboamide bridge. As seen in the previous sets (Tables 6.2 – 6.5), the compounds with linker groups showed a much lower efficiency score upon comparison to the γ -lactam and THIQ-based compounds (**5.1** and **5.56**). In Table 6.6,

CHAPTER 6 | Biological evaluation of the THIQ analogues

entries 1 and 2 showed low scores of -0.022 (for ER α) and \sim -0.026 (for ER β), while entry 3 had a more reasonable score of -0.033 for ER α and -0.035 for ER β .

Table 6.6. Ligand efficiency scores obtained for compounds from set 6.

Entry	Compound	Structure	Ligand efficiency score
			α/β ER
1	4.46d		-0.022 (α)/-0.027 (β)
2	4.46f		-0.022 (α)/-0.026 (β)
3	5.1f		-0.033 (α)/-0.035 (β)

6.1.1.7 Overall results obtained for Table 6.1 to 6.6

Compounds (3.49b – d, 4.46, 4.66, 4.74, 4.80, 5.1 and 5.56) shown in the Tables on the preceding pages in the active site of the receptor (ER), followed by their rankings *via* a ligand efficiency scoring function are summarized in the Tables 6.1 – 6.6 and depicted graphically in Figure 6.1.

CHAPTER 6 | Biological evaluation of the THIQ analogues

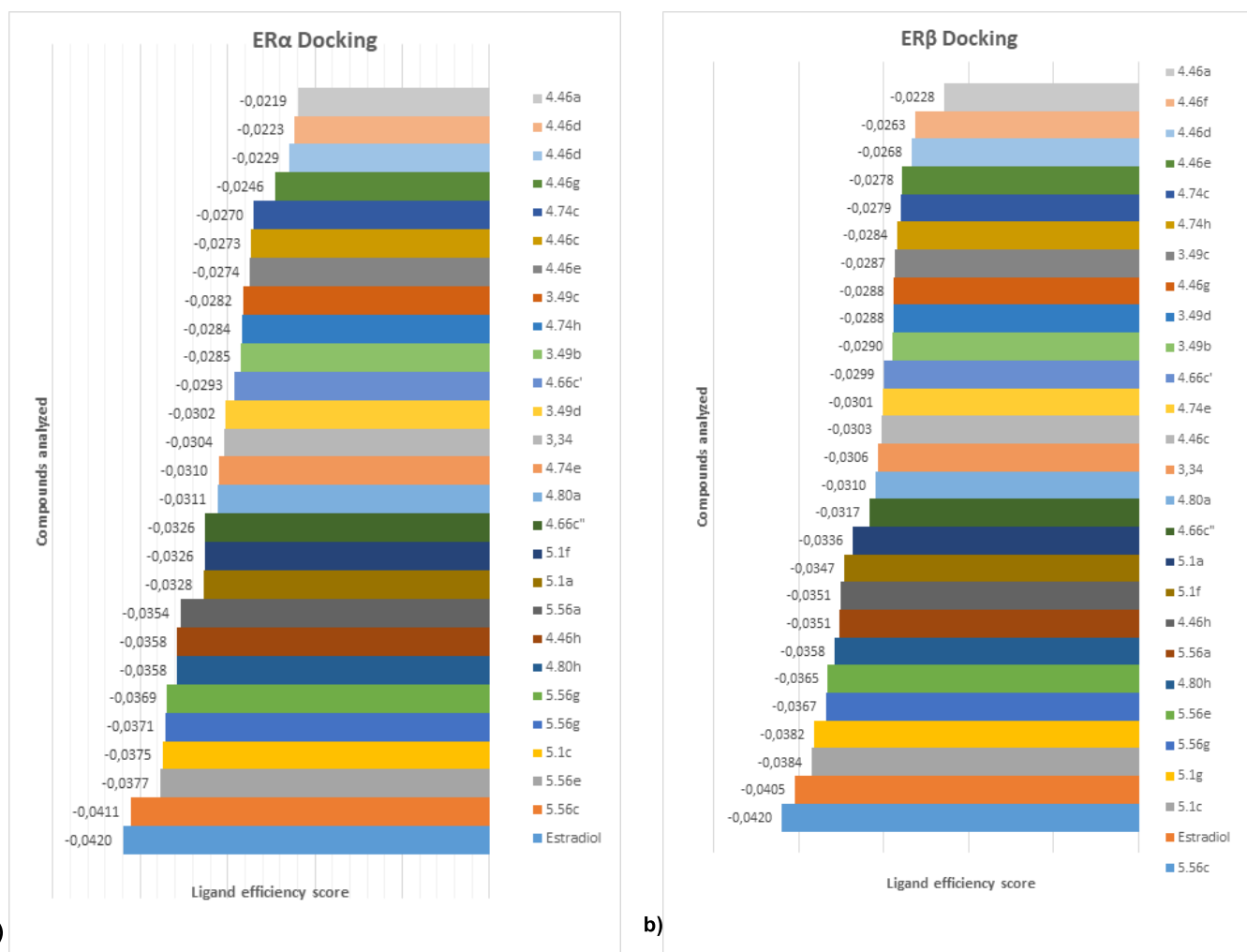


Figure 6.1. a) ER α scoring and b) ER β scoring of the virtual ligand efficiency scores.

The results obtained from the virtual efficiency scores motivated further EC₅₀ and anti-proliferation evaluations of the compounds listed in Figure 6.1. The additional biological evaluations for some of the compounds are thus discussed below.

6.2 EC₅₀ results obtained for set 1 compounds

The synthesis of compounds **3.49b** and **3.49d** was prompted by the continuation of the work reported by Brunsveld, L. *et al.*, where compound **3.34** showed an enhanced 10-fold affinity for ER β .⁴⁰ However, for this study, unlike the reference compound **3.34**, analogues **3.49** included two R-groups at the 4-position of the THIQ skeleton as shown in Figure 6.2 below.

CHAPTER 6 | Biological evaluation of the THIQ analogues

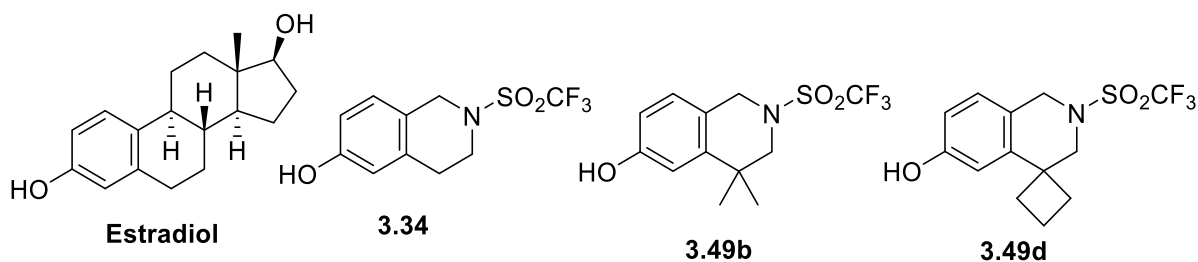


Figure 6.2. The reference compound **3.34** with the 4-substituted analogues **3.49**.

This variation was used to determine the effect the R-groups would have on the results with respect to compound **3.34**. Particularly, with the impact of additional steric bulk in this section of the scaffold. It was hoped that this additional bulk would provide the ligands with an increased discretion for ER α or ER β . The data measured for estradiol was analysed using a non-linear regression graph, with single-site binding and used to calculate the EC₅₀ value of 86 nM (\pm 5 nM), which is in reasonable agreement with the value report for estradiol versus ER α in Brunsveld, L.*et al.*, in previous work (EC₅₀ value of 0.13 μ M \pm 0.04 μ M) demonstrated in Figure 6.3.⁴⁰ It should be noted that the value for estradiol were determined using the same experimental set-up.

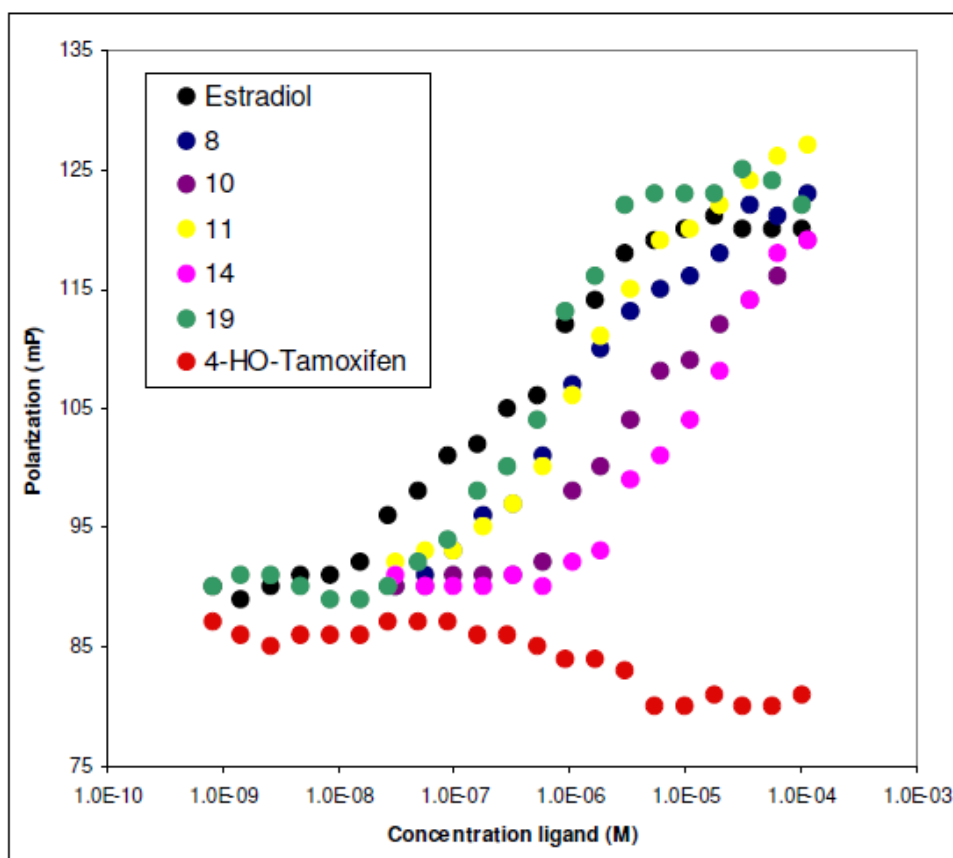


Figure 6.3. Representative ER β -Fluorescein LXXLL peptide fluorescence polarization curves upon increasing ligand concentration. Estradiol and all tested ligands lead to an increase in fluorescence polarization (agonistic

CHAPTER 6 | Biological evaluation of the THIQ analogues

effect). 4-Hydroxy tamoxifen, as an antagonistic reference, leads to a decrease in polarization. (Source: Taken from Brunsveld, L.*et al.*, *J. Med. Chem* 2011, 54, 2005)

Comparison between the reference compound **3.34**, and its derivatives **3.49b** and **3.49d**, is shown in Figure 6.4. Compounds **3.49d**, **3.49b** and **4.46h**, versus the use of estradiol as a positive control, were evaluated in a fluorescence polarization cofactor recruitment assay against SUMO-tagged ER α , using a protocol similar to the study described by Brunsveld, L.*et al.*⁴⁰ In this bioevaluation, a 1 μ M solution of SUM-ER α , 0.1 μ M fluorescein-labelled SRC1-Box2 peptide and a dilution series of each compound from a 5 mM EtOH stock solution for estradiol was utilized. In addition, a 10 mM DMSO stock solution was prepared for each of the test compounds. The measurements were performed in triplicate in coregulator buffer E in black 384 round-bottomed well plates. It should be noted the error bars are included, but are obscured by the symbols, which means the data are highly reproducible within each set of triplicate measurements. The final DMSO content was a constant 10% in each well.

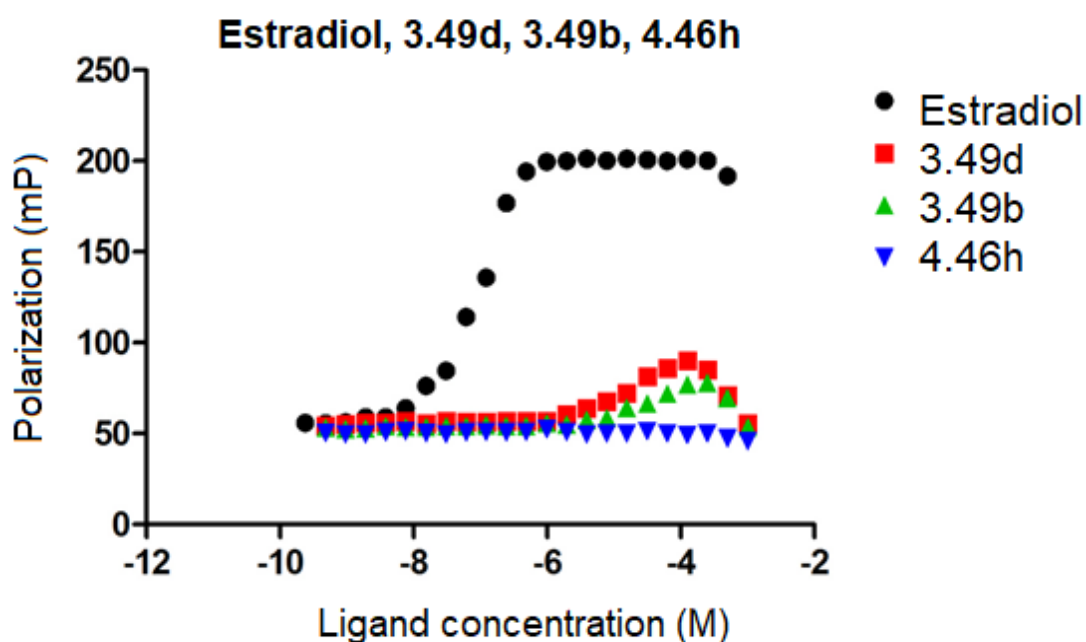


Figure 6.4. Interpreted EC₅₀ results obtained. Fluorescein LXXLL peptide fluorescence polarization curves upon increasing ligand concentration. Estradiol and tested compounds **3.49b**, **3.49d** and **4.46h** which lead to a decrease in fluorescence polarization upon comparison to estradiol.

As shown by Figure 6.4, compound **4.46h** did not induce SRC1 Box2 peptide binding under these conditions up to the highest test concentration (100 μ M), while **3.49d** and **3.49b** both appeared to induce a partial response (i.e. at a fraction of the maximum response induced

CHAPTER 6 | Biological evaluation of the THIQ analogues

by estradiol) at concentrations above 1 μM . The activity of neither compounds plateaued at higher concentrations, which meant that determining an EC_{50} for both compounds was unfortunately not possible.

6.3 Methodology used in screening of sets 2 – 6 against MCF7

Despite the number of compounds submitted for EC_{50} analysis, only a few of the results were obtained for the compounds shown in Figure 6.2. It was decided to send the remaining compounds for proliferation analysis to the CSIR in Pretoria where whole cell testing was performed.¹⁸⁹ The testing procedure included loading of the whole cell assays into sterile 24-well tissue culture plates at 1.50×10^6 M of MCF7 (invasive ductal carcinoma) cell line, after which they were exposed to 2.50 mg/mL of compounds **4.46h**, **4.66c''**, **4.66c'**, **4.46d**, **4.74h**, **4.46f**, **4.46g**, **5.1a**, **5.56a**, **5.56c**, **5.1c**, **5.56e**, **5.1f**, **5.1g** and **5.56e** for 4 days. Post culturing, the array of plates were treated with immunofluorescence and imaged using a Cytation3 cell imaging Multi-Mode Reader, where three channels were used, as illustrated in Figure 6.5.

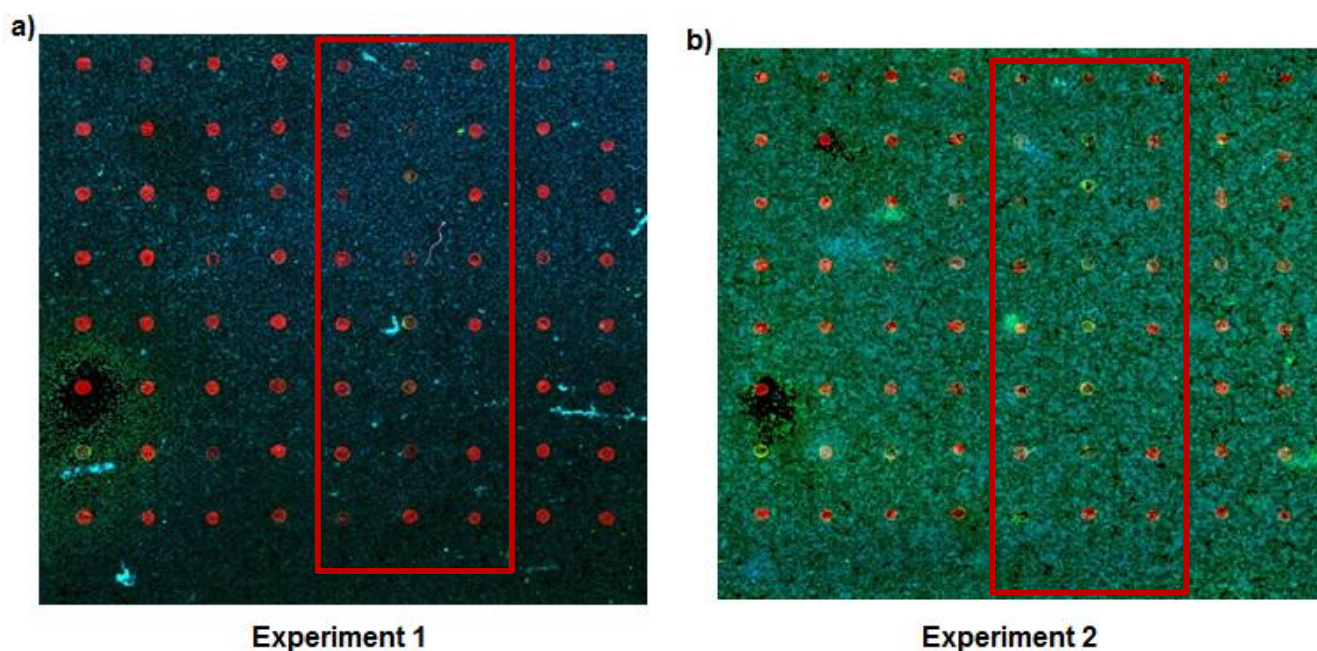


Figure 6.5. MCF7 cell line on a mini compound array. The spots were imaged in the red channel (sulfurhodamine b, 568 nm), the actin cytoskeleton in the green channel (phalloidin, 488 nm) and the DNA in the blue channel [4,6-diamidino-2-phenylindole, dihydrochloride (DAPI, 408 nm)].

The changes in fluorescent intensity were taken to be indicative of changes in MCF7 apoptosis or cell proliferation. Individual experiments were subjected to Persomics analysis

CHAPTER 6 | Biological evaluation of the THIQ analogues

software for the processing and analysis on images was performed using cell profiler and data quantification using Microsoft Excel.

6.3.1 MCF7 cellular anti-proliferation results and discussion

The structural characteristics of the compounds employed in determining the MCF7 anti-proliferation results, included either the substitution of aryl groups (compounds **5.1a**, **5.56a**, **5.56c**, **5.1c**, **5.56e**, **5.1f**, **5.1g** and **5.56e**) or the aryl-linked modified amido groups (**4.46h**, **4.66c''**, **4.66c'**, **4.46d**, **4.74h**, **4.46f** and **4.46g**) *via* the nitrogen of the THIQ scaffold. These aryl rings, in addition to their heteroatoms, were intended to extend toward the His475 residue within the receptors pocket.

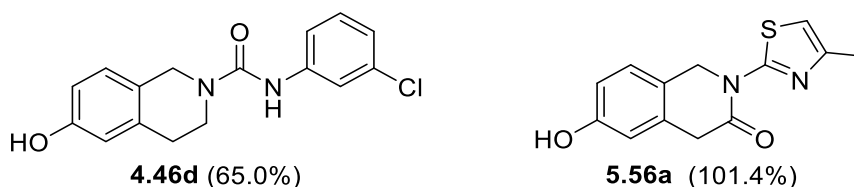


Figure 6.6. The best cellular anti-proliferation effects was shown by the compounds **4.46d** and **5.56a** (Proliferation percentage shown in brackets).

The inhibition displayed by compound **4.46d** was reasonable in terms of MCF7 anti-proliferation), while **5.56a** essentially did not affect the cellular growth (both structures shown in Figure 6.6). All other compounds showed poor inhibition (effectively the promotion of cellular growth) upon comparison to reference compounds, which included fulvestrant and zileuton.

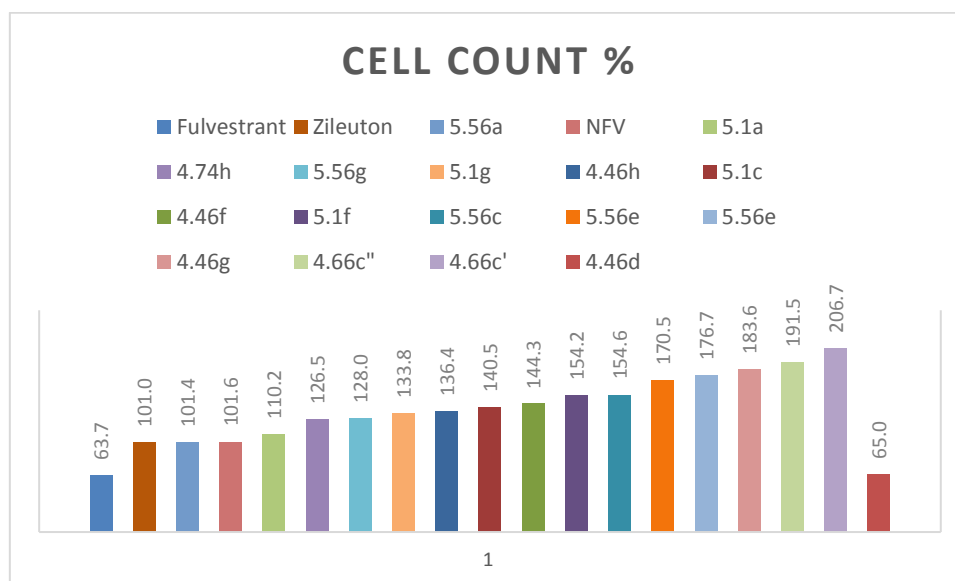
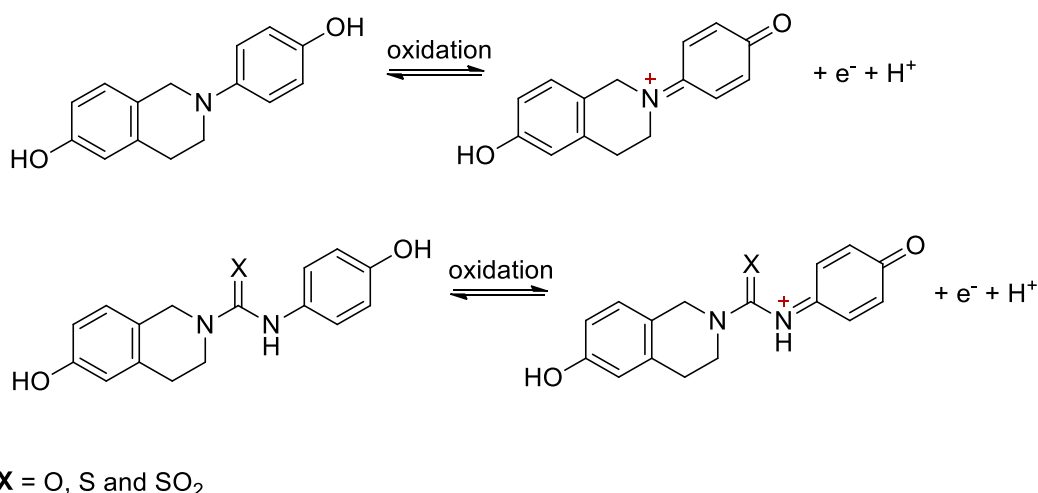


Figure 6.7. MCF7 anti-proliferation values obtained for compounds from sets 2 – 6 (vs reference compounds).

6.4 Summary and concluding remarks

The compounds generated from Libraries 1, 2 and 3, were structurally designed to accommodate the receptors binding pocket and improve the potency and selectivity toward the ER β protein. Upon reviewing the ligand efficiency scores obtained from the virtual screening process of compounds listed in Table 6.1 – 6.6, some reasonable results were obtained indicating the possibility that these compounds would be worthy of further biochemical studies. The virtual screening scores reflected good ligand efficiency for most of compounds. However, when doing whole cell testing only two compounds (**4.46d** and **5.56a**) showed potential activity with the rest showing quite poor activity. A common problem associated with the compounds listed in Table 6.1 was their sediment formation, when trying to solubilize the compounds for EC₅₀ and cellular anti-proliferation analysis. This was commonly associated with the THIQ skeletons that included the 4-phenol (for example shown in Table 6.3; **4.46c**, **4.66c'**, **4.74c** and **5.1c**) which could be explained by Scheme 6.1, as well as the 4-haloaryl substituents (demonstrated in Tables 6.5 and 6.6; **4.46g**, **5.1g**, **4.46f** and **5.1f**).



Scheme 6.1. Possible oxidation of the hydroxyl-functional group resulting in the quinone species.

Not being able to completely dissolve the sample could result in the calculation of incorrect concentrations of the prepared samples with inaccurate results being expected. In addition, slow precipitation of the compounds could also result in the results being less reliable.

Overall, it should be noted that due to rather poor results obtained from the admittedly limited bio-testing performed it is currently not possible to utilize these results for a reasonable SAR analysis. Further evaluations will therefore need to be planned to enable a better SAR evaluation on the THIQ compounds synthesized thus far (see Future work section).

Chapter 7

Future work

The purpose of this study was aimed toward generating sets of small compounds, to then test their ability to bind with ER, and for some of these new compounds to potentially bind with a greater affinity to the ER β subtype. Three small libraries were generated (i) where the THIQ skeleton contained the trifluoromethylsulfonyl substituent as discussed in Chapter 3, (ii) in which the THIQ skeleton contained a number of variations of urea groups as elaborated upon in Chapter 4, and (iii) a lactam skeleton, in addition to the THIQ skeleton, with a number of aryl substituents as discussed in Chapter 5 (all general scaffolds depicted in Figure 7.1).

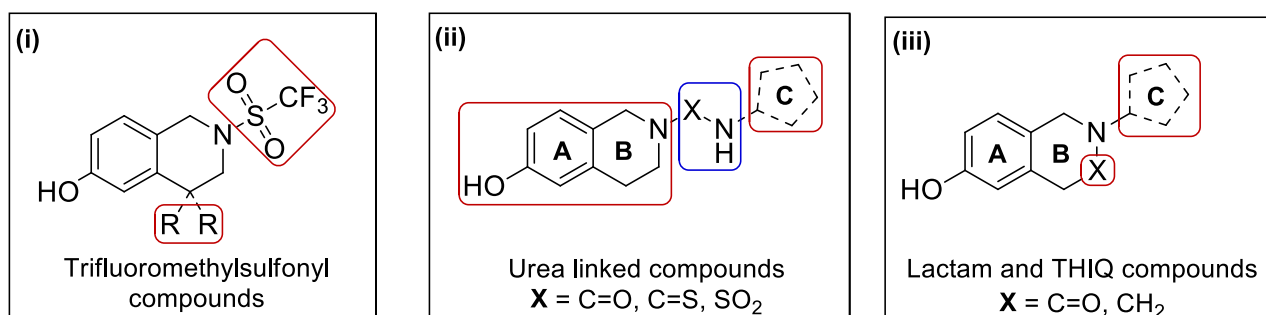


Figure 7.1. General scaffolds upon which the varied sets of compounds synthesized in this project were designed.

Once the compounds were successfully synthesised, based preliminary docking studies and previously published work,⁴⁰ the use of virtual screening was employed to investigate computationally the potential binding and selectivity of the compounds generated (Compound structures shown in Table 6.1 – 6.6 for libraries 1 – 3 (in Chapter 6). The results obtained from the virtual screening indicated overall good to reasonable ligand binding efficiency scores when compared with estradiol as discussed in Chapter 6, although disappointingly little difference was found in terms of the potential to bind the ER β subtype in preference to the α form. Finally, results obtained from the whole cell evaluation of these compounds in a number of bioassays were unfortunately inauspicious. The design of the compounds in libraries 1 – 3 were targeted to mimic the phenolic portion as well as the cyclopentanol portion of the estradiol structure, resulting in the requirement that for our final compounds the arylmethyl ether needed to be demethylated to expose the phenolic

functional group shown by other groups to be required for a significant portion of the binding affinity. In the biological assays the evaluation of the compounds turned out to be problematic with many of them not showing good activity. Compounding this matter was that a significant number of compounds demonstrated poor solubility in the media utilized for the bioactivity testing frequently resulting in time-dependant sedimentation and resulting in opaque solutions which posed problems during the actual biological evaluation. In addition, these problems often increased with the compounds in which the arylmethyl ether had been converted into the phenol group.

It was frequently found that after demethylation a number of the compounds showed sensitivity toward environmental conditions and decomposed easily. This resulted in NMR spectra initially being good followed by gradual degradation of the samples was observed (for some compounds this degradation was already evident during purification by column chromatography or during NMR spectroscopy experiments. These significant problems need to be corrected or prevented by putting a number of strategies in place as will be discussed in some of the suggestions in this final chapter of the thesis.

7.1 Addressing solubility problems

Since a number of problems were discovered once the methoxy-compounds were demethylated, it would be interesting to evaluate the phenolic compounds biochemical interactions while maintaining the methoxy functional group. Despite the positive results obtained from computational docking studies, the compounds behaved poorly in aqueous media when tested. Thus, the methoxy-masked phenoxy groups could be evaluated by determining the inhibitory concentration and efficient concentration testing. The presence of the methoxy functional group would improve stability and prevent decomposition. However, it is expected that the loss of the phenoxy group would result in reduced interactions with amino acids Glu and His in the ER active site.⁴⁰ Another possibility would be to replace the phenoxy group with a nitrogen-based functional group such as an aniline NH₂ or NHMe so as to maintain the ability to hydrogen bond with the amino acids present in the binding site.

7.2 Maintaining solubility while retaining the phenoxy functional group – a possible pro-drug strategy

As seen from the design of most SERM's, antiestrogens or estrogens, and supporting reports by Katzenellenbogen,⁶⁰ Anstead,⁵² Komm,³¹ Dowers⁷⁰ and co-workers, the phenol

functional group is a paramount structural feature. With that mentioned, the incorporation of cleavable protecting groups such as the sulfonate group **a**, as shown in Figure 7.2, could be considered.¹⁹⁰ This type of functional group could easily undergo enzymatic hydrolysis, revealing the intended hydroxy group. The unmasked hydroxyl group would then be free for hydrogen bond interactions within the active binding site without generating solubility problems.

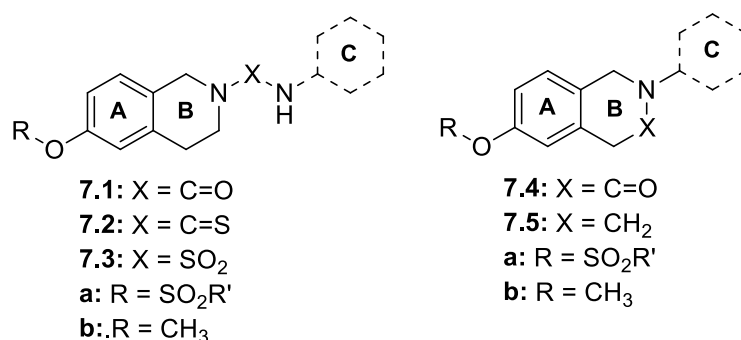
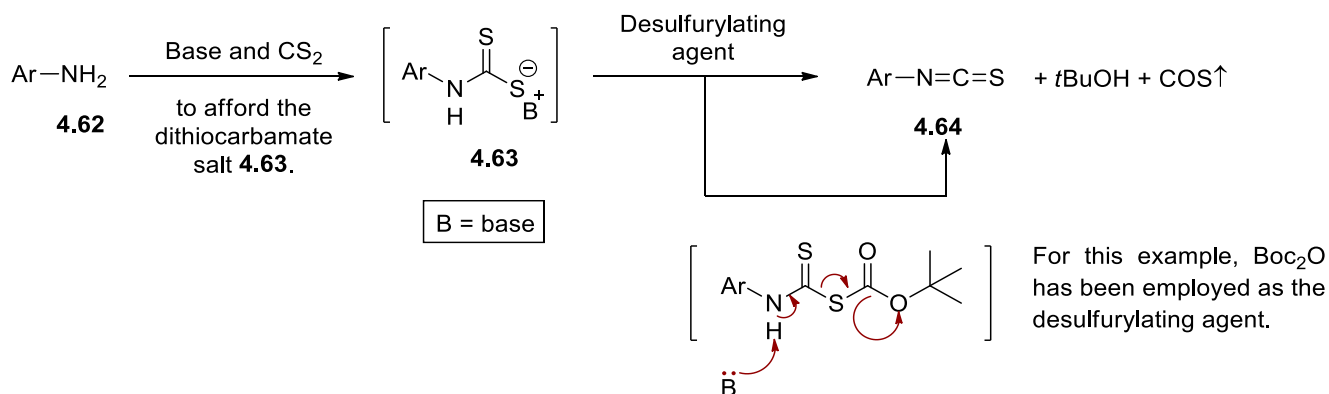


Figure 7.2. Minor modifications to the compounds from libraries 2 and 3.

7.3 Modification to the synthesis of the thiourea linked compounds 4.66

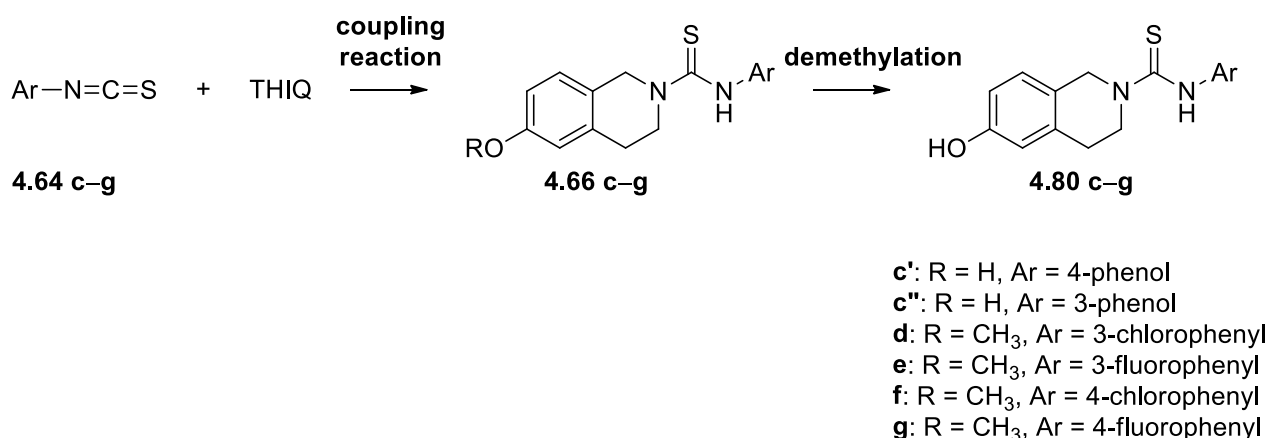
The synthesis of compounds **4.66** were described in section 4.4.3.1 are re-illustrated in Scheme 7.1.



Scheme 7.1. Description of the protocol used in the preparation of the isothiocyanates **4.64**.

The isothiocyanates (**4.64**) were generated by synthesizing the dithiocarbamate salts followed by desulfurization; however, it was found that when using the halogenated anilines (**4.62**) the results were not reproducible when repeated. An interesting protocol recently described recently by Mandapati and co-workers¹⁹¹ describes the use of copper as a desulfurization agent for halogenated anilines and provides good yields in the examples investigated (up to 80%). Improved yield for the isothiocyanate intermediates **4.64** would

provide enough material for optimization of the sequential reactions. Nonetheless, the demethylation of compounds **4.66** resulted in the complete decomposition of the final compound **4.80**. Methods to decrease the harsh nature of the demethylating procedures applied (resulting in the decomposition issues) could be overcome by use of the demethylated THIQ substrate, which proved to be successful in the synthesis of compounds **4.66c'** and **4.66c''**. This would of course require reaction conditions that allowed for chemoselectivity of the THIQ amine over the competing phenol group as shown in Scheme 7.2.



Scheme 7.2. Illustration of the thiourea groups discussed above.

7.4 Boron-containing phenol-fused heterocycles to potentially mimic the tetrahydroisoquinoline scaffold

Apart from our current approach in generating a scaffold able to selectively mediate estrogenic responses, the introduction of a heteroatom, such as boron presents numerous auspicious avenues in finding a suitable scaffold. Use of the element boron has rarely been observed in biological systems but with passing of the 20th century a plethora of research has contributed to boron's coalescence within biologically active compounds.^{192,193} Despite the few mentioned, an immense amount of research reported by Endo *et al.*,^{108,194-197} has described boronic esters/clusters being employed as potential selective estrogen receptor modulators. In addition, the use of computational screening of the carboborane compounds listed below in Figure 7.3, does indicate their potential as estrogenic mediators.

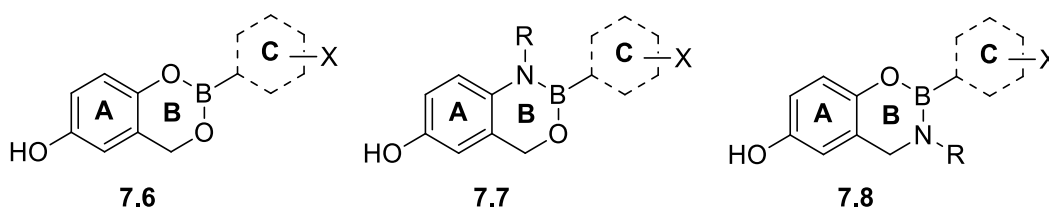
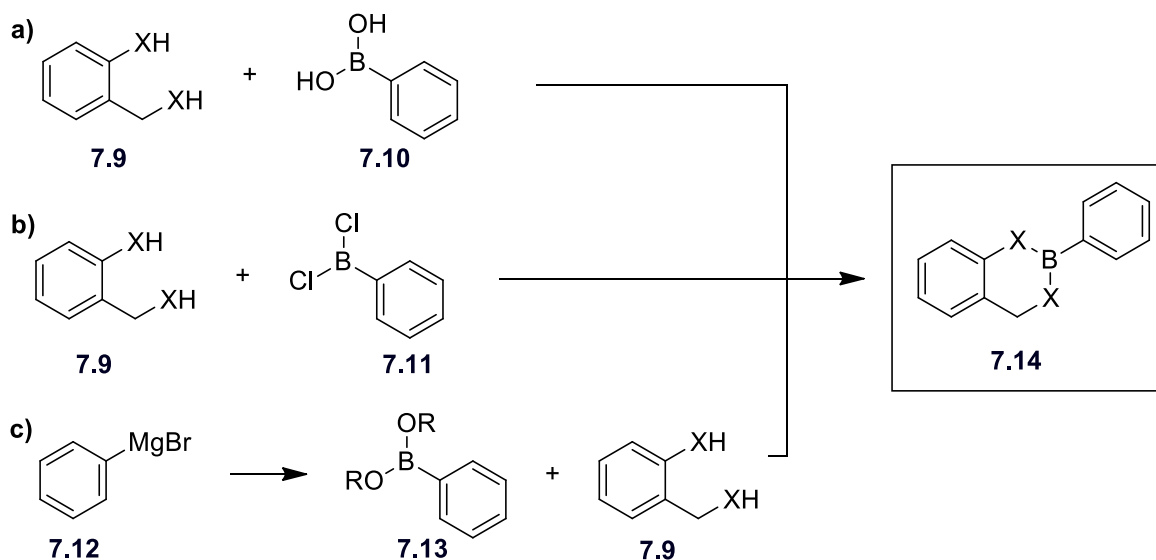


Figure 7.3. Examples of possible major modifications to the THIQ skeleton.

The general scaffold structure below entails a number of viable routes to easily generate compounds containing the organoborane skeleton **7.14**. Method a) includes dehydration of the boronic acid, method b) includes displacement of the chlorine atoms, and lastly, method c) where the boronic ester would be generated from the Grignard reagent **7.12**, followed by reaction with the diheteroatom-containing molecules **7.9** under reflux to produce analogues of compound **7.14** demonstrated in Scheme 7.3.



Where X = O, NH or NR

Scheme 7.3. Synthetic routes to obtain the general skeleton of compound **7.14**.

Work on these scaffolds with the inclusion of the phenoxy-group by compounds such as compounds **7.6 – 7.8** shown in Figure 7.3 could lead to interesting biological results.

7.5 Concluding remarks

As reported throughout this dissertation, the THIQ – core compounds have displayed very good pharmacological activity and quite challenging in to work with in the laboratory. We hope to address these challenges by application of methodologies mentioned above. In

addition, the introduction of boron – based compounds could further expand our library and therapeutic targets.

Chapter 8

Experimental and Analytical results

8.1 Glassware preparation

For reactions performed under anhydrous conditions, all glassware and stirrer bars were prepared by rinsing with acetone followed with overnight drying in a 90°C oven. Once removed, the glassware was placed under vacuum conditions for 10 minutes, followed by back filling of the reaction vessel with nitrogen unless stated otherwise in the experimental section.

8.2 Reagent preparation

Syntheses were carried out with commercially available chemicals purchased from Sigma Aldrich or Merck. Compounds that were impure were purified using methods from the purification of laboratory chemicals book.¹⁹⁸ The solvents used for chromatography and experiments were redistilled prior to use. Generally used reaction solvents such as tetrahydrofuran, toluene, diethyl ether, methanol and ethanol were analytical grade and dried under standard anhydrous conditions prior to use.¹⁹⁹ Drying agents for example sieves, were placed in a 300°C oven for 48 hours cooled to 100°C followed by storing under nitrogen, prior to its use.

8.3 Temperature control

Reactions being heated was monitored by use of a thermal couple attached to the heating plate in addition to the use of a thermometer as a reference. Cool reactions were monitored using a -100 °C alcohol thermometer. Low temperatures of -78 °C were maintained by use of a mixture of carbon dioxide/acetone. Temperatures of 0 to -5 °C were maintained with a mixture of a saturated brine solution/ice.

8.4 Chromatography

All crude residues/compounds were purified with column chromatography using silica gel 60 (70 – 230 mesh used for gravity column chromatography and 230 – 400 mesh used for flash chromatography unless stated otherwise) purchased from Merck. Silica sensitive

compounds were purified using Aluminium oxide 90 active neutral 0.063 – 0.200 mm (70 – 230 mesh ASTM) purchased Merck. Thin layer chromatography (TLC) analysis was carried out on aluminium plates precoated with silica gel 60 F₂₅₄ (0.2 mm). Visualization of TLC spots were observed under a UV visible light at 254 nm or using agents such as potassium permanganate, ninhydrin, *p*-anisaldehyde, cerium ammonium molybdate, 2,4-dinitrophenyl hydrazine solution and silica coated iodine.

8.5 Characterization

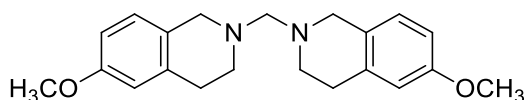
All nuclear magnetic resonance (NMR) spectroscopic data was obtained using Varian Gemini-300 (¹H NMR at 300 MHz and ¹³C NMR at 75 MHz) as well as a Varian VXR-400 spectrometer (¹H NMR at 400 MHz and ¹³C NMR at 101 MHz). Chemical shifts (δ) are denoted in units (ppm) relative to the respective deuterated solvents, where ¹H NMR spectral signals at: δ 7.26 ppm for CDCl₃, δ 2.50 ppm for DMSO-*d*₆ and δ 3.30 ppm for CD₃OD. ¹³C NMR spectral signals were observed at: δ 77.16 ppm for CDCl₃, δ 39.52 ppm for DMSO-*d*₆ and δ 49.00 ppm for CD₃OD. The following abbreviations are used to indicate the signal multiplicity's and characteristics: b (broad), s (singlet), d (doublet), dd (double of doublet), t (triplet), q (quartet), and m (multiplet). In the following ArC is a representation of quaternary carbons and ArCH refers to the aryl protons.

Positive electron spray impact (ESI+) high resolution mass spectrometry (HRMS) were recorded on a Unicam Automass mass spectrometer in conjunction with a gas chromatograph. Infrared spectra were obtained using a Nexus Thermo-Nicolet FT-IR instrument using thin film (NaCl plate) or using the ATR attachment or using an ATi Perkin Elmer Spectrum RX1 FTIR spectrometer using thin film (NaCl). Melting points were obtained using a Gallen lamp melting point apparatus and were uncorrected. However, not all compounds were submitted for HRMS which was generally employed for final compounds.

General experimental methods

8.6 Synthesis of 2-[(trifluoromethyl)sulfonyl]-1,2,3,4-tetrahydroisoquinolin-6-ol 3.34

8.6.1 General procedure for the synthesis of bis[6-methoxy-3,4-dihydroisoquinoline - 2(1*H*)-yl]methane 3.36

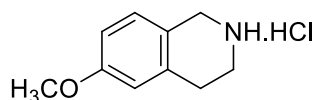


According to the general procedure described by Zhong and co-workers,¹¹⁹ a mixture of 2-(3-methoxyphenyl) ethylamine **3.35** (0.500 mL,

3.43 mmol), aqueous 1 N HCl solution (5.00 mL, 4.96 mmol) and 37% aqueous formaldehyde (1.00 mL, 13.0 mmol) were stirred at 60 °C for 4 h resulting in a yellow translucent solution. This solution was cooled to 0 °C after which a 50% aqueous NaOH solution (1.03 mL, 5.62 mmol) was added until the mixture was neutralized, forming a white sticky gum-like residue, which solidified with further stirring and was pulverized very carefully.

Aminal dimer **3.36** was obtained in quantitative (1.16 g) yield as a white clay powder; **mp** = 119 – 121 °C; R_f = 0.60 (60:40 EtOAc/Hexane). **¹H NMR** (400 MHz, CDCl₃): δ (ppm) 6.96 (d, J = 8.4 Hz, 2H, 2xArH), 6.76 – 6.61 (m, 4H, 4xArH), 3.78 (s, 6H, 2xOCH₃), 3.68 (s, 4H, 2xArCH₂N), 3.26 (s, 2H, CH₂-bridge), 2.90 – 2.86 (m, 8H, 2xCH₂CH₂). **¹³C NMR** (101 MHz, CDCl₃): δ (ppm) 29.73 (2xArCH₂), 49.36 (2XCH₂), 54.26 (2xArCH₂N), 55.60 (2xOCH₃), 81.05 (CH₂-bridge), 112.36 (2xArCH), 113.64 (2xArCH), 127.68 (2xArCH), 127.97 (2xArC), 136.34 (2xArC), 158.22 (2xArCOMe). The experimental spectroscopic information corresponded well with the reported literature spectroscopic information.¹¹⁹

8.6.2 General procedure for the synthesis of 6-methoxy-1,2,3,4-tetrahydroisoquinoline hydrochloride 3.37

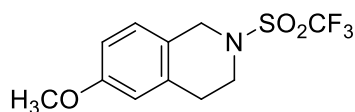


According to the general procedure described by Zhong and co-workers,¹¹⁹ the synthesis of 6-methoxy-1,2,3,4-tetrahydroisoquinoline hydrochloride was as follows. An aqueous 11 M HCl solution (0.360 mL, 3.84 mmol) was slowly added to a suspension of the aminal dimer **3.36** (590 mg, 1.74 mmol) in isopropyl alcohol (IPA) (10 mL) providing a yellow

translucent mixture. The resulting solution was stirred at RT for 18 h, after which MTBE (1.00 mL per mmol of dimer) was added. This was followed by additional stirring of 4 h and the resultant white solid was filtered, washed with IPA/MTBE (1:1) and air dried to yield the hydrochloride salt **3.37**.

Compound **3.37** was obtained in quantitative (348 mg) yield as a white amorphous powder; mp = 238 – 239 °C; R_f = 0.00 (100% EtOAc). **¹H NMR** (400 MHz, DMSO-*d*₆): δ (ppm) 9.47 (brs, 2H, NH), 7.13 (d, J = 8.4 Hz, 1H, ArH), 6.88 – 6.75 (m, 2H, 2xArH), 4.16 (s, 2H, ArCH₂N), 3.74 (s, 3H, OCH₃), 3.32 (t, J = 4.4 Hz, 2H, ArCH₂CH₂), 2.98 (t, J = 4.4 Hz, 2H, CH₂). **¹³C NMR** (101 MHz, DMSO-*d*₆): δ (ppm) 24.90 (ArCH₂), 40.28 (CH₂), 42.92 (OCH₃), 55.15 (ArCH₂N), 113.09 (ArCH), 113.11 (ArCH), 120.82 (ArCH), 127.88 (ArC), 133.39 (ArC), 158.36 (ArCOMe). The experimental spectroscopic information, corresponded well with the reported literature spectroscopic information.¹¹⁹

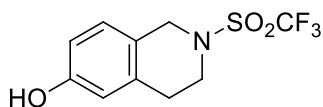
8.6.3 General procedure for the preparation of 6-methoxy-2-[(trifluoromethyl) sulfonyl] -1,2,3,4-tetrahydroisoquinoline **3.38**



According to the general procedure described by Brunsveld, L. *et al.*,⁴⁰ the hydrochloride salt **3.37** (200 mg, 1.00 mmol) was suspended in anhydrous CH₂Cl₂ (20 mL) and treated at -60 °C with Et₃N (0.560 mL, 4.00 mmol). Trifluoromethanesulfonyl anhydride (0.370 mL, 2.20 mmol) was slowly added, followed by stirring at -20 °C for 2 h, and additional stirring at RT for 3 h. Once complete, the reaction mixture was partitioned between an aqueous saturated NaHCO₃ solution and CH₂Cl₂ and extracted (25 mL x 3). The organic layers were separated, dried over MgSO₄, filtered and concentrated under reduced pressure affording a brown residue which was purified by flash chromatography (5:95 EtOAc/Hexane).

Compound **3.38** was obtained in 258 mg in 89% yield as a yellow/orange oil; R_f = 0.46 (30:70, EtOAc/Hexane). **¹H NMR** (300 MHz, CDCl₃): δ (ppm) 7.01 (d, J = 8.5 Hz, 1H, ArH), 6.80 (dd, J = 8.5, 2.6 Hz, 1H, ArH), 6.70 (d, J = 2.6 Hz, 1H, ArH), 4.61 (s, 2H, ArCH₂N), 3.88 – 3.65 (m, 5H, overlapping signals-OCH₃ and CH₂), 2.96 (t, J = 6.0 Hz, 2H, ArCH₂CH₂). **¹³C NMR** (75 MHz, CDCl₃, no C-F coupling was clearly visible): δ (ppm) 29.41 (ArCH₂CH₂), 44.59 (CH₂), 47.46 (ArCH₂N), 55.59 (OCH₃), 113.47 (ArCH), 114.02 (ArCH), 122.56 (ArCH), 123.07 (ArC), 134.16 (ArC), 158.99 (ArCOMe).

8.6.4 General procedure for the synthesis of 2-[(trifluoromethyl)sulfonyl]-1,2,3,4-tetrahydroisoquinolin-6-ol **3.34**

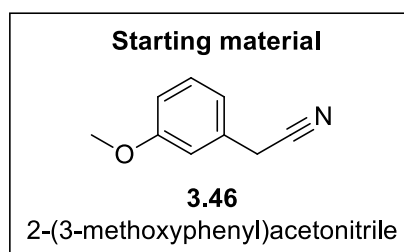


According to the general procedure described by McOmie and co-workers,¹²¹ a solution of the sulfonamide **3.38** (250 mg, 0.850 mmol) in anhydrous CH₂Cl₂ (0.90 mL) was added at -78 °C to a solution of 1 M boron tribromide (BBr₃) (0.730 mL, 7.75 mmol) in anhydrous CH₂Cl₂ (7.30 mL). The reaction mixture was stirred at RT overnight and then quenched with water (15 mL) at 0 °C hydrolysing excess BBr₃ and boron complexes, and finally extracted with CH₂Cl₂ (25 mL x 3). The organic layers were combined, dried over MgSO₄, filtered and concentrated under reduced pressure yielding compound **3.34** in 80 – 95% yield as an orange-brown oil; R_f = 0.20 (100% EtOAc). **¹H NMR** (400 MHz, CDCl₃): δ (ppm) 7.02 – 6.84 (m, 1H, ArH), 6.79 – 6.56 (m, 2H, 2xArH), 6.33 (s, 1H, ArH), 4.57 (brs, 1H, OH), 3.72 (s, 2H, ArCH₂N), 3.00 (s, 2H, ArCH₂CH₂), 2.95 – 2.86 (m, 2H, CH₂). **¹³C NMR** (101 MHz, CDCl₃, C-F coupling was not clearly visible): δ (ppm) 29.15 (ArCH₂), 44.55 (CH₂CH₂N), 47.47 (CH₂), 114.67 (ArCH), 115.66 (ArCH), 122.79 (ArCH), 127.48 (ArC), 134.34 (ArC), 155.30 (ArCOH).

8.7 Synthesis of the C4 analogues of

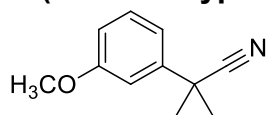
2-[(trifluoromethyl)sulfonyl]-1,2,3,4-tetrahydro-isoquinolin-6-ol analogues **3.49**

8.7.1 General alkylation procedure for 2-(3-methoxyphenyl)acetonitrile **3.47a – d**



According to the general procedure described by Melvin and co-workers,¹²² a solution of 2-(3-methoxyphenyl)acetonitrile **3.46** (263 mg, 0.250 mL, 1.79 mmol) in anhydrous DMF (5.0 mL) was added to a cooled (3 °C) 60% suspension of NaH in mineral oil (180 mg, 7.50 mmol) in anhydrous DMF (5.0 mL). The resulting mixture was stirred for 30 min providing a red coloured mixture. The haloalkanes, *viz.*, 1,2-dibromoethane (0.230 mL, 2.68 mmol), iodomethane (1.33 mL, 21.5 mmol), 1,3-bromoethane (1.33 mL, 21.5 mmol) and 1,3-dibromopropane (0.230 mL, 2.68 mmol) were added, followed by stirring at RT for 16 h. Once complete, the mixture was treated with an aqueous saturated NH₄Cl solution (20 mL) and further extracted with EtOAc (20 mL x 3). The organic layers were dried with MgSO₄, filtered and concentrated under reduced pressure providing a residue. Purification of the residue was performed with flash chromatography (5:95 EtOAc/Hexane), yielding products **3.47a – d** as oils, characterization of which are described below:

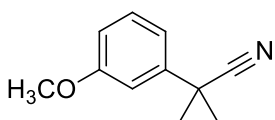
1-(3-Methoxyphenyl)cyclopropane carbonitrile 3.47a was obtained in 86% (273 mg)



yield from 263 mg of starting material **3.46**. Yellow oil; $R_f = 0.30$ (20:80 EtOAc/Hexane). $^1\text{H NMR}$ (400 MHz, CDCl_3): δ (ppm) 7.47 (d, $J = 7.8$ Hz, 1H, ArH), 7.07 – 7.00 (m, 3H, ArH), 4.01 (s, 3H, OCH_3), 1.93 – 1.88 (m, 2H, CH_2), 1.62

– 1.57 (m, 2H, CH_2). $^{13}\text{C NMR}$ (75 MHz, CDCl_3): δ (ppm) 13.97 (C), 18.33 ($2\times\text{CH}_2$ -spiro cyclopropyl), 55.45 (OCH_3), 112.02 (ArCH), 113.00 (ArCH), 117.96 (CN), 122.65 (ArCH), 130.09 (ArCH), 137.73 (ArC), 160.11 (ArCOMe). The experimental spectroscopic information, was similar to the literature spectroscopic information reported by O’Niel and co-workers.²⁰⁰

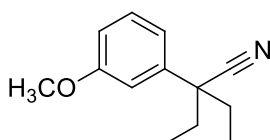
2-(3-Methoxyphenyl)-2-methylpropane nitrile 3.47b was obtained in quantitative (125



mg) yield from 263 mg of starting material **3.46**. Colourless oil; $R_f = 0.60$ (50:50 EtOAc/Hexane). $^1\text{H NMR}$ (300 MHz, CDCl_3): δ (ppm) 7.33

– 7.17 (m, 1H, ArH), 7.06 – 6.92 (m, 2H, $2\times\text{ArH}$), 6.80 – 6.78 (m, 1H, ArH), 3.78 (s, 3H, OCH_3), 1.67 (s, 6H, $2\times\text{CH}_3$). $^{13}\text{C NMR}$ (75 MHz, CDCl_3): δ (ppm) 29.26 (C), 37.31 ($2\times\text{CH}_3$), 55.47 (OCH_3), 111.63 (ArCH), 112.86 (ArCH), 117.46 (ArCH), 126.61 (CN), 130.12 (ArCH), 143.18 (ArC), 160.06 (ArCOMe). The experimental spectroscopic information, was similar to the literature spectroscopic information reported by Zacheis and co-workers.¹⁴⁶

2-Ethyl-2-(3-methoxyphenyl)butane nitrile 3.47c was obtained in 77% (212 mg) yield

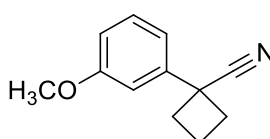


from 263 mg of starting material **3.46**. Translucent oil; $R_f = 0.57$ (20:80

CH_2Cl_2 /Hexane). $^1\text{H NMR}$ (300 MHz, CDCl_3): δ (ppm) 7.29 – 7.22 (m, 1H, ArH), 6.95 – 6.78 (m, 3H, $3\times\text{ArH}$), 3.79 (s, 3H, OCH_3), 2.03 – 1.82

(m, 4H, $2\times\text{CH}_2$), 0.880 (t, $J = 7.50$ Hz, 6H, $2\times\text{CH}_3$). $^{13}\text{C NMR}$ (75 MHz, CDCl_3 , it is important to note one ArC not visible): δ (ppm) 10.02 (C), 34.14 ($2\times\text{CH}_3$), 50.18 ($2\times\text{CH}_2$), 55.59 (OCH_3), 112.84 (ArCH), 118.74 (ArCH), 122.58 (CN), 130.11 (ArCH), 140.06 (ArCH), 160.20 (ArCOMe).

1-(3-Methoxyphenyl)cyclobutene carbonitrile 3.47d was obtained in 81% (656 mg) yield



from 263 mg of starting material **3.46**. Yellow oil; $R_f = 0.52$ (100%

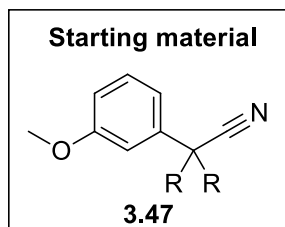
Hexane). The crude compound was used in generating the ^1H - and

^{13}C - NMR spectra. $^1\text{H NMR}$ (300 MHz, CDCl_3): δ (ppm) 7.23 – 7.16

(m, 1H, ArH), 6.93 – 6.80 (m, 2H, $2\times\text{ArH}$), 6.78 – 6.69 (m, 1H, ArH), 3.73 (s, 3H, OCH_3), 2.77 – 2.61 (m, 2H, CH_2), 2.58 – 2.40 (m, 2H, CH_2), 2.30 – 2.07 (m, 2H, CH_2). $^{13}\text{C NMR}$ (75

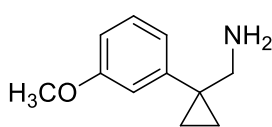
MHz, CDCl₃): δ (ppm) 17.16 (C), 29.81 (CH₂), 34.67 (CH₂), 40.26 (CH₂), 55.38 (OCH₃), 111.81 (ArCH), 113.06 (ArCH), 117.86 (ArCH), 124.43 (CN), 130.10 (ArCH), 141.44 (ArC), 160.10 (ArCOMe).

8.7.2 General procedure for the reduction of nitriles **3.47a – d**



The general reduction procedure described by Nystrom, Davis and co-workers,^{123,124} was as follows. Lithium aluminium hydride (LiAlH₄) (41.0 mg, 1.07 mmol) was suspended in anhydrous THF (30 mL) and cooled to -3 °C in an ice bath. Aluminium chloride (AlCl₃) (140 mg, 1.07 mmol) was then carefully added in small portions while maintaining the temperature at -3 °C. The resulting hydride (AlH₂Cl) suspension was stirred at RT for 30 min, to which the nitrile derivatives **3.47a – d** (0.713 mmol) in THF (4.0 mL) were added. The reaction mixture was stirred under reflux for 5 h, cooled to RT and carefully treated with water until no further effervescence occurred. The white solid (lithium aluminate) was separated by vacuum filtration and the filtrate extracted with EtOAc (20 mL x 2). The organic layers were combined, dried over MgSO₄, filtered and concentrated under reduced pressure to give the corresponding amines **3.50a – d**, as oils with no further purification required. The amine characteristics are described below:

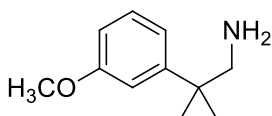
1-[(3-Methoxyphenyl)cyclopropyl]methanamine 3.50a was obtained in 93% (161 mg)



yield from ~123 mg of starting material **3.47a**. Yellow oil. ¹H NMR (300MHz, CDCl₃, no amine signal was visible): δ (ppm) 7.29 – 7.21 (m, 1H, ArH), 6.98 – 6.88 (m, 2H, ArH), 6.78 (m, *J* = 8.2, 2.6, 1.0 Hz, 1H, ArH), 3.82 (s, 3H, OCH₃), 2.79 (s, 2H, CCH₂NH₂), 0.88 – 0.82 (m, 2H, CH₂), 0.78 – 0.72 (m, 2H, CH₂).

¹³C NMR (75 MHz, CDCl₃): δ (ppm) 11.95 (2xCH₂), 29.67 (C), 52.22 (CCH₂N), 55.50 (OCH₃), 111.84 (ArCH), 115.48 (ArCH), 121.93 (ArCH), 129.62 (ArCH), 145.45 (ArC), 159.89 (ArCOMe).

2-(3-Methoxyphenyl)-2-methylpropan-1-amine 3.50b was obtained in 81% (205 mg)

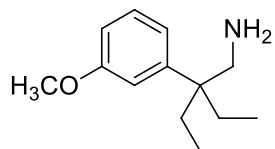


yield from ~125 mg of starting material **3.47b**. Yellow oil. ¹H NMR (300MHz, CDCl₃, no amine signal was visible): δ (ppm) 7.33 – 7.17 (m, 1H, ArH), 6.98 – 6.75 (m, 3H, 3xArH), 3.81 (s, 3H, OCH₃), 2.79 (s, 2H, CH₂), 1.36 – 1.23 (s, 6H, 2xCH₃).

¹³C NMR (75 MHz, CDCl₃, not all quaternary carbon signals were visible): δ (ppm) 26.45 (2xCH₃), 54.95 (CH₂), 55.24 (OCH₃), 110.43 (ArCH), 113.07 (ArCH), 118.77 (ArCH), 129.33 (ArCH), 149.21 (ArC), 159.69 (ArCOMe). The experimental spectroscopic

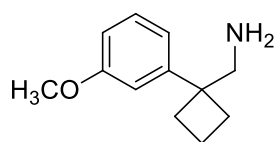
information, was similar to the literature spectroscopic information reported by Johnson and co-workers.²⁰¹

2-[Ethyl-2-(3-methoxyphenyl)]butan-1-amine 3.50c was obtained in quantitative (140



mg) yield from ~145 mg of starting material **3.47c**. Yellow oil. **¹H NMR** (300 MHz, CDCl₃): δ (ppm) 7.29 – 7.23 (m, 1H, ArH), 6.93 – 6.73 (m, 3H, 3xArH), 3.82 (s, 3H, OCH₃), 2.86 (s, 2H, CH₂), 1.70 (q, *J* = 7.4 Hz, 4H, 2xCH₂), 0.95 (brs, 2H, NH₂), 0.76 – 0.71 (m, 6H, 2xCH₃). **¹³C NMR** (75 MHz, CDCl₃): δ (ppm) 8.04 (2xCH₃), 26.53 (2xCH₂), 45.93 (C), 48.32 (CH₂), 55.26 (OCH₃), 110.18 (ArCH), 113.99 (ArCH), 119.62 (ArCH), 129.17 (ArCH), 147.57 (ArC), 159.73 (ArCOMe).

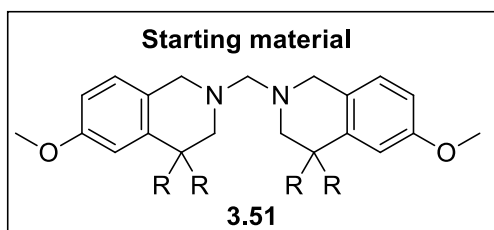
1-[(3-Methoxyphenyl)cyclobutyl]methanamine 3.50d was obtained in 54% (365 mg)



yield from ~133 mg of starting material **3.47d**. Yellow translucent oil. **¹H NMR** (300 MHz, CDCl₃, no amine signal was visible): δ (ppm) 7.20 – 7.15 (m, 1H, ArH), 6.71 – 6.53 (m, 3H, 3xArH), 3.78 – 3.69 (s, 3H, OCH₃), 2.85 (s, 2H, CH₂), 2.34 – 2.16 (m, 2H, CH₂), 2.13 – 1.91 (m, 4H, 2xCH₂). **¹³C NMR** (75 MHz, CDCl₃, not all quaternary carbon signals were visible): δ (ppm) 15.87 (CH₂), 30.52 (CH₂), 52.68 (CH₂), 55.26 (OCH₃), 110.68 (ArCH), 112.19 (ArCH), 118.50 (ArCH), 129.20 (ArCH), 144.00 (ArC), 146.00 (ArC), 159.59 (ArCOMe).

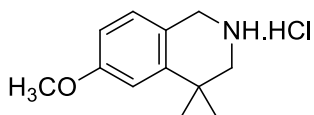
8.7.3 General procedure for the synthesis of 3.51a – d

The general procedure described by Zhong and co-workers,¹¹⁹ was implemented for the synthesis of the amina dimers **3.50a – d**. A solution of 37% aqueous formaldehyde (1.00 mL, 13.0 mmol) was added to a solution of **3.50a – d** (0.500 mL, 3.31 mmol) in 1 N aqueous HCl solution (5.00 mL, 4.96 mmol). The mixture was heated and stirred at 60 °C for 4 h. This was followed by the mixture being cooled to 0 °C and neutralized by the slow addition of a 50% aqueous NaOH solution (1.03 mL, 5.62 mmol). The resulting heavy suspension was extracted using EtOAc (20 mL x 2) providing compounds **3.51a – d**, which were directly used as is in the subsequent reactions with no further purification.

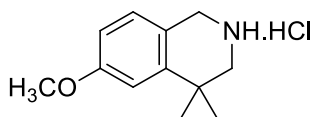
8.7.4 General procedure for the synthesis of THIQ hydrochloride salts **3.52a – d**

The general procedure described by Zhong and co-workers,¹¹⁹ was implemented for the synthesis of **3.52a – d**. Amino dimers **3.51a – d** (2.00 mmol) were suspended in IPA (4.20 mL, 5.50 mmol), to which a concentrated aqueous 11 M HCl solution (0.420 mL,

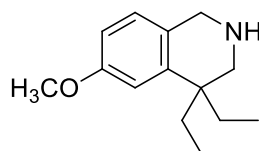
4.60 mmol) was slowly added with a slight exotherm being noted. Addition of the aqueous HCl solution resulted in a colour change, after which a solid precipitated. The resulting suspension was stirred at RT for 18 h. MTBE (1.00 mL per mmol of dimer) was added and the resulting mixture was left to stir for an additional 4 h. The solid was collected by vacuum filtration providing products **3.52a – d** which were washed with a 1:1 ratio of IPA/MTBE and air dried to yield amorphous powders that are described below:

6'-Methoxy-2',3'-dihydro-1'H-spiro(cyclopropane-1,4'-isoquinoline)

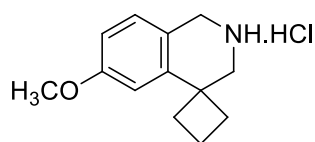
hydrochloride 3.52a was obtained in quantitative (170 mg) yield from 159 mg of starting material **3.51a**. White solid; $R_f = 0.00$ (100% EtOAc). $^1\text{H NMR}$ (300 MHz, DMSO- d_6): δ (ppm) 9.78 (brs, 2H, NH₂), 7.12 (d, $J = 8.5$ Hz, 1H, ArH), 6.78 (dd, $J = 8.5, 2.5$ Hz, 1H, ArH), 6.34 (d, $J = 2.5$ Hz, 1H, ArH), 4.25 (s, 2H, ArCH₂N), 3.72 (s, 3H, OCH₃), 3.17 (s, 2H, CH₂), 1.11 – 1.07 (m, 4H, CH₂-CH₂). $^{13}\text{C NMR}$ (75 MHz, DMSO- d_6): δ (ppm) 16.49 (CH₂), 16.95 (CH₂), 44.35 (C), 48.82 (OCH₃), 55.28 (ArCH₂N), 106.89 (ArCH), 112.13 (ArCH), 121.25 (ArCH), 127.77 (ArC), 138.91 (ArC), 159.27 (ArCOMe). **HRMS ESI⁺**: m/z [M-36.4609]⁺ calcd for C₁₂H₁₅NO, 190.1232; found, 190.1243 (5.80 ppm).

6-Methoxy-4,4-dimethyl-1,2,3,4-tetrahydroisoquinoline hydrochloride 3.52b was

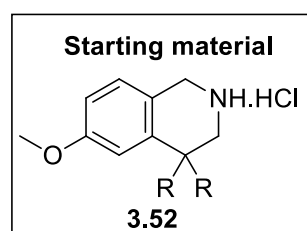
obtained in quantitative (457 mg) yield from 426 mg of starting material **3.51b**. White solid; $R_f = 0.00$ (100% EtOAc). $^1\text{H NMR}$ (300 MHz, DMSO- d_6): δ (ppm) 9.63 (brs, 2H, NH₂), 7.12 (d, $J = 8.6$ Hz, 1H, ArH), 6.97 (d, $J = 2.5$ Hz, 1H, ArH), 6.83 (dd, $J = 8.6, 2.5$ Hz, 1H, ArH), 4.15 (s, 2H, ArCH₂N), 3.77 (s, 3H, OCH₃), 3.14 (s, 2H, CH₂), 1.35 (s, 6H, 2xCH₃). $^{13}\text{C NMR}$ (75 MHz, DMSO- d_6): δ (ppm) 25.60 (2xCH₃), 28.82 (C), 32.92 (CH₂), 44.07 (OCH₃), 55.32 (ArCH₂N), 111.26 (ArCH), 112.81 (ArCH), 119.47 (ArCH), 127.95 (ArC), 142.68 (ArC), 159.06 (ArCOMe). **HRMS ESI⁺**: m/z [M-36.4609]⁺ calcd for C₁₂H₁₈NO, 192.1388; found, 192.1388 (0.00 ppm).

4,4-Diethyl-6-methoxy-1,2,3,4-tetrahydroisoquinoline hydrochloride 3.52c was

obtained in quantitative (400 mg) yield from 377 mg of starting material **3.51c**. Brown powder; $R_f = 0.00$ (100% EtOAc). $^1\text{H NMR}$ (300 MHz, DMSO- d_6): δ (ppm) 9.62 (brs, 2H, NH_2), 7.13 (d, $J = 7.5$ Hz, 1H, ArH), 6.84 – 6.80 (m, 2H, 2xArH), 4.12 (s, 2H, ArCH_2N), 3.75 (s, 3H, OCH_3), 3.13 (s, 2H, CH_2), 1.89 – 1.84 (m, 2H, CH_2), 1.68 – 1.60 (m, 2H, CH_2), 0.74 (t, $J = 7.4$ Hz, 6H, 2x CH_3). $^{13}\text{C NMR}$ (75 MHz, DMSO- d_6): δ (ppm) 8.26 (2x CH_3), 25.49 (CH_2), 30.35 (C), 43.68 (CH_2), 45.34 (OCH_3), 55.19 (ArCH_2N), 111.80 (ArCH), 112.46 (ArCH), 120.74 (ArC), 127.98 (ArCH), 140.15 (ArC), 158.67 (ArCOMe). **HRMS ESI⁺**: m/z [$\text{M}-36.4609$]⁺ calcd for $\text{C}_{14}\text{H}_{21}\text{NO}$, 220.1701; found, 220.1693 (3.60 ppm).

6'-Methoxy-2',3'-dihydro-1'H-spiro(cyclobutane-1,4'-isoquinoline)hydrochloride

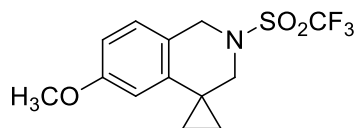
3.52d was obtained in quantitative (170 mg) yield from 159 mg of starting material **3.51d**. Yellow oil; $R_f = 0.00$ (100% EtOAc). $^1\text{H NMR}$ (300 MHz, DMSO- d_6): δ (ppm) 9.73 (brs, 2H, NH_2), 7.21 – 7.20 (m, 2H, 2xArH), 6.85 (dd, $J = 8.4, 2.5$ Hz, 1H, ArH), 4.11 (s, 2H, CH_2), 3.80 (s, 3H, OCH_3), 3.43 (brs, 2H, CH_2), 2.40 – 2.36 (m, 2H, CH_2), 2.19 – 2.16 (m, 4H, 2x CH_2). $^{13}\text{C NMR}$ (75 MHz, DMSO- d_6): δ (ppm) 14.43 (CH_2), 25.49 (CH_2), 33.29 (CH_2), 43.6 (C), 49.41 (CH_2), 55.26 (OCH_3), 61.99 (ArCH_2N), 111.10 (ArCH), 112.91 (ArCH), 119.91 (ArCH), 127.59 (ArC), 141.31 (ArC), 159.16 (ArCOMe). **HRMS ESI⁺**: m/z [$\text{M}-36.4609$]⁺ calcd for $\text{C}_{13}\text{H}_{17}\text{NO}$, 204.1344; found, 204.1384 (4.89 ppm).

8.7.5 General procedure for the synthesis of trifluorosulfonamides 3.53a – d

The general procedure described by Brunsveld⁴⁰ Bailey¹²⁰ and co-workers was implemented for sulfonation of **3.52a – d**. A mixture of the analogues **3.52a – d** (~0.878 mmol) and Et_3N (0.490 mL, 3.50 mmol) in anhydrous CH_2Cl_2 (20 mL) were stirred at RT for 30 min to ensure the complete solubilizing of the suspension. The resulting mixture was cooled to -40°C , to which trifluoromethanesulfonic anhydride (0.160 mL, 0.966 mmol) was slowly added. The mixture was stirred at -20°C for an additional 2 h, followed by stirring at RT for 3 h with progress being monitored by TLC. After consumption of starting material, the reaction mixture was extracted with an aqueous 5 N HCl solution followed by CH_2Cl_2 (25 mL x 3). The organic layers were combined and further washed with an aqueous saturated NaHCO_3 solution, followed by a final washing with a saturated brine solution. The organic layers were combined, dried with MgSO_4 and concentrated under reduced pressure.

The residue was purified with flash chromatography (5:95 EtOAc/Hexane), yielding products as oils, which crystalized upon freezing with moderate yields. The characteristics of compounds **3.53a – d** is described below:

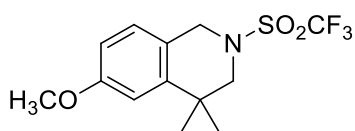
6'-Methoxy-2'-[(trifluoromethyl)sulfonyl]-2',3'-dihydro-1'H-spirocyclopropane-1,



4'-isoquinoline 3.53a was obtained in 69% (195 mg) yield from 167 mg of starting material **3.52a**. Brown oil; $R_f = 0.62$ (20:80 EtOAc/Hexane). $^1\text{H NMR}$ (400 MHz, CDCl_3): δ (ppm) 7.00 (d, $J = 8.5$ Hz, 1H, ArH), 6.74 (dd, $J = 8.5, 2.5$ Hz, 1H, ArH), 6.30 (d, $J = 2.5$ Hz, 1H, ArH), 4.70

(brs, 2H, ArCH_2N), 3.76 (s, 3H, OCH_3), 3.51 (brs, 2H, CH_2), 1.09 – 1.04 (m, 4H, $2\times\text{CH}_2$). $^{13}\text{C NMR}$ (101 MHz, CDCl_3 , C–F coupling was not clearly visible): δ (ppm) 20.18 ($\text{CH}_2\text{--CH}_2$), 48.70 (CH_2), 53.53 (CH_2), 55.77 (OCH_3), 108.22 (ArCH), 111.97 (ArCH), 123.85 (ArCH), 127.28 (ArC), 139.79 (ArC), 159.77 (ArCOMe). **HRMS ESI⁺**: m/z $[\text{M}+\text{H}]^+$ calcd for $\text{C}_{13}\text{H}_{14}\text{F}_3\text{NO}_3\text{S}$, 322.0680; found, 290.2690 (101.54 ppm). The HRMS further confirmed the instability and decomposition of compound **5.53a** and was not used in any further reactions.

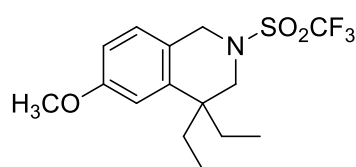
6-Methoxy-4,4-dimethyl-2-[(trifluoromethyl)sulfonyl]-1,2,3,4-tetrahydroisoquinoli



ne 3.53b was obtained in 86% (129 mg) yield from 89.2 mg of starting material **3.52b**. Orange oil; $R_f = 0.55$ (20:80 EtOAc/Hexane). $^1\text{H NMR}$ (300 MHz, CDCl_3): δ (ppm) 6.98 (d, $J = 8.5$ Hz, 1H, ArH), 6.88 (d, $J = 2.6$ Hz, 1H, ArH), 6.77 (d, $J = 8.5$ Hz, 2.6 Hz, 1H, ArH), 4.62

(brs, 2H, ArCH_2N), 3.81 (s, 3H, OCH_3), 3.44 (brs, 2H, CH_2), 1.35 (s, 6H, $2\times\text{CH}_3$). $^{13}\text{C NMR}$ (75 MHz, CDCl_3 , C–F coupling was not clearly visible): δ (ppm) 35.86 ($2\times\text{CH}_3$), 55.73 (CH_2), 65.58 (OCH_3), 109.27 (ArCH), 119.32 (ArC), 119.83 (ArCH), 129.95 (ArC), 132.53 (ArC), 155.27 (ArCOMe).

4,4-Diethyl-6-methoxy-2-[(trifluoromethyl)sulfonyl]-1,2,3,4-tetrahydroisoquinoline

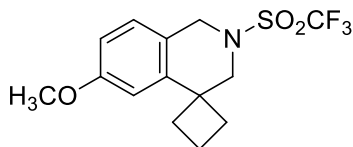


3.53c was obtained in 70% (239 mg) yield from 214 mg of starting material **3.52c**. Orange oil; $R_f = 0.75$ (30:70 EtOAc/Hexane). $^1\text{H NMR}$ (300 MHz, CDCl_3): δ (ppm) 6.98 – 6.79 (m, 1H, ArH), 6.77 – 6.60 (m, 2H, $2\times\text{ArH}$), 4.49 (brs, 2H,

Ar CH_2N), 3.71 (s, 3H, OCH_3), 3.55 – 3.24 (m, 2H, CH_2), 1.79 – 1.49 (m, 4H, $2\times\text{CH}_2$), 0.820 – 0.630 (m, 6H, $2\times\text{CH}_3$). $^{13}\text{C NMR}$ (75 MHz, CDCl_3 , C–F coupling was not clearly visible): δ (ppm) 8.43 (CH_3), 29.79 (CH_2), 41.31 (CH_2), 47.91 (C), 50.80 (CH_2), 55.40 (OCH_3), 112.74

(ArCH), 118.32 (ArCH), 122.73 (ArCH), 127.17 (ArC), 140.81 (ArC), 158.60 (ArCOMe).
HRMS ESI⁺: m/z [M+H]⁺ calcd for C₁₅H₂₀F₃NO₃S, 350.1038; found, 350.1046 (2.30 ppm).

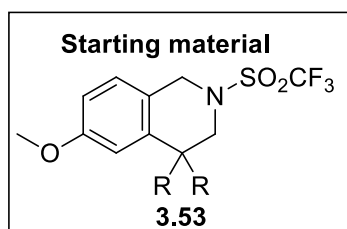
6'-Methoxy-2'-[(trifluoromethyl)sulfonyl]-2',3'-dihydro-1'H-spirocyclobutane-1,4'



-isoquinoline 3.53d was obtained in 69% (194 mg) yield from 171 mg of starting material **3.52d**. Orange oil; R_f = 0.76 (30:70 EtOAc/Hexane). **¹H NMR** (300 MHz, CDCl₃): δ (ppm) 7.03 (d, J = 2.6 Hz, 1H, ArH), 6.87 (d, J = 8.5 Hz, 1H, ArH), 6.69 (dd, J =

8.5, 2.6 Hz, 1H, ArH), 4.58 (brs, 2H, ArCH₂N), 3.75 (s, 3H, OCH₃), 2.38 – 2.07 (m, 6H, 3xCH₂). **¹³C NMR** (75 MHz, CDCl₃, C–F coupling was not clearly visible): δ (ppm) 15.12 (CH₂), 41.81 (CH₂), 48.11 (CH₂), 53.80 (CH₂), 55.67 (OCH₃), 111.87 (C), 112.55 (ArCH), 120.75 (q, J = 322.5 Hz, CF₃), 122.16 (ArCH), 127.16 (ArC), 142.41 (CF₃), 159.60 (ArCOMe). **HRMS ESI⁺**: m/z [M+H]⁺ calcd for C₁₄H₁₆F₃NO₃S, 336.0837; found, 336.1977 (2.65 ppm).

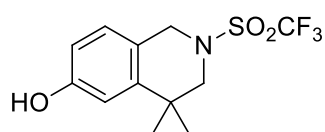
8.7.6 General procedure for the demethylation of aryl ethers 3.53a – d



The general procedure described by McOmie and co-workers,¹²¹ was implemented for the demethylation of aryl methyl ethers **3.53a – d**. Thus, a mixture of 1 M BBr₃ (0.346 mL, 3.65 mmol) in anhydrous CH₂Cl₂ (3.46 mL) was cooled to –40 °C, to which sulfonamide derivatives **3.53a – d** (0.398 mmol)

dissolved in anhydrous CH₂Cl₂ (0.90 mL), were slowly added and stirred at –40 °C for 2 h. The mixture was allowed to warm to RT and stirred for an additional 4 h. This was followed by quenching any excess BBr₃ and boron complexes formed with water at 0 °C. Product was collected by extracting with CH₂Cl₂ (25 mL x 3), the organic solvent was dried over MgSO₄, filtered and concentrated under reduced pressure. The spectroscopic details of compounds **3.54b – d** are described below:

4,4-Dimethyl-2-[(trifluoromethyl)sulfonyl]-1,2,3,4-tetrahydroisoquinolin-6-ol 3.49b



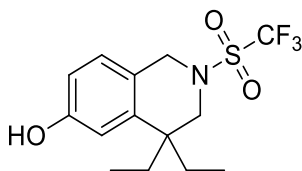
was obtained in 85% (104 mg) yield from 127 mg of starting material **3.53b**. Yellow oil; R_f = 0.43 (30:70 EtOAc/Hexane). **¹H NMR** (300 MHz, CDCl₃): δ (ppm) 6.92 (d, J = 8.4 Hz, 1H, ArH), 6.83

(d, J = 2.6 Hz, 1H, ArH), 6.70 (dd, J = 8.4, 2.6 Hz, 1H, ArH), 4.89 (brs, 1H, OH), 4.61 (s, 2H, ArCH₂N), 3.44 (d, J = 6.6 Hz, 2H, CH₂), 1.34 (s, 6H, 2xCH₃). **¹³C NMR** (75 MHz, CDCl₃, no C–F coupling was clearly visible): δ (ppm) 35.43 (2xCH₃), 48.21 (CH₂), 56.09 (ArCH₂N),

112.74 (ArCH), 114.45 (ArCH), 121.67 (C), 127.50 (ArCH), 144.10 (ArC), 155.16 (ArCOH).

HRMS ESI⁺: m/z [M+H]⁺ calcd for C₁₂H₁₄F₃NO₃S, 310.0725; found, 310.0721 (1.3 ppm).

4,4-Diethyl-2-[(trifluoromethyl)sulfonyl]-1,2,3,4-tetrahydroisoquinolin-6-ol **3.49c**



was obtained in 36% (83.9 mg) yield from 242 mg of starting material

3.53c. Orange oil; R_f = 0.55 (30:70 EtOAc/Hexane). **¹H NMR** (300

MHz, CDCl₃): δ (ppm) 6.89 (d, J = 8.2 Hz, 1H, ArH), 6.71 (m, 2H,

2xArH), 5.70 (brs, 1H, OH), 4.55 (brs, 2H, ArCH₂N), 3.51 (brs, 2H,

CH₂), 1.86 – 1.78 (m, 2H, CH₂), 1.66 – 1.59 (m, 2H, CH₂), 0.740 (t, J = 7.5 Hz, 6H, 2xCH₃).

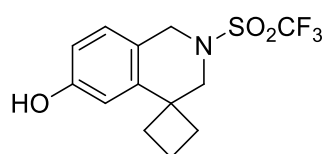
¹³C NMR (75 MHz, CDCl₃, no C–F coupling was clearly visible): δ (ppm) 8.33 (2xCH₃), 41.23

(CH₂), 47.96 (CH₂), 50.75 (ArCH₂N), 113.59 (ArCH), 114.09 (ArCH), 122.67 (ArCH), 127.36

(ArC), 141.11 (ArC), 154.64 (ArCOH). **HRMS ESI⁺**: m/z [M+H]⁺ calcd for C₁₄H₁₈F₃NO₃S,

336.0881; found, 336.0881 (0.00 ppm).

2'-[(Trifluoromethyl)sulfonyl]-2',3'-dihydro-1'H-spirocyclobutane-1,4'-isoquinolin



-6'-ol 3.49d was obtained in 65% (109 mg) yield from 175 mg of

starting material **3.53d**. Colourless oil; R_f = 0.53 (30:70

EtOAc/Hexane). **¹H NMR** (300 MHz, CDCl₃): δ (ppm) 7.00 (d, J =

2.5 Hz, 1H, ArH), 6.83 (d, J = 8.3 Hz, 1H, ArH), 6.63 (dd, J = 8.3,

2.5 Hz, 1H, ArH), 4.99 (brs, 1H, OH), 4.47 (brs, 2H, ArCH₂N), 3.63 (s, 2H, CH₂), 2.47 – 1.82

[m, 6H, 3x(CH₂)]. **¹³C NMR** (75 MHz, CDCl₃, no C–F coupling was clearly visible): δ (ppm)

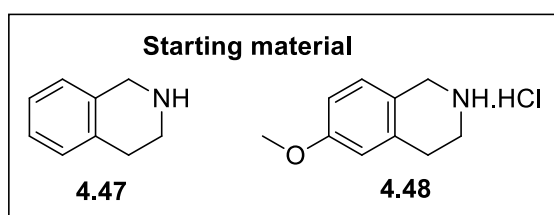
15.07 (CH₂), 41.65 (CH₂), 48.11 (CH₂), 53.77 (ArCH₂N), 112.86 (ArCH), 114.44 (ArCH),

118.56 (q, J = 322.5 Hz, CF₃), 122.24 (ArCH), 127.35 (ArC), 142.76 (ArC), 155.48 (ArCOH).

HRMS ESI⁺: m/z [M+H]⁺ calcd for C₁₃H₁₄F₃NO₃S, 322.0646; found, 322.0706 (3.10 ppm).

8.8 Synthesis of urea analogues

8.8.1 General procedure for the synthesis of THIQ–carbamoyl imidazoles



According to the general procedure described by

Grzyb and co-workers,¹³¹ a cooled (0°C) solution of 1,1'-carbonyldiimidazole (350 mg, 2.20 mmol)

in anhydrous CH₃CN (25 mL) was treated with the

THIQ (**4.47** or **4.48**) (2.00 mmol) and K₂CO₃ (4.00

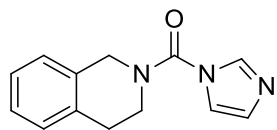
mmol). This was followed by overnight stirring at RT, which resulted in a yellow mixture. The

mixture was concentrated under reduced pressure and the residue further purified with

the mixture was concentrated under reduced pressure and the residue further purified with

column chromatography (100% EtOAc). The spectroscopic details of the compounds are described below:

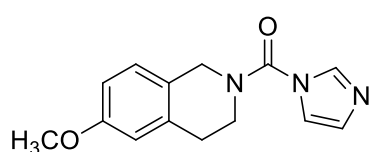
[3,4-Dihydroisoquinolin-2(1H)-yl](1H-imidazol-1-yl)methanone 4.49 was obtained in



84% (307 mg) yield from 0.200 mL of starting material **4.47**. Bright yellow solid; mp = 82 – 83 °C; R_f = 0.25 (100% EtOAc). $^1\text{H NMR}$ (300 MHz, CDCl_3): δ (ppm) 7.86 (s, 1H, ArH), 7.25 – 6.97 (m, 6H, 6xArH),

4.68 (s, 2H, ArCH_2N), 3.75 (t, J = 6.0 Hz, 2H, CH_2), 2.94 (t, J = 6.0 Hz, 2H, ArCH_2CH_2). $^{13}\text{C NMR}$ (75 MHz, CDCl_3 , not all aromatic signals were clearly visible): δ (ppm) 28.68 (ArCH_2CH_2), 44.65 (CH_2), 48.55 (ArCH_2N), 117.99 (ArCH), 126.97 (ArCH), 127.43 (ArCH), 129.00 (ArCH), 129.96 (ArC), 131.87 (ArCH), 133.80 (ArC), 136.93 (ArCH), 151.22 (C=O). **HRMS ESI⁺**: m/z $[\text{M}+\text{H}]^+$ calcd for $\text{C}_{13}\text{H}_{13}\text{ON}_3$, 228.1137; found, 228.1135 (0.90 ppm). The experimental spectroscopic information, was similar to that reported in the literature.¹³¹

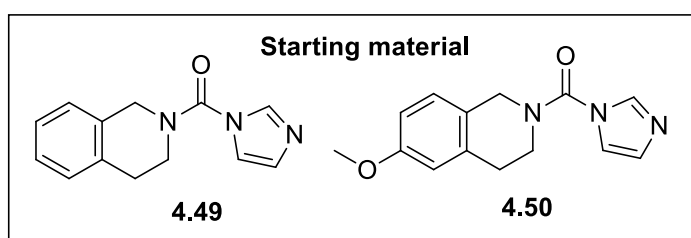
(1H-Imidazol-1-yl)[6-methoxy-3,4-dihydroisoquinolin-2(1H)-yl]methanone 4.50



was obtained in 96% (449 mg) yield from 362 mg of starting material **4.48**. Colourless oil; R_f = 0.31 (100% EtOAc). $^1\text{H NMR}$ (300 MHz, CDCl_3): δ (ppm) 7.86 (d, J = 0.9 Hz, 1H, imidazole-ArH),

7.20 (d, J = 1.4 Hz, 1H, imidazole-ArH), 7.05 (d, J = 1.4 Hz, 1H, imidazole-ArH), 6.95 – 6.92 (m, J = 8.4 Hz, 1H, ArH), 6.71 – 6.64 (m, 2H, ArH), 4.61 (s, 2H, ArCH_2N), 3.78 – 3.67 (m, 5H, overlapping signals- CH_2 and OCH_3), 2.90 (t, J = 6.0 Hz, 2H, ArCH_2CH_2). $^{13}\text{C NMR}$ (75 MHz, CDCl_3): δ (ppm) 29.11 (ArCH_2CH_2), 44.67 (CH_2), 48.34 (ArCH_2N), 55.64 (OCH_3), 113.32 (ArCH), 113.87 (ArCH), 118.17 (ArCH), 124.14 (ArC), 127.59 (ArCH), 130.08 (ArCH), 135.29 (ArC), 137.11 (ArCH), 151.36 (C=O), 159.00 (ArCOMe).

8.8.2 General procedure for the synthesis of THIQ-carbamoyl imidazolium salts

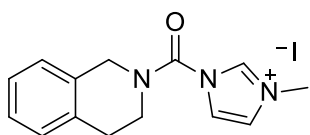


According to the general procedure described by Grzyb and co-workers,¹³¹ iodomethane (MeI) (0.960 mL, 15.5 mmol) was added to a suspension of the tetrahydroisoquinoline carbamoyl

imidazole (**4.49** and **4.50**) (1.55 mmol) in anhydrous CH_3CN (24 mL) and stirred overnight affording a precipitate. The solvent and excess MeI were removed under reduced pressure

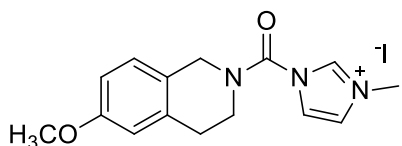
to afford the product in quantitative yield as a solid iodium salt, with no further purification required. The spectroscopic details of the compounds are described below:

1-[3,4 Dihydroisoquinolin-2(1H)-yl]carbonyl-3'-methyl-1H-imidazol-3-ium iodide



4.51 was obtained in quantitative (572 mg) yield from 353 mg of starting material **4.49**. Bright yellow powder; **mp** = 166 – 168 °C; R_f = 0.00 (100% EtOAc). **¹H NMR** (400 MHz, DMSO- d_6): δ (ppm) 8.79 (s, 1H, *imidazole*-ArH), 7.27 (d, J = 1.8 Hz, 1H, ArH), 7.06 (d, J = 1.7 Hz, 1H, ArH), 6.41 (d, J = 6.6 Hz, 4H, 4xArH), 3.92 (s, 2H, ArCH₂N), 3.11 (s, 3H, *imidazole*-CH₃), 2.90 (s, 2H, CH₂), 2.14 (t, J = 5.9 Hz, 2H, ArCH₂CH₂). **¹³C NMR** (101 MHz, DMSO- d_6 , not all methylene signals were visible as two were hidden in the DMSO signal): δ (ppm) 36.46 (ArCH₂CH₂), 121.07 (ArCH), 123.72 (ArCH), 126.50 (ArCH), 127.02 (ArCH), 128.45 (ArC), 131.86 (ArCH), 134.19 (ArCH), 137.78 (ArC), 147.22 (C=O). **HRMS ESI⁺**: m/z [M-126.9045]⁺ calcd for C₁₄H₁₆IN₃O, 242.1293; found, 242.1284 (3.7 ppm).

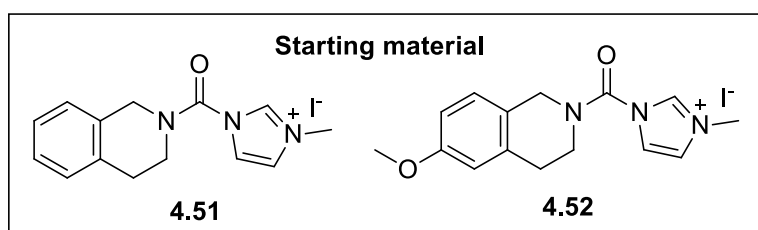
1-(6-Methoxy-1,2,3,4-tetrahydroisoquinoline-2-carbonyl)-3'-methyl-1H-imidazol-3-ium



4.52 was obtained in quantitative (1.16 g) yield from 748 mg of starting material **4.50**. Off white solid; **mp** = 172 – 173 °C; R_f = 0.00 (100% EtOAc). **¹H NMR** (300 MHz, DMSO- d_6): δ (ppm) 9.62 (s, 1H, *imidazole*-ArH), 8.10 – 8.09 (m, 1H, *imidazole*-ArH), 7.89 – 7.88 (m, 1H, ArH), 7.13 (brs, 1H, ArH), 6.84 – 6.81 (m, 2H, 2xArH), 4.67 (s, 2H, ArCH₂N), 3.94 (s, 3H, *imidazole*-CH₃), 3.75 – 3.68 (m, 5H, overlapping signals-OCH₃ and CH₂), 2.95 (t, J = 5.8 Hz, 2H, ArCH₂CH₂). **¹³C NMR** (75 MHz, DMSO- d_6 , no methylene, methyl and one ArC signals were not visible): δ (ppm) 55.33 (OCH₃), 112.85 (ArCH), 113.22 (ArCH), 121.14 (ArC), 123.79 (ArCH), 127.59 (ArCH), 135.66 (ArC), 137.84 (ArCH), 147.26 (C=O), 158.33 (ArCOMe).

8.8.3 Coupling of THIQ – carbamoyl imidazolium salts with heteroaryls amines

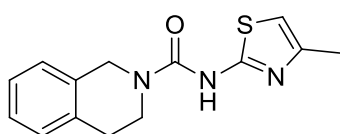
8.8.3.1 General procedure for the synthesis of compound 4.54



According to the general procedure described by Grzyb and co-workers,¹³¹ a combined mixture of 2-amino-4-methyl thiazole (120 mg, 1.08 mmol), and

Et₃N (0.150 mL, 1.08 mmol) in anhydrous CH₃CN (15 mL) were stirred at RT for 30 min. Subsequently, the tetrahydroisoquinoline carbamoyl imidazolium salts (**4.51** or **4.52**) (0.542 mmol) were then added. The work-up procedure included washing of the reaction mixture with an aqueous 1 N HCl solution (50 mL x 2) followed by an extraction with EtOAc (20 mL x 2). The organic layers were combined, dried over MgSO₄, filtered and concentrated under reduced pressure providing oily residues. The residues were purified using column chromatography (50:50 EtOAc/Hexane). The spectroscopic details of the compounds are described below:

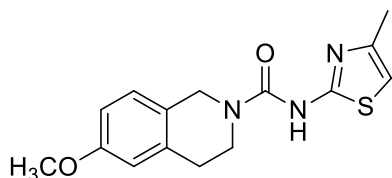
N-(4'-Methylthiazol-2-yl)-3,4-dihydroisoquinoline-2(1H)-carboxamide 4.53a was



obtained in 44% (53.5 mg) yield from 164 mg of starting material **4.51**. Bright yellow foam/powder; $R_f = 0.48$ (50:50 EtOAc/Hexane). ¹H NMR (300 MHz, CDCl₃): δ (ppm) 7.18 – 7.01

(m, 4H, 4xArH), 6.38 (s, 1H, *thiazole*-ArH), 4.61 (s, 2H, ArCH₂N), 3.70 (t, $J = 5.9$ Hz, 2H, CH₂), 2.85 (t, $J = 5.9$ Hz, 2H, ArCH₂CH₂), 2.26 (s, 3H, *thiazole*-CH₃). ¹³C NMR (75 MHz, CDCl₃, one ArC signal was not visible): δ (ppm) 16.69 (*thiazole*-CH₃), 28.80 (ArCH₂CH₂), 41.61 (CH₂), 45.82 (ArCH₂N), 106.98 (ArCH), 126.51 (ArCH), 126.93 (ArCH), 128.52 (ArCH), 132.69 (ArC), 134.55 (ArCH), 144.53 (ArCNH), 154.70 (C=O), 162.39 (*thiazole*-ArC).

6-Methoxy-N-(4'-methylthiazol-2-yl)-3,4-dihydroisoquinoline-2(1H)-carboxamide 4.54a was

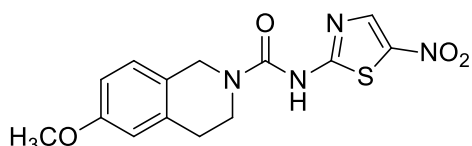


obtained in 80% (203 mg) yield from 334 mg of starting material **4.52**. Orange oil; $R_f = 0.39$ (50:50 EtOAc/Hexane). ¹H NMR (300 MHz, CDCl₃): δ (ppm) 6.95 (d,

$J = 8.4$ Hz, 1H, ArH), 6.75 (dd, $J = 8.4, 2.5$ Hz, 1H, ArH), 6.66 (d, $J = 2.5$ Hz, 1H, ArH), 6.39 (s, 1H, *thiazole*-ArH), 4.55 (s, 2H, ArCH₂N), 3.78 (s, 3H, OCH₃), 3.70 (t, $J = 5.9$ Hz, 2H, CH₂), 2.84 (t, $J = 5.9$ Hz, 2H, ArCH₂CH₂), 2.27 (s, 3H, *thiazole*-CH₃). ¹³C NMR (75 MHz, CDCl₃, one ArC signal was not visible): δ (ppm) 16.81 (*thiazole*-CH₃), 29.14 (ArCH₂CH₂), 41.50 (CH₂), 45.34 (ArCH₂N), 55.41 (OCH₃), 107.07 (ArCH), 112.76 (ArCH), 113.40 (ArCH), 124.75 (ArC), 127.45 (ArCH), 135.87 (ArCNH), 154.54 (C=O), 158.54 (ArCOMe). HRMS ESI⁺: m/z [M+H]⁺ calcd for C₁₅H₁₇N₃O₂S, 304.1120; found, 304.1111 (3.00 ppm).

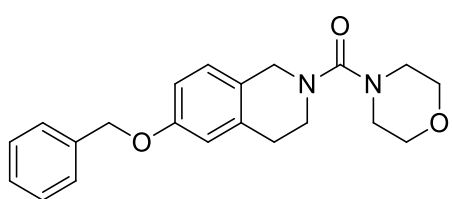
8.8.3.2 General procedure for the synthesis of compounds 4.54

The general procedure described by Grzyb and co-workers¹³¹ was followed. A suspension of 2-amino-5-nitrothiazole (100 mg, 0.714 mmol), and Cs₂CO₃ (310 mg, 0.952 mmol) in anhydrous CH₃CN (20 mL) was stirred at RT for 30 min, to which the tetrahydroisoquinoline imidazolium salt **4.52** (190 mg, 0.476 mmol) was added. The work-up procedure included rinsing of the reaction mixture with an aqueous 1 N HCl solution (15 mL x 2), followed by an EtOAc extraction (25 mL x 2). The organic layers were combined, dried over MgSO₄, filtered and concentrated under reduced pressure affording a solid residue. The residue was purified using column chromatography (30:70 EtOAc/Hexane). The spectroscopic details of the compounds are described below:

6-Methoxy-N-(5'-nitrothiazol-2-yl)-3,4-dihydroisoquinoline-2(1H)-carboxamide

4.54b was obtained in 90% (90.0 mg) yield from 119 mg of starting material **4.52**. Yellow powder; $R_f = 0.50$ (30:70 EtOAc/Hexane). **¹H NMR** (300 MHz, DMSO-*d*₆): δ (ppm)

12.17 (s, 1H, NH), 8.58 (s, 1H, *thiazole*-ArH), 7.10 (d, $J = 8.4$ Hz, 1H, ArH), 6.89 – 6.67 (m, 2H, 2xArH), 4.64 (s, 2H, ArCH₂N), 3.89 – 3.62 (m, 5H, overlapping signals-OCH₃ and CH₂), 2.84 (t, $J = 5.9$ Hz, 2H, ArCH₂CH₂). **¹³C NMR** (75 MHz, DMSO-*d*₆): δ (ppm) 28.31 (ArCH₂CH₂), 41.53 (CH₂), 44.95 (ArCH₂N), 55.05 (OCH₃), 112.50 (ArCH), 113.17 (ArCH), 124.89 (ArCH), 127.23 (ArCH), 135.65 (ArC), 140.53 (ArCH), 142.10 (ArCNH), 153.84 (C=O), 157.90 (ArCOMe), 165.54 (ArCNO₂). **HRMS ESI⁺**: m/z [M+H]⁺ calcd for C₁₄H₁₄N₄O₄S, 335.0814; found, 335.0805 (2.7 ppm).

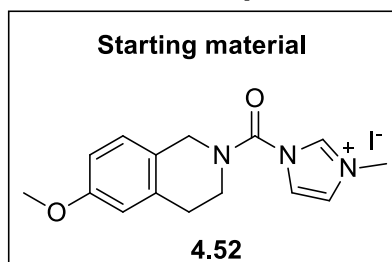
6-[Benzyloxy-3,4-dihydroisoquinolin-2(1H)-yl(morpholino)]methanone 4.54h was

obtained in 96% (260 mg) yield from 365 mg of starting material. White oil solidified at low temperatures; $R_f = 0.48$ (100% EtOAc). **¹H NMR** (300 MHz, CDCl₃): δ (ppm) 7.39

– 7.15 (m, 5H, 5xBnH), 6.93 (d, $J = 8.4$ Hz, 1H, ArH), 6.80 – 6.62 (m, 2H, 2xArH), 4.96 (s, 2H, ArCH₂O), 4.31 (s, 2H, ArCH₂N), 3.74 – 3.53 (m, 4H, *morpholine*-2xOCH₂), 3.42 (t, $J = 5.8$ Hz, 2H, CH₂), 3.29 – 3.13 (m, 4H, *morpholine*-2xNCH₂), 2.79 (t, $J = 5.8$ Hz, 2H, ArCH₂CH₂). **¹³C NMR** (75 MHz, CDCl₃): δ (ppm) 29.00 (ArCH₂CH₂), 44.49 (*morpholine*-2xNCH₂), 47.41 (CH₂), 48.44 (ArCH₂N), 66.78 (*morpholine*-2xCH₂O), 70.15 (BnCH₂O), 113.46 (ArCH), 114.71 (ArCH), 126.13 (ArC), 127.42 (ArCH), 128.04 (ArCH), 128.68 (ArCH), 135.92 (ArC), 137.10 (BnC), 157.49 (C=O),

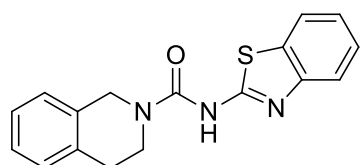
164.03 (ArCOBn). **HRMS ESI⁺**: m/z [M+H]⁺ calcd for C₂₁H₂₄N₂O₃, 353.1865; found, 353.1866 (0.30 ppm).

8.8.3.3 General procedure for the synthesis of compounds 4.54c – g



The general procedure described by Grzyb and co-workers,¹³¹ was implemented as follows. A cooled (−78 °C) solution of the aniline analogues (**c – g**) (80.0 mg, 0.649 mmol), 1.4 M *n*BuLi (0.690 mL, 0.974 mmol) in anhydrous THF (15 mL) was stirred for 1 h at −78 °C. The temperature was gradually allowed to increase to RT. Compound **4.52** (310 mg, 0.779 mmol) was then added and the reaction mixture was stirred at RT overnight. The work-up procedure involved a wash with an aqueous 1 N HCl solution (10 mL x 2), followed by an extraction with EtOAc (20 mL x 2). The organic layers were combined, dried over MgSO₄, filtered and concentrated under reduced pressure affording a residue which was purified by column chromatography (50:50 EtOAc/Hexane). The spectroscopic details of the compounds are described below:

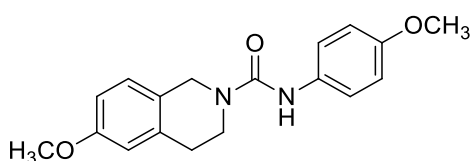
N-[Benzo(d)thiazol-2-yl]-3,4-dihydroisoquinoline-2(1H)-carboxamide was obtained



in 60% (102 mg) yield from 219 mg of starting material **4.51**. White solid; **mp** = 180 – 182 °C; R_f = 0.56 (50:50 EtOAc/Hexane). **¹H NMR** (400 MHz, CDCl₃): δ (ppm) 7.77 (d, J = 7.7 Hz, 1H, *benzothiazole*-ArH), 7.62 (d, J = 7.7 Hz, 1H, *benzothiazole*-ArH), 7.37 (d, J = 7.7 Hz, 1H, *benzothiazole*-ArH), 7.31 – 7.09 (m, 2H, 2xArH), 7.01 (s, 1H, ArH), 4.69 (s, 2H, ArCH₂N), 3.78 (t, J = 5.9 Hz, 2H, CH₂), 2.89 (t, J = 5.9 Hz, 2H, ArCH₂CH₂).

¹³C NMR (101 MHz, CDCl₃): δ (ppm) 29.02 (ArCH₂CH₂), 42.02 (CH₂), 45.87 (ArCH₂N), 121.76 (*benzothiazole*-ArCH), 123.62 (*benzothiazole*-ArCH), 126.38 (*benzothiazole*-ArCH), 126.61 (ArCH), 126.90 (ArCH), 127.23 (ArCH), 128.71 (ArCH), 134.68 (ArCNH). **HRMS ESI⁺**: m/z [M+H]⁺ calcd for C₁₄H₁₄N₄O₄S, 310.0969; found, 310.1017 (3.22 ppm).

6-Methoxy-N-(4'-methoxyphenyl)-3,4-dihydroisoquinoline-2(1H)-carboxamide



4.54c was obtained in 98% (270 mg) yield from 352 mg of starting material **4.52**. Brown oil; R_f = 0.50 (50:50 EtOAc/Hexane). **¹H NMR** (300 MHz, CDCl₃): δ (ppm) 7.30 – 7.14 (m, 2H, 2xArH), 6.99 (d, J = 8.4 Hz, 1H,

ArH), 6.84 – 6.60 (m, 4H, 4xArH), 6.32 (s, 1H, NH), 4.52 (s, 2H, ArCH₂N), 3.73 (s, 3H, OCH₃), 3.74 (s, 3H, OCH₃), 3.63 (t, *J* = 5.9 Hz, 2H, CH₂), 2.82 (t, *J* = 5.9 Hz, 2H, ArCH₂CH₂). ¹³C NMR (75 MHz, CDCl₃): δ (ppm) 29.69 (ArCH₂CH₂), 41.68 (CH₂), 45.58 (ArCH₂N), 55.73 (2xOCH₃), 112.86 (ArCH), 113.59 (ArCH), 114.41 (ArCH), 122.85 (ArCH), 125.64 (ArCH), 127.65 (ArC), 132.35 (ArC), 136.64 (ArCNH), 155.80 (C=O), 156.21 (ArCOMe), 158.69 (ArCOMe).

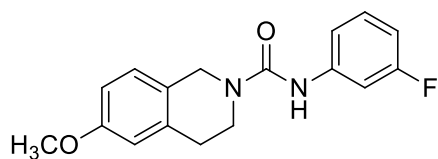
***N*-(3'-Chlorophenyl)-6-methoxy-3,4-dihydroisoquinoline-2(1*H*)-carboxamide**



4.54d was obtained in 50% (70.0 mg) yield from 177 mg of starting material **4.52**. Brown oil that solidified at low temperatures; *R_f* = 0.50 (50:50 EtOAc/Hexane). ¹H NMR (300 MHz, CDCl₃): δ (ppm) 7.47 (dd, *J* = 1.9 Hz, 1H, ArH),

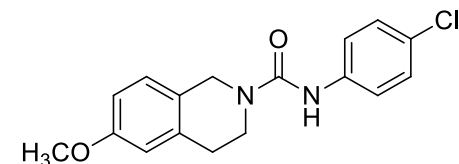
7.31 – 7.07 (m, 2H, 2xArH), 7.06 – 6.90 (m, 2H, 2xArH), 6.85 – 6.61 (m, 3H, 2xArH and NH), 4.55 (s, 2H, ArCH₂N), 3.77 (s, 3H, OCH₃), 3.65 (t, 6.0 Hz, 2H, CH₂), 2.83 (t, *J* = 6.0 Hz, 2H, ArCH₂CH₂). ¹³C NMR (75 MHz, CDCl₃): δ (ppm) 29.33 (ArCH₂CH₂), 41.60 (CH₂), 45.39 (ArCH₂N), 55.42 (OCH₃), 112.68 (ArCH), 113.38 (ArCH), 118.26 (ArCH), 120.27 (ArCH), 123.09 (ArCH), 125.16 (ArCH), 127.40 (ArC), 129.83 (ArCH), 134.43 (ArC), 136.21 (ArCCl), 140.52 (ArCNH), 154.90 (C=O), 158.52 (ArCOMe). **HRMS ESI⁺** *m/z* [M+H]⁺ calcd for C₁₇H₁₇ClN₂O₂, 317.1057 (³⁵Cl); found, 317.1052 (1.60 ppm) and 319.1027 (³⁷Cl).

***N*-(3'-Fluorophenyl)-6-methoxy-3,4-dihydroisoquinoline-2(1*H*)-carboxamide**



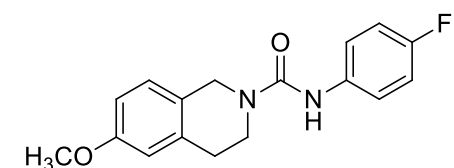
4.54e was obtained in 98% (270 mg) yield from 366 mg of starting material **4.52**. Brown oil that solidified at low temperatures; *R_f* = 0.50 (50:50 EtOAc/Hexane). ¹H NMR (300 MHz, CDCl₃): δ (ppm) 7.38 – 7.18 (m, 1H, 1xArH),

7.09 – 7.03 (m, 2H, 2xArH), 6.80 – 6.70 (m, 2H, 2xArH), 6.45 (s, 2H, NH), 4.62 (s, 2H, ArCH₂N), 3.83 (s, 3H, OCH₃), 3.70 (t, *J* = 5.8 Hz, 2H, CH₂), 2.93 (t, *J* = 5.8 Hz, 2H, ArCH₂CH₂). ¹³C NMR (75 MHz, CDCl₃, some ArC signals were not observed): δ (ppm) 29.31 (ArCH₂CH₂), 41.45 (CH₂), 45.27 (ArCH₂N), 55.33 (OCH₃), 107.35 (ArCH), 109.52 (ArCH), 112.64 (ArCH), 113.31 (ArCH), 114.86 (ArC), 127.33 (ArCH), 136.18 (ArCNH), 158.51 (ArCOMe). **HRMS ESI⁺**: *m/z* [M+H]⁺ calcd for C₁₇H₁₇FN₂O₂, 301.1356 (¹⁸F); found, 301.1356 (0.00 ppm) and 302.1383 (¹⁹F).

***N*-(4'-Chlorophenyl)-6-methoxy-3,4-dihydroisoquinoline-2(1*H*)-carboxamide**

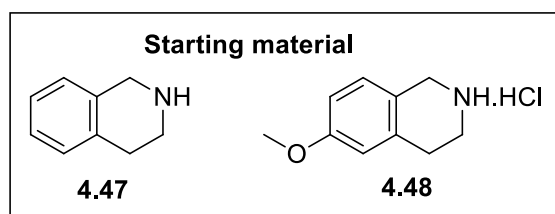
4.54f was obtained in 44% (53.0 mg) yield from 152 mg of starting material **4.52**. Brown solid; **mp** = 105 – 107 °C;

R_f = 0.50 (50:50 EtOAc/Hexane). **¹H NMR** (300 MHz, CDCl₃): δ (ppm) 7.40 – 7.19 (m, 4H, 4xArH), 7.06 (d, J = 8.4 Hz, 1H, ArH), 6.88 – 6.65 (m, 2H, 2xArH), 6.45 (s, 1H, NH), 4.59 (s, 2H, ArCH₂N), 3.80 (s, 3H, OCH₃), 3.76 – 3.65 (m, 2H, CH₂), 2.90 (t, J = 5.3 Hz, 2H, ArCH₂CH₂). **¹³C NMR** (75 MHz, CDCl₃, some ArC signals were not observed): δ (ppm) 29.68 (ArCH₂CH₂), 41.78 (CH₂), 45.63 (ArCH₂N), 55.69 (OCH₃), 112.99 (ArCH), 113.67 (ArCH), 121.53 (ArC), 125.14 (ArCH), 127.68 (ArCH), 129.21 (ArC), 136.44 (ArCCl), 138.06 (ArCNH), 154.95 (ArCH), 155.21 (C=O), 158.38 (ArCOMe). **HRMS ESI⁺**: m/z [M+H]⁺ calcd for C₁₇H₁₇ClN₂O₂, 317.1057 (³⁵Cl); found, 317.1060 (0.90 ppm) and 319.1036 (³⁷Cl).

***N*-(4'-Fluorophenyl)-6-methoxy-3,4-dihydroisoquinoline-2(1*H*)-carboxamide**

4.46g was obtained in 81% (94.1 mg) yield from 154 mg of starting material **4.52**. Brown solid; **mp** = 136 – 137 °C;

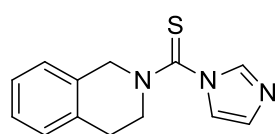
R_f = 0.50 (50:50 EtOAc/Hexane). **¹H NMR** (300 MHz, CDCl₃): δ (ppm) 7.38 – 7.28 (m, 2H, 2xArH), 7.10 – 6.91 (m, 3H, 3xArH), 6.83 – 6.68 (m, 2H, 2xArH), 6.43 (s, 1H, NH), 4.59 (s, 2H, ArCH₂N), 3.80 (s, 3H, OCH₃), 3.70 (t, J = 5.9 Hz, 2H, CH₂), 2.89 (t, J = 5.9 Hz, 2H, ArCH₂CH₂). **¹³C NMR** (75 MHz, CDCl₃): δ (ppm) 29.70 (ArCH₂CH₂), 41.78 (CH₂), 45.64 (ArCH₂N), 55.71 (OCH₃), 112.98 (ArCH), 113.68 (ArCH), 115.81 (d, J = 22.5 Hz, ArCH-F), 122.48 (d, J = 7.7 Hz, ArCH-F), 125.49 (ArC), 127.70 (ArCH), 135.30 (ArC), 136.61 (ArCNH), 155.45 (C=O), 157.56 (d, J = 67.5 Hz, ArC-F), 158.84 (ArCOMe). **HRMS ESI⁺**: m/z [M+H]⁺ calcd for C₁₇H₁₇FN₂O₂, 302.1308 (¹⁸F); found, 302.1381 (3.30 ppm).

8.9 Synthesis of thiourea analogues**8.9.1 General procedure for the synthesis of [3,4-dihydroisoquinolin-2(1*H*)-yl]****(1*H*-imidazol-1-yl)methanethione**

The general procedure described by Grzyb and co-workers¹³¹ was followed. Thus, a cooled (0 °C) diluted mixture of 1,1'-thiocarbonyldiimidazole (210 mg, 1.20 mmol) in anhydrous CH₃CN (100 mL) was

treated by the portion-wise addition of THIQ (**4.47** or **4.48**) (1.00 mmol) [in the case of the hydrochloric salt Et₃N (0.420 mL, 3.00 mmol) was included] while maintaining a temperature of 0 °C for 2 h, followed by gradual heating to RT. Stirring was continued for 18 h. The reaction mixture was concentrated under reduced pressure to afford a residue which was purified with column chromatography (100% EtOAc), yielding product as an orange oil. It is important to note that in order to prevent the preferential formation of the dimer, the portion-wise addition of **4.47** or **4.48** was essential. The spectroscopic details of the compounds are described below:

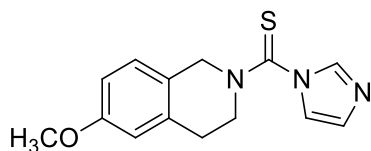
{[3,4-Dihydroisoquinolin-2(1H)-yl]1H-imidazol-1-yl}methanethione **4.55** was



obtained in 86% (329 mg) yield from 213 mg of starting material **4.47**.

Yellow oil; $R_f = 0.25$ (100% EtOAc). **¹H NMR** (300 MHz, CDCl₃): δ (ppm) 7.88 – 7.79 (m, 1H, *imidazole-ArH*), 7.24 – 7.11 (m, 4H, 4xArH), 7.07 – 6.96 (m, 2H, *imidazole-2xArH*), 4.88 (s, 2H, ArCH₂N), 4.00 (t, $J = 5.8$ Hz, 2H, CH₂), 2.99 (t, $J = 5.8$ Hz, 2H, ArCH₂CH₂). No **¹³C NMR** was reported since, the spectrum corresponded well with that described by Grzyb and co-workers.¹³¹

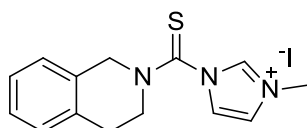
(1H-Imidazol-1-yl)[6-methoxy-3,4-dihydroisoquinolin-2(1H)-yl]methanethione



4.56 was obtained in quantitative (754 mg) yield from 550 mg of starting material **4.48**. Yellow oil; $R_f = 0.21$ (100% EtOAc). **¹H**

NMR (300 MHz, CDCl₃): δ (ppm) 7.92 – 7.83 (m, 1H, *imidazole-ArH*), 7.26 – 7.19 (m, 1H, *imidazole-ArCH*), 7.08 (dd, $J = 1.4, 0.9$ Hz, 1H, *imidazole-ArH*), 6.98 (s, 1H, ArH), 6.84 – 6.67 (m, 2H, 2xArH), 4.85 (s, 2H, ArCH₂N), 4.00 (d, $J = 7.2$ Hz, 2H, CH₂), 3.78 (s, 3H, OCH₃), 3.01 (t, $J = 5.6$ Hz, 2H, ArCH₂CH₂). **¹³C NMR** (75 MHz, CDCl₃, one of the methylene and ArC signals were not visible): δ (ppm) 49.95 (ArCH₂CH₂), 53.25 (CH₂), 55.42 (OCH₃), 113.13 (ArCH), 113.35 (ArCH), 119.29 (*imidazole-ArCH*), 123.52 (ArC), 127.40 (ArCH), 129.87 (ArC), 137.23 (*imidazole-ArCH*), 159.01 (ArCOMe), 178.24 (C=S).

8.9.2 General procedure for the synthesis of 1-[3,4 dihydroisoquinolin-2(1H)-yl]-3'-methyl-1H-imidazole-3-ium iodide

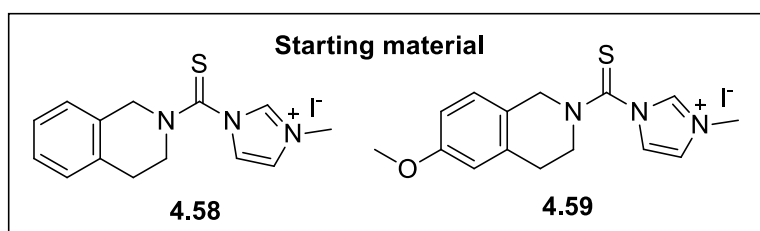


The general procedure described by Grzyb and co-worker¹³¹ was employed. Thus, a solution of **4.55** (110 mg, 0.400 mmol) in anhydrous CH₃CN (24.0 mL) was treated with MeI (0.200 mL, 3.32 mmol) and stirred at RT overnight. The reaction mixture was concentrated under reduced

pressure affording a brown froth in quantitative yields and was used as such without further purification.

Compound **4.50** was obtained in 80% (139 mg) yield. Yellow froth; $R_f = 0.00$ (100% EtOAc). $^1\text{H NMR}$ (400 MHz, CDCl_3): δ (ppm) 7.87 (s, 1H, *imidazole*-ArH), 7.25 (dd, $J = 10.5, 0.4$ Hz, 1H, *imidazole*-ArH), 7.08 (s, 1H, *imidazole*-ArH), 6.99 (s, 1H, ArH), 6.84 – 6.66 (m, 2H, 2xArH), 4.85 (s, 2H, ArCH_2N), 3.99 (d, 2H, CH_2), 3.77 (s, 3H, *imidazole*- CH_3), 3.01 (d, 2H, ArCH_2CH_2). $^{13}\text{C NMR}$ (75 MHz, CDCl_3 , one ArC signal was visible): δ (ppm) 28.65 (*imidazole*- CH_3), 49.73 (ArCH_2CH_2), 53.02 (CH_2), 55.20 (ArCH_2N), 113.01 (*imidazole*-ArCH), 119.09 (ArCH), 123.31 (ArCH), 127.17 (ArCH), 129.62 (ArCH), 134.95 (ArC), 137.04 (ArC), 158.76 (*imidazole*-NCHN), 177.93 (C=S). **HRMS ESI⁺**: m/z [M-126.9045]⁺ calcd for $\text{C}_{14}\text{H}_{16}\text{IN}_3\text{S}$, 258.1060; found, 258.1068 (3.10 ppm).

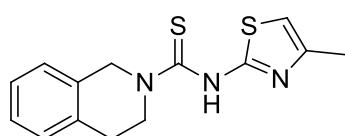
8.9.3 General procedure for the coupling of THIQ thiocarbamoyl imidazolium salts with heteroaryl amines



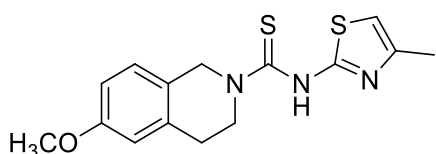
The general procedure described by Grzyb and co-workers¹³¹ was adopted. Thus, a mixture of the heteroaryl amine derivatives (**a**, **b**, **d**, **h**) (0.578 mmol) and K_2CO_3

(133 mg, 0.963 mmol) in anhydrous CH_3CN (15 mL) was stirred for 30 min at RT, to which the tetrahydroisoquinoline imidazolium salt (**4.58** or **4.59**) (4.81 mmol) was added. The reaction mixture was stirred at RT (however, for 2-amino-5-nitrothiazole the reaction was stirred at 120 °C) for 24 – 48 h (and monitored with TLC). The work-up procedure included partitioning of the reaction mixture between an aqueous 1 N HCl solution (15 mL x 2) and EtOAc (20 mL x 2). The organic layers were combined, dried over MgSO_4 , filtered and concentrated under reduced pressure providing a residue, purified with column chromatography (50:50 EtOAc/Hexane). The spectroscopic details of the compounds are described below:

N*-(4'-Methylthiazol-2-yl)-3,4-dihydroisoquinoline-2(1*H*)-carbothioamide **4.60a*



was obtained in 40% (80.0 mg) yield from 258 mg of starting material **4.58**. Yellow oil; $R_f = 0.73$ (20:80 EtOAc/Hexane). $^1\text{H NMR}$ (300 MHz, $\text{DMSO}-d_6$): δ (ppm) 12.45 (brs, 1H, NH), 7.19 (s, 4H, 4xArH), 6.32 (s, 1H, *thiazole*-ArH), 5.15 (s, 2H, ArCH_2N), 4.22 (t, $J = 5.9$ Hz, 2H, CH_2), 2.87 (t, $J = 5.9$ Hz, 2H, ArCH_2CH_2), 2.17 (s, 3H, *thiazole*- CH_3).

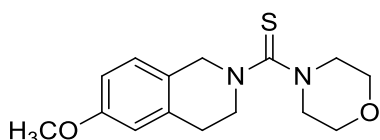
6-Methoxy-*N*-(4'-methylthiazol-2-yl)-3,4-dihydroisoquinoline-2(1*H*)-carbothioamide 4.61a

ide 4.61a was obtained in 80% (184 mg) yield from 284 mg of starting material **4.59**. Orange oil; $R_f = 0.63$ (40:60 EtOAc/Hexane). $^1\text{H NMR}$ (300 MHz, CDCl_3): δ (ppm) 12.42 (s, 1H, NH), 7.08 (d, $J = 7.3$ Hz, 1H, ArH), 6.86 – 6.67 (m, 2H, 2xArH), 6.30 (s, 1H, *thiazole*-ArH), 5.05 (s, 2H, ArCH_2N), 4.18 (t, $J = 5.9$ Hz, 2H, CH_2), 3.72 (s, 3H, OCH_3), 2.83 (t, $J = 5.9$ Hz, 2H, ArCH_2CH_2), 2.16 (s, 3H, *thiazole*- CH_3). $^{13}\text{C NMR}$ (75 MHz, CDCl_3 , two extra signals were visible in the aromatic region): δ (ppm) 29.20 (*thiazole*- CH_3), 46.71 (ArCH_2CH_2), 50.04 (CH_2), 55.45 (ArCH_2N), 55.49 (OCH_3), 112.66 (ArCH), 113.06 (ArCH), 114.10 (ArCH), 124.99 (ArC), 127.36 (ArCH), 127.56 (ArCH), 132.83 (ArCH), 136.42 (ArC), 157.71 (*thiazole*- ArCNH), 158.75 (ArCOMe), 182.29 ($\text{C}=\text{S}$). **HRMS ESI⁺**: m/z $[\text{M}+\text{H}]^+$ calcd for $\text{C}_{15}\text{H}_{17}\text{N}_3\text{OS}_2$, 320.0847; found, 320.0887 (3.13 ppm).

***N*-(3'-Chlorophenyl)-6-methoxy-3,4-dihydroisoquinoline-2(1*H*)-carbothioamide 4.61d**

4.61d was obtained in 6% (14.0 mg) yield from 291 mg of starting material **4.59**. White solid; **mp** = 184 – 186 °C; $R_f = 0.20$ (10:90 EtOAc/Hexane). $^1\text{H NMR}$ (300 MHz, CDCl_3): δ (ppm) 7.30 – 7.21 (m, 3H, 3xArH), 7.19 – 7.00

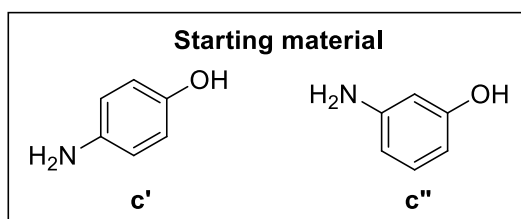
(m, 4H, 4xArH), 6.86 – 6.68 (m, 2H, 2xArH), 4.86 (s, 2H, ArCH_2N), 4.02 (t, $J = 5.7$ Hz, 2H, ArCH_2N), 3.80 (s, 3H, OCH_3), 2.96 (t, $J = 5.7$ Hz, 2H, ArCH_2CH_2). $^{13}\text{C NMR}$ (75 MHz, CDCl_3 , one of the aromatic signals could not be detected): δ (ppm) 29.34 (ArCH_2CH_2), 47.45 (CH_2), 50.75 (ArCH_2N), 55.73 (OCH_3), 113.07 (ArCH), 113.44 (ArCH), 122.43 (ArC), 124.33 (ArCH), 125.80 (ArCH), 127.81 (ArCH), 130.06 (ArCCl), 134.88 (ArCH), 136.42 (ArCH), 141.46 (ArCNH), 158.98 (ArCOMe), 183.48 ($\text{C}=\text{S}$). **HRMS ESI⁺**: m/z $[\text{M}+\text{H}]^+$ calcd for $\text{C}_{17}\text{H}_{17}\text{ClN}_2\text{OS}$, 333.0828 (^{35}Cl); found, 333.0821 (2.10 ppm) and 335.0786 (^{37}Cl).

[6-Methoxy-3,4-dihydroisoquinolin-2(1*H*)-yl](morpholino)methanethione 4.61h

obtained in 65% (220 mg) yield from 480 mg of starting material **4.59**. Yellow oil; $R_f = 0.25$ (30:70 EtOAc/Hexane). $^1\text{H NMR}$ (300 MHz, CDCl_3): δ (ppm) 7.01 (d, $J = 8.4$ Hz, 1H, ArH), 6.84 – 6.63 (m, 2H, 2xArH), 4.66 (s, 2H, ArCH_2N), 3.91 – 3.82 (m, 4H, *morpholine*-2x CH_2N), 3.81 – 3.64 (m, 7H, overlapping signals- *morpholine*-2x CH_2 and OCH_3), 3.62 – 3.50 (m, 4H, *morpholine*-overlapping signals- CH_2), 2.98 (t, $J = 5.8$ Hz, 2H, ArCH_2CH_2). $^{13}\text{C NMR}$ (75 MHz, CDCl_3): δ (ppm) 28.62 (ArCH_2CH_2), 49.07 (CH_2), 51.86

(*morpholine*-NCH₂), 52.82 (ArCH₂N), 55.13 (OCH₃), 66.30 (*morpholine*-CH₂O), 112.55 (ArCH), 113.18 (ArCH), 124.94 (ArCH), 126.98 (ArC), 135.59 (ArC), 158.29 (ArCOMe), 193.69 (C=S). **HRMS ESI⁺**: *m/z* [M+H]⁺ calcd for C₁₅H₂₀N₂O₂S, 293.1279; found, 293.1324 (3.41 ppm).

8.9.4 Method A: General procedure for the synthesis of isothiocyanates 4.64 from hydroxy anilines

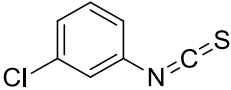


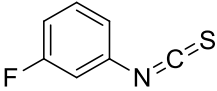
According to the general procedure described by Munch and co-workers,¹¹⁴ the corresponding aniline derivatives (**c'** or **c''**) (200 mg, ~1.83 mmol) were dissolved in analytical grade EtOH (20 mL), to which an excess of carbon disulphide (1.10 mL, 6.32

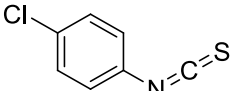
mmol) and Et₃N (0.260 mL, 1.83 mmol) were added at RT. Upon stirring for 30 min a precipitate became visible. Di-*tert*-butyl dicarbonate (Boc₂O) (380 mg, 1.76 mmol) and 4-dimethylaminopyridine (DMAP) (67.0 mg, 0.550 mmol, 10.0 mol%) was then added to the reaction mixture and stirred for 30 min (whilst monitored by TLC). Once complete, the reaction mixture was concentrated under reduced pressure to afford the product in moderate yields. No further purification was performed, and the compounds were used as is in the next reaction.

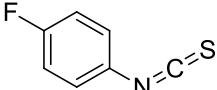
8.9.5 Method B: General procedure for the synthesis of isothiocyanates 4.64 from haloanilines

According to the general procedure described by Wong and co-workers,¹⁴⁵ the corresponding haloanilines (**d – g**) (200 mg, 1.83 mmol) were dissolved in anhydrous THF (20 mL), to which a 60% suspension of NaH in mineral oil (0.260 mL, 1.83 mmol) was added at 0 °C. The suspension was stirred at RT for 2 h, after which an excess of carbon disulphide (1.10 mL, 6.32 mmol) was added and stirring was continued for 24 h at RT. A precipitant was noted and tosyl chloride (380 mg, 1.76 mmol) was added. The reaction mixture was stirred overnight (whilst monitored by TLC). Once complete, the reaction mixture was quenched with an aqueous 1 N HCl (5.0 mL) solution and extracted with CH₂Cl₂ (15 mL x 3). The organic layers were concentrated under reduced pressure and purified with column chromatography (100% Hexane). The spectroscopic details of the compounds are described below:

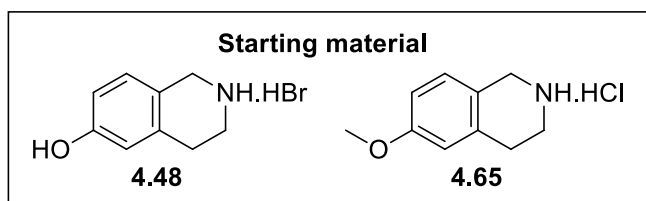
1-Chloro-3-isothiocyanatobenzene 4.64d was obtained in 34% (52.2 mg) yield from 98.0 mg of starting material **d**. Colourless oil; $R_f = 0.85$ (100% Hexane).  **$^1\text{H NMR}$** (300 MHz, CDCl_3): δ (ppm) 7.89 (s, 1H, ArH), 7.57 – 6.98 (m, 3H, 3xArH). **$^{13}\text{C NMR}$** (75 MHz, CDCl_3): δ (ppm) 123.24 (ArCH), 125.24 (ArCH), 127.36 (ArCH), 130.59 (ArCH), 135.09 (ArCN), 138.02 (ArCCL), 179.79 (C=S).

1-Fluoro-3-isothiocyanatobenzene 4.64e was obtained in 85% (150 mg) yield from 128 mg of starting material **e**. colourless oil; $R_f = 0.90$ (100% Hexane).  **$^1\text{H NMR}$** (300 MHz, CDCl_3): δ (ppm) 7.53 – 6.79 (m, 4H, 4xArH). **$^{13}\text{C NMR}$** (75 MHz, CDCl_3 , no C=S signal was visible): δ (ppm) 113.09 (d, $J = 25.5$ Hz, ArCH-F), 114.62 (d, $J = 21.00$ Hz, ArCH-F), 121.73 (ArCH), 130.68 (ArCH), 130.81 (ArCH).

1-Chloro-4-isothiocyanatobenzene 4.64f was obtained in 77% (200 mg) yield from 166 mg of starting material **f**. Yellow transparent oil; $R_f = 0.85$ (100% Hexane).  **$^1\text{H NMR}$** (300 MHz, CDCl_3): δ (ppm) 7.34 (dd, $J = 8.5, 1.6$ Hz, 2H, 2xArH), 7.22 – 7.12 (m, 2H, 2xArH). **$^{13}\text{C NMR}$** (75 MHz, CDCl_3 , no C=S signal was visible): δ (ppm) 126.99 (ArCH), 129.88 (ArCH).

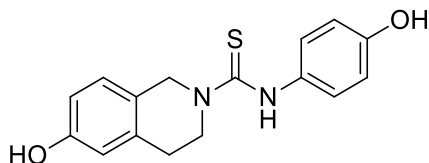
1-Fluoro-4-isothiocyanatobenzene 4.64g was obtained in 36% (90.0 mg) yield from 181 mg of starting material **g**. Yellow oil; $R_f = 0.85$ (100% Hexane).  **$^1\text{H NMR}$** (300 MHz, CDCl_3 , ArC signal was not clearly visible): δ (ppm) 7.28 – 7.13 (m, 2H, 2xArH), 7.11 – 6.97 (m, 2H, 2xArH). **$^{13}\text{C NMR}$** (75 MHz, CDCl_3 , no C=S signal was visible): δ (ppm) 116.48 (d, $J = 23.25$ Hz, ArCH-F), 127.13 (ArCH), 127.24 (ArCH).

8.9.6 General procedure for the coupling of isothiocyanates **4.64** with **4.65**

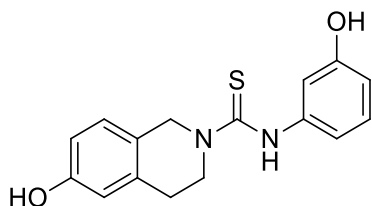


The general procedure described by Ganellin and co-workers²⁰² was adopted. Thus, a mixture of amines **4.48** or **4.65** (~0.782 mmol), isothiocyanates (**4.64**)

(140 mg, ~0.939 mmol) and Et_3N (0.330 mL, 2.35 mmol) in anhydrous MeCN (10 mL) were stirred overnight at 80 °C. The mixture was cooled to RT, partitioned between an aqueous saturated brine solution (5.0 mL) and EtOAc (20 mL x 2). The organic layers were combined, dried over MgSO_4 , concentrated under reduced pressure and the residue further purified using column chromatography (50:50 EtOAc/Hexane). The spectroscopic details of the compounds are described below:

6-Hydroxy-N-(4'-hydroxyphenyl)-3,4-dihydroisoquinoline-2(1H)-carbothioamide

4.66c' was obtained in 41% (110 mg) yield from 178 mg of starting material **4.48**. White solid; **mp** = 220 – 222 °C; R_f = 0.43 (50:50 EtOAc/Hexane). **¹H NMR** (300 MHz, DMSO-*d*₆): δ (ppm) 9.31 (d, J = 5.6 Hz, 2H, NH), 9.04 (s, 1H, OH), 7.06 – 6.94 (m, 2H, 2xArH), 6.72 – 6.58 (m, 3H, 3xArH), 4.88 (s, 2H, ArCH₂N), 3.98 (t, J = 6.0 Hz, 2H, CH₂), 2.85 (t, J = 6.0 Hz, 2H, ArCH₂CH₂). **¹³C NMR** (75 MHz, DMSO-*d*₆, ArC was not clearly visible): δ (ppm) 28.65 (ArCH₂CH₂), 46.05 (CH₂), 49.62 (ArCH₂N), 113.76 (ArCH), 114.75 (ArCH), 124.26 (ArCNH), 127.45 (ArC), 128.21 (ArCH), 132.58 (ArCH), 136.62 (ArC), 155.02 (ArCOH), 156.30 (ArCOH), 181.30 (C=S). **HRMS ESI⁺**: m/z [M+H]⁺ calcd for C₁₆H₁₆N₂O₂S, 301.1011; found, 301.1017 (2.00 ppm).

6-Hydroxy-N-(3'-hydroxyphenyl)-3,4-dihydroisoquinoline-2(1H)-carbothioamide

4.66c'' was obtained in 39% (92.5 mg) yield from 157 mg of starting material **4.48**. White solid; **mp** = 174 – 176 °C; R_f = 0.68 (50:50 EtOAc/Hexane). **¹H NMR** (300 MHz, DMSO-*d*₆): δ (ppm) 9.31 (s, 1H, NH), 8.32 (s, 1H, OH), 7.44 – 7.29 (m, 2H, 2xArH), 7.16 – 7.02 (m, 4H, 4xArH), 6.66 – 6.61 (m, 2H, 2xArH), 4.68 (s, 2H, ArCH₂N), 3.83 (t, J = 6.0 Hz, 2H, CH₂), 2.88 (t, J = 6.0 Hz, 2H, ArCH₂CH₂). **¹³C NMR** (75 MHz, DMSO-*d*₆): δ (ppm) 28.04 (ArCH₂CH₂), 43.12 (CH₂), 46.64 (ArCH₂N), 109.19 (ArCH), 114.00 (ArCH), 115.13 (ArCH), 116.01 (ArCH), 120.65 (ArCH), 123.03 (ArCH), 124.25 (ArC), 127.61 (ArCH), 135.43 (ArC), 143.37 (ArCNH), 148.67 (ArCOH), 156.23 (ArCOH), 162.07 (C=S). **HRMS ESI⁺**: m/z [M+H]⁺ calcd for C₁₆H₁₆N₂O₂S, 301.1011; found, 301.1023 (2.00 ppm).

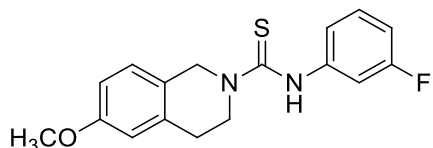
N-(3'-Chlorophenyl)-6-methoxy-3,4-dihydroisoquinoline-2(1H)-carbothioamide

4.66d was obtained in 6% (14.0 mg) yield from 140 mg of starting material **4.48**. White solid; **mp** = 184 – 186 °C; R_f = 0.20 (10:90 EtOAc/Hexane). **¹H NMR** (300 MHz, CDCl₃): δ (ppm) 7.30 – 7.21 (m, 3H, 3xArH), 7.19 – 7.00 (m, 4H, 4xArH), 6.86 – 6.68 (m, 2H, 2xArH), 4.86 (s, 2H, ArCH₂N), 4.02 (t, J = 5.7 Hz, 2H, ArCH₂N), 3.80 (s, 3H, OCH₃), 2.96 (t, J = 5.7 Hz, 2H, ArCH₂CH₂). **¹³C NMR** (75 MHz, CDCl₃, one ArC signal was not able to be identified): δ (ppm) 29.34 (ArCH₂CH₂), 47.45 (CH₂), 50.75 (ArCH₂N), 55.73 (OCH₃), 113.07 (ArCH), 113.44 (ArCH), 122.43 (ArC), 124.33 (ArCH), 125.80 (ArCH), 127.81 (ArCH), 130.06

(ArCCl), 134.88 (ArCH), 136.42 (ArCH), 141.46 (ArCNH), 158.98 (ArCOMe), 183.48 (C=S).

HRMS ESI⁺: m/z [M+H]⁺ calcd for C₁₇H₁₇ClN₂OS, 333.0828 (³⁵Cl); found, 333.0821 (2.10 ppm) and 335.0786 (³⁷Cl).

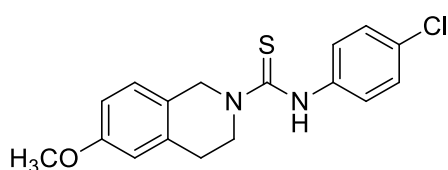
***N*-(3'-Fluorophenyl)-6-methoxy-3,4-dihydroisoquinoline-2(1*H*)-carbothioamide**



4.66e was obtained in 56% (146 mg) yield from 165 mg of starting material **4.48**. White solid; **mp** = 184 – 186 °C; R_f = 0.53 (50:50 EtOAc/Hexane). **¹H NMR** (300 MHz, CDCl₃):

δ (ppm) 7.31 – 7.28 (m, 2H, 2xArH overlapping with CDCl₃), 7.14 – 6.75 (m, 6H, 5xArH and NH), 4.87 (s, 2H, ArCH₂N), 4.03 (t, J = 5.9 Hz, 2H, CH₂), 3.82 (s, 3H, OCH₃), 2.98 (t, J = 5.9 Hz, 2H, ArCH₂CH₂). **¹³C NMR** (75 MHz, CDCl₃, not all ArC were visible): δ (ppm) 29.26 (ArCH₂CH₂), 47.54 (CH₂), 50.89 (ArCH₂N), 55.66 (OCH₃), 111.29 (d, J = 24.0 Hz, ArCH-F), 112.36 (d, J = 17.25 Hz, ArCH-F), 113.18 (d, J = 28.5 Hz, ArCH-F), 119.33 (ArCH), 127.73 (ArC), 130.47 (ArCH), 136.40 (ArC).

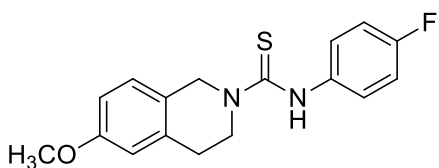
***N*-(4'-Chlorophenyl)-6-methoxy-3,4-dihydroisoquinoline-2(1*H*)-carbothioamide**



4.66f was obtained in 79% (150 mg) yield from 114 mg of starting material **4.48**. White solid; **mp** = 170 – 171 °C; R_f = 0.33 (30:70 EtOAc/Hexane). **¹H NMR** (300 MHz, CDCl₃, two extra ArH are attributed to overlapping of the

CDCl₃ signal and the NH signal in the aromatic region): δ (ppm) 7.32 – 7.17 (m, 2H, 2xArH), 7.07 – 7.04 (m, 3H, 3xArH), 6.80 – 6.75 (m, 2H, 2xArH), 4.88 (s, 2H, ArCH₂N), 4.02 (t, J = 5.5 Hz, 2H, CH₂), 3.81 (m, 2H, OCH₃), 2.96 (t, J = 5.5 Hz, 2H, ArCH₂CH₂). **¹³C NMR** (75 MHz, CDCl₃): δ (ppm) 29.35 (ArCH₂CH₂), 47.27 (CH₂), 50.59 (OCH₃), 55.68 (ArCH₂N), 113.01 (ArCH), 113.38 (ArCH), 124.66 (ArC), 126.12 (ArCH), 127.77 (ArCH), 129.38 (ArCH), 131.07 (ArCCl), 137.85 (ArC), 138.78 (ArCNH), 159.13 (ArCOMe), 182.66 (C=S). **HRMS ESI⁺**: m/z [M+H]⁺ calcd for C₁₇H₁₇ClN₂OS, 333.0721 (³⁵Cl); found, 333.0825 (2.99 ppm).

***N*-(4'-Fluorophenyl)-6-methoxy-3,4-dihydroisoquinoline-2(1*H*)-carbothioamide**



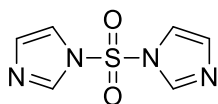
4.66g was obtained in 62% (161 mg) yield from 164 mg of starting material **4.48**. White solid; **mp** = 156 – 158 °C; R_f = 0.44 (30:70 EtOAc/Hexane). **¹H NMR** (300 MHz, CDCl₃):

δ (ppm) 7.27 – 7.20 (m, 2H, ArH and NH), 7.08 – 7.01 (m, 4H, 4xArH), 6.81 – 6.75 (m, 2H, 2xArH), 4.89 (s, 2H, ArCH₂N), 4.03 (t, J = 5.9 Hz, 2H, CH₂),

3.81 (s, 3H, OCH₃), 2.97 (t, *J* = 5.9 Hz, 2H, ArCH₂CH₂). ¹³C NMR (75 MHz, CDCl₃): δ (ppm) 29.16 (ArCH₂CH₂), 46.84 (CH₂), 50.14 (OCH₃), 55.44 (ArCH₂N), 112.93 (d, *J* = 28.5 Hz, ArCH–F), 115.84 (d, *J* = 22.5 Hz, ArCH–F), 124.73 (ArCH), 127.09 (ArCH), 127.20 (ArC), 135.52 (ArCNH), 136.33 (ArCH), 158.91 (ArCOMe), 182.52 (C=S).

8.10 Synthesis of sulfonyl urea analogues

8.10.1 General procedure for the synthesis of 1,1 – sulfonyl bisimidazole 4.72

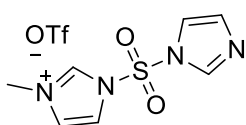


The general procedure described by Cívicos and co-workers¹⁴⁷ for the synthesis of 1,1 – sulfonyl bisimidazole was adopted. Thus, sulfonyl chloride (0.740 mL, 9.19 mmol) was slowly added to a cooled (0°C) solution of imidazole (2.00 g, 37.0 mmol) in anhydrous CH₂Cl₂ (50 mL). The reaction mixture was monitored by TLC and after starting material had been consumed, the reaction mixture was filtered, and the resulting filtrate partitioned between water (20 mL) and CH₂Cl₂. Extraction with CH₂Cl₂ (25 mL x 2) followed by removal of the organic layer under reduced pressure provided a white solid which was recrystallized from IPA to afford white crystals of product **4.72** (1.54 g) in 97% yield. White crystals; **mp** = 128 – 129 °C; *R_f* = 0.30 (100% EtOAc). ¹H NMR (400 MHz, CDCl₃): δ (ppm) 8.04 (s, 1H, ArH), 7.31 (d, *J* = 1.3 Hz, 1H, ArH), 7.17 (s, 1H, ArH). **HRMS ESI⁺**: *m/z* [M+H]⁺ calcd for C₆H₆N₄O₂S, 199.0245; found, 199.0294 (5.01 ppm). The experimental spectroscopic data, corresponded with literature as reported by Cívicos and co-workers.¹⁴⁷

8.10.2 General procedure for the preparation of sulfamoyl imidazolium salts 4.73

The general procedure described by Beaudoin and co-workers¹⁴⁰ was adopted. Thus, methyl triflate (0.310 mL, 2.77 mmol) was slowly added to a cooled (0°C) solutions of the different sulfamoyl imidazoles (**4.72**) (~2.52 mmol) in anhydrous CH₂Cl₂ (10 mL) and stirred for 4 h at 0°C. The reaction mixtures were concentrated under reduced pressure, yielding product with no further purification required and the crude material was used as is in subsequent reactions.

1-(1*H*-imidazol-1-ylsulfonyl)-3-methyl-1*H*-imidazol-3-ium trifluoromethane

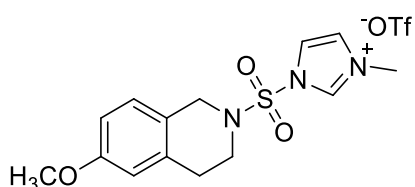


sulfonate 4.73 was obtained in 83% (1.82 g) yield from 1.23 g of starting material **4.72**. White powder; **mp** = 84 – 85 °C; *R_f* = 0.00 (100% EtOAc).

Due to the hygroscopic nature of the triflate salt, the crude material was used as such in subsequent reactions and for NMR analysis. ¹H NMR (400 MHz, CD₃OD):

δ (ppm) 8.91 (s, 1H, ArH), 8.45 (s, 1H, ArH), 7.77 (d, $J = 1.5$ Hz, 1H, ArH), 7.62 – 7.51 (m, 2H, 2xArH), 7.18 (d, $J = 0.9$ Hz, 1H, ArH), 3.98 (s, 3H, CH₃). **¹³C NMR** (101 MHz, CD₃OD): δ (ppm) 23.12 (CH₃), 73.50 (ArCH), 119.45 (ArCH), 120.32 (ArCH), 120.85 (ArCH), 124.31 (ArCH), 132.46 (ArCH), 135.17 (ArCH), 136.82 (ArCH), 138.80 (ArCH). **HRMS ESI⁺**: m/z [M-149.0697]⁺ calcd for C₇H₉N₄O₂S⁺, 213.0441; found, 213.0428 (4.71 ppm).

1-[6-Methoxy-3,4-dihydroisoquinolin-2(1H)-yl]sulfonyl-3'-methyl-1H-imidazol-3

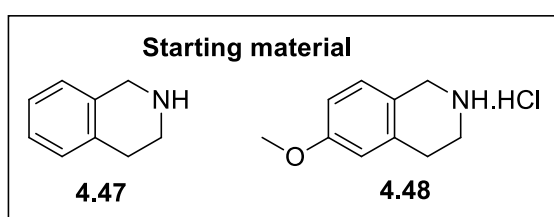


-ium trifluoromethane sulfonate **4.76** was obtained in 87% (563 mg) yield from 416 mg of starting material **4.48**. Beige semi-solid; **mp** = RT (hygroscopic and when handled at RT, it melted forming a brown oil); $R_f = 0.00$ (100% EtOAc).

¹H NMR (300 MHz, DMSO-*d*₆): δ (ppm) 9.60 (m, 1H, *imidazole*-ArH), 8.04 (d, $J = 2.0$ Hz, 1H, *imidazole*-ArH), 7.76 – 7.67 (m, 1H, *imidazole*-ArH), 7.11 (d, $J = 8.5$ Hz, 1H, ArH), 6.82 (dd, $J = 8.5, 2.6$ Hz, 1H, ArH), 6.75 (d, $J = 2.6$ Hz, 1H, ArH), 4.64 (s, 2H, ArCH₂N), 3.98 (s, 3H, OCH₃), 3.86 – 3.74 (m, 5H, overlapping signals-CH₂ and CH₃), 2.99 (t, $J = 6.2$ Hz, 2H, ArCH₂CH₂). **¹³C NMR** (75 MHz, DMSO-*d*₆, one methylene signal was not visible): δ (ppm) 29.03 (*imidazole*-CH₃), 37.43 (ArCH₂CH₂), 46.36 (ArCH₂N), 55.90 (OCH₃), 114.33 (ArCH), 114.62 (ArCH), 121.95 (ArC), 123.32 (ArCH), 126.52 (ArC), 128.64 (*imidazole*-ArCH), 135.32 (*imidazole*-ArCH), 139.18 (*imidazole*-ArCH), 160.60 (ArCOMe).

8.10.3 General procedure for the synthesis of

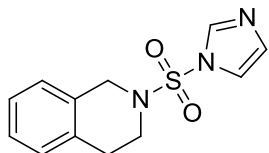
2-[(1H-Imidazol-1-yl)sulfonyl]-1,2,3,4- tetrahydroisoquinolines **4.64** and **4.75**



The general procedure described by Beaudoin and co-workers¹⁴⁰ was implemented as follows. THIQ analogues (**4.47** or **4.48**) (1.00 mmol) were added to a cooled (0°C) mixture of **4.64** (400 mg, 1.10 mmol) in anhydrous CH₂Cl₂ (50 mL), which

was gradually allowed to heat to RT and stirred for 18 h. Once complete, the reaction mixture was concentrated under reduced pressure and provided a residue, which was further purified by column chromatography (50:50 EtOAc/Hexane). Since the usual tendency is for the dimer to preferably form. It was necessary to dilute the solution and maintain low temperatures during the protocol. The spectroscopic details of the compounds are described below:

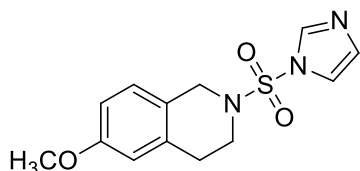
2-[(1*H*-Imidazol-1-yl)sulfonyl]-1,2,3,4-tetrahydroisoquinoline 4.64 was obtained in



61% (179 mg) yield from 148 mg of starting material **4.47**. Yellow oil; $R_f = 0.48$ (50:50 EtOAc/Hexane). $^1\text{H NMR}$ (400 MHz, CDCl_3 , none of the *imidazole*-ArH signals were visible): δ (ppm) 7.94 (s, 1H, ArH),

7.29 – 7.00 (m, 3H, 3xArH), 4.41 (s, 2H, ArCH₂N), 3.52 (t, $J = 6.0$ Hz, 2H, CH₂), 2.91 (t, $J = 6.0$ Hz, 2H, ArCH₂CH₂). $^{13}\text{C NMR}$ (101 MHz, CDCl_3): δ (ppm) 28.13 (ArCH₂CH₂), 44.24 (CH₂), 47.68 (ArCH₂N), 117.49 (*imidazole*-ArCH), 126.17 (ArCH), 126.81 (ArCH), 127.35 (ArCH), 128.87 (ArCH), 129.92 (ArCH), 130.65 (*imidazole*-ArCH), 132.24 (ArC), 136.67 (*imidazole*-NCHN). **HRMS ESI⁺**: m/z [M+H]⁺ calcd for C₁₂H₁₃N₃O₂S, 264.0762; found, 264.0814 (19.7 ppm).

2-[(1*H*-Imidazol-1-yl)sulfonyl]-6-methoxy-1,2,3,4-tetrahydroisoquinoline 4.75 was



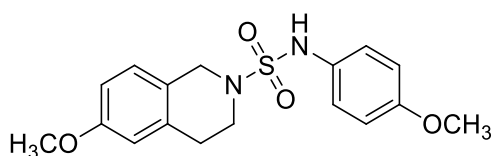
obtained in 70% (408 mg) yield from 396 mg of starting material **4.48**. Transparent oil; $R_f = 0.58$ (100% EtOAc). $^1\text{H NMR}$ (300 MHz, CDCl_3): δ (ppm) 7.93 (d, $J = 3.0$ Hz, 1H, *imidazole*-ArH),

7.31 (d, $J = 3.0$ Hz, 1H, *imidazole*-ArH), 7.15 (d, $J = 3.0$ Hz, 1H, *imidazole*-ArH), 6.96 (d, $J = 8.5$ Hz, 1H, ArH), 6.75 (dd, $J = 8.5, 2.5$ Hz, 1H, ArH), 6.61 (d, $J = 2.5$ Hz, 1H, ArH), 4.35 (s, 2H, ArCH₂N), 3.76 (s, 3H, OCH₃), 3.51 (t, $J = 6.0$ Hz, 2H, CH₂), 2.88 (t, $J = 6.0$ Hz, 2H, ArCH₂CH₂). **HRMS ESI⁺**: m/z [M+H]⁺ calcd for C₁₃H₁₅N₃O₃S, 294.0914; found, 294.0908 (1.40 ppm).

8.10.4 General procedure for the coupling of 4.76 with heteroaryl amines

A modified procedure, based on the general procedure described by Beaudoin and co-workers¹⁴⁰ was implemented as follows. Aniline analogues (**c – g**) (~0.739 mmol) were added to a solution of the sulfamoyl imidazolium salt **4.76** (~200 mg, 0.615 mmol) in anhydrous CH₃CN (20 mL) and stirred at RT overnight yielding product. However, for the haloanilines (**d – g**) heating under reflux was required. The spectroscopic details of the compounds are described below:

6-Methoxy-*N*-(4'-methoxyphenyl)-3,4-dihydroisoquinoline-2(1*H*)-sulfonamide

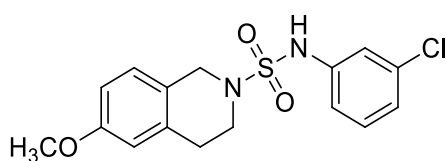


4.77c was obtained in 87% (122 mg) yield from 184 mg of starting material **4.76** as a brown oil, which solidified at low temperatures; $R_f = 0.41$ (50:50 EtOAc/Hexane). $^1\text{H NMR}$ (300 MHz, CDCl_3): δ (ppm)

7.13 (dd, $J = 8.9, 0.9$ Hz, 2H, 2xArH), 6.99 – 6.86 (m, 2H, 2xArH), 6.83 – 6.67 (m, 3H,

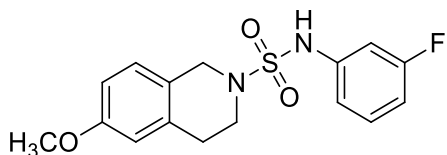
3xArH), 6.60 (s, 1H, NH), 4.39 (s, 2H, ArCH₂N), 3.86 (s, 3H, OCH₃), 3.65 (s, 3H, OCH₃), 3.49 (t, *J* = 5.6 Hz, 2H, CH₂), 2.76 (t, *J* = 5.6 Hz, 2H, ArCH₂CH₂). **¹³C NMR** (75 MHz, CDCl₃): δ (ppm) 29.25 (ArCH₂CH₂), 44.22 (CH₂), 47.30 (ArCH₂N), 55.49 (2xOCH₃), 112.85 (ArCH), 113.56 (ArCH), 114.58 (ArCH), 124.24 (ArCH), 124.56 (ArCH), 127.40 (ArC), 129.61 (ArCNH), 134.73 (ArC), 157.64 (ArCOMe), 158.40 (ArCOMe). **HRMS ESI⁺**: *m/z* [M+H]⁺ calcd for C₁₇H₂₀N₂O₄S, 349.1177; found, 349.1207 (2.87 ppm).

***N*-(3'-Chlorophenyl)-6-methoxy-3,4-dihydroisoquinoline-2(1*H*)-sulfonamide**

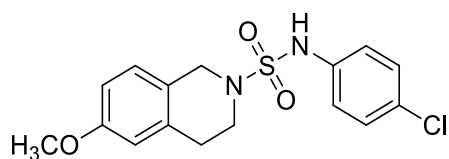


4.77d was obtained in 83% (130 mg) yield from 202 mg of starting material **4.76**. Orange oil; *R_f* = 0.22 (15:85 EtOAc/Hexane). **¹H NMR** (300 MHz, CDCl₃): δ (ppm) 7.37 – 6.86 (m, 4H, 4xArH), 6.84 – 6.48 (m, 3H, 3xArH), 4.43 (d, *J* = 3.9 Hz, 2H, ArCH₂N), 3.68 (brm, 5H, overlapping signals–OCH₃ and CH₂), 3.00 – 2.67 (m, 2H, ArCH₂CH₂). **¹³C NMR** (75 MHz, CDCl₃, one aromatic signal was not visible): δ (ppm) 28.99 (ArCH₂CH₂), 44.27 (CH₂), 47.30 (ArCH₂N), 55.41 (OCH₃), 113.01 (ArCH), 113.61 (ArCH), 118.02 (ArCH), 120.02 (ArCH), 123.84 (ArCH), 124.66 (ArC), 127.40 (ArCH), 130.42 (ArC), 134.48 (ArCCl), 135.04 (ArCNH), 138.45 (ArCOMe). **HRMS ESI⁺**: *m/z* [M+H]⁺ calcd for C₁₆H₁₇ClN₂O₃S, 351.0570 (³⁵Cl); found, 351.0551 (5.40 ppm).

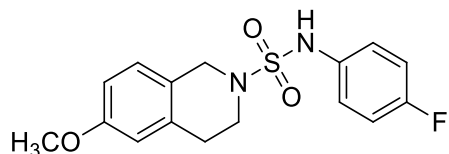
N*-(3'-Fluorophenyl)-6-methoxy-3,4-dihydroisoquinoline-2(1*H*)-sulfonamide **4.77e*



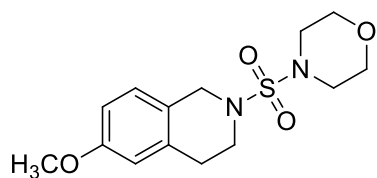
was obtained in 46% (70.0 mg) yield from 207 mg of starting material **4.76**. Colourless oil; *R_f* = 0.37 (30:70 EtOAc/Hexane). **¹H NMR** (300 MHz, CDCl₃): δ (ppm) 7.20 (m, 2H, 2xArH), 6.99 – 6.67 (m, 4H, 4xArH), 6.60 (d, *J* = 2.3 Hz, 1H, ArH), 4.42 (s, 2H, ArCH₂N), 3.80 – 3.51 (m, 5H, overlapping signals–OCH₃ and CH₂), 2.81 (t, *J* = 5.9 Hz, 2H, ArCH₂CH₂). **¹³C NMR** (75 MHz, CDCl₃, no C–F coupling was visible): δ (ppm) 29.05 (ArCH₂CH₂), 44.25 (CH₂), 47.29 (ArCH₂N), 55.41 (OCH₃), 107.04 (ArCH), 107.38 (ArCH), 111.16 (ArCH), 111.44 (ArCH), 113.00 (ArCH), 113.60 (ArCH), 115.28 (ArCH), 123.84 (ArCH), 127.41 (ArC), 130.64 (ArCH), 134.49 (ArC), 138.86 (ArCNH), 158.52 (ArCOMe), 164.86 (ArCF). **HRMS ESI⁺**: *m/z* [M+H]⁺ calcd for C₁₆H₁₈N₂O₃FS, 337.1022 (¹⁸F); found, 337.1024 (0.60 ppm) and 338.1052 (¹⁹F).

***N*-(4'-Chlorophenyl)-6-methoxy-3,4-dihydroisoquinoline-2(1*H*)-sulfonamide 4.77f**

was obtained in 54% (81.2 mg) yield from 194 mg of starting material **4.76**. Brown translucent oil; $R_f = 0.22$ (15:85 EtOAc/Hexane). $^1\text{H NMR}$ (300 MHz, CDCl_3): δ (ppm) 7.22 – 7.19 (m, 3H, 3xArH), 7.10 – 7.06 (m, 2H, 2xArH), 6.94 – 6.91 (m, 1H, ArH), 6.73 – 6.70 (m, 1H, ArH), 6.60 (brs, 1H, NH), 4.48 (s, 2H, ArCH_2N), 3.84 (s, 3H, OCH_3), 3.61 (t, $J = 5.9$ Hz, 2H, CH_2), 2.86 (t, $J = 5.9$ Hz, 2H, ArCH_2CH_2). $^{13}\text{C NMR}$ (75 MHz, CDCl_3): δ (ppm) 29.21 (ArCH_2CH_2), 44.44 (CH_2), 47.49 (ArCH_2N), 55.60 (OCH_3), 113.13 (ArCH), 113.81 (ArCH), 121.88 (ArCH), 124.05 (ArC), 127.59 (ArCH), 129.65 (ArC), 130.29 (ArCH), 134.66 (ArCNH), 135.96 (ArCCl), 158.71 (ArCOMe). **HRMS ESI⁺**: m/z $[\text{M}+\text{H}]^+$ calcd for $\text{C}_{16}\text{H}_{17}\text{ClN}_2\text{O}_3\text{S}$, 353.0727 (^{35}Cl); found, 353.0723 (1.10 ppm) and 355.0706 (^{37}Cl).

***N*-(4'-Fluorophenyl)-6-methoxy-3,4-dihydroisoquinoline-2(1*H*)-sulfonamide 4.77g**

was obtained in 94% (190 mg) yield from 274 mg of starting material **4.76**. Colourless oil; $R_f = 0.37$ (30:70 EtOAc/Hexane). $^1\text{H NMR}$ (300 MHz, CDCl_3): δ (ppm) 7.01 – 6.95 (m, 2H, 2xArH), 6.78 – 6.77 (m, 3H, 3xArH), 6.74 – 6.63 (m, 1H, ArH), 6.61 (m, 1H, ArH), 6.31 (brs, 1H, NH), 4.40 (s, 2H, ArCH_2N), 3.77 (s, 3H, OCH_3), 3.51 (t, $J = 5.9$ Hz, 2H, CH_2), 2.78 (t, $J = 5.9$ Hz, 2H, ArCH_2CH_2). No $^{13}\text{C NMR}$ was included, despite best efforts, the spectrum was not very clear and therefore not incorporated in the experimental section. **HRMS ESI⁺**: m/z $[\text{M}+\text{H}]^+$ calcd for $\text{C}_{16}\text{H}_{18}\text{N}_2\text{O}_3\text{FS}$, 337.1022 (^{18}F); found, 337.1018 (1.80 ppm) and 338.1044 (^{19}F).

4-[[6-Methoxy-3,4-dihydroisoquinolin-2(1*H*)-yl]sulfonyl]morpholine 4.77h

obtained in 67% (120 mg) yield from 262 mg of starting material **4.76**. White amorphous solid; **mp** = 119 – 121 °C; $R_f = 0.44$ (40:60 EtOAc/Hexane). $^1\text{H NMR}$ (300 MHz, CDCl_3): δ (ppm) 6.99 (d, $J = 8.4$ Hz, 1H, ArH), 6.82 – 6.71 (m, 1H, ArH), 6.67 (s, 1H, ArH), 4.39 (s, 2H, ArCH_2N), 3.85 – 3.64 (m, 7H, overlapping signals— OCH_3 and $\text{morpholine-2xOCH}_2$), 3.54 (t, $J = 5.9$ Hz, 2H, CH_2), 3.28 – 3.15 (m, 4H, $\text{morpholine-2xNCH}_2$), 2.91 (t, $J = 5.9$ Hz, 2H, ArCH_2CH_2). $^{13}\text{C NMR}$ (75 MHz, CDCl_3): δ (ppm) 29.31 (ArCH_2CH_2), 44.12 ($\text{morpholine-2xNCH}_2$), 46.55 (CH_2), 47.60 (ArCH_2N), 55.44 (OCH_3), 66.49 ($\text{morpholine-2xOCH}_2$), 112.98 (ArCH), 113.71 (ArCH), 124.44 (ArCH),

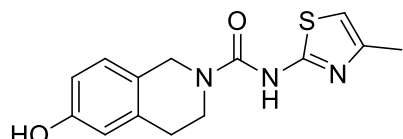
127.43 (ArC), 134.63 (ArC), 158.53 (ArCOMe). **HRMS ESI⁺**: m/z [M+H]⁺ calcd for C₁₄H₂₀N₂O₄S, 313.1222; found, 313.1218 (1.30 ppm).

8.11 Deprotection of aryl methyl ethers

8.11.1 General procedure for the demethylation using BBr₃

A general procedure described by McOmie and co-workers¹²¹ was adopted and performed as followed. Thus, a mixture of 1 M BBr₃ (0.190 mL, 1.97 mmol) in anhydrous CH₂Cl₂ (1.90 mL) was prepared using a Schlenk tube cooled to -78 °C, to which compounds **4.46**, **4.80** and **4.74** (0.659 mmol) in anhydrous CH₂Cl₂ (0.50 mL) were slowly added. The reaction mixture was stirred for 2 h at -60 °C followed by stirring for an additional 4 h (while being monitored by TLC) at RT. Ethanol was then slowly added until fuming ceased, after which the reaction mixture was poured into an aqueous saturated NaHCO₃ solution (15 mL) and extracted with EtOAc (20 mL x 3). The organic layers were combined, dried over MgSO₄, concentrated under reduced pressure and purified with column chromatography (40:60 EtOAc/Hexane). The following compounds were synthesised in this manner.

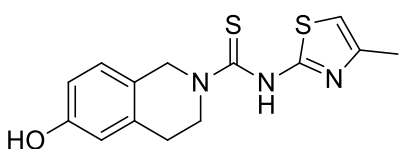
6-Hydroxy-*N*-(4'-methylthiazol-2-yl)-3,4-dihydroisoquinoline-2(1*H*)-carboxamide



4.46a was obtained in 64% (49.0 mg) yield from 0.80 mg of starting material **4.54a**. Yellow solid; mp = 199 – 200 °C; R_f = 0.22 (50:50 EtOAc/Hexane). **¹H NMR** (300 MHz, DMSO-*d*₆)

δ (ppm) 6.36 – 6.33 (s, 1H, ArH), 6.05 – 5.99 (m, 2H, 2xArH), 5.79 (s, 1H, *thiazole*-ArH), 4.29 (brs, 2H, NH and OH), 3.98 (s, 2H, ArCH₂N), 3.13 – 3.09 (m, 2H, NCH₂), 2.19 (t, *J* = 5.9 Hz, 2H, ArCH₂CH₂), 1.63 (d, *J* = 1.1 Hz, 3H, *thiazole*-CH₃). **¹³C NMR** (75 MHz, DMSO-*d*₆, no C=O signal was visible) δ 6.75 (*thiazole*-CH₃), 20.56 (ArCH₂CH₂), 33.43 (CH₂), 36.99 (ArCH₂N), 70.10 (*thiazole*-ArCH), 97.49 (ArCH), 105.44 (ArCH), 106.40 (ArC), 115.89 (ArCH), 118.91 (ArC), 127.82 (*thiazole*-ArC), 134.47 (ArCNH), 147.77 (C=O), 148.56 (ArCOH). **HRMS ESI⁺**: m/z [M+H]⁺ calcd for C₁₇H₂₀N₂O₄S, 290.0963; found, 290.0955 (2.80 ppm).

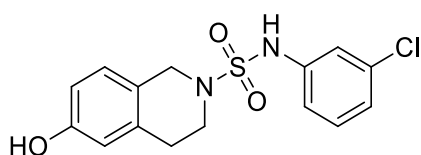
6-Hydroxy-*N*-(4'-methylthiazol-2-yl)-3,4-dihydroisoquinoline-2(1*H*)-carbothioamide



4.80a was obtained in 36% (54.0 mg) yield from 157 mg of starting material **4.61a**. Orange oil; R_f = 0.37 (40:60 EtOAc/Hexane). **¹H NMR** (300 MHz, DMSO-*d*₆): δ (ppm) 6.19 – 6.15 (m, 1H, ArH), 5.83 – 5.79 (m, 2H, 2xArH), 5.60

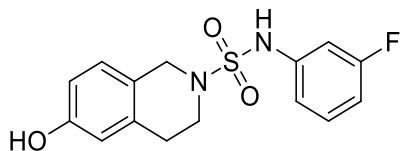
(s, 1H, *thiazole*-ArH), 3.79 (s, 2H, ArCH₂N), 2.96 – 2.90 (m, 2H, NCH₂), 2.02 – 1.98 (m, 2H, ArCH₂CH₂), 1.43 (s, 3H, *thiazole*-CH₃). ¹³C NMR (75 MHz, DMSO-*d*₆, C=S and one ArC signal was not visible): δ (ppm) 6.65 (*thiazole*-CH₃), 20.55 (ArCH₂CH₂), 33.45 (CH₂), 36.98 (ArCH₂N), 97.39 (ArCH), 101.63 (ArCH), 105.40 (ArC), 106.36 (ArC), 115.93 (ArCH), 118.80 (ArCH), 127.82 (ArCNH), 147.60 (ArCOH). HRMS ESI⁺: *m/z* [M+H]⁺ calcd for C₁₇H₂₀N₂O₄S, 306.0735; found, 306.0722 (4.20 ppm).

***N*-(3'-Chlorophenyl)-6-hydroxy-3,4-dihydroisoquinoline-2(1*H*)-sulfonamide 4.74d**

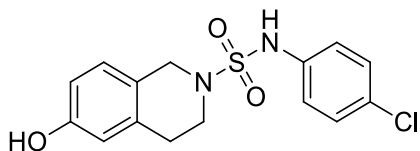


was obtained in 34% (41.0 mg) yield from 126 mg of starting material **4.77d**. Colourless oil; *R_f* = 0.41 (50:50 EtOAc/Hexane). ¹H NMR (300 MHz, CDCl₃): δ (ppm) 7.28 – 7.24 (m, 1H, NH), 7.18 (d, *J* = 8.0 Hz, 1H, ArH), 7.13 – 6.96 (m, 2H, 2xArH), 6.90 (d, *J* = 8.3 Hz, 1H, ArH), 6.71 – 6.51 (m, 2H, 2xArH), 4.71 (brs, 1H, OH), 4.41 (s, 2H, ArCH₂N), 3.55 (t, *J* = 6.0 Hz, 2H, NCH₂), 2.77 (t, *J* = 6.0 Hz, 2H, ArCH₂CH₂). ¹³C NMR (75 MHz, CDCl₃): δ (ppm) 28.98 (ArCH₂CH₂), 44.40 (CH₂), 47.52 (ArCH₂N), 114.32 (ArCH), 115.47 (ArCH), 118.36 (ArCH), 120.38 (ArCH), 121.27 (ArC), 124.14 (ArCH), 124.99 (ArCH), 127.78 (ArCH), 130.65 (ArCCl), 134.96 (ArC), 135.29 (ArCNH), 154.63 (ArCOH). HRMS ESI⁺: *m/z* [M+H]⁺ calcd for C₁₅H₁₅ClN₂O₃S, 339.0570 (³⁵Cl); found 339.0570 (0.00 ppm) and 341.0549 (³⁷Cl).

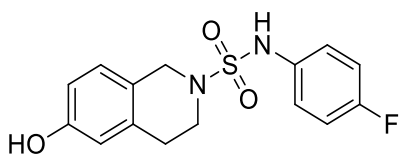
***N*-(3'-Fluorophenyl)-6-hydroxy-3,4-dihydroisoquinoline-2(1*H*)-sulfonamide 4.74e**



was obtained in 10% (6.49 mg) yield from 643 mg of starting material **4.77e**. Brown oil; *R_f* = 0.32 (50:50 EtOAc/Hexane). ¹H NMR (300 MHz, CDCl₃): δ (ppm) 7.38 – 7.08 (m, 2H, ArH and NH), 7.01 – 6.44 (m, 6H, 6xArH), 4.87 (s, 1H, OH), 4.41 (d, *J* = 6.0 Hz, 2H, ArCH₂N), 3.54 (t, *J* = 6.0 Hz, 2H, NCH₂), 2.77 (t, *J* = 6.0 Hz, 2H, ArCH₂CH₂). ¹³C NMR (75 MHz, CDCl₃): δ (ppm) 29.04 (ArCH₂CH₂), 44.38 (CH₂), 47.57 (ArCH₂N), 107.55 (d, *J* = 25.5 Hz, ArCH-F), 111.65 (d, *J* = 30.75 Hz, ArCH-F), 114.29 (ArCH), 115.45 (ArCH), 115.57 (ArCH), 115.61 (ArC), 124.14 (ArCH), 127.79 (ArCH), 130.81 (ArCH), 130.94 (ArC), 134.97 (ArCH), 148.55 (ArCNH), 154.64 (ArCOH). HRMS ESI⁺: *m/z* [M+H]⁺ calcd for C₁₅H₁₅FN₂O₃S, 323.0821 (¹⁸F); found, 323.0854 (3.10 ppm).

***N*-(4'-Chlorophenyl)-6-hydroxy-3,4-dihydroisoquinoline-2(1*H*)-sulfonamide 4.74f**

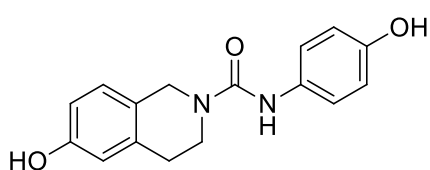
was obtained in 41% (31.3 mg) yield from 79.0 mg of starting material **4.77f**. Colourless oil; $R_f = 0.41$ (50:50 EtOAc/Hexane). $^1\text{H NMR}$ (300 MHz, CDCl_3 , no OH signal was visible): δ (ppm) 7.27 – 7.21 (m, 3H, 2xArH and NH), 7.09 – 7.06 (m, 2H, 2xArH), 6.90 – 6.56 (m, 3H, 3xArH), 4.39 (s, 2H, ArCH_2N), 3.71 – 3.35 (m, 2H, NCH_2), 2.76 (m, 2H, ArCH_2CH_2). $^{13}\text{C NMR}$ (75 MHz, CDCl_3 , not all ArCH signals were visible): δ (ppm) 29.03 (ArCH_2CH_2), 44.35 (CH_2), 47.51 (ArCH_2N), 114.25 (ArCH), 115.43 (ArCH), 122.17 (ArC), 127.75 (ArCH), 129.70 (ArCH), 130.44 (ArC), 134.80 (ArCCl), 135.75 (ArCNH), 154.60 (ArCOH). **HRMS ESI⁺**: m/z $[\text{M}+\text{H}]^+$ calcd for $\text{C}_{15}\text{H}_{15}\text{ClN}_2\text{O}_3\text{S}$, 339.0571 (^{35}Cl); found 339.0556 (1.40 ppm) and 341.0534 (^{37}Cl).

***N*-(4'-Fluorophenyl)-6-hydroxy-3,4-dihydroisoquinoline-2(1*H*)-sulfonamide 4.74g**

was obtained in 33% (64.4 mg) yield from 204 mg of starting material **4.77g**. Brown oil; $R_f = 0.32$ (50:50 EtOAc/Hexane). $^1\text{H NMR}$ (300 MHz, CDCl_3 , no OH signal was visible): δ (ppm) 7.12 – 7.06 (m, 2H, 2xArH), 7.96 – 6.83 (m, 6H, 5xArH and NH), 4.36 (d, $J = 10.3$ Hz, 2H, ArCH_2N), 3.51 – 3.47 (m, 2H, NCH_2), 2.71 (t, $J = 6.0$ Hz, 2H, ArCH_2CH_2). $^{13}\text{C NMR}$ (75 MHz, CDCl_3): δ (ppm) 29.78 (ArCH_2CH_2), 44.03 (CH_2), 47.32 (ArCH_2N), 112.90 (ArCH), 114.19 (ArCH), 116.03 (ArC), 116.33 (ArCH), 123.49 (d, $J = 8.2$ Hz, $\text{ArCH}-\text{F}$), 125.73 (ArC), 126.55 (ArCH), 133.50 (ArCNH), 151.31 ($\text{ArC}-\text{F}$), 161.77 (ArCOH). **HRMS ESI⁺**: m/z $[\text{M}+\text{H}]^+$ calcd for $\text{C}_{15}\text{H}_{15}\text{FN}_2\text{O}_3\text{S}$, 323.0866 (^{18}F); found, 323.0858 (2.50 ppm).

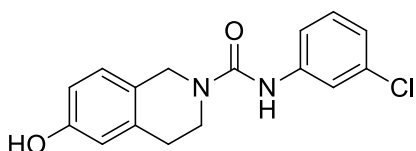
8.11.2 General procedure for the synthesis of demethylation using AlI_3

The general procedure described by Bhatt and co-workers⁹³ was adopted. Thus, iodine (I_2) (1.31 g, 10.0 mmol) was added to a cooled suspension of clean aluminium powder (180 mg, 6.88 mmol) in anhydrous toluene (20 mL) followed by heating to 110 °C until the red colour dissipated. The reaction mixture was cooled to RT, to which the various methoxy substrates **4.54**, **4.66** and **4.77** (0.688 mmol) were added and stirred at 60 °C overnight. The reaction mixture was cooled to RT and the excess AlI_3 was quenched by the slow addition of water (20 mL). The reaction mixture was extracted with EtOAc (20 mL x 3) and the organic layers combined and dried over MgSO_4 . The organic layer was concentrated under reduced pressure affording a brown residue, further purified by column chromatography (40:60 EtOAc/Hexane) to afford compounds as described below:

6-Hydroxy-N-(4'-hydroxyphenyl)-3,4-dihydroisoquinoline-2(1H)-carboxamide

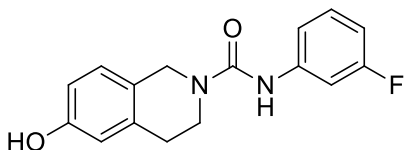
4.46c was obtained in 42% (50.0 mg) yield from 110 mg of starting material **4.54c**. White oil that solidified at low temperatures; $R_f = 0.14$ (50:50 EtOAc/Hexane). **^1H and ^{13}C NMR** was not very clear and therefore not incorporated in

the experimental section however, HRMS was further employed to confirm product formation. **HRMS ESI⁺**: m/z $[\text{M}+\text{H}]^+$ calcd for $\text{C}_{17}\text{H}_{20}\text{N}_2\text{O}_4\text{S}$, 285.1239; found, 285.1240 (0.40 ppm).

N-(3'-Chlorophenyl)-6-hydroxy-3,4-dihydroisoquinoline-2(1H)-carboxamide

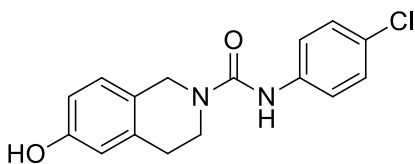
4.46d was obtained in 50% (70.0 mg) yield from 146 mg of starting material **4.54d**. Brown solid; **mp** = 188 – 190 °C; $R_f = 0.50$ (50:50 EtOAc/Hexane). **^1H NMR** (300 MHz, CD_3OD , no OH or NH signals were visible): δ (ppm) 7.57 – 6.99 (m, 5H, 5xArH), 6.67 – 6.64 (m, 2H, 2xArH), 4.59 (s, 2H, ArCH_2N), 3.71 (t, $J = 5.9$ Hz, 2H, NCH_2), 2.86 (t, $J = 5.9$ Hz, 2H, ArCH_2CH_2).

^{13}C NMR (75 MHz, CD_3OD): δ (ppm) 30.04 (ArCH_2CH_2), 42.93 (CH_2), 46.49 (ArCH_2N), 114.78 (ArCH), 115.69 (ArCH), 119.94 (ArCH), 121.69 (ArC), 123.66 (ArCCl), 125.38 (ArCH), 128.27 (ArCH), 130.75 (ArCH), 134.99 (ArC), 135.33 (ArCHCl), 137.34 (ArCNH), 157.13 ($\text{C}=\text{O}$), 157.43 (ArCOH). **HRMS ESI⁺**: m/z $[\text{M}+\text{H}]^+$ calcd for $\text{C}_{16}\text{H}_{15}\text{ClN}_2\text{O}_2$, 303.0900 (^{35}Cl); found, 303.0910 (0.30 ppm) and 305.0875 (^{37}Cl).

N-(3'-Fluorophenyl)-6-hydroxy-3,4-dihydroisoquinoline-2(1H)-carboxamide 4.46e

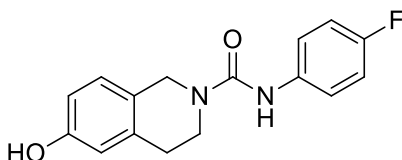
was obtained in 35% (40.0 mg) yield from 120 mg of starting material **4.54e**. White solid; **mp** = 166 – 168 °C; $R_f = 0.33$ (50:50 EtOAc/Hexane). **^1H NMR** (300 MHz, $\text{DMSO}-d_6$): δ

(ppm) 9.25 (s, 1H, NH), 8.71 (brs, 1H, OH), 7.54 – 7.37 (m, 1H, ArH), 7.34 – 7.17 (m, 2H, 2xArH), 6.96 (d, $J = 8.2$ Hz, 1H, ArH), 6.80 – 6.53 (m, 3H, 3xArH), 4.51 (s, 2H, ArCH_2N), 3.63 (t, $J = 5.9$ Hz, 2H, NCH_2), 2.75 (t, $J = 5.9$ Hz, 2H, ArCH_2CH_2). **^{13}C NMR** (75 MHz, $\text{DMSO}-d_6$, no C-F coupling was observable): δ (ppm) 28.72 (ArCH_2CH_2), 41.61 (CH_2), 45.40 (ArCH_2N), 106.13 (ArCH), 106.48 (ArCH), 108.02 (ArCH), 108.30 (ArCH), 113.77 (ArCH), 114.97 (ArCH), 115.33 (ArCH), 124.21 (ArC), [one extra signal 127.39 (ArCH)], 130.00 (ArC), 136.05 (ArCNH), 142.86 ($\text{ArC}-\text{F}$), 154.92 ($\text{C}=\text{O}$), 156.01 (ArCOH). **HRMS ESI⁺**: m/z $[\text{M}+\text{H}]^+$ calcd for $\text{C}_{16}\text{H}_{15}\text{FN}_2\text{O}_2$, 287.1196 (^{18}F); found, 287.1198 (0.30 ppm) and 288.1228 (^{19}F).

***N*-(4'-Chlorophenyl)-6-hydroxy-3,4-dihydroisoquinoline-2(1*H*)-carboxamide 4.46f**

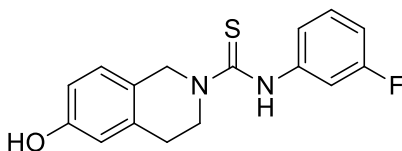
was obtained in 50% (12.2 mg) yield from 26.0 mg of starting material **4.54f**. Brown oil; $R_f = 0.50$ (50:50 EtOAc/Hexane). $^1\text{H NMR}$ (300 MHz, CD_3OD , both OH and NH signals were not visible): δ (ppm) 7.57 – 6.99 (m, 5H,

5xArH), 6.67 – 6.64 (m, 2H, 2xArH), 4.59 (s, 2H, ArCH_2N), 3.72 (t, $J = 5.7$ Hz, 2H, NCH_2), 2.86 (t, $J = 5.7$ Hz, 2H, ArCH_2CH_2). $^{13}\text{C NMR}$ (75 MHz, CD_3OD , one ArC signal was not visible): δ (ppm) 28.62 (ArCH_2CH_2), 41.44 (CH_2), 45.04 (ArCH_2N), 113.35 (ArCH), 114.33 (ArCH), 114.67 (ArC), 123.10 (ArCH), 123.57 (ArCH), 124.12 (ArCH), 126.85 (ArCNH), 135.97 (ArCCl), 155.01 (ArCOH), 156.03 (C=O). **HRMS ESI⁺**: m/z $[\text{M}+\text{H}]^+$ calcd for $\text{C}_{16}\text{H}_{15}\text{ClN}_2\text{O}_2$, 303.0793 (^{35}Cl); found, 303.0899 (3.28 ppm).

***N*-(4'-Fluorophenyl)-6-hydroxy-3,4-dihydroisoquinoline-2(1*H*)-carboxamide 4.46g**

was obtained in 2% (4.50 mg) yield from 236 mg of starting material **4.54g**. White solid; **mp** = 225 – 226 °C; $R_f = 0.33$ (50:50 EtOAc/Hexane). $^1\text{H NMR}$ (300 MHz, CD_3OD , both OH and NH signals were not visible): δ (ppm) 7.47 – 7.19 (m, 3H, 3xArH), 7.00 (d, $J = 7.9$

Hz, 2H, 2xArH), 6.66 (d, $J = 7.9$ Hz, 2H, 2xArH), 4.58 (s, 2H, ArCH_2N), 3.71 (t, $J = 5.7$ Hz, 2H, CH_2), 2.85 (t, $J = 5.7$ Hz, 2H, ArCH_2CH_2). $^{13}\text{C NMR}$ (75 MHz, CD_3OD , no C–F coupling was not visible): δ (ppm) 30.02 (ArCH_2CH_2), 42.89 (CH_2), 46.48 (ArCH_2N), 114.77 (ArCH), 115.71 (ArCH), 123.54 (ArC), 125.43 (ArC), 128.26 (ArCH), 128.96 (ArCH), 129.46 (ArCH), 137.35 (ArCF), 139.87 (ArCNH), 157.19 (C=O), 157.69 (ArCOH). **HRMS ESI⁺**: m/z $[\text{M}+\text{H}]^+$ calcd for $\text{C}_{16}\text{H}_{15}\text{FN}_2\text{O}_2$, 287.1196 (^{18}F); found, 287.1204 (3.48 ppm).

***N*-(3'-Fluorophenyl)-6-hydroxy-3,4-dihydroisoquinoline-2(1*H*)-carbothioamide**

4.80e was obtained in 2% (5.0 mg) yield from 146 mg of starting material **4.66e**. Brown oil; $R_f = 0.33$ (50:50 EtOAc/Hexane). $^1\text{H NMR}$ (300 MHz, CDCl_3): δ (ppm) 7.30 –

7.16 (m, 2H, 2xArH), 7.13 (brs, 1H, NH), 7.08 – 6.94 (m, 3H, 3xArH), 6.78 – 6.57 (m, 2H, 2xArH), 4.87 (s, 2H, ArCH_2N), 4.00 (t, $J = 5.8$ Hz, 2H, NCH_2), 2.90 (t, $J = 5.8$ Hz, 2H, ArCH_2CH_2), 2.06 (brs, 1H, OH). $^{13}\text{C NMR}$ (75 MHz, CDCl_3): δ (ppm) 28.99 (ArCH_2CH_2), 46.85 (CH_2), 50.22 (ArCH_2N), 114.15 (ArCH), 114.70 (ArCH), 115.73 (ArCH), 116.03 (ArCH), 124.75 (ArC), 127.33 (d, $J = 8.4$ Hz, ArCH-F), [one extra ArCH

127.75 (ArCH)], 135.70 (ArC), 136.60 (ArCH), 155.04 (ArCOH), 159.11 (ArCNH), 162.34 (d, $J = 18.0$ Hz, ArCH-F), 166.26 (d, $J = 67.5$ Hz, ArC-F), 182.35 (C=S).

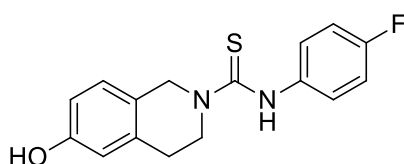
***N*-(4'-Chlorophenyl)-6-hydroxy-3,4-dihydroisoquinoline-2(1*H*)-carbothioamide**



4.80f was obtained in 44% (61.5 mg) yield from 145 mg of starting material **4.66f**. Yellow froth; $R_f = 0.23$ (50:50 EtOAc/Hexane). **¹H NMR** (300 MHz, CDCl₃, OH and NH signals were not visible): δ (ppm) 7.30 – 6.89 (m, 5H, 5xArH), 6.77 – 6.63 (m, 2H, 2xArH), 4.86 (s, 2H, ArCH₂N), 3.99 (t, $J = 5.9$ Hz, 2H, NCH₂), 2.90 (t, $J = 5.9$ Hz, 2H, ArCH₂CH₂).

¹³C NMR (75 MHz, CDCl₃): δ (ppm) 29.17 (ArCH₂CH₂), 47.04 (CH₂), 50.41 (ArCH₂N), 114.34 (ArCH), 114.89 (ArCH), 115.92 (ArCH), 124.94 (ArCH), 127.51 (d, $J = 8.4$ Hz, ArCCl), 127.93 (ArC), 135.97 (ArCH), 136.78 (ArC), 155.22 (ArCNH), 162.53 (ArCOH), 182.53 (C=S).

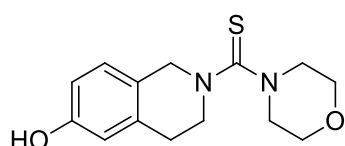
***N*-(4'-Fluorophenyl)-6-hydroxy-3,4-dihydroisoquinoline-2(1*H*)-carbothioamide**



4.80g was obtained in trace amounts from 161 mg of starting material **4.66g**. Opaque oil that solidified at low temperatures; $R_f = 0.23$ (50:50 EtOAc/Hexane). **¹H NMR** (300 MHz, CDCl₃): δ (ppm) 7.30 – 7.16 (m, 2H, ArH and NH), 7.13 (single signal, 1H, ArH), 7.08 – 6.94 (m, 3H, 3xArH), 6.78 – 6.57 (m, 2H, 2xArH), 4.87 (s, 2H, ArCH₂N), 4.00 (t, $J = 5.9$ Hz, 2H, NCH₂), 2.90 (t, $J = 5.9$ Hz, 2H, ArCH₂CH₂), 2.06 (brs, 1H, OH).

¹³C NMR (75 MHz, CDCl₃): δ (ppm) 29.17 (ArCH₂CH₂), 47.04 (CH₂), 50.41 (ArCH₂N), 114.34 (ArCH), 114.89 (ArCH), 115.92 (ArC), 116.22 (ArCH), 124.94 (ArC), 127.51 (d, $J = 8.4$ Hz, ArCHF), 135.97 (ArCH), 136.78 (ArCNH), 155.22 (ArCOH), 162.06 (ArCF), 182.53 (C=S).

[6-Hydroxy-3,4-dihydroisoquinolin-2(1*H*)-yl](morpholino)methanethione **4.80h**

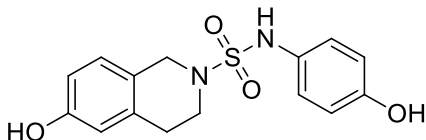


obtained in 20% (41.8 mg) yield from 219 mg of starting material **4.61h** with unreacted starting material being recovered. Brown oil;

$R_f = 0.32$ (30:70 EtOAc/Hexane). **¹H NMR** (300 MHz, CDCl₃): δ (ppm) 6.94 (d, $J = 8.2$ Hz, 1H, ArH), 6.76 – 6.53 (m, 2H, 2xArH), 4.64 (s, 2H, ArCH₂N), 3.90 – 3.71 (m, 4H, morpholine-2xOCH₂), 3.64 – 3.44 (m, 6H, morpholine-2xNCH₂ and NCH₂), 2.94 (t, $J = 5.8$ Hz, 2H, ArCH₂CH₂), 1.21 (brs, 1H, OH). **¹³C NMR** (75 MHz, CDCl₃): δ (ppm) 28.89 (ArCH₂CH₂), 49.53 (CH₂), 52.30 (ArCH₂N), 53.34 (morpholine-2xCH₂O), 66.82 (morpholine-2xNCH₂), 114.20 (ArCH), 115.30 (ArCH), 125.17 (ArC), 127.58 (ArCH), 136.24

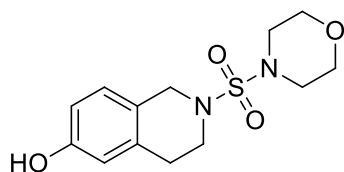
(ArC), 155.00 (ArCOH), 193.98 (C=S). **HRMS ESI⁺**: m/z [M+H]⁺ calcd for C₁₄H₁₈N₂O₂S, 279.1167; found, 279.1166 (0.40 ppm).

6-Hydroxy-*N*-(4-hydroxyphenyl)-3,4-dihydroisoquinoline-2(1*H*)-sulfonamide



4.74c was obtained in 32% (70.6 mg) yield from 240 mg of starting material **4.77c**. White oil that solidified at low temperatures; R_f = 0.24 (50:50 EtOAc/Hexane). **¹H NMR** (300 MHz, CD₃OD): δ (ppm) 7.09 – 6.97 (m, 2H, ArH and NH), 6.85 (d, J = 8.3 Hz, 1H, ArCH), 6.77 – 6.54 (m, 3H, 3xArH), 6.50 (d, J = 2.5 Hz, 2H, 2xArH), 4.59 (brs, 1H, OH), 4.26 (s, 2H, ArCH₂N), 3.38 (t, J = 5.9 Hz, 2H, NCH₂), 2.65 (t, J = 5.9 Hz, 2H, ArCH₂CH₂). **¹³C NMR** (75 MHz, CD₃OD): δ (ppm) 20.68 (ArCH₂CH₂), 36.10 (NCH₂), 39.06 (ArCH₂N), 105.56 (ArCH), 106.68 (ArCH), 107.33 (ArC), 107.43 (ArCH), 115.22 (ArCH), 115.31 (ArCH), 116.19 (ArCH), 119.01 (ArCH), 121.29 (ArCH), 121.54 (ArC), 126.77 (ArCNH), 146.83 (ArCOH), 147.72 (ArCOH). **HRMS ESI⁺**: m/z [M+H]⁺ calcd for C₁₇H₂₀N₂O₄S, 321.0864; found, 321.0912 (3.11 ppm).

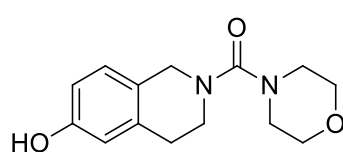
2-(Morpholinofonyl)-1,2,3,4-tetrahydroisoquinolin-6-ol 4.74h was obtained in



25% (35.0 mg) yield from 147 mg of starting material **4.77h**. White solid; **mp** = 168 – 170 °C; R_f = 0.53 (100% EtOAc). **¹H NMR** (300 MHz, DMSO-*d*₆): δ (ppm) 6.94 (d, J = 8.2 Hz, 1H, ArH), 6.72 – 6.51 (m, 2H, 2xArH), 4.37 (s, 2H, ArCH₂N), 3.69 (single signal, 4H, *morpholine*-2xCH₂O), 3.54 (t, J = 5.5 Hz, 2H, NCH₂), 3.22 – 3.18 (m, 4H, *morpholine*-2xNCH₂), 2.86 (t, J = 5.5 Hz, 2H, ArCH₂CH₂). **¹³C NMR** (75 MHz, DMSO-*d*₆): δ (ppm) 29.88 (ArCH₂CH₂), 45.32 (*morpholine*-2xNCH₂), 47.70 (CH₂), 48.56 (ArCH₂N), 67.40 (*morpholine*-2xCH₂O), 114.90 (ArCH), 116.01 (ArCH), 124.56 (ArC), 128.25 (ArCH), 135.92 (ArC), 157.11 (ArCOH). **HRMS ESI⁺**: m/z [M+H]⁺ calcd for C₁₃H₁₈N₂O₄S, 299.1066; found, 299.1061 (1.70 ppm).

8.11.3 Debenzylation of

6-[Benzyloxy-3,4-dihydroisoquinolin-2(1*H*)-yl](morpholino) methanone



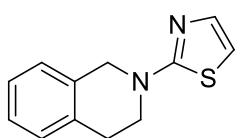
The general procedure described by Silverman and co-workers²⁰³ was adopted. Thus, a mixture of **4.54h** (270 mg, 0.766 mmol), Pd 10% on activated charcoal (81.0 mg, 0.766 mmol), acetic acid (0.096 mL, 1.68 mmol) and anhydrous MeOH (6.00 mL) was stirred under a hydrogen atmosphere (balloon) at 40 °C for 48 h. The mixture

was filtered through celite and concentrated under reduced pressure. The residue was partitioned between EtOAc (30 mL) and washed with saturated aqueous NaHCO₃ (10 mL x 3). The organic layer was dried over MgSO₄, followed by concentrating under reduced pressure. The residue was purified by column chromatography (100% EtOAc).

[6-Hydroxy-3,4-dihydroisoquinolin-2(1H)-yl](morpholino)methanone 4.46h was obtained in 79% (89.0 mg) yield. White solid; mp = 188 – 190 °C; R_f = 0.21 (50:50 EtOAc/Hexane). ¹H NMR (400 MHz, DMSO-*d*₆): δ (ppm) 9.02 (brs, 1H, OH), 6.90 (d, *J* = 8.1 Hz, 1H, ArH), 6.67 (dd, *J* = 8.1 and 2.1 Hz, 1H, ArH), 6.55 – 6.46 (m, H, ArH), 3.58 – 3.48 (m, 4H, *morpholine*-2xOCH₂), 3.28 – 3.21 (m, 6H, *morpholine*-2xNCH₂ and NCH₂), 3.13 (dd, *J* = 9.0, 3.8 Hz, 2H, CH₂), 2.59 (dd, *J* = 9.0, 3.8 Hz, 2H, ArCH₂CH₂). ¹³C NMR (101 MHz, DMSO-*d*₆): δ (ppm) 18.60 (ArCH₂CH₂), 34.62 (*morpholine*-2xNCH₂), 41.48 (CH₂), 44.45 (ArCH₂N), 66.61 (*morpholine*-2xOCH₂), 113.56 (ArCH), 116.68 (ArCH), 126.37 (ArC), 131.36 (ArCH), 139.40 (ArC), 155.95 (ArCOH), 158.20 (C=O).

8.12 Coupling protocols for the synthesis of THIQ analogues

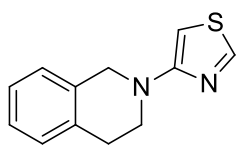
8.12.1 2'-[3,4-Dihydroisoquinolin-2(1H)-yl]thiazole 5.5a



The general procedure described by Klapars and co-workers¹⁵⁰ was followed. Thus, a solution of THIQ **5.4** (0.200 mL, 1.66 mmol) and 2-bromothiazole (0.100 mL, 1.11 mmol) in anhydrous DMF (2.0 mL) were stirred at RT for 1 h. The reaction mixture was treated with Et₃N (0.340 mL, 2.44 mmol) and stirred for 18 h at 80 °C, after which the reaction mixture was poured into water (5.0 mL) and extracted with EtOAc (20 mL x 2). The organic layers were combined, dried over MgSO₄ and concentrated under reduced pressure providing a brown residue purified with column chromatography (30:70 EtOAc/Hexane).

Compound **5.5a** was obtained in 23% (44.0 mg) yield. Orange oil; R_f = 0.55 (50:50 EtOAc/Hexane). ¹H NMR (400 MHz, DMSO-*d*₆, one ArH signal was not visible): δ (ppm) 7.33 – 7.08 (m, 4H, 4xArH), 6.83 (d, *J* = 3.6 Hz, 1H, *thiazole*-ArH), 4.60 (s, 2H, ArCH₂N), 3.71 (t, *J* = 6.0 Hz, 2H, CH₂), 2.93 (t, *J* = 6.0 Hz, 2H, ArCH₂CH₂). ¹³C NMR (101 MHz, DMSO-*d*₆): δ (ppm) 27.80 (ArCH₂CH₂), 46.00 (CH₂), 49.80 (ArCH₂N), 107.73 (*thiazole*-ArCH), 126.34 (ArCH), 126.62 (ArCH), 126.73 (ArCH), 128.69 (ArCH), 133.10 (ArC) 134.47 (ArC), 139.70 (*thiazole*-ArCH), 170.74 (*thiazole*-ArCN).

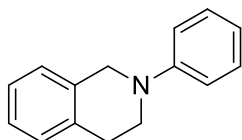
8.12.2 4'-[3,4-Dihydroisoquinolin-2(1H)-yl]thiazole 5.5b



The general procedure described by Klapars and co-workers¹⁵⁰ was followed. Thus, L-proline (17.0 mg, 0.149 mmol, 20.0 mol%), CuI (14.2 mg, 74.6x10⁻³ mmol, 10.0 mol%) and K₃PO₄ (470 mg, 2.24 mmol) were mixed in DMF (1.0 mL) followed by addition of THIQ **5.4** (9.30x10⁻³ mL, 0.747 mmol) and 4-bromothiazole (0.100 mL, 1.12 mmol) under anhydrous conditions. The reaction vessel was sealed and set to stir at 150 °C for 24 h, after which the reaction mixture was diluted with water (5.0 mL) and extracted with EtOAc (20.0 mL x 2). The organic layers were combined, dried over MgSO₄ and concentrated under reduced pressure to afford a red/brown coloured residue, purified by column chromatography (30:70 EtOAc/Hexane).

Compound **5.5b** was obtained in 9.5% (15.2 mg) yield. Orange oil; R_f = 0.62 (50:50 EtOAc/Hexane). ¹H NMR (400 MHz, CDCl₃): δ (ppm) 8.75 (s, 1H, *thiazole*-SCHN), 7.39 – 7.08 (m, 4H, 4xArH), 6.43 (s, 1H, *thiazole*-ArH), 4.65 (s, 2H, ArCH₂N), 3.75 (t, J = 5.1 Hz, 2H, CH₂), 2.99 (t, J = 5.1 Hz, 2H, ArCH₂CH₂). ¹³C NMR was not very clear and therefore not reported.

8.12.3 2-Phenyl-1,2,3,4-tetrahydroisoquinoline 5.5c

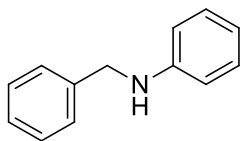


L-Proline (37.0 mg, 0.32 mmol, 20.0 mol%), K₂CO₃ (22.0 mg, 0.160 mmol, 10.0 mol%) and CuI (80.0 mg, 0.160 mmol, 10.0 mol%) were combined, to which THIQ **5.4** (0.200 mL, 1.60 mmol) and bromobenzene (0.170 mL, 1.60 mmol) in anhydrous DMSO (1.50 mL) were added. The mixture was stirred for 30 seconds followed by heating in a Microwave oven at 150 °C for 15 min at 24 – 37 W with a pressure of 1 bar forming a brown suspension. The suspension was diluted with water (5.0 mL) and extracted with EtOAc (20 mL x 3). The organic layers were combined, dried over MgSO₄ and purified with column chromatography (40:60 EtOAc/Hexane).

Compound **5.5c** was obtained in 60% yield. Yellow-brown oil, which solidified at low temperatures; R_f = 0.39 (90:10 EtOAc/Hexane). ¹H NMR (300 MHz, CDCl₃): δ (ppm) 7.25 – 7.09 (m, 5H, 5xArH), 6.93 – 6.90 (m, 2H, 2xArH), 6.78 – 6.73 (m, 2H, 2xArH), 4.34 (s, 2H, ArCH₂N), 3.49 (t, J = 5.8 Hz, 2H, NCH₂), 2.92 (t, J = 5.8 Hz, 2H, ArCH₂CH₂). ¹³C NMR (75 MHz, CDCl₃, one ArC was not visible): δ (ppm) 29.30 (ArCH₂CH₂), 46.70 (CH₂), 50.90 (ArCH₂N), 115.27 (ArCH), 118.79 (ArCH), 126.16 (ArCH), 126.46 (ArCH), 126.57 (ArCH), 128.65 (ArCH), 134.61 (ArC), 135.01 (ArC), 150.69 (ArCN).

8.13 Intramolecular Friedel–Crafts cyclization protocol toward synthesis of THIQ analogues

8.13.1 Procedure for the synthesis of *N*-benzyl aniline **5.16**



The general procedure described by Romero and co-workers¹⁴⁹ was adopted. Thus, benzaldehyde (0.200 mL, 1.96 mmol), aniline (0.200 mL, 2.17 mmol), $\text{Mg}(\text{ClO}_4)_3$ (44.0 mg, 0.196 mmol) and MgSO_4 (237 mg, 1.96 mmol) were combined in anhydrous CH_3CHCl_2 (15 mL). The mixture was stirred at 60 °C for 5 h then cooled to RT. The solid was filtered off and the eluent concentrated under reduced pressure to afford crude material which was dissolved in anhydrous EtOH (3.0 mL) and cooled to –3 °C. NaBH_4 (50.0 mg, 1.30 mmol) was added and the mixture was stirred at RT overnight and solvent removed. Removal of the solvent under reduced pressure provided a residue, which was purified by column chromatography (20:80 EtOAc/Hexane).

Compound **5.16** was obtained in quantitative (359 mg) yield. Colourless oil; $R_f = 0.53$ (20:80 EtOAc/Hexane). $^1\text{H NMR}$ (400 MHz, CDCl_3): δ (ppm) 7.48 – 7.02 (m, 7H, 7xArH), 6.79 – 6.55 (m, 3H, 3xArH), 4.34 (s, 2H, ArCH₂), 4.03 (brs, 1H, NH). $^{13}\text{C NMR}$ (101 MHz, CDCl_3 , one ArCH was not visible): δ (ppm) 48.60 (CH₂), 113.09 (ArCH), 117.82 (ArCH), 127.48 (ArCH), 127.76 (ArCH), 128.88 (ArCH), 129.52 (BnC), 139.68 (ArCN). This data corresponded well with the literature as reported by Wang and co-workers.²⁰⁴

8.13.2 $\text{S}_{\text{N}}2$ substitution protocol for the synthesis of THIQ analogues

8.13.2.1 Method A: General procedure for of *N*-benzyl–5-methylthiazol–2-amine

5.19

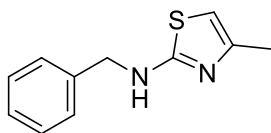
The general procedure described by Krishnaiah and co-workers¹⁶⁵ was followed. Thus, a stirred suspension of 2-amino-4-methylthiazole (105 mg, 0.925 mmol), benzyl bromide (0.100 mL, 0.840 mmol) and Cs_2CO_3 (600 mg, 1.85 mmol) were combined in anhydrous DMF (5.0 mL). The mixture was stirred overnight at RT followed by addition of water (20 mL). Extraction with EtOAc (10 mL x 3) afforded a brown residue which was purified with column chromatography (30:70 EtOAc/Hexane), yielding 34% of **5.19**.

8.13.2.2 Method B: General procedure for 5.19 using the Ullmann conditions

The general procedure described by Klapars and co-workers¹⁵⁰ was adopted. Thus, a suspension of 2-amino-4-methylthiazole (105 mg, 0.925 mmol), Cs_2CO_3 (600 mg, 1.85 mmol), L-proline (9.70 mg, 84.2×10^{-3} mmol, 5.00 mol%) and CuI (16.0 mg, 84.2×10^{-3} mmol, 5.00 mol%) in anhydrous DMF (2.0 mL) were combined followed by the addition of benzyl

bromide (0.100 mL, 0.840 mmol). The reaction mixture was stirred overnight at RT followed by the addition of water (20 mL) and extraction with EtOAc (20 mL x 3) which afforded a brown residue purified by column chromatography (30:70 EtOAc/Hexane).

Compound **5.19** was obtained in 48% (164 mg) yield. Yellow oil; $R_f = 0.48$ (50:50 EtOAc/Hexane).



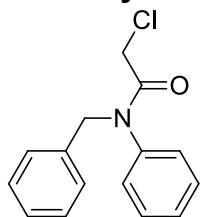
$^1\text{H NMR}$ (300 MHz, CDCl_3 , doubling of signals are attributed to rotamers): δ (ppm) 7.54 – 6.89 (m, 5H, rotamers 5xArH), 6.42 (s, 1H, thiazole-ArH), 5.50 – 5.01 (m, 2H, rotamers ArCH₂), 4.40 (s, 1H, NH), 2.23 (s, 3H, thiazole-CH₃). **HRMS ESI⁺**: m/z [M+H]⁺ calcd for C₁₁H₁₂N₂S, 205.0755; found, 205.0793 (4.87 ppm). The experimental data, corresponded well with the literature as reported by Aoyama and co-workers.²⁰⁵

8.13.3 General procedure for acylation of amines

8.13.3.1 Chloroacetylation of amines (a and b)

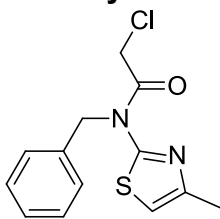
The protocol described by Velavan and co-workers¹³⁸ was followed. Thus, chloroacetyl chloride (78.0×10^{-3} mL, 9.82 mmol) was slowly added to a stirred solution of **5.16** (150 mg, 0.818 mmol) or **5.19** (164 mg, 0.800 mmol) and DIPEA (0.170 mL, 9.82 mmol) in anhydrous CH_2Cl_2 (20 mL) at -3°C . The solution was stirred for 6 – 18 h at RT, resulting in a yellow mixture, which changed to a red-brown colour. The reaction mixture was treated with water (10 mL) and extracted with EtOAc (20 mL x 2) to afford a brown residue, further purified by column chromatography (20:80 EtOAc/Hexane). The spectroscopic details of the compounds are described below:

N-Benzyl-2-chloro-N-phenylacetamide 5.20 was obtained in 89% (203 mg) yield.

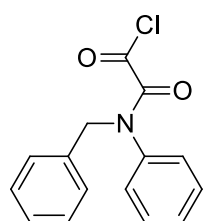


Colourless oil; $R_f = 0.19$ (20:80 EtOAc/Hexane). **$^1\text{H NMR}$** (300 MHz, CDCl_3): δ (ppm) 7.43 – 7.33 (m, 3H, 3xArH), 7.33 – 7.18 (m, 5H, 5xArH), 7.08 – 6.99 (m, 2H, 2xArH), 4.92 (s, 2H, COCH₂Cl), 3.87 (s, 2H, ArCH₂). **$^{13}\text{C NMR}$** (75 MHz, CDCl_3): δ (ppm) 42.20 (ArCH₂), 53.90 (CH₂), 126.60 (ArCH), 127.80 (ArCH), 128.40 (ArCH), 128.73 (ArCH), 128.87 (ArCH), 129.11 (ArCH), 129.97 (BnCCH₂), 136.69 (ArCN), 166.29 (C=O). Spectral data corresponded well with that reported by Flipo and co-workers.²⁰⁶

N-Benzyl-2-chloro-N-(5-methylthiazol-2-yl)acetamide 5.21 was obtained in 70% (158 mg) yield. Pale yellow crystal; **mp** = 68 – 70 °C; R_f = 0.23 (20:80 EtOAc/Hexane). **¹H NMR** (300 MHz, CDCl₃): δ (ppm) 7.39 – 6.97 (m, 5H, 5xArH), 6.43 (d, J = 1.0 Hz, 1H, *thiazole*-ArH), 5.31 (s, 2H, COCH₂Cl), 5.18 (s, 2H, ArCH₂), 2.24 (s, 3H, *thiazole*-CH₃). **¹³C NMR** (75 MHz, CDCl₃): δ (ppm) 17.8 (single signal *thiazole*-CH₃), 50.3 (ArCH₂), 68.9 (CH₂), 109.39 (*thiazole*-ArCH), 127.58 (ArCH), 128.59 (ArCH), 128.73 (ArCH), 128.86 (ArCH), 135.40 (*thiazole*-ArCN), 137.82 (BnC), 147.76 (C=O).



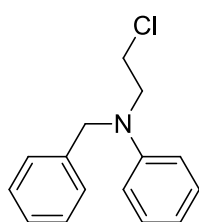
8.13.3.2 2-[Benzyl(phenyl)amino]-2-oxoacetyl chloride 5.33



The protocol described by Vekemans and co-worker²⁰⁷ was followed. Thus, oxalyl chloride (0.240 mL, 2.83 mmol) was slowly added to a stirred solution of **5.16** (413 mg, 2.36 mmol) in anhydrous CCl₄ (20 mL) at 0 °C. The mixture was stirred for 6 – 18 h at RT. The resulting yellow mixture was treated with water (10 mL) and extracted with EtOAc (20 mL x 2) to afford a residue purified with column chromatography (20:80 EtOAc/Hexane).

Compound **5.33** was obtained in 56% (272 mg) yield. Yellow oil; R_f = 0.32 (100% Hexane). **¹H NMR** (300 MHz, CDCl₃): δ (ppm) 7.34 – 6.73 (m, 10H, 10xArH), 4.67 (s, 2H, ArCH₂). **¹³C NMR** (75 MHz, CDCl₃, not all ArCH signals were visible): δ (ppm) 52.18 (ArCH₂), 127.50 (ArCH), 128.26 (ArCH), 128.91 (ArCH), 129.19 (ArCH), 136.54 (BnC), 139.64 (ArC), 164.73 (C=O). **HRMS ESI⁺**: m/z [M+H]⁺ calcd for C₁₅H₁₁ClNO₂, 275.0527; found, 274.1513 (6.92 ppm).

8.13.4 N-Benzyl-N-(2-chloroethyl)aniline 5.22



The protocol described by Nystrom,¹²³ Davis¹²⁴ and co-workers was followed. Thus, to a suspension of LiAlH₄ (88.9 mg, 2.34 mmol) in anhydrous THF (10.0 mL) at -3 °C, AlCl₃ (312 mg, 2.34 mmol) was added in small portions maintaining the temperature at -3 °C. The resulting monochloroalane solution was then stirred for 30 min at RT, to which **5.20** (203 mg, 0.780 mmol) in anhydrous THF (2.0 mL) was added. The reaction mixture was stirred under reflux for 5 h, cooled to RT and later to 0 °C. Water (15 mL) was slowly added till no further effervescence occurred. The lithium aluminate was separated by vacuum filtration and the eluent extracted with EtOAc (20 mL x 2) to afford an oily residue purified by column chromatography (10:90 CH₂Cl₂/Hexane).

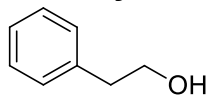
Compound **5.22** was obtained in 59% (113 mg) yield. Orange oil; $R_f = 0.45$ (5:95 $\text{CH}_2\text{Cl}_2/\text{Hexane}$). $^1\text{H NMR}$ (400 MHz, CDCl_3 , doubling of signals is due to rotamers): δ (ppm) 7.60 – 7.11 (m, 6H, rotamers 6xArH), 6.99 – 6.64 (m, 4H, 4xArH), 4.71 (s, 2H, ArCH_2N), 3.87 – 3.83 (m, 2H, CH_2), 3.75 – 3.71 (m, 2H, CH_2). $^{13}\text{C NMR}$ (101 MHz, CDCl_3): δ (ppm) 40.5 (CH_2), 53.20 (CH_2Cl), 55.00 (ArCH_2), 112.42 (ArCH), 117.38 (ArCH), 126.65 (ArCH), 127.18 (ArCH), 128.83 (ArCH), 129.59 (ArCH), 138.51 (BnC), 147.74 (ArCN).

8.14 Synthesis of isochromanone as a route to THIQ analogues

8.14.1 Reduction of phenyl acetic acid to 2-phenylethanol 5.35

The procedure described by Shindikar and co-workers¹⁶⁹ was followed. The phenyl acetic acid (3.00 mmol) in anhydrous THF (9.0 mL) was slowly added to a mixture of LiAlH_4 (460 mg, 12.0 mmol) in anhydrous THF (18 mL) at RT and the resulting mixture was heated under reflux for 3 h whilst monitoring with TLC. the reaction mixture was cooled to 0°C, to which water was added until all effervescence ceased and water (10 mL) was added followed by extraction with EtOAc (20 mL x 3) which afforded a colourless oil in excellent yields with no further purification required. The spectroscopic details of the compounds are described below:

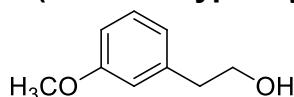
2-Phenylethanol 5.35 was obtained in 91% (409 mg) yield from 501 mg of starting material



phenyl acetic acid. Translucent liquid; $R_f = 0.47$ (50:50 EtOAc/Hexane). $^1\text{H NMR}$

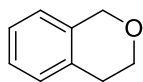
(300 MHz, CDCl_3): δ (ppm) 7.38 – 7.16 (m, 5H, 5xArH), 3.81 (t, $J = 6.7$ Hz, 2H, ArCH_2CH_2), 2.85 (t, $J = 6.7$ Hz, 2H, $\text{CH}_2\text{CH}_2\text{OH}$), 2.37 (brs, 1H, OH). $^{13}\text{C NMR}$ (75 MHz, CDCl_3): δ (ppm) 39.30 (ArCH_2), 63.70 (CH_2), 126.53 (ArCH), 128.66 (ArCH), 129.18 (ArCH), 138.77 (ArC). The experimental data corresponded with that reported by Chapman and co-workers.¹⁷⁴

2-(3-Methoxyphenyl)ethanol 5.40 was obtained in 87% (411 mg) yield from 516 mg of starting material 3-methoxyphenyl acetic acid. Colourless oil; $R_f =$



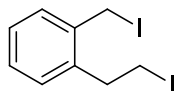
0.48 (50:50 EtOAc/Hexane). $^1\text{H NMR}$ (300 MHz, CDCl_3): δ (ppm) 7.13 (m, 1H, ArH), 6.76 – 6.61 (m, 3H, 3xArH), 3.81 – 3.62 (m, 5H, overlapping signals – OCH_3 , CH_2OH), 2.72 (t, $J = 6.5$ Hz, 2H, ArCH_2), 1.93 (brs, 1H, OH). $^{13}\text{C NMR}$ (75 MHz, CDCl_3): δ (ppm) 39.50 (ArCH_2), 55.50 (OCH_3), 63.80 (CH_2OH), 112.03 (ArCH), 115.08 (ArCH), 121.66 (ArCH), 129.82 (ArCH), 140.48 (ArC), 160.03 (ArCOMe).

8.14.2 Isochroman 5.36



The procedure described by Deady and co-workers¹⁶⁸ was followed. Thus, phosphorous trichloride (0.870 mL, 9.82 mmol) was added to a suspension of phenyl ethanol **5.35** (400 mg, 3.27 mmol), paraformaldehyde (60.0 mg, 1.64 mmol) and aqueous 11 M HCl (0.100 mL, 0.900 mmol). The reaction mixture was stirred at 40 °C for 4 h, cooled to RT neutralized to a pH7 with an aqueous 2 N NaOH and extracted with EtOAc (20 mL x 2), to give the product as an oil, which solidified at low temperatures. Compound **5.36** was obtained in 96% (420 mg) yield. Yellow oil; $R_f = 0.70$ (50:50 EtOAc/Hexane). **¹H NMR** (300 MHz, CDCl₃): δ (ppm) 7.23 – 7.17 (m, 3H, 3xArH), 7.05 – 7.02 (m, 1H, ArH), 4.83 (s, 2H, ArCH₂O), 4.03 (t, $J = 5.7$ Hz, 2H, ArCH₂CH₂), 2.92 (t, $J = 5.7$ Hz, 2H, CH₂). **¹³C NMR** (75 MHz, CDCl₃): δ (ppm) 28.40 (ArCH₂CH₂), 65.40 (CH₂), 68.00 (ArCH₂O) 124.45 (ArCH), 126.03 (ArCH), 126.40 (ArCH), 128.96 (ArCH), 133.27 (ArC), 134.99 (ArC). The spectroscopic data, corresponded with the literature.¹⁶⁸

8.14.3 1-(2-Iodoethyl)-2-(iodomethyl)benzene 5.37



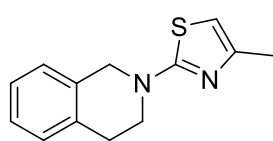
The protocol described by Ma and co-workers¹⁷³ was adopted. Thus, isochroman **5.36** (173 mg, 1.29 mmol) was treated with aqueous 57% HI (0.680 mL, 9.00 mmol) and stirred overnight under reflux (130 °C) in a darkened environment. The reaction mixture was cooled to RT, diluted with water (5.0 mL) and extracted with ether (20 mL x 2) to afford the product.

Compound **5.37** was obtained in 92% (444 mg) yield. Orange oil which crystallized upon being cooled to below zero; $R_f = 0.28$ (100% Hexane). **¹H NMR** (300 MHz, CDCl₃): δ (ppm) 7.41 – 7.12 (m, 4H, 4xArH), 4.49 (s, 2H, ArCH₂I), 3.51 – 3.39 (m, 2H, CH₂CH₂I), 3.28 (dd, $J = 9.0, 9.0$ Hz, 2H, ArCH₂CH₂). **¹³C NMR** (75 MHz, CDCl₃): δ (ppm) 3.24 (ArCH₂I), 3.62 (CH₂CH₂I), 36.85 (ArCH₂CH₂), 127.76 (ArCH), 128.79 (ArCH), 129.9 (ArCH), 130.43 (ArCH), 136.82 (ArC), 138.87 (ArC). The spectroscopic data corresponds with reported literature.¹⁷³

8.14.4 General procedure for the THIQ formation from 5.37

The protocol described by Ma and co-workers¹⁷³ was adopted. Thus, a mixture of **5.37** (200 mg, 0.538 mmol), amines (**a – c**) (0.538 mmol), NaHCO₃ (90.0 mg, 1.07 mmol) and catalytic amounts of SDS (15.0 mg, 53.8x10⁻⁴ mmol) in distilled water (10 mL) were stirred under reflux for 4 h. The reaction mixture was cooled to RT, followed by an extraction with EtOAc (20 mL x 2) which afforded residues purified by column chromatography (20:80 EtOAc/Hexane). The spectroscopic details of the compounds are described below:

2-[3,4-Dihydroisoquinolin-2(1H)-yl]4'-methylthiazole 5.38a was obtained in 29%

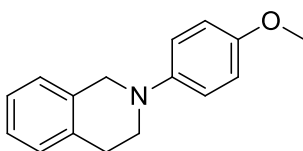


(34.8 mg) yield. Orange oil; $R_f = 0.67$ (50:50 EtOAc/Hexane). $^1\text{H NMR}$

(300 MHz, CDCl_3): δ (ppm) 7.21 – 7.16 (m, 4H, 4xArH), 6.13 (s, 1H, thiazole-ArH), 4.65 (s, 2H, ArCH₂N), 3.76 (t, $J = 5.9$ Hz, 2H, NCH₂),

2.99 (t, $J = 5.9$ Hz, 2H, ArCH₂CH₂), 2.30 (s, 3H, thiazole-CH₃). $^{13}\text{C NMR}$ (75 MHz, CDCl_3 , one of the aromatic signals were not visible): δ (ppm) 17.70 (thiazole-CH₃), 28.70 (ArCH₂CH₂), 45.90 (CH₂), 49.60 (ArCH₂N), 100.84 (thiazole-ArCH), 126.35 (ArCH), 126.39 (ArCH), 126.60 (ArCH), 128.51 (ArCH), 132.84 (ArC), 134.39 (ArC), 149.58 (thiazole-ArCN).

2-(4'-Methoxyphenyl)-1,2,3,4-tetrahydroisoquinoline 5.38b was obtained in 86% (80.9

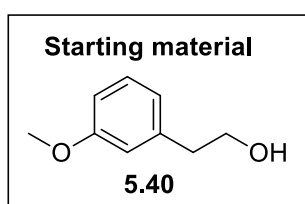


mg) yield. Beige oil; $R_f = 0.57$ (50:50 EtOAc/Hexane). $^1\text{H NMR}$ (300

MHz, CDCl_3): δ (ppm) 7.22 – 7.10 (m, 4H, 4xArH), 7.04 – 6.96 (m, 2H, 2xArH), 6.92 – 6.85 (m, 2H, 2xArH), 4.31 (s, 2H, ArCH₂N), 3.79

(s, 3H, OCH₃), 3.46 (t, $J = 5.8$ Hz, 2H, NCH₂), 3.00 (t, $J = 5.8$ Hz, 2H, ArCH₂CH₂). $^{13}\text{C NMR}$ (75 MHz, CDCl_3): δ (ppm) 29.27 (ArCH₂CH₂), 48.59 (CH₂), 52.82 (OCH₃), 55.79 (ArCH₂N), 114.71 (ArCH), 118.16 (ArCH), 126.04 (ArCH), 126.52 (ArCH), 128.83 (ArCH), 134.69 (ArCH), 145.51 (ArCN), 153.63 (ArCOCH₃). **HRMS ESI⁺**: m/z [M+H]⁺ calcd for C₁₅H₁₅NO, 226.1232 found, 226.1225 (3.09 ppm).

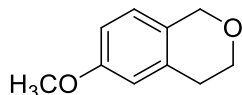
8.14.5 6-Methoxyisochroman 5.44



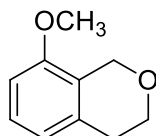
The protocol described by Taber and co-workers¹⁷⁶ was followed.

Thus, 3-methoxy phenyl ethanol **5.40** (0.200 mL, 1.41 mmol) in anhydrous THF (0.50 mL) was slowly added to a 60% suspension of NaH in mineral oil (47.0 mg, 1.98 mmol) in anhydrous THF (15 mL) and stirred for 30 min at 0 °C. Chloromethyl methyl ether (0.110 mL, 1.50 mmol) was slowly added to the mixture and left to stir overnight at RT. The reaction was quenched aqueous saturated NH₄Cl solution (10 mL), followed by extraction with ether (10 mL x 3) to afford an orange oil. The crude oil in anhydrous toluene (5.0 mL), containing *p*-toluene sulfonic acid (80.0 mg, 0.141 mmol) was stirred under reflux overnight. Water (15 mL) was added to the cooled reaction mixture which was extracted with EtOAc (20 mL x 2) to a brown oil, purified by column chromatography (2:98 EtOAc/Hexane) yielding compounds **5.44** and **5.44a**.

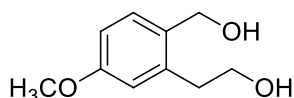
6-Methoxyisochroman 5.44 was obtained in 39% (244 mg) yield. Colourless oil; $R_f = 0.41$ (20:80 EtOAc/Hexane). $^1\text{H NMR}$ (300 MHz, CDCl_3): δ (ppm) 7.27 (d, $J = 2.2$ Hz, 1H, ArH), 6.92 (d, $J = 8.4$ Hz, 1H, ArH), 6.72 (dd, $J = 8.4$ and 2.2 Hz, 1H, ArH), 4.75 (s, 2H, ArCH_2O), 4.03 – 3.92 (m, 2H, NCH_2), 3.79 (s, 3H, OCH_3), 2.86 (t, $J = 5.6$ Hz, 2H, ArCH_2CH_2). $^{13}\text{C NMR}$ (75 MHz, CDCl_3): δ (ppm) 28.70 (ArCH_2CH_2), 55.30 (OCH_3), 65.30 (OCH_2), 67.80 (ArCH_2O), 112.36 (ArCH), 113.56 (ArCH), 125.43 (ArCH), 127.08 (ArC), 134.41 (ArCCH_2), 158.08 (ArCOMe). **HRMS ESI⁺**: m/z $[\text{M}+\text{H}]^+$ calcd for $\text{C}_{10}\text{H}_{12}\text{O}_2$, 165.0871; found, 165.0910 (6.04 ppm). The experimental data, corresponded with the literature.¹⁷⁶



8-Methoxyisochroman 5.44a was obtained in 6% (42.7 mg) yield. Yellow oil; $R_f = 0.52$ (20:80 EtOAc/Hexane). $^1\text{H NMR}$ (300 MHz, CDCl_3): δ (ppm) 7.17 – 7.12 (m, 1H, ArH), 6.75 – 6.67 (m, 2H, 2xArH), 4.75 (s, 2H, ArCH_2O), 3.93 (t, $J = 5.6$ Hz, 2H, OCH_2), 3.81 (s, 3H, OCH_3), 2.83 (t, $J = 5.6$ Hz, 2H, ArCH_2CH_2). $^{13}\text{C NMR}$ (75 MHz, CDCl_3): δ (ppm) 28.40 (ArCH_2CH_2), 55.20 (OCH_3), 64.50 (CH_2), 64.90 (ArCH_2O), 107.40 (ArCH), 121.21 (ArCH), 123.87 (ArCH), 127.02 (ArC), 134.93 (ArC), 155.65 (ArCOMe). **HRMS ESI⁺**: m/z $[\text{M}+\text{H}]^+$ calcd for $\text{C}_{10}\text{H}_{12}\text{O}_2$, 165.0871; found, 165.0910 (6.04 ppm).



8.14.6 2-[2-(Hydroxymethyl)-5-methoxyphenyl]ethanol 5.48

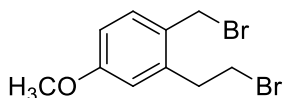


The protocol described by Shindikar and co-workers¹⁶⁹ was followed. Thus, LiAlH_4 (130 mg, 3.36 mmol) was added to a cooled mixture of **5.47** (300 mg, 4.68 mmol) in anhydrous THF (20 mL) followed by heating at 60 °C for 5 h. The reaction mixture was cooled to 0 °C and quenched by the slow addition of water (5.0 mL) followed by extracting with EtOAc (20 mL x 3) which afforded a residue, purified by column chromatography (50:50 EtOAc/Hexane).

Compound **5.48** was obtained in 98% (299 mg) yield. White solid; **mp** = 79 – 81 °C; $R_f = 0.33$ (75:25 EtOAc/Hexane). $^1\text{H NMR}$ (400 MHz, CDCl_3): δ (ppm) 7.20 (d, $J = 8.0$ Hz, 1H, ArH), 6.74 (d, $J = 9.2$ Hz, 2H, 2xArH), 4.52 (s, 2H, ArCH_2OH), 3.89 – 3.71 (m, 5H, overlapping signals – OCH_3 and CH_2), 2.87 (t, $J = 5.8$ Hz, 2H, ArCH_2CH_2). $^{13}\text{C NMR}$ (101 MHz, CDCl_3): δ (ppm) 35.60 (ArCH_2CH_2), 55.50 (OCH_3), 62.80 (ArCH_2O), 63.60 (ArCH_2), 111.91 (ArCH), 115.88 (ArCH), 131.53 (ArCH), 132.13 (ArC), 140.19 (ArC), 159.91 (ArCOMe).

8.14.7 General procedure for the halogenation of diol 5.48

8.14.7.1 2-(2-Bromoethyl)-1-(bromomethyl)-4-methoxybenzene 5.49

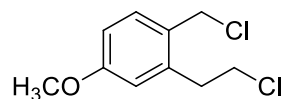


The protocol described by Taylor and co-workers¹⁷⁹ was followed.

Thus, phosphorous tribromide (1.17 mL, 12.5 mmol) was added to a cooled solution of **5.48** (900 mg, 4.94 mmol) in anhydrous toluene (10 mL) and heated at 60 °C overnight. The reaction mixture was cooled to 0 °C, water (20 mL) was added and extracted with EtOAc (10 mL x 3) to afford a residue purified by column chromatography (100% Hexane).

Compound **5.49** was obtained in 9% (105 mg) yield. $R_f = 0.31$ (20:80 EtOAc/Hexane). **¹H NMR** (300 MHz, CDCl₃): δ (ppm) 7.25 – 7.12 (m, 1H, ArH), 6.77 – 6.63 (m, 2H, 2xArH), 4.52 – 4.54 (m, 2H, CH₂CH₂Br), 4.46 (s, 2H, ArCH₂Br), 3.71 (s, 3H, OCH₃), 3.59 – 3.51 (m, 2H, ArCH₂CH₂), 3.18 (t, $J = 7.7$ Hz, 2H, CH₂CH₂Br). **¹³C NMR** (75 MHz, CDCl₃): δ (ppm) 31.80 (CH₂CH₂Br), 32.20 (ArCH₂Br), 36.20 (CH₂), 55.60 (OCH₃), 112.85 (ArCH), 115.97 (ArCH), 128.13 (ArC), 132.26 (ArCH), 139.64 (ArC), 160.29 (ArCOMe).

8.14.7.2 2-(2-Chloroethyl)-1-(chloromethyl)-4-methoxybenzene 5.49



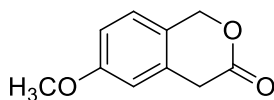
The protocol described by Batey and co-workers¹³⁶ was followed.

Thus, thionyl chloride (0.800 mL, 11.7 mmol) was added to a solution of **5.40** (200 mg, 1.10 mmol) in CH₃CHCl₂ (20 mL). The reaction mixture was stirred at 60 °C overnight. Excess thionyl chloride was removed under reduced pressure and the product purified by column chromatography (100% Hexane).

Compound **5.49** was obtained in 50% (212 mg) yield. Yellow oil; $R_f = 0.37$ (20:80 EtOAc/Hexane). **¹H NMR** (300 MHz, CDCl₃): δ (ppm) 6.90 (d, $J = 8.4$ Hz, 1H, ArH), 6.80 – 6.5 (m, 2H, 2xArH), 4.73 (s, 2H, ArCH₂Cl), 3.95 (t, $J = 5.5$ Hz, 2H, CH₂CH₂Cl), 3.79 (s, 3H, OCH₃), 2.84 (t, $J = 5.5$ Hz, 2H, ArCH₂CH₂). **¹³C NMR** (75 MHz, CDCl₃): δ (ppm) 28.96 (ArCH₂CH₂), 55.56 (CH₂CH₂Cl), 65.53 (ArCH₂Cl), 68.00 (OCH₃), 112.66 (ArCH), 113.86 (ArCH), 125.73 (ArCH), 127.38 (ArC), 134.72 (ArC), 158.38 (ArCOMe).

8.15 Synthesis of isochromanone as a route to THIQ analogues

8.15.1 General procedure for the synthesis of 6-methoxyisochroman-3-one 5.47



The protocol described by Spangler and co-workers¹⁷² was adopted.

Thus, a mixture of 3-methoxyphenyl acetic acid (4.80 g, 28.8 mmol), 34% aqueous formaldehyde solution (7.20 mL, 261 mmol) and

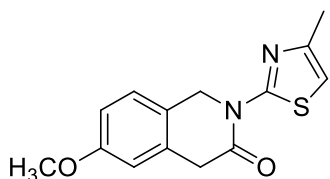
concentrated aqueous 11 M HCl (1.44 mL, 15.8 mmol) in glacial acetic acid (22.0 mL, 38.0 mmol) was stirred under atmospheric conditions for 5 days. Heating resulted in the formation of multiple products. The reaction mixture was treated with an aqueous saturated NaHCO₃ solution (40 mL) and extracted with EtOAc (20 mL x 3) to afford a residue, purified using flash chromatography (20:80 EtOAc/Hexane).

Compound **5.47** was obtained in a 50% (2.56 g) yield. White crystals; **mp** = 66 – 67 °C; *R_f* = 0.45 (50:50 EtOAc/Hexane). **¹H NMR** (300 MHz, CDCl₃): δ (ppm) 7.16 (d, *J* = 8.3 Hz, 1H, ArH), 6.88 – 6.70 (m, 2H, 2xArH), 5.26 (s, 2H, ArCH₂O), 3.82 (s, 3H, OCH₃), 3.68 (s, 2H, ArCH₂). **¹³C NMR** (75 MHz, CDCl₃): δ (ppm) 36.67 (ArCH₂C=O), 55.58 (OCH₃), 69.93 (ArCH₂O), 112.70 (ArCH), 112.92 (ArCH), 123.80 (ArCH), 126.01 (ArC), 132.68 (ArC), 160.20 (ArCOMe), 170.82 (C=O). **HRMS ESI⁺**: *m/z* [M+H]⁺ calcd for C₁₀H₁₀O₃, 179.0708; found, 179.0702 (3.40 ppm). The experimental data, corresponded with literature.¹⁷²

8.15.2 General procedure for the lactamisation 5.47

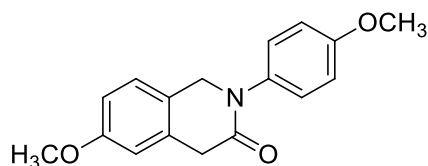
The protocol described by Chen and co-workers¹⁸⁰ was followed. A mixture of 6-methoxyisochroman-3-one **5.47** (300 mg, 1.68 mmol), aniline analogues (**a – g**) (2.52 mmol) and 10 mol% of AlCl₃ (45.0 mg, 0.340 mmol) were combined under anhydrous conditions in a sealed tube while being heated for 48 h at 150 °C. The reaction mixture was poured into aqueous 1 N HCl (5.0 mL) and extracted with EtOAc (20 mL x 2) providing a brown residue purified with column chromatography (30:70 EtOAc/Hexane). The spectroscopic details of the compounds are described below:

6-Methoxy-2-(4'-methylthiazol-2-yl)-1,2-dihydroisoquinolin-3(4H)-one 5.51a was



obtained in 29% (136 mg) yield. Pale yellow powder; **mp** = °C; *R_f* = 0.76 (50:50 EtOAc/Hexane). **¹H NMR** (300 MHz, CDCl₃): δ (ppm) 7.27 – 7.25 (m, 1H, ArH), 6.84 – 6.75 (m, 2H, 2xArH), 6.58 (s, 1H, *thiazole*-ArH), 5.29 (s, 2H, ArCH₂N), 3.83 – 3.80 (m, 5H, overlapping signals-OCH₃ and CH₂), 2.33 (s, 3H, *thiazole*-CH₃). **¹³C NMR** (75 MHz, CDCl₃): δ (ppm) 17.7 (*thiazole*-CH₃), 39.10 (ArCH₂), 49.70 (ArCH₂N), 55.70 (OCH₃), 109.98 (*thiazole*-ArCH), 112.52 (ArCH), 113.33 (ArCH), 123.68 (ArCH), 127.37 (ArC), 132.78 (ArC), 147.04 (*thiazole*-ArCMe), 158.71 (*thiazole*-ArCN), 159.75 (ArCOMe), 168.36 (C=O). **HRMS ESI⁺**: *m/z* [M+H]⁺ calcd for C₁₄H₁₄N₂O₂S, 275.0854; found, 275.0855 (0.40 ppm).

6-Methoxy-2-(4'-methoxyphenyl)-1,2-dihydroisoquinolin-3(4H)-one 5.51b was



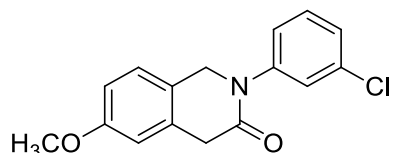
obtained in 40% (117 mg) yield. Beige oily residue; $R_f = 0.17$ (50:50 EtOAc/Hexane). $^1\text{H NMR}$ (300 MHz, CDCl_3): δ (ppm) 7.26 – 7.19 (m, 2H, 2xArH), 7.09 – 7.07 (m, 1H, ArH), 6.93 – 6.90 (m, 2H, 2xArH), 6.81 – 6.75 (m, 2H, 2xArH), 4.75 (s, 2H, ArCH_2N), 3.81 – 3.73 (m, 8H, overlapping signals–2x OCH_3 and ArCH_2). $^{13}\text{C NMR}$ (75 MHz, CDCl_3): δ (ppm) 39.20 (ArCH_2), 54.30 (2x OCH_3), 55.80 (ArCH_2N), 112.56 (ArCH), 112.96 (ArCH), 114.49 (ArCH), 124.50 (ArCH), 126.51 (ArCH), 127.25 (ArCH), 134.28 (ArC), 135.63 (ArC), 158.49 (ArCN), 159.60 (ArCOMe), 169.45 (C=O). **HRMS ESI⁺**: m/z [$\text{M}+\text{H}$]⁺ calcd for $\text{C}_{17}\text{H}_{17}\text{NO}_3$, 284.1287; found, 284.1292 (1.80 ppm).

6-Methoxy-2-(5'-nitro-3H-pyrrol-2-yl)-1,2-dihydroisoquinolin-3(4H)-one 5.51c



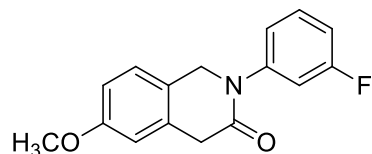
was obtained in 15% (42.0 mg) yield. Orange solid; **mp** = °C; $R_f = (20:80 \text{ EtOAc/Hexane})$. $^1\text{H NMR}$ (300 MHz, CDCl_3): δ (ppm) 8.39 (s, 1H, *thiazole*-ArH), 7.35 – 7.18 (m, 1H, ArH), 6.97 – 6.69 (m, 2H, 2xArH), 5.37 (s, 2H, ArCH_2N), 3.92 (s, 3H, OCH_3), 3.84 (s, 2H, ArCH_2). **HRMS ESI⁺**: m/z [$\text{M}+\text{H}$]⁺ calcd for $\text{C}_{13}\text{H}_{11}\text{N}_3\text{O}_4\text{S}$, 306.0549; found, 306.0547 (0.70 ppm).

2-(3'-Chlorophenyl)-6-methoxy-1,2-dihydroisoquinolin-3(4H)-one 5.51d was



obtained in 57% (80.0 mg) yield. White solid; **mp** = 87 – 88 °C; $R_f = 0.36$ (40:60 EtOAc/Hexane). $^1\text{H NMR}$ (300 MHz, CDCl_3): δ (ppm) 7.37 – 7.10 (m, 5H, 5xArH), 6.82 – 6.78 (m, 2H, 2xArH), 4.80 (d, $J = 6.0$ Hz, 2H, ArCH_2N), 3.85 – 3.75 (m, 5H, overlapping signals– OCH_3 and ArCH_2). $^{13}\text{C NMR}$ (75 MHz, CDCl_3 , not all ArCH and ArC were not visible): δ (ppm) 39.12 (ArCH_2), 53.38 (OCH_3), 55.45 (ArCH_2N), 112.35 (ArCH), 112.73 (ArCH), 123.81 (ArCH), 125.79 (ArCH), 126.28 (ArCH), 126.81 (ArC), 129.99 (ArCCl), 132.74 (ArCH), 134.84 (ArCN), 158.38 (ArCOMe), 160.26 (C=O). **HRMS ESI⁺**: m/z [$\text{M}+\text{H}$]⁺ calcd for $\text{C}_{16}\text{H}_{14}\text{ClNO}_2$, 288.0791 (^{35}Cl); found, 288.0785 (2.10 ppm) and 290.0757 (^{37}Cl).

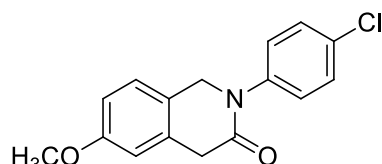
2-(3'-Fluorophenyl)-6-methoxy-1,2-dihydroisoquinolin-3(4H)-one 5.51e was



obtained in 89% (150 mg) yield. White solid; **mp** = 108 – 110 °C; $R_f = 0.41$ (50:50 EtOAc/Hexane). $^1\text{H NMR}$ (300 MHz, CDCl_3 , the extra proton can be attributed to the overlapping of the CDCl_3 signal): δ (ppm) 7.38 – 6.78 (m, 8H, 8xArH), 4.79 (s, 2H, ArCH_2N), 4.01 – 3.55 (m, 5H, overlapping signals– ArCH_2 and OCH_3). $^{13}\text{C NMR}$ (75 MHz, CDCl_3 , one ArCH and two

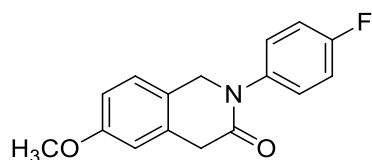
ArC were not visible): δ (ppm) 39.31 (ArCH₂), 53.49 (OCH₃), 55.58 (ArCH₂N), 112.67 (d, J = 28.50 Hz, ArCH-F), 113.70 (d, J = 21.00 Hz, ArCH-F), 120.99 (ArCH), 123.93 (ArCH), 126.29 (ArCH), 130.16 (ArC), 133.72 (ArCH), 159.32 (ArCOMe), 169.80 (ArCF), 172.86 (C=O). **HRMS ESI⁺**: m/z [M+H]⁺ calcd for C₁₆H₁₄FNO₂, 272.1087 (¹⁸F); found, 272.1086 (0.40 ppm).

2-(4'-Chlorophenyl)-6-methoxy-1,2-dihydroisoquinolin-3(4H)-one 5.51f was



obtained in 35% (84.0 mg) yield. Yellow solid; mp = 123 – 125 °C; R_f = 0.38 (40:60 EtOAc/Hexane). **¹H NMR** (300 MHz, CDCl₃): δ (ppm) 7.39 – 7.28 (m, 4H, 4xArH), 7.12 – 7.09 (m, 1H, ArH), 6.82 – 6.78 (m, 2H, 2xArH), 4.76 (s, 2H, ArCH₂N), 3.92 – 3.63 (m, 5H, overlapping signals–ArCH₂ and OCH₃). **¹³C NMR** (75 MHz, CDCl₃, one ArC was not visible): δ (ppm) 39.19 (ArCH₂), 53.59 (ArCH₂N), 55.59 (OCH₃), 112.48 (ArCH), 112.88 (ArCH), 124.04 (ArC), 126.41 (ArCH), 126.99 (ArCH), 129.37 (ArCH), 132.21 (ArCH), 133.91 (ArCH), 140.67 (ArCCl), 157.21 (ArCN), 159.60 (ArCOMe), 169.25 (C=O). **HRMS ESI⁺**: m/z [M+H]⁺ calcd for C₁₆H₁₄ClNO₂, 288.0684 (³⁵Cl); found, 288.0782 (3.45 ppm).

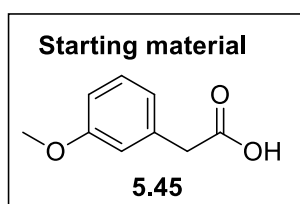
2-(4'-Fluorophenyl)-6-methoxy-1,2-dihydroisoquinolin-3(4H)-one 5.51g was



obtained in 29% (67.3 mg) yield as an oil; R_f = 0.38 (40:60 EtOAc/Hexane). **¹H NMR** (300 MHz, CDCl₃): δ (ppm) 7.47 – 7.23 (m, 5H, 5xArH), 7.00 – 6.95 (m, 2H, 2xArH), 4.93 (s, 2H, ArCH₂N), 3.97 (m, 5H, overlapping signals–OCH₃ and CH₂). **¹³C NMR** (75 MHz, CDCl₃): δ (ppm) 39.23 (ArCH₂CH₂), 54.09 (ArCH₂N), 55.76 (OCH₃), 112.84 (d, J = 30.00 Hz, ArCH-F), 116.17 (ArC), 116.47 (ArCH), 124.26 (ArC), 126.56 (ArCH), 127.74 (ArCH), 127.80 (ArCH), 134.13 (ArCN), 159.72 (ArCF), 162.89 (ArCOMe), 169.50 (C=O). **HRMS ESI⁺**: m/z [M+H]⁺ calcd for C₁₆H₁₄FNO₂, 272.1042 (¹⁸F); found, 272.1090 (3.67 ppm) and 273.1119 (¹⁹F).

8.15.3 Synthesis of THIQ analogues *via.*, amide formation

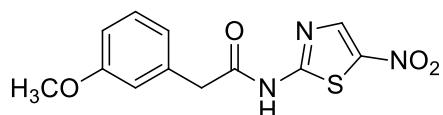
8.15.3.1 Coupling of amines with carboxylic acid 5.45



The protocol described by Pelly and co-workers,¹⁸¹ was modified where *N,N*-dicyclohexylcarbodiimide (220 mg, 1.08 mmol); *f* DMAP (11.1 mg, 9.03x10⁻⁵ mmol) and carboxylic acid **5.45** (150 mg, 0.903 mmol) were combined at 0 °C. To this was added a mixture of amines (**d – g**) (0.903 mmol) in anhydrous CH₂Cl₂ (5.0 mL) and the resultant reaction mixture was

stirred at RT for 12 h. The suspension was filtered, and the eluent concentrated under reduced pressure to yield a solid residue purified by flash chromatography (15:85 EtOAc/Hexane). The spectroscopic details of the compounds are described below:

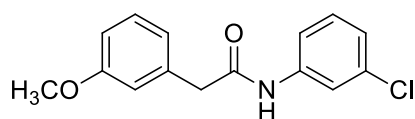
2-(3-Methoxyphenyl)-N-(5'-nitrothiazol-2-yl)acetamide 5.53c was obtained in 16%



(42.0 mg) yield. Orange solid; **mp** = 119 – 120 °C; R_f = 0.29 (30:70 EtOAc/Hexane). **¹H NMR** (300 MHz, CDCl₃): δ (ppm) 9.52 (brs, 1H, NH), 8.22 (s, 1H, *thiazole*-ArH), 7.29

– 7.19 (m, 1H, ArH), 6.85 – 6.76 (m, 3H, 3xArH), 4.17 – 3.55 (m, 5H, overlapping signals-OCH₃ and CH₂). **¹³C NMR** (75 MHz, CDCl₃, one ArCH signal was not visible): δ (ppm) 43.42 (ArCH₂), 55.56 (OCH₃), 113.82 (*thiazole*-ArCH), 115.68 (ArCH), 121.79 (ArCH), 130.99 (ArCH), 133.36 (ArC), 140.44 (*thiazole*-ArC), 160.66 (*thiazole*-ArCN), 161.17 (ArCOMe), 169.54 (C=O). **HRMS ESI⁺**: m/z [M+H]⁺ calcd for C₁₂H₁₁N₃O₄S, 294.0549; found, 294.0547 (0.70 ppm).

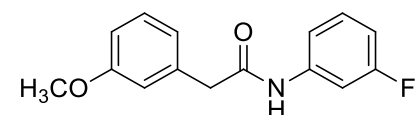
N-(3'-Chlorophenyl)-2-(3-methoxyphenyl)acetamide 5.53d was obtained in 66% (330



mg) yield. White oil which solidified at low temperatures; R_f = 0.66 (50:50 EtOAc/Hexane). **¹H NMR** (300 MHz, CDCl₃): δ (ppm) 7.51 (d, J = 1.8 Hz, 1H, ArH), 7.38 – 7.14 (m, 3H,

3xArH), 7.11 – 7.00 (m, 1H, ArH), 6.95 – 6.80 (m, 3H, 3xArH), 3.83 (s, 3H, OCH₃), 3.71 (s, 2H, ArCH₂). **¹³C NMR** (75 MHz, CDCl₃): δ (ppm) 45.06 (ArCH₂), 55.43 (OCH₃), 113.38 (ArCH), 115.31 (ArCH), 117.89 (ArCH), 120.00 (ArCH), 121.80 (ArCH), 124.61 (ArCH), 130.04 (ArCH), 130.54 (ArCH), 134.71 (ArCCl), 135.65 (ArCCH₂), 138.86 (ArCN), 160.21 (ArCOMe), 169.04 (C=O). **HRMS ESI⁺**: m/z [M+H]⁺ calcd for C₁₅H₁₅NO₂Cl, 276.0684 (³⁵Cl); found, 276.0792 (3.60 ppm) and 278.0765 (³⁷Cl).

N-(3'-Fluorophenyl)-2-(3-methoxyphenyl)acetamide 5.53e was obtained in 94% (220

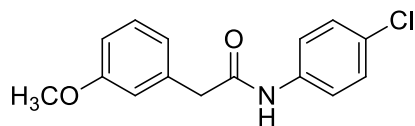


mg) yield. White solid; **mp** = 57 – 58 °C; R_f = 0.46 (20:80 EtOAc/Hexane). **¹H NMR** (300 MHz, CDCl₃, no NH signal

was detected): δ (ppm) 7.45 – 7.11 (m, 3H, 3xArH), 7.06 – 6.69 (m, 5H, 5xArH), 3.80 (s, 3H, OCH₃), 3.69 (s, 2H, ArCH₂). **¹³C NMR** (75 MHz, CDCl₃, two of the aromatic signals were not visible): δ (ppm) 44.85 (ArCH₂), 55.49 (OCH₃), 107.77 (d, J = 26.25 Hz, ArCH-F), 111.38 (d, J = 21.00 Hz, ArCH-F), 113.27 (ArCH), [too many ArCHF 115.53 (d, J = 12.75 Hz, ArCH-F)], 121.93 (ArCH), 130.32 (m, J = 9.00 Hz, ArCH-F), 136.03 (ArCN), 139.63 (d, J = 10.50 Hz, ArCH-F), 161.55 (ArCOMe), 164.79 (ArCF), 170.01 (C=O). **HRMS ESI⁺**: m/z

$[M+H]^+$ calcd for $C_{15}H_{15}NO_2F$, 260.1087 (^{18}F); found, 260.1083 (1.50 ppm) and 261.1115 (^{19}F).

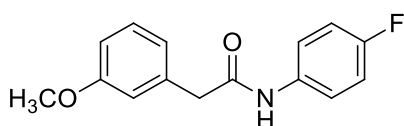
***N*-(4'-Chlorophenyl)-2-(3-methoxyphenyl)acetamide 5.53f** was obtained in 87% (210



mg) yield. White oil which solidified at low temperatures; $R_f = 0.41$ (30:70 EtOAc/Hexane). 1H NMR (300 MHz, $CDCl_3$, no NH signal was observed): δ (ppm) 7.51 – 7.50 (m, 5H,

5xArH), 7.11 – 6.80 (m, 3H, 3xArH), 3.83 (s, 3H, OCH_3), 3.71 (s, 2H, $ArCH_2$). ^{13}C NMR (75 MHz, $CDCl_3$, no C=O was not visible): δ (ppm) 45.06 ($ArCH_2$), 55.43 (OCH_3), 113.40 ($ArCH$), 115.33 ($ArCH$), 117.85 ($ArCH$), 119.96 ($ArCH$), 121.82 ($ArCH$), 124.61 ($ArCH$), 130.06 ($ArCCl$), 130.75 ($ArCH$), 130.36 (ArC), 135.74 ($ArCNH$), 135.53 ($ArCOMe$). **HRMS ESI⁺**: m/z $[M+H]^+$ calcd for $C_{15}H_{15}NO_2Cl$, 276.0791 (^{35}Cl); found, 276.0780 (4.0 ppm) and 278.0752 (^{37}Cl).

***N*-(4'-Fluorophenyl)-2-(3-methoxyphenyl)acetamide 5.53g** was obtained in 56% (130



mg) yield. White solid; **mp** = 70 – 72 °C; $R_f = 0.46$ (30:70 EtOAc/Hexane). 1H NMR (300 MHz, $CDCl_3$): δ (ppm) 7.45 – 7.11 (m, 3H, 3xArH), 7.06 – 6.69 (m, 5H, 5xArH), 3.80 (s,

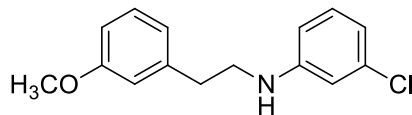
3H, OCH_3), 3.69 (s, 2H, $ArCH_2$). ^{13}C NMR (75 MHz, $CDCl_3$): δ (ppm) 44.70 ($ArCH_2$), 55.27 (OCH_3), 113.12 ($ArCH$), 115.20 ($ArCH$), 115.55 (d, $J = 22.5$ Hz, $ArCH-F$), 121.76 (m, $J = 7.50$ Hz, $ArCH-F$), 130.33 ($ArCH$), 133.45 ($ArCH$), 135.78 ($ArCN$), 157.89 ($ArCCH_2$), 160.20 ($ArCOMe$), 161.06 ($ArCF$), 169.00 (C=O). **HRMS ESI⁺**: m/z $[M+H]^+$ calcd for $C_{15}H_{15}NO_2F$, 260.1042 (^{18}F); found, 260.1083 (3.14 ppm).

8.15.3.2 General procedure for the reduction of the carbonyl function

This protocol described by Nystrom, Davis and co-workers^{123,124} was adopted. Thus, $LiAlH_4$ (41.0 mg, 1.07 mmol) was suspended in anhydrous THF (30 mL) and cooled to -3 °C in an ice bath $AlCl_3$ (140 mg, 1.07 mmol) was added in small portions maintaining the temperature at -3 °C. The resulting hydride suspension (AlH_2Cl) was stirred at RT for 30 min, to which the amides **5.53d – g** (0.713 mmol) in THF (4.0 mL) were added. The reaction mixture was stirred under reflux for 5 h, cooled to RT and carefully treated with water until no further effervescence occurred. The white solid (lithium aluminate) was separated by vacuum filtration and the filtrate extracted with EtOAc (20 mL x 2) to give the corresponding amines

5.54 as oils with no further purification required. The spectroscopic details of the compounds are described below:

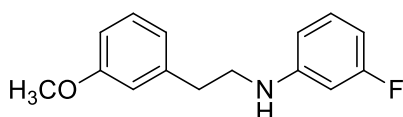
3'-Chloro-N-(3-methoxyphenethyl)aniline 5.54d was obtained in 98% (100 mg) yield



from 114 mg of starting material **5.53d**. Yellow oil solidified at low temperatures; $R_f = 0.82$ (50:50 EtOAc/Hexane). $^1\text{H NMR}$ (300 MHz, CDCl_3 , no clean spectra was recorded, therefore no spectral information was recorded).

$^{13}\text{C NMR}$ (75 MHz, CDCl_3): δ (ppm) 35.66 (ArCH₂), 45.01 (CH₂), 55.52 (OCH₃), 111.63 (ArCH), 112.14 (ArCH), 112.85 (ArCH), 114.93 (ArCH), 117.56 (ArCH), 121.43 (ArCH), 130.02 (ArCH), 130.55 (ArCH), 135.58 (ArCCl), 140.92 (ArCNH), 149.48 (ArC), 160.20 (ArCOMe). **HRMS ESI⁺**: m/z [M+H]⁺ calcd for C₁₅H₁₅NO₂Cl, 262.0999 (³⁵Cl); found, 262.0988 (4.20 ppm) and 264.0961 (³⁷Cl).

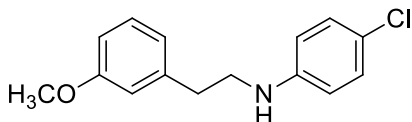
3'-Fluoro-N-(3-methoxyphenethyl)aniline 5.54e was obtained in 73% (153 mg) yield



from 235 mg of starting material **5.53e**. White oil; $R_f = 0.63$ (50:50 EtOAc/Hexane). $^1\text{H NMR}$ (300 MHz, CDCl_3 , no NH signal was visible): δ (ppm) 7.77 – 7.29 (m, 5H, 5xArH), 6.42 – 6.28 (m, 3H, 3xArH), 3.80 (s, 3H, OCH₃), 3.38 (t, $J = 6.9$ Hz, 2H, ArCH₂CH₂), 2.89 (t, $J = 6.9$ Hz, 2H, CH₂CH₂NH).

$^{13}\text{C NMR}$ (75 MHz, CDCl_3): δ (ppm) 35.33 (ArCH₂CH₂), 44.75 (CH₂CH₂NH), 55.18 (OCH₃), 99.55 (d, $J = 26.25$ Hz, ArCH–F), 103.91 (d, $J = 9.00$ Hz, ArCH–F), 108.84 (ArCH), 111.76 (ArCH), 114.58 (ArCH), 121.08 (ArCH), 129.95 (ArCH), 130.20 (ArCH), 130.37 (ArC), 140.82 (ArCNH), 150.00 (ArCOMe). **HRMS ESI⁺**: m/z [M+H]⁺ calcd for C₁₅H₁₅NO₂F, 246.1294 (¹⁸F); found, 246.1290 (1.6 ppm) and 247.1321 (¹⁹F).

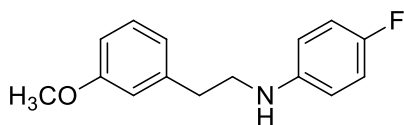
4'-Chloro-N-(3-methoxyphenethyl)aniline 5.54f was obtained in 88% (176 mg) yield



from 198 mg of starting material **5.53f**. Yellow oil which solidified at low temperatures; $R_f = 0.80$ (50:50 EtOAc/Hexane). $^1\text{H NMR}$ (300 MHz, CDCl_3): δ (ppm) 7.30 – 7.18 (m, 1H, ArH), 7.17 – 7.08 (m, 2H, 2xArH), 6.87 – 6.67 (m, 3H, 3xArH), 6.58 – 6.47 (m, 2H, 2xArH), 3.80 (s, 3H, OCH₃), 3.68 (brs, 1H, NH), 3.37 (t, $J = 6.8$ Hz, 2H, ArCH₂CH₂), 2.88 (t, $J = 6.8$ Hz, 2H, CH₂CH₂NH).

$^{13}\text{C NMR}$ (75 MHz, CDCl_3 , one of the ArCH was not visible): δ (ppm) 35.55 (ArCH₂CH₂), 45.28 (CH₂CH₂NH), 55.50 (OCH₃), 112.03 (ArCH), 114.34 (ArCH), 114.91 (ArCH), 121.39 (ArCH), 122.48 (ArCCl), 129.39 (ArCH), 129.96 (ArC), 141.62 (ArCNH), 159.79 (ArCOMe). **HRMS ESI⁺**: m/z [M+H]⁺ calcd for C₁₅H₁₅NO₂Cl, 262.0891 (³⁵Cl); found, 262.0988 (3.79 ppm).

4'-Fluoro-N-(3-methoxyphenethyl)aniline 5.54g was obtained in 96% (120 mg) yield



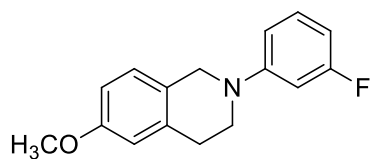
from 140 mg of starting material **5.53g**. Translucent oil; $R_f = 0.71$ (50:50 EtOAc/Hexane). $^1\text{H NMR}$ (300 MHz, CDCl_3 , no NH signal was observed): δ (ppm) 7.29 – 7.23 (s, 1H, ArH),

6.78 – 6.03 (m, 5H, 5xArH), 6.58 – 6.54 (m, 2H, 2xArH), 3.90 (s, 3H, OCH_3), 3.38 (t, $J = 6.0$ Hz, 2H, $\text{CH}_2\text{CH}_2\text{NH}$), 2.90 (t, $J = 6.0$ Hz, 2H, ArCH_2CH_2). $^{13}\text{C NMR}$ (75 MHz, CDCl_3): δ (ppm) 35.49 (ArCH_2CH_2), 45.58 ($\text{CH}_2\text{CH}_2\text{NH}$), 55.20 (OCH_3), 111.71 (ArCH), 113.85 (d, $J = 7.50$ Hz, ArCH-F), 114.62 (ArCH), 115.69 (d, $J = 21.75$ Hz, ArCH-F), 121.12 (ArCH), 129.65 (ArCH), 141.05 (ArC), 144.06 (ArCNH), 156.77 (ArCF), 159.90 (ArCOMe). **HRMS ESI⁺**: m/z $[\text{M}+\text{H}]^+$ calcd for $\text{C}_{15}\text{H}_{15}\text{NO}_2\text{F}$, 246.1249 (^{18}F); found, 246.1290 (4.06 ppm).

8.15.3.3 General procedure for the Pictet–Spengler cyclization of amines 5.54

The protocol described by Kano and co-workers¹⁸² was adopted. Thus, the amine substrates **5.54** (1.05 mmol) and paraformaldehyde (1.15 mmol) were heated in formic acid (5.0 mL) at 80 °C overnight. The reaction mixture was diluted with water (20 mL) and the pH adjusted to 5 with NaHCO_3 solution, followed by extraction with EtOAc (20 mL x 2). The organic layers afforded crude material which was purified by chromatography in (20:80 EtOAc/Hexane). The spectroscopic details of the compounds are described below:

2-(3'-Fluorophenyl)-6-methoxy-1,2,3,4-tetrahydroisoquinoline 5.55e was obtained

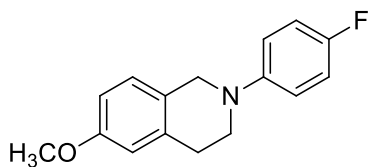


in 75% (120 mg) yield from 153 mg of starting material **5.54e**.

Orange oil; $R_f = 0.00$ (40:60 EtOAc/Hexane). $^1\text{H NMR}$ (300 MHz, CDCl_3 , one ArH was not visible): δ (ppm) 7.28 – 7.00 (m, 2H, 2xArH), 6.87 – 6.37 (m, 4H, 4xArH), 4.36 (s, 2H, ArCH_2N),

3.80 (s, 3H, OCH_3), 3.55 (t, $J = 5.8$ Hz, 2H, CH_2), 2.96 (t, $J = 5.8$ Hz, 2H, ArCH_2CH_2). $^{13}\text{C NMR}$ (75 MHz, CDCl_3 , one ArC signal was not visible): δ (ppm) 29.28 (ArCH_2CH_2), 45.80 (CH_2), 49.55 (ArCH_2N), 55.30 (OCH_3), 101.30 (d, $J = 25.5$ Hz, ArCH-F), 104.44 (d, $J = 21.75$ Hz, ArCH-F), 109.85 (ArCH), 112.41 (ArCH), 113.15 (ArCH), 126.18 (ArCH), 127.48 (ArCH), 130.14 (ArC), 136.03 (ArCN), 157.18 (ArCOMe), 159.29 (ArCF). **HRMS ESI⁺**: m/z $[\text{M}+\text{H}]^+$ calcd for $\text{C}_{16}\text{H}_{16}\text{FNO}$ 258.1294 (^{18}F); found, 258.1288 (2.30 ppm) and 259.1317 (^{19}F).

2-(4'-Fluorophenyl)-6-methoxy-1,2,3,4-tetrahydroisoquinoline 5.55g was obtained



in 98% (120 mg) yield from 117 mg of starting material **5.54g**.

Brown solid; **mp** = 75 – 78 °C; R_f = 0.00 (40:60 EtOAc/Hexane).

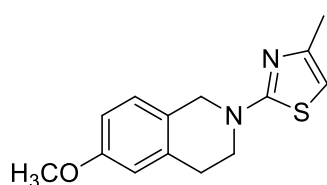
¹H NMR (300 MHz, CDCl₃): δ (ppm) 7.12 – 6.87 (m, 5H, 5xArH), 6.82 – 6.66 (m, 2H, 2xArH), 4.28 (s, 2H, ArCH₂N), 3.81 (s, 3H,

OCH₃), 3.48 (t, J = 5.8 Hz, 2H, NCH₂), 2.97 (t, J = 5.8 Hz, 2H, ArCH₂CH₂). **¹³C NMR** (75 MHz, CDCl₃): δ (ppm) 29.61 (ArCH₂CH₂), 48.05 (CH₂), 51.69 (ArCH₂N), 55.60 (OCH₃), 112.70 (ArCH), 113.56 (ArCH), 115.86 (d, J = 22.50 Hz, ArCH-F), 117.46 (d, J = 7.50 Hz, ArCH-F), 126.77 (ArCH), 127.78 (ArC), 136.02 (ArC), 147.50 (ArCN), 155.17 (ArCF), 158.41 (ArCOMe). **HRMS ESI⁺**: m/z [M+H]⁺ calcd. C₁₆H₁₆FNO, 258.1249 (¹⁸F); found, 258.1292 (3.87 ppm) and 259.1319 (¹⁹F).

8.15.4 General procedure for the reduction of Isochromanones 5.43

The protocol described by Nystrom, Davis and co-workers^{123,124} was followed. Thus, LiAlH₄ (99.0 mg, 2.62 mmol) in anhydrous THF (50 mL) was cooled to 0 °C, to which AlCl₃ (350 mg, 2.62 mmol) was added portion-wise. The mixture was stirred at RT providing AlH₂Cl, to which **5.43a** and **b** (0.873 mmol) were added and the mixture stirred at RT for 5 h. Water (15 mL) was added and the resulting solution extracted with EtOAc (20 mL x 3) affording products **5.55a** and **b** as oils after chromatographic purification (20:80 EtOAc/Hexane). The spectroscopic details of the compounds are described below:

2-[6-Methoxy-3,4-dihydroisoquinolin-2(1H)-yl]-4'-methylthiazole 5.55a was



obtained in 82% (189 mg) yield from 243 mg of starting material

5.43a. Yellow oil that solidified after exposure to low temperatures;

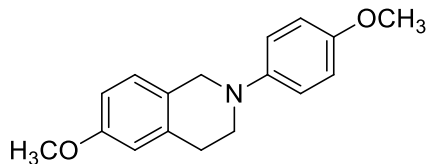
R_f = 0.33 (20:80 EtOAc/Hexane). **¹H NMR** (300 MHz, CDCl₃): δ

(ppm) 7.09 (d, J = 8.4 Hz, 1H, ArH), 6.83 – 6.65 (m, 2H, 2xArH),

6.12 (single signal, 1H, thiazole-ArH), 4.58 (s, 2H, ArCH₂N), 3.87 – 3.65 (m, 5H, overlapping signals-OCH₃ and CH₂), 2.95 (t, J = 5.8 Hz, 2H, ArCH₂CH₂), 2.28 (d, J = 1.1 Hz, 3H,

thiazole-CH₃). **¹³C NMR** (75 MHz, CDCl₃): δ (ppm) 21.40 (thiazole-CH₃), 29.40 (ArCH₂CH₂), 46.10 (CH₂), 49.60 (ArCH₂N), 55.60 (OCH₃), 101.16 (ArCH), 112.94 (ArCH), 113.61 (ArCH), 125.31 (ArC), 127.74 (ArC), 136.00 (ArC), 149.83 (ArC), 158.58 (ArCOMe), 170.82 (ArCN). **HRMS ESI⁺**: m/z [M+H]⁺ calcd for C₁₄H₁₆N₂OS, 261.1062; found, 261.1070 (3.10 ppm).

6-Methoxy-2-(4'-methoxyphenyl)-1,2,3,4-tetrahydroisoquinoline 5.55b was



obtained in 67% (107 mg) yield from 168 mg of starting material **5.43b**. Off white solid, **mp** = 116 – 118 °C; R_f = 0.73 (50:50 EtOAc/Hexane). **¹H NMR** (300 MHz, CDCl₃): δ (ppm) 7.12 – 7.11 (m, 1H, ArH), 6.93 – 6.90 (m, 2H, 2xArH),

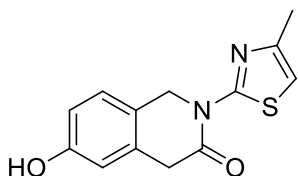
6.78 – 6.69 (m, 3H, 3xArH), 6.58 (s, 1H, ArH), 4.38 (s, 2H, ArCH₂N), 3.80 and 3.82 (each as a s, 6H, 2xOCH₃), 3.47 (t, J = 5.7 Hz, 2H, CH₂), 2.75 (t, J = 5.7 Hz, 2H, ArCH₂CH₂). **¹³C NMR** (75 MHz, CDCl₃): δ (ppm) 29.40 (ArCH₂CH₂), 44.40 (CH₂), 47.50 (ArCH₂N), 55.60 (OCH₃), 55.70 (OCH₃), 113.04 (ArCH), 113.75 (ArCH), 114.77 (ArCH), 124.43 (ArCH), 124.75 (ArCH), 127.60 (ArC), 129.80 (ArC), 134.92 (ArCN), 157.83 (ArCOMe), 158.59 (ArCOMe). **HRMS ESI⁺**: m/z [M+H]⁺ calcd for C₁₇H₁₉NO₂, 270.1494; found, 270.1494 (0.00 ppm).

8.16 Demethylation protocols for 6-hydroxy THIQ analogues

8.16.1 Method A: Using BBr₃

The protocol described by McOmie and co-workers¹²¹ was followed. Thus, a mixture of 1 M BBr₃ (0.670 ml, 6.68 mL) in anhydrous CH₂Cl₂ (6.7 mL) was prepared in a Schlenk tube cooled to –78 °C. Compounds **5.51** and **5.55** (0.729 mmol) in anhydrous CH₂Cl₂ (0.5 mL) were slowly added, and stirred for 2 h while maintaining the temperature at –60 °C. The mixture was stirred for an additional 4 h and then warmed to RT. Water (15 mL) was slowly added to the cooled (0 °C) solution until effervescence ceased. Extraction with CH₂Cl₂ (15 mL x 3) yielded an orange-brown oil in low to moderate yields after chromatographic purification (40:60 EtOAc/Hexane). The spectroscopic details of the compounds are described below:

6-Hydroxy-2-(4'-methylthiazol-2-yl)-1,2-dihydroisoquinolin-3(4H)-one 5.56a was

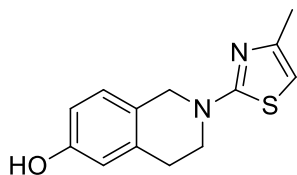


obtained in 45% (52.6 mg) yield from 123 mg of starting material **5.51a**. Yellow solid; **mp** = 204 – 206 °C; R_f = 0.79 (5:95 MeOH/CH₂Cl₂). **¹H NMR** (300 MHz, DMSO-*d*₆): δ (ppm) 9.58 (brs, 1H, OH), 7.25 (d, J = 8.1 Hz, 1H, ArH), 6.86 (sharp m, 1H, thiazole-ArH),

6.69 – 6.66 (m, 2H, 2xArH), 5.23 (s, 2H, ArCH₂N), 3.83 (s, 2H, ArCH₂CH₂), 2.32 (d, J = 1.0 Hz, 3H, thiazole-CH₃). **¹³C NMR** (75 MHz, DMSO-*d*₆): δ (ppm) 17.03 (thiazole-CH₃), 38.13 (ArCH₂O), 48.69 (ArCH₂N), 109.57 (thiazole-ArCH), 113.36 (ArCH), 113.61 (ArCH), 121.74 (ArCH), 126.88 (ArC), 132.86 (ArC), 145.89 (thiazole-ArC), 156.93

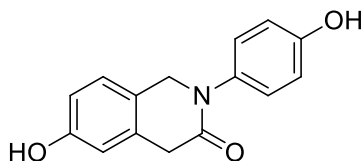
(ArCOH), 158.37 (*thiazole*-ArCN), 168.46 (C=O). **HRMS ESI⁺**: m/z [M+H]⁺ calcd for C₁₃H₁₂N₂O₂S, 261.0653; found, 261.0701 (3.83 ppm).

2-(4'-Methylthiazol-2-yl)-1,2,3,4-tetrahydroisoquinolin-6-ol 5.1a was obtained in



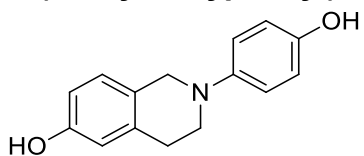
45% (52.6 mg) yield from 149 mg of starting material **5.55a**. Yellow solid; **mp** = 120 – 122 °C; R_f = 0.24 (40:60 EtOAc/Hexane). **¹H NMR** (300 MHz, DMSO-*d*₆): δ (ppm) 6.34 (d, J = 8.2 Hz, 1H, ArH), 6.10 – 5.94 (m, 2H, 2xArH), 5.78 (sharp m, 1H, *thiazole*-ArH), 4.29 (brs, 1H, OH), 3.97 (s, 2H, ArCH₂N), 3.10 (t, J = 6.0 Hz, 2H, CH₂), 2.18 (t, J = 6.0 Hz, 2H, ArCH₂CH₂), 1.63 (d, J = 1.1 Hz, 3H, *thiazole*-CH₃). **¹³C NMR** (75 MHz, DMSO-*d*₆): δ (ppm) 20.24 (*thiazole*-CH₃), 33.11 (ArCH₂CH₂), 36.67 (CH₂), 69.79 (ArCH₂N), 97.17 (*thiazole*-ArCH), 105.12 (ArCH), 106.09 (ArCH), 115.57 (ArCH), 118.59 (ArC), 127.50 (ArC), 134.15 (*thiazole*-ArC), 147.45 (ArCOH), 148.24 (*thiazole*-ArCN). **HRMS ESI⁺**: m/z [M+H]⁺ calcd for C₁₃H₁₄N₂OS, 247.0860; found, 247.0910 (4.04 ppm).

6-Hydroxy-2-(4'-hydroxyphenyl)-1,2-dihydroisoquinolin-3(4H)-one 5.56b was



obtained in a 78% (110 mg) yield from 156 mg of starting material **5.51b**. Beige solid; decomposition temperature = 230 – 240 °C; R_f = 0.21 (40:60 EtOAc/Hexane). **¹H NMR** (300 MHz, DMSO-*d*₆): δ (ppm) 9.45 (brs, 2H, 2xOH), 7.09 – 7.06 (m, 3H, 3xArH), 6.75 (d, J = 8.6 Hz, 2H, 2xArH), 6.63 (d, J = 8.6 Hz, 2H, 2xArH), 4.65 (s, 2H, ArCH₂N), 3.57 (s, 2H, ArCH₂CH₂). **¹³C NMR** (75 MHz, DMSO-*d*₆, two ArCH signals were not visible): δ (ppm) 38.50 (ArCH₂CH₂), 53.06 (ArCH₂N), 113.33 (ArCH), 115.21 (ArCH), 123.27 (ArCH), 126.32 (ArC), 126.82 (ArC), 134.15 (ArCN), 155.50 (ArCOH), 156.70 (ArCOH), 168.49 (C=O). **HRMS ESI⁺**: m/z [M+H]⁺ calcd for C₁₅H₁₃NO₃, 256.0929; found, x.

2-(4'-Hydroxyphenyl)-1,2,3,4-tetrahydroisoquinolin-6-ol 5.1c was obtained in a 38%



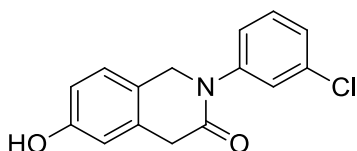
(17.7 mg) yield from 52.0 mg of starting material **5.55c**. Yellow solid; **mp** = 178 – 180 °C. **¹H NMR** (300 MHz, CD₃OD): δ (ppm) 7.05 – 6.89 (m, 3H, 3xArH), 6.83 – 6.69 (m, 2H, 2xArH), 6.67 – 6.53 (m, 2H, 2xArH), 4.12 (s, 2H, ArCH₂N), 2.92 (t, J = 5.8 Hz, 2H, ArCH₂CH₂). **¹³C NMR** (75 MHz, CD₃OD, the methylene signals were hidden behind the CD₃OD signal and the ArCOH signals were not visible): δ (ppm) 29.98 (ArCH₂CH₂), 51.05 (CH₂), 54.60 (ArCH₂N), 114.52 (ArCH), 115.69 (ArCH), 116.71 (ArC), 120.73 (ArCH), 126.13 (ArC), 126.84 (ArCH),

135.79 (ArCH), 136.74 (ArCH). **HRMS ESI⁺**: m/z [M+H]⁺ calcd for C₁₅H₁₅NO₂, 242.1181; found, 242.1185 (1.65 ppm).

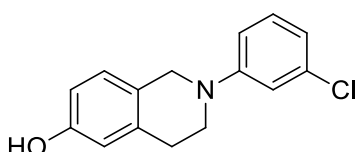
8.16.2 Method B: Using AlI₃

The protocol described by Bhatt and co-workers⁹³ was adopted. Thus, I₂ (990 mg, 7.80 mmol) was added to a cooled suspension of Al powder (160 mg, 6.00 mmol) in anhydrous toluene (20 mL) stirred under reflux for 6 h (red colour dissipates). The mixture was cooled to RT, to which the methoxy substrates **5.55d – g** (0.600 mmol) were added and stirred overnight at 60 °C. The reaction was cooled to RT and excess AlI₃ was quenched by the slow addition of water (15 mL). The suspension was extracted with EtOAc (20 mL x 3) to yield a brown residue purified by column chromatography (50:50 EtOAc/Hexane). The spectroscopic details of the compounds are described below:

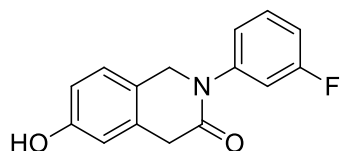
2-(3'-Chlorophenyl)-6-hydroxy-1,2-dihydroisoquinolin-3(4H)-one 5.56d was obtained in 57% (80.0 mg) yield from 146 mg of starting material **5.51d**. Translucent oil which solidified to a white solid at low temperatures; R_f = 0.36 (40:60 EtOAc/Hexane). **¹H NMR** and **¹³C NMR** spectra were not clear enough and not recorded, therefore no spectral information was recorded. **HRMS ESI⁺**: m/z [M+H]⁺ calcd for C₁₅H₁₂ClNO₂, 275.0527 (³⁵Cl); found, 275.0527 (3.65 ppm).



2-(3'-Chlorophenyl)-1,2,3,4-tetrahydroisoquinolin-6-ol 5.1d was obtained in 57% (80.0 mg) yield from 148 mg of starting material **5.55d**. White crystal; **mp** = 128 – 130 °C; R_f = 0.36 (40:60 EtOAc/Hexane). **¹H NMR** (300 MHz, CDCl₃): δ (ppm) 7.27 – 7.06 (m, 1H, ArH), 6.99 (d, J = 8.0 Hz, 1H, ArH), 6.87 (d, J = 1.9 Hz, 1H, ArH), 6.82 – 6.51 (m, 4H, 4xArH), 4.30 (s, 2H, ArCH₂N), 3.49 (t, J = 5.3 Hz, 2H, CH₂), 2.87 (t, J = 5.3 Hz, 2H, ArCH₂CH₂). **¹³C NMR** (75 MHz, CDCl₃): δ (ppm) 29.44 (ArCH₂CH₂), 46.25 (CH₂), 49.99 (ArCH₂N), 113.02 (ArCH), 114.05 (ArCH), 114.77 (ArCH), 115.23 (ArCH), 118.35 (ArCH), 126.34 (ArCH), 128.03 (ArC), 130.47 (ArCH), 135.42 (ArC), 136.60 (ArCCl), 151.76 (ArCN), 154.77 (ArCOH). **HRMS ESI⁺**: m/z [M+H]⁺ calcd for C₁₅H₁₄ClNO, 261.0842 (³⁵Cl); found, 261.0833 (3.50 ppm) and 262.0807 (³⁷Cl).

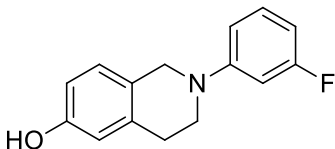


2-(3'-Fluorophenyl)-6-hydroxy-1,2-dihydroisoquinolin-3(4H)-one 5.56e was



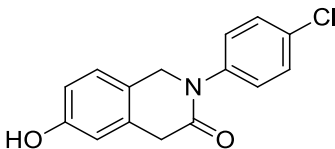
obtained in 89% (150 mg) yield from 177 mg of starting material **5.51e**. White solid; **mp** = 118 – 200 °C; R_f = 0.41 (50:50 EtOAc/Hexane). **¹H NMR** (300 MHz, CD₃OD, no OH signal was detected): δ (ppm) 7.56 – 7.33 (m, 1H, ArH), 7.23 – 6.96 (m, 4H, 4xArH), 6.84 – 6.58 (m, 2H, 2xArH), 4.81 (s, 2H, ArCH₂N), 3.70 (s, 2H, ArCH₂). **¹³C NMR** (75 MHz, CD₃OD): δ (ppm) 37.27 (ArCH₂CH₂), 52.35 (ArCH₂N), 114.14 (d, J = 21.75 Hz, ArCH-F), 114.47 (d, J = 24.00 Hz, ArCH-F), 122.42 (ArCH), 122.38 (ArCH), 123.98 (ArC), 127.25 (ArCH), 131.22 (ArCH), 131.34 (ArCH), 145.05 (ArC), 158.24 (ArCOH), 162.47 (ArCN), 165.86 (ArCF), 170.05 (C=O). **HRMS ESI⁺**: m/z [M+H]⁺ calcd for C₁₅H₁₂FNO₂, 258.0930 (¹⁸F); found, 258.0919 (4.30 ppm).

2-(3'-Fluorophenyl)-1,2,3,4-tetrahydroisoquinolin-6-ol 5.1e was obtained in 48%



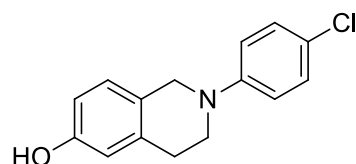
(63.8 mg) yield from 140 mg of starting material **5.55e**. Yellow solid; **mp** = °C; R_f = 0.41 (50:50, EtOAc/Hexane). **¹H NMR** and **¹³C NMR** spectra were not clear enough and not recorded, therefore no spectral information was recorded. **HRMS ESI⁺**: m/z [M+H]⁺ calcd for C₁₅H₁₄FNO, 244.1093 (¹⁸F); found, 244.1140 (4.09 ppm).

2-(4'-Chlorophenyl)-6-hydroxy-1,2-dihydroisoquinolin-3(4H)-one 5.56f was



obtained in trace amounts 9% (7 mg) yield from 84.0 mg of starting material **5.51f**. White solid; **mp** = 156 – 158 °C; R_f = 0.41 (50:50 EtOAc/Hexane). **¹H NMR** (300 MHz, CD₃OD): δ (ppm) 7.49 – 7.40 (m, 1H, ArH), 7.39 – 7.30 (m, 2H, 2xArH), 7.11 (d, J = 6.6 Hz, 2H, 2xArH), 6.71 (d, J = 6.6 Hz, 2H, 2xArH), 4.80 (s, 2H, ArCH₂N), 4.59 (brs, 1H, OH), 3.70 (s, 2H, ArCH₂). Unfortunately, not enough product was obtained for a good **¹³C NMR**. **HRMS ESI⁺**: m/z [M+H]⁺ calcd for C₁₅H₁₂ClNO₂, 275.0527 (³⁵Cl); found, 274.0634 (3.60 ppm) and 276.0611 (³⁷Cl).

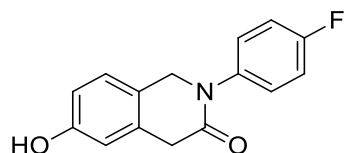
2-(4'-Chlorophenyl)-1,2,3,4-tetrahydroisoquinolin-6-ol 5.1f was obtained in 58%



(81.7 mg) yield from 133 mg of starting material **5.55f**. Brown solid; **mp** = 116 – 117 °C; R_f = 0.41 (50:50 EtOAc/Hexane). **¹H NMR** (300 MHz, CDCl₃, no OH signal was visible): δ (ppm) 7.27 – 7.15 (m, 2H, 2xArH), 7.00 (d, J = 8.2 Hz, 1H, ArH), 6.90 – 6.81 (m, 2H, 2xArH), 6.71 – 6.58 (m, 2H, 2xArH), 4.28 (s, 2H, ArCH₂N), 3.48 (t, J = 5.9 Hz, 2H, CH₂), 2.89 (t, J = 5.9 Hz,

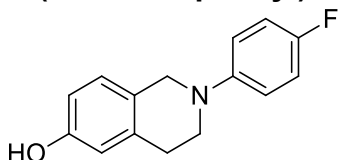
2H, ArCH₂CH₂). ¹³C NMR (75 MHz, CDCl₃): δ (ppm) 29.11 (ArCH₂CH₂), 46.63 (CH₂), 50.32 (ArCH₂N), 113.68 (ArCH), 114.97 (ArCH), 116.36 (ArCH), 123.15 (ArCH), 123.95 (ArCH), 126.46 (ArC), 127.82 (ArCCL), 129.13 (ArCH), 136.29 (ArCH), 149.13 (ArC), 149.60 (ArCN), 154.18 (ArCOH). HRMS ESI⁺: *m/z* [M+H]⁺ calcd for C₁₅H₁₄CINO, 261.0842 (³⁵Cl); found, 260.0833 (3.50 ppm) and 262.0803 (³⁷Cl).

2-(4'-Fluorophenyl)-6-hydroxy-1,2-dihydroisoquinolin-3(4H)-one 5.56g was



obtained in 24% (5.50 mg) yield from 24.2 mg of starting material **5.51g**. Brown solid; mp = 115 – 117 °C; R_f = 0.41 (50:50 EtOAc/Hexane). ¹H NMR (300 MHz, DMSO-*d*₆): δ (ppm) 6.53 (m, 2H, 2xArH), 6.42 – 6.22 (m, 3H, 3xArH), 5.88 (d, *J* = 6.1 Hz, 2H, 2xArH), 3.97 (d, *J* = 3.2 Hz, 2H, ArCH₂N), 3.77 (brs, 1H, OH), 2.88 (s, 2H, ArCH₂). ¹³C NMR (75 MHz, DMSO-*d*₆, no ArC and C=O signals were visible): δ (ppm) 29.97 (ArCH₂CH₂), 45.69 (ArCH₂N), 105.41 (d, *J* = 31.5 Hz, ArCH-F), 107.57 (d, *J* = 23.0 Hz, ArCH-F), 118.10 (ArCH), 119.82 (ArCH), 125.43 (ArCH). HRMS ESI⁺: *m/z* [M+H]⁺ calcd for C₁₅H₁₂FNO₂, 258.0886 (¹⁸F); found, 258.0934 (3.87 ppm).

2-(4'-Fluorophenyl)-1,2,3,4-tetrahydroisoquinolin-6-ol 5.1g was obtained in 55%



(60.8 mg) yield from 116 mg of starting material **5.55g**. Orange solid; mp = 105 – 107 °C; R_f = 0.53 (50:50 EtOAc/Hexane). ¹H NMR (300 MHz, CDCl₃): δ (ppm) 7.06 – 6.88 (m, 5H, 5xArH), 6.74 – 6.59 (m, 2H, 2xArH), 4.26 (s, 2H, ArCH₂N), 3.46 (t, *J* = 5.7 Hz, 2H, NCH₂), 2.92 (t, *J* = 5.7 Hz, 2H, ArCH₂CH₂). ¹³C NMR (75 MHz, CDCl₃, no C-F coupling was visible): δ (ppm) 29.41 (ArCH₂CH₂), 48.16 (CH₂), 51.87 (ArCH₂N), 113.87 (ArCH), 115.27 (ArCH), 115.80 (ArCH), 116.09 (ArCH), 117.68 (ArCH), 126.05 (ArCH), 126.80 (ArCH), 128.04 (ArC), 136.35 (ArC), 154.38 (ArCN), 157.79 (ArCOH), 159.89 (ArCF). HRMS ESI⁺: *m/z* [M+H]⁺ calcd for C₁₅H₁₄FNO, 244.1038 (¹⁸F); found, 244.1140 (0.80 ppm) and 245.1168 (¹⁹F).

References

- (1) Chesworth, R.; Zawistoski, M. P.; Lefker, B. A.; Cameron, K. O.; Day, R. F.; Mangano, F. M.; Rosati, R. L.; Colella, S.; Petersen, D. N.; Brault, A.; Lu, B.; Pan, L. C.; Perry, P.; Ng, O.; Castleberry, T. A.; Owen, T. A.; Brown, T. T.; Thompson, D. D.; DaSilva-Jardine, P. *Bioorg. Med. Chem. Lett.* **2004**, *14*, 2729.
- (2) Gangapuram, M.; Eyunni, S.; Redda, K. K. *J. Cancer Sci. Ther.* **2014**, *6*, 161.
- (3) Abe, K.; Saitoh, T.; Horiguchi, Y.; Utsunomiya, I.; Taguchi, K. *Biol. Pharm. Bull.* **2005**, *28*, 1355.
- (4) Renaud, J.; Bischoff, S. F.; Buhl, T.; Floersheim, P.; Fournier, B.; Geiser, M.; Halleux, C.; Kallen, J.; Keller, H.; Ramage, P. *J. Med. Chem.* **2005**, *48*, 364.
- (5) Gitto, R.; Caruso, R.; Pagano, B.; De Luca, L.; Citraro, R.; Russo, E.; De Sarro, G.; Chimirri, A. *J. Med. Chem.* **2006**, *49*, 5618.
- (6) Wen Ng, H.; Perkins, R.; Tong, W.; Hong, H. *Int. J. Environ. Res. Public Health* **2014**, *11*, 8709.
- (7) Cui, J.; Shen, Y.; Li, R. *Trends Mol. Med.* **2013**, *19*, 197.
- (8) Kraemer, W. J.; Rogol, A. D. In *The Endocrine System in Sports and Exercise.*; Blackwell: **2005**, p 2.
- (9) Anand, P.; Kunnumakara, A. B.; Sundaram, C.; Harikumar, K. B.; Tharakan, S. T.; Lai, O. S.; Sung, B.; Aggarwal, B. B. *Pharm. Res.* **2008**, *25*, 2097.
- (10) Jemal, A.; Bray, F.; Forman, D.; O'Brien, M.; Ferlay, J.; Center, M.; Parkin, D. M. *Cancer* **2012**, *118*, 4372.
- (11) Singh, P. *ICMR Bulletin* **2003**, *33*, 4377.
- (12) Key, T. J.; Allen, N. E.; Spencer, E. A.; Travis, R. C. *Lancet* **2002**, *360*, 861.
- (13) Tsuchiya, Y.; Nakajima, M.; Yokoi, T. *Cancer Lett.* **2005**, *227*, 115.
- (14) Platet, N. *Crit. Rev. Oncology/Hematology* **2004**, *51*, 55.
- (15) Ascenzi, P.; Bocedi, A.; Marino, M. *Mol. Aspects. Medicine* **2006**, *27*, 299.
- (16) Gustafsson, J. A. *J. Endocrinol.* **1999**, *163*, 379.
- (17) Hewitt, S. C.; Korach, K. S. *Endocrine & Metabolic Disorders* **2002**, *3*, 193.
- (18) Yagar, J. D.; Davidson, N. E. *N. Engl. J. Med.* **2006**, *354*, 270.
- (19) Russo, J.; Russo, I. H. *J. Steroid Biochem. Molec. Biol.* **2006**, *102*, 89.
- (20) Pearce, S. T.; Jordan, V. C. *Crit. Rev. Oncology/Hematology* **2004**, *50*, 3.
- (21) Kang, H.; Kim, S.-W.; Kim, H.-J.; Ahn, S.-J.; Bae, J.-Y.; Park, S. K.; Khang, D.; Hirvonen, A.; Choe, K. J.; Noh, D.-Y. *Cancer Lett.* **2002**, *178*, 175.
- (22) Maximov, P. Y.; Lee, T. M.; Jordan, V. C. *Curr. Clin. Pharmacol.* **2013**, *8*, 135.
- (23) Maalouf, G. J.; Xu, W.; Smith, T. F.; Mohr, S. C. *J. Biomol. Struct. Dyn.* **1998**, *15*, 841.
- (24) Mueller-Fahrnow, A.; Egner, U. *Curr. Opin. Biotechnol.* **1999**, *10*, 550.
- (25) Ruff, M.; Gangloff, M.; Wurtz, J. M.; Moras, D. *Breast Cancer Res.* **2000**, *2*, 353.
- (26) Canadian Cancer Society, 2017; Vol. 2017.
- (27) von Rueden, D. F.; Wilson, R. E. *Surg. Gynecol. Obstet.* **1984**, *158*, 105.
- (28) Singletary, S. E.; Patel-Parekh, L.; Bland, K. I. *Ann. Surg.* **2005**, *242*, 281.
- (29) Sudhakar, A. *J. Cancer Sci. Ther.* **2009**, *1*, 1.
- (30) Bansal, R.; Acharya, P. C. *Chem. Rev.* **2014**, *114*, 6986.
- (31) Komme, B. S.; Mrkin, S. *J. Steroid Biochem. Mol. Biol.* **2014**, *143*, 207.
- (32) Howell, S. J.; Johnston, S. R. D.; Howell, A. *Best Pract. Res., Clin. Endocrinol. Metab.* **2004**, *18*, 47.
- (33) Dillman, R. O. *Cancer Metastasis Rev.* **1999**, *18*, 465.
- (34) Harris, M. *Lancet Oncol.* **2004**, *5*, 292.
- (35) In www.cancer.gov/cancertopics/treatment/types_of_treatment, American Cancer Society: 2015 (Accessed January 2019).
- (36) Jemal, A.; Bray, F.; Center, M. M.; Ferlay, J.; Ward, E.; Forman, D. *CA: Cancer J. Clin.* **2011**, *61*, 69.
- (37) Vorobiof, D. A.; Sitas, F.; Vorobiof, G. *Am. Soc. Clin. Oncol.* **2001**, *19*, 125.
- (38) Wallace, O. B.; Richardson, T. I.; Dodge, J. A. *Curr. Top. Med. Chem.* **2003**, *3*, 1663.
- (39) Renaud, J.; Bischoff, S. E.; Buhl, T.; Floersheim, P.; Fournier, B.; Halleux, C.; Kallen, J.; Keller, H.; Schlaeppli, J.-M.; Stark, W. *J. Med. Chem.* **2003**, *46*, 2945.

- (40) Möcklinghoff, S.; van Otterlo, W. A. L.; Rose, R.; Fuchs, S.; Zimmermann, T. J.; Seoane, M. D.; Waldmann, H.; Ottmann, C.; Brunsveld, L. *J. Med. Chem.* **2011**, *54*, 2005.
- (41) Barkhem, T.; Carlsson, B.; Nilsson, Y.; Enmark, E.; Gustafsson, J. A.; Nilsson, S. *Mol. Pharmacol.* **1998**, *54*, 105.
- (42) Heldring, N.; Pike, A.; Andersson, S.; Matthews, J.; Cheng, G.; Hartman, J.; Tujague, M.; Strom, A.; Treuter, E.; Warner, M.; Gustafsson, J. A. *Physiol. Rev.* **2007**, *87*, 905.
- (43) Nilsson, S.; Makela, S.; Treuter, E.; Tujague, M.; Thomsen, J.; Andersson, G.; Enmark, E.; Pettersson, K.; Warner, M.; Gustafsson, J.-A. *Physiol. Rev.* **2001**, *81*, 1535.
- (44) Pettersson, K.; Gustafsson, J. A. *Annu. Rev. Physiol.* **2001**, *63*, 165.
- (45) Martin-Santamaria, S.; Rodriguez, J.; de Pascual-Teresa, S.; Gordon, S.; Bengtsson, M.; Garrido-Laguna, I.; Rubio-Viqueira, B.; Lopez-Casas, P. P.; Hidalgo, M.; de Pascual-Teresa, B.; Ramos, A. *Org. Biomol. Chem.* **2008**, *6*, 386.
- (46) Riggs, B. L.; Hartmann, L. C. *N. Engl. J. Med.* **2003**, *348*, 618.
- (47) Rahman, R. L.; Pruthi, S. *Cancers* **2012**, *4*, 1146.
- (48) Martinkovich, S.; Shah, D.; Planey, S. L.; Arnott, J. A. *Clin. Interventions Aging* **2014**, *9*, 1437.
- (49) Smith, E.; Boyd, J.; Frank, G.; Lubahn, D.; Korach, K. *N. Engl. J. Med.* **1994**, *331*, 1056.
- (50) Korach, K. S. *Science* **1994**, *266*, 1524.
- (51) Lin, H.; Safo, M. K.; Abraham, D. J. *Bioorg. Med. Chem. Lett.* **2007**, *17*, 2581.
- (52) Anstead, G. M.; Carlson, K. E.; Katzenellenbogen, J. A. *Steroids* **1997**, *62*, 268.
- (53) Kumar, R.; Zakharov, M. N.; Khan, S. H.; Miki, R.; Jang, H.; Toraldo, G.; Singh, R.; Bhasin, S.; Jasuja, R. *J. Amino Acids* **2011**, *7*.
- (54) Zheng, J.; Li, W.; Zhao, Y.; Liu, G.; Tang, Y.; Jiang, H. *J. Phys. Chem. B* **2008**, *112*, 2719.
- (55) Patrick, G. L. *An Introduction to Medicinal Chemistry*; 5th ed.; Oxford University Press, 2013.
- (56) Levin, E. R. *J. Appl. Physiol.* **2001**, *91*, 1860.
- (57) Shoa, D.; Berrodin, T. J.; Manas, E.; Hauze, D.; Powers, R.; Bapat, A.; Gonder, D.; Winneker, R. W.; Frail, D. E. *J. Steroid Biochem. Mol. Biol.* **2004**, *88*, 351.
- (58) Freedman, L. P. (Editor) *Molecular Biology of Steroid and Nuclear Hormone Receptors*; Birkhauser (Springer), 1998.
- (59) Harrington, W. R.; Sheng, S.; Barnette, D. H.; Petz, L. N.; Katzenellenbogen, J. A.; Katzenellenbogen, B. A. *Mol. Cell. Endocrin.* **2003**, *203*, 13.
- (60) Katzenellenbogen, B. S.; Katzenellenbogen, J. A. *Breast Cancer Res.* **2000**, *2*, 335.
- (61) Shiau, A. K.; Barstad, D.; Loria, P. M.; Cheng, L.; Kushner, P. J.; Agard, D. A.; Greene, G. L. *Cell* **1998**, *95*, 927.
- (62) Perissi, V.; Rosenfeld, M. G. *Nat. Rev. Mol. Cell Biol.* **2005**, *6*, 542.
- (63) Klinge, C. M. *Steroids* **2000**, *65*, 227.
- (64) Baniahmad, A. *J. Steroid Biochem. Mol. Biol.* **2005**, *93*, 89.
- (65) Dobrzycka, K. M.; Townson, S. M.; Jiang, S.; Oesterreich, S. *Endocr.-Relat. Cancer* **2003**, *10*, 517.
- (66) Li, J.; Soroka, J.; Buchner, J. *Biochim. Biophys. Acta.* **2012**, *1823*, 624.
- (67) Compston, J. E. *Physiol. Rev.* **2001**, *81*, 419.
- (68) Bjornstrom, L.; Sjoberg, M. *Mol. Endocrinol.* **2005**, *19*, 833.
- (69) Gruber, C. J.; Gruber, D. M.; Gruber, I. M. L.; Wieser, F.; Huber, J. C. *Trends Endocrinol. Metab.* **2004**, *15*, 73.
- (70) Dowers, T. S.; Qin, Z.-H.; Thatcher, G. R. J.; Bolton, J. L. *Chem. Res. Toxicol.* **2006**, *19*, 1125.
- (71) Schiff, R.; Massarweh, S.; Shou, J.; Osborne, C. K. *Clin. Cancer Res.* **2003**, *9*, 447s.
- (72) Hall, J. M.; McDonnell, D. P. *Menopausal Medicine* **2008**, *16*, S1.
- (73) Bryant, H. U. *Rev. Endocr. Metab. Disord.* **2002**, *3*, 231.
- (74) Lewis, R. M. *Yale J. Biol. Med.* **1939**, *12*, 235.
- (75) Herbst, A. L.; Kurman, R. J.; Scully, R. E. *Ob/Gyn* **1972**, *40*, 287.
- (76) Cutler, B. S.; Forbes, A. P.; Ingersoll, F. M.; Scully, R. E. *N. Engl. J. Med.* **1972**, *287*, 628.
- (77) Lanier, A. P.; Noller, K. L.; Decker, D. G.; Elveback, L. R.; Kurland, L. T. *Obstetrics and Gynecology Survey* **1974**, *29*, 407.
- (78) Gabriel, E. M.; Jatoi, I. *Expert Rev. Anticancer Ther.* **2012**, *12*, 223.
- (79) Ning, M.; Zhou, C.; Weng, J.; Zhang, S.; Chen, D.; Yang, C.; Wang, H.; Ren, J.; Zhou, L.; Jin, C.; Wang, M.-W. *J. Pharmacol.* **2007**, *150*, 19.
- (80) Jackson, L. R.; Cheung, K. L.; Buzdar, A. U.; Robertson, J. F. R. *Core Evid.* **2007**, *2*, 251

- (81) Vajdos, F. F.; Hoth, L. R.; Geoghegan, K. F.; Simons, S. P.; Lemotte, P. K.; Danley, D. E.; Ammirati, M. J.; Pandit, J. *Protein Sci.* **2007**, *16*, 897.
- (82) Gennari, L.; Merlotti, D.; Nuti, R. *Clin. Investigations Aging* **2010**, *5*, 19.
- (83) Brzezinski, A.; Debi, A. *Eur. J. Obstet. Gynecol. Reprod. Biol.* **1999**, *85*, 47.
- (84) Bolton, J. L. *Curr. Org. Chem.* **2014**, *18*, 61.
- (85) Yu, L.; Liu, H.; Li, W.; Zhang, F.; Luckie, C.; van Breemen, R. B.; Thatcher, G. R. J.; Bolton, J. L. *Chem. Res. Toxicol.* **2004**, *17*, 879.
- (86) Newman, D. J.; Cragg, G. M. *Future Med. Chem.* **2009**, *8*, 1415.
- (87) Harvey, A. L. *Drug Discovery Today* **2008**, *13*, 894.
- (88) Pieters, L.; Vlietinck, A. J. *J. Ethnopharmacol.* **2005**, *100*, 57.
- (89) Dahanukar, S. A.; Kulkarni, R. A.; Rege, N. N. *Indian J. Pharmacol.* **2002**, *32*, 81
- (90) Barz, W.; Reinhard, E.; Zenk, E. H. In *Plant Tissue Culture and its Bio-Technological Applications. Proceedings in Life Sciences.*; Zenk, M. H., El-Shagi, H., Avens, H., Stockigt, J., Weiler, E. W., Deus, B., Eds.; Springer: Berlin, Heidelberg, 1977.
- (91) Wright, A. E.; Forleo, D. A.; Gunawardana, G. P.; Gunasekera, S. P.; Koehn, F. E.; McConnell, O. J. *J. Org. Chem* **1990**, *55*, 4508.
- (92) Aubry, S.; Pellet-Rostaing, S.; Fournier dit Chabert, J.; Ducki, S.; Lemaire, M. *Bioorg. Med. Chem. Lett.* **2007**, *17*, 2598.
- (93) Bhatt, V. M.; Babu, R. J. *Tetrahedron Lett.* **1984**, *25*, 3497.
- (94) Ouellet, C.; Ouellet, E.; Poirier, D. *Invest. New Drugs* **2015**, *33*, 95.
- (95) Dong, H.; Lee, C.-M.; Huang, W.-L.; Peng, S.-X. *Br. Pharmacol. Soc.* **1992**, *107*, 262.
- (96) Amat, M.; Elias, V.; Llor, N.; Subrizi, F.; Molins, E.; Bosch, J. *Eur. J. Org. Chem.* **2010**, *2010*, 4017.
- (97) Martinez, S.; Perezl, L.; Galmarini, C. M.; Aracil, M.; Tercero, J. C.; Gago, F.; Albella, B.; Bueren, J. A. *Br. J. Pharmacol.* **2013**, *170*, 871.
- (98) Eyunni, S.; Gangapuram, M.; Redda, K. K. *Lett. Drug Des. Discovery* **2014**, *11*, 428.
- (99) Liu, W.; Liu, S.; Jin, R.; Guo, H.; Zhao, J. *Org. Chem. Front.* **2015**, *2*, 288.
- (100) Mukherjee, S.; Saha, A.; Roy, K. *Bioorg. Med. Chem. Lett.* **2005**, *15*, 957.
- (101) Scott, J. S.; Bailey, A.; Davies, R. D. M.; Degorce, S. L.; MacFaul, P. A.; Gingell, H.; Moss, T.; Norman, R. A.; Pink, J. H.; Rabow, A. A.; Roberts, B.; Smith, P. D. *ACS Med. Chem. Lett.* **2016**, *7*, 94.
- (102) Zou, Z.-H.; Lan, X.-b.; Qian, H.; Huang, W.-l.; Li, Y.-M. *Bioorg. Med. Chem. Lett* **2011**, *21*, 5934.
- (103) Zhang, Y.; Liu, C.; Chou, C. J.; Wang, X.; Jia, Y.; Xu, W. *Chem. Biol. Drug Des.* **2013**, *82*, 125.
- (104) Pingaew, R.; Prachayasittikul, S.; Ruchirawat, S.; Prachayasittikul, V. *Med. Chem. Res.* **2013**, *22*, 267.
- (105) Kubota, H.; Kakefuda, A.; Watanabe, T.; Ishii, N.; Wada, K.; Masuda, N.; Sakamoto, S.; Tsukamoto, S.-I. *J. Med. Chem.* **2003**, *46*, 4728.
- (106) Berger, T.; French, E. D.; Siggins, G. R.; Shier, W. T.; Bloom, F. E. *Pharmacol. Biochem. Behav.* **1982**, *17*, 813.
- (107) Giorgioni, G.; Ruggieri, S.; Claudi, F.; Di Stefano, A.; Ljung, E.; Carlsson, T. *J. Med. Chem.* **2008**, *4*, 1.
- (108) Endo, Y.; Yoshimi, T.; Miyaura, C. *Pure Appl. Chem.* **2003**, *75*, 1197.
- (109) Al-Horani, R. A.; Desai, U. R. *Tetrahedron* **2012**, *68*, 2027.
- (110) Dua, R.; Shrivastavas, S.; Sonwane, S. K.; Srivastavas, S. K. *Adv. Bio. Res.* **2011**, *5*, 120.
- (111) Vitaku, E.; Smith, D. T.; Njardarson, J. T. *J. Med. Chem* **2014**, *57*, 10257.
- (112) Norman, S. R. *Drug Dev. Res.* **2008**, *69*, 15.
- (113) Lemoucheux, L.; Rouden, J.; Ibazizene, M.; Sobrio, F.; Lasne, M. *J. Org. Chem.* **2003**, *6*, 7289.
- (114) Munch, H.; Hansen, J. S.; Pittelkow, M.; Christensen, J. B.; Boas, U. *Tetrahedron Lett.* **2008**, *49*, 3117.
- (115) Ponzio, M. G.; Evindar, G.; Batey, R. A. *Tetrahedron Lett.* **2002**, *43*, 7601.
- (116) Wang, X.-J.; Tan, J.; Grozinger, K. *Tetrahedron Lett.* **1998**, *39*, 6609.
- (117) Zografos, A. L. In *Heterocyclic Chemistry in Drug Discovery*, John Wiley & Sons, Inc.: Hoboken, New Jersey, 2013, p 471.
- (118) Zarranz de Ysern, M. E.; Odonez, L. A. *Prog. Neuro-Psychopharmacol.* **1981**, *5*, 343.

- (119) Zhong, H. M.; Villani, F. J.; Marzouq, R. *Org. Process Res. Dev.* **2007**, *11*, 463.
- (120) Bailey, J. M.; Booth, H.; Al-Shirayda, H. A. R. Y. *J. Chem. Soc. Perkin Trans. 2* **1984**, 583.
- (121) McOmie, J. F. W.; Watts, M. L.; West, D. E. *Tetrahedron* **1968**, *24*, 2289.
- (122) Melvin, L. S.; Johnson, M. R.; Harbert, C. A.; Milne, G. M.; Weissman, A. *J. Med. Chem.* **1984**, *27*, 67.
- (123) Nystrom, R. F. *J. Am. Chem. Soc.* **1955**, *77*, 2544.
- (124) Davis, H. A.; Brown, R. K. *Canadian J. Chem.* **1971**, *49*, 2166.
- (125) Dalence-Guzman, M. F.; Berglund, M.; Skogvall, S.; Sterner, O. *J. Bioorg. Med. Chem.* **2008**, *16*, 2499.
- (126) Berglund, M.; Dalence-Guzman, M. F.; Skogvall, S.; Sterner, O. *J. Bioorg. Med. Chem.* **2008**, *16*, 2513.
- (127) Montalbetti, C. A. G. N.; Falque, V. *Tetrahedron* **2005**, *61*, 10827.
- (128) Lippa, K. A.; Demel, S.; Lau, H. I.; Roberts, A. L. *J. Agric. Food Chem.* **2004**, *52*, 3010
- (129) Vishnyakova, T. P.; Golubeva, I. A.; Glebova, E. V. *Russ. Chem. Rev.* **1985**, *54*, 249.
- (130) Kreye, O.; Mutlu, H.; Meier, A. M. R. *Green Chem.* **2013**, *15*, 1431.
- (131) Grzyb, J. A.; Shen, M.; Yoshina-Ishii, C.; Chi, W.; Brown, S.; Batey, R. A. *Tetrahedron* **2005**, *61*, 7153.
- (132) Valeur, E.; Bradley, M. *Chem. Soc. Rev.* **2009**, *38*, 606.
- (133) Bodanszky, M. *Int. J. Pep. Potein Res.* **1985**, *25*, 449.
- (134) Han, S.-Y.; Kim, Y.-A. *Tetrahedron* **2004**, *61*, 2447.
- (135) Ozaki, S. *Chem. Rev.* **1972**, *72*, 457.
- (136) Batey, R. A.; Yoshina-Ishii, C.; Taylor, S. D.; Santhakuma, V. *Tetrahedron Lett.* **1999**, *40*, 2669.
- (137) Padiya, K. J.; Gavade, S.; Kardile, B.; Tiwari, M.; Bajare, S.; Mane, M.; Gaware, V.; Harel, D.; Kurhade, S. *Org. Lett.* **2012**, *14*, 2814.
- (138) Velavan, A.; Sumathi, S.; Balasubramanian, K. K. *Org. Biomol. Chem.* **2012**, *10*, 6420.
- (139) Le, T. C.; Berlin, D.; Benson, S. D.; Eastman, M. A.; Bell-Eunice, G.; Nelson, A. C.; Benbrook, D. M. *Open Med. Chem. J.* **2007**, *1*, 11.
- (140) Beaudoin, S.; Kinsey, K. E.; Burns, J. F. *J. Org. Chem.* **2003**, *68*, 115.
- (141) Katrizky, A. R.; Witek, R. M.; Rodriguez-Garcia, V.; Mohapatra, P. P.; Rogers, J. W.; Cusido, J.; Abdel-Fattah, A. A. A.; Sted, P. J. *J. Org. Chem.* **2005**, *70*, 7866.
- (142) Yella, R.; Ghosh, H.; Murru, S.; Sahoo, S. K.; Patel, B. K. *Synth. Comm.* **2010**, *40*, 2083.
- (143) Sun, N.; Li, B.; Shao, J.; Mo, W.; Hu, B.; Shen, Z.; Hu, X. *Beilstein J. Org. Chem.* **2012**, *8*, 61.
- (144) Chaskar, A. C.; Yewale, S.; Bhagat, R.; Langi, B. P. *Synth. Comm.* **2008**, *38*, 1972.
- (145) Wong, R.; Dolman, S. J. *J. Org. Chem.* **2007**, *72*, 3969.
- (146) Zacheis, D.; Dhar, A.; Lu, S.; Madler, M. M.; Klucik, J.; Brown, O. W.; Liu, S.; Clement, I.; Subramanian, S.; Weeraseskare, G. M.; Berlin, K. D.; Gold, M. A.; Houck, J. R.; Fountain, K. R.; Benbrook, D. M. *J. Med. Chem.* **1999**, *42*, 4434.
- (147) Civicos, J. F.; Alonso, D. A.; Nájera, C. *Eur. J. Org. Chem.* **2012**, 3670.
- (148) Monnier, F.; Taillefer, M. *Angew. Chem. Int. Ed.* **2009**, *48*, 6954.
- (149) Romero, M.; Harrak, Y.; Basset, J.; Ginet, L.; Constans, P.; Pujol, M. D. *Tetrahedron* **2006**, *52*, 9010.
- (150) Klapars, A.; Antilla, J. C.; Huang, X.; Buchwald, S. L. *J. Am. Chem. Soc.* **2001**, *123*, 7727.
- (151) Hennessy, E. J.; Buchwald, S. L. *J. Am. Chem. Soc.* **2003**, *125*, 12084.
- (152) Surry, D. S.; Buchwald, S. L. *Chem. Sci* **2011**, *2*, 27.
- (153) Rao, K. S.; Wu, T. S. *Tetrahedron* **2012**, *68*, 7735.
- (154) Sambigiagio, C.; Marsden, S. P.; Blacker, A. J.; McGowan, P. C. *Chem. Soc. Rev.* **2014**, *43*, 3525.
- (155) Sperotto, E.; van Klink, G. P. M.; van Koten, G.; de Vries, J. *Dalton Trans.* **2010**, *39*, 10338.
- (156) Fischer, C.; Koenig, B. *Beilstein J. Org. Chem.* **2007**, *7*, 59.
- (157) Ma, D.; Cai, Q.; Zheng, H. *Org. Lett.* **2003**, *5*, 2453.
- (158) Ganapathi, K.; Kulkarni, K. D. *Proc. Indian Acad. Sci.* **1953**, *38*, 45
- (159) Qin, W.; Long, S.; Panunzio, M.; Biondi, S. *Molecules* **2013**, *18*, 12264.
- (160) de Silva, C. M.; de Silva, D. L.; Modolo, L. V.; Alves, R. B.; de Resende, M. A.; Martins, C. V. B.; de Fatima, A. *J. Adv. Res.* **2011**, *2*, 1.
- (161) Zhang, P.; Shi, B.; Wei, T.; Zhang, Y.; Lin, Q.; Yoa, H.; You, X. *Dyes Pigm.* **2013**, *99*, 857.

- (162) Kang, J.; Kim, H. S.; Jang, D. O. *Tetrahedron Lett.* **2005**, *46*, 6079.
- (163) da Settimo, A.; Primofiore, G.; da Settimo, F.; Calzolari, L.; Cazzulani, P.; Passoni, A.; Tofanetti, O. *Eur. J. Med. Chem.* **1992**, *27*, 395.
- (164) Hwang, J. Y.; Kim, H.; Jo, S.; Park, E.; Choi, J.; Khong, S.; Park, D.-S.; Heo, J. M.; Lee, J. S.; Ko, Y.; Choi, I.; Cechetto, J.; Kim, J. H.; Lee, J.; No, Z.; Windisch, M. P. *Eur. J. Med. Chem.* **2013**, *70*, 315.
- (165) Krishnaiah, M.; Jin, C. H.; Sreenu, D.; Subrahmanyam, V. B.; Rao, K. S.; Son, D.-H.; Park, H.-J.; Kim, S. K.; Sheen, Y. Y.; Kim, D.-K. *Eur. J. Med. Chem.* **2012**, *57*, 74.
- (166) Magnus, P.; Matthews, K. S. *Tetrahedron* **2012**, *68*, 6343.
- (167) Meyer, A. L.; Turner, R. B. *Tetrahedron* **1971**, *27*, 2609.
- (168) Deady, L. W.; Pirzada, N.; Topsom, R. D. *Chem. Comm.* **1971**, 571, 799.
- (169) Shindikar, A. V.; Khan, F.; Viswanathan, C. L. *Eur. J. Med. Chem.* **2006**, *41*, 786.
- (170) Meyers, A. I.; Dickman, D. A. *J. Am. Chem. Soc.* **1986**, *109*, 1263.
- (171) Bonnet-Delpon, D.; Charpentier-Morize, M.; Jacquot, R. *J. Org. Chem.* **1988**, *53*, 759.
- (172) Spangler, R. J.; Beckmann, B. G.; Kim, J. H. *J. Org. Chem.* **1977**, *42*, 2989.
- (173) Ma, Y. N.; Yang, X. J.; Pan, L.; Hou, Z.; Geng, H. L.; Song, X. P.; Zhou, L.; Miao, F. *Chem. Pharm. Bull.* **2013**, *61*, 204.
- (174) Chapman, O. L.; Miller, M. D.; Pitzemberger, S. M. *J. Am. Chem. Soc.* **1987**, *109*, 6867.
- (175) Larghi, E. L.; Kaufman, T. S. *Synthesis* **2006**, *2*, 187.
- (176) Taber, D. F.; Raciti, D. M. *Tetrahedron* **2011**, *67*, 10229.
- (177) Altenbach, R. J.; Black, L. A.; Chang, S.-J.; Cowart, M. D.; Faghieh, R.; Gfesser, G. A.; Ku, Y.-Y.; Liu, H.; Lukin, K. A.; Nersesian, D. L.; Pu, Y. M. Patent US20040092521A1, 2004, Preparation of pyrrolidine derivatives as histamine-3 receptor ligands.
- (178) Black, L. A.; Nersesian, D. L.; Sharma, P.; Ku, Y. Y.; Bennani, Y. L.; Marsh, K. C.; Miller, T. R.; Esben, S. T. A.; Hancock, A. A.; Cowart, M. *Bioorg. Med. Chem. Lett.* **2007**, *17*, 1443.
- (179) Taylor, J. B.; Lewis, J. W.; Jacklin, M. *J. Med. Chem.* **1970**, *13*, 1226.
- (180) Cheng, C.-Y.; Tsai, H.-B.; Lin, M.-S. *J. Heterocycl. Chem.* **1995**, *32*, 73.
- (181) Hassam, M.; Basson, A. E.; Liotta, D. C.; van Otterlo, W. A. L.; Pelly, S. C. *ACS Med. Chem. Lett.* **2012**, *3*, 470
- (182) Kano, S.; Yokomatsu, T.; Yuasa, Y. *Heterocycles* **1984**, *21*, 700.
- (183) Meng, X.; Zhang, H.; Mezei, M.; Cui, M. *Curr. Comput. Aided Drug Des.* **2011**, *7*, 146.
- (184) Carlson, H. A.; McCammon, J. A. *Mol. Pharmacol.* **2000**, *57*, 213.
- (185) Schultes, S.; de Graaf, C.; Haaksma, E. E. J.; de Esch, I. J. P.; Leurs, R.; Krämer, O. *Drug Discov. Today: Technol.* **2010**, *7*, e157.
- (186) Friesner, R. A.; Murphy, R. B.; Repasky, M. P.; Frye, L. L.; Greenwood, J. R.; Halgren, T. A.; Sanschagrín, P. C.; Mainz, D. T. *J. Med. Chem.* **2006**, *49*, 6177.
- (187) Ghersi, D.; Sanchez, R. *Proteins* **2009**, *74*, 417.
- (188) Huang, S.; Zou, X. *Int. J. Mol. Sci.* **2010**, *11*, 3016.
- (189) Erfle, H.; Pepperkok, R. *Methods Enzymol.* **2005**, *404*, 1
- (190) Hostetler, K. Y. *Antiviral Res.* **2009**, *82*, A84
- (191) Mandapati, U.; Pinapati, S.; Rudraraju, R. R. *Tetrahedron Lett.* **2017**, *58*, 125.
- (192) Yang, F.; Zhu, M.; Zhang, J.; Zhou, H. *Med. Chem. Comm.* **2018**, *9*, 201
- (193) Ban, H. S.; Nakamura, H. *Chem. Rec.* **2015**, *15*, 616
- (194) Endo, Y.; Yamakoshi, Y.; Kagechika, H. *Bioorg. Med. Chem. Lett.* **2003**, *13*, 4089
- (195) Endo, Y.; Iijima, T.; Amakoshi, Y.; Kubo, A.; Itai, A. *Bioorg. Med. Chem. Lett.* **1999**, *9*, 3313
- (196) Endo, Y.; Iijima, T.; Yamakoshi, Y.; Fukasawa, H.; Miyaura, C.; Inada, M.; Kubo, A.; Itai, A. *Chem. Biol.* **2001**, *8*, 341
- (197) Ogawa, T.; Endo, Y.; Ohta, K.; Yoshimi, T.; Yamazaki, H.; Suzuki, T.; Ohta, S. *Bioorg. Med. Chem. Lett.* **2006**, *16*, 3943
- (198) Perrin, D. D.; Armarego, W. L. F. *Purification of Laboratory Chemicals.*; 3rd ed., Elsevier Science, Amsterdam, 1988.
- (199) Williams, D. B. G.; Lawton, M. *J. Org. Chem.* **2010**, *75*, 8351.
- (200) O' Niel, J. D.; Bamat, M. K.; von Borstel, R. W.; Sharma, S.; Arudchandran, R.; Patent A01N 43/08 (2006, 01) ed. 2009, p 89, Compounds and method for reducing uric acid.
- (201) Johnson, J. A.; Yoon, J.; Lloyd, J.; Finlay, H.; Patent C37D231/56; C07D261/20; C07D275/06; C07D498/04 ed. 2007, Acyclic IKur inhibitors.

- (202) Ganellin, C. R.; Hosseini, S. K.; Khalaf, Y. S.; Tertiuk, W.; Arrang, J.-M.; Garbarg, M.; Ligneau, X.; Schwartz, J.-C. *J. Med. Chem.* **1995**, *38*, 3342.
- (203) Ji, H.; Jing, Q.; Huang, J.; Silverman, R. B. *Tetrahedron* **2012**, *68*, 1359.
- (204) Wang, C.; Chen, C.; Han, J.; Zhang, J.; Yao, Y.; Zhao, Y. *Eur. J. Org. Chem.* **2015**, *2015*, 2972.
- (205) Aoyama, T.; Murata, S.; Arai, I.; Araki, N.; Takido, T.; Suzuki, Y.; Kodomari, M. *Tetrahedron* **2006**, *62*, 3201.
- (206) Flipo, M.; Willand, N.; Lecat-Guillet, N.; Hounsou, C.; Desroses, M.; Leroux, F.; Lens, Z.; Villeret, V.; Wohlkönig, A.; Wintjens, R.; Christophe, T.; Kyoung Jeon, H.; Locht, C.; Brodin, P.; Baulard, A. R.; Déprez, B. *J. Med. Chem.* **2012**, *55*, 6391.
- (207) Vekemans, J.; Hoornaert, G. *Tetrahedron* **1979**, *36*, 943.